Regionalized Gene Expression during Human Neocorticogenesis

Bui Kar IP

A thesis submitted to Newcastle University for the degree of Doctor of Philosophy (PhD)

Faculty of Medical Sciences

Institute of Human Genetics

Institute of Neuroscience

December 2010

Abstract

Introduction: The mammalian neocortical areas arise from graded/regionalized gene expression from the earliest stages of corticogenesis. However, little is known about the establishment of the human motor cortex, despite being a common site of perinatal damage causing cerebral palsy. Affymetrix gene chip analysis of human neocortical tissue from 8-12.5 post-conceptional weeks (PCW) previously discovered genes expressed in gradients along the anterior-posterior human neocortex.

Aims: i) Identify putative anterior/posterior molecular determinants of the developing human neocortex. ii) Test the hypothesis that the anterior pole of the human neocortex as an early site of the developing motor cortex generating corticofugal neurones and understand their development. iii) Establish a human *in-vitro* regionalisation model and study potential regulatory mechanisms of some corticofugal neurone-related genes.

Results and Conclusion: Graded expression of some putative anterior/posterior markers was confirmed in the human neocortex by real-time PCR (8-12 PCW). Among them, the corticofugal neurone-related genes (transcription factor *CTIP2*, axon guidance molecule *ROBO1* and its downstream signalling molecule *SRGAP1*) were up-regulated anteriorly. Their spatiotemporal expression patterns were examined further by tissue *in-situ* hybridization and immunohistochemistry, and compared with other corticofugal neurone-related transcription factors that showed no/opposite expression gradients (FEZF2 and SOX5) and various laminar-enriched markers previously established in humans (ER81, TBR1, TBR2, GAP43 and Synaptophysin) or validated in the current project (SATB2 and NURR1). Layer V was shown to arise as early as 12 PCW in humans. Prominent medullary pyramids containing corticospinal fibres strongly expressed both ROBO1/SRGAP1 by 14-17 PCW, when a distinct ROBO1/SRGAP1-positive Layer V emerges. Co-expression of the three genes in anterior neocortex might mark the site of the emerging human motor cortex, which is the predominant origin of corticofugal neurones such as corticospinal/corticopontine projection neurones. Dissociated neocortical cell cultures were established from anteriorly-/posteriorly-derived foetal neocortex that maintained regional intrinsic molecular identities. This *in-vitro* model of regionalization allowed gene regulation study to be performed in which a preliminary investigation of fibroblast growth factor signalling in controlling the expression of corticofugal neurone-related genes was initiated.

Dedication

For my beloved and supportive grandparents,

parents, *Wing Kee Ip* and *Marita Wai Yu Ng*,

and my brother, *Brian Pui Lam Ip*.

Acknowledgements

I am sincerely grateful to Dr. Gavin Clowry and Professor Susan Lindsay for their continued supervision, encouragement and support, and for allowing me to accomplish this work in their laboratories.

I owe my deepest gratitude to Dr. Nadhim Bayatti for his infinite help, guidance, and inspiration throughout my time of study. He has made available his support in a number of ways including the training of different laboratory techniques, advice on writing skills as well as the use of various computer software. The Affymetrix gene chip analysis presented here was performed by Dr. Nadhim Bayatti.

I would also like to thank members of our group and the Institute of Human Genetics, Dr. Steven Lisgo, Moira Crosier, Lynne Overman and Dr. YuZhu Cheng from the Human Developmental Biology Resource (HDBR), Dr. Subrot Sarma, Dr. Janet Kerwin, Dr. Demetrius Vouyiouklis, Dr. Nahidh Al-Jaberi, Charmaine Belinda George, Dr. Simon Fitch and Lisa Hodgson for their continuous technical support, advice and discussion. The human embryonic and foetal materials were collected and processed by members of the HDBR. Thanks to Dr. Simon Fitch for his assistance in real-time PCR and Lisa Hodgson for helping with confocal microscopy.

Thanks to Professor Zoltan Molnar, Dr. Anna Hoerder-Suabedissen and Dr. Wei Zhi Wang from University of Oxford for their generous gift of the NURR1 antibody used in this study and the interesting discussion on the development of subplate in rodents and humans.

Much appreciation is also given to the Anatomical Society of Great Britain and Ireland for funding this research studentship.

Table of Contents

List of Figures

List of Tables

Abbreviations

aa	Amino acids
ANK2	Ankyrin 2
ANOVA	Analysis of variance
ANR	Anterior neural ridge
ARHGAP4	Rho GTPase-activating protein 4
ARRDC3	Arrestin domain-containing 3
Ascl1	Achaete-scute complex homolog 1 (Murine)
BLAST	Basic Local Alignment Search Tool
Bmp2/4/5/7	Bone morphogenetic protein 2/4/5/7
bp	Base pairs
BrdU	Bromodeoxyuridine (5-bromo-2-deoxyuridine)
cAMP	Cyclic adenosine monophosphate
CAMs	Cell adhesion molecules
CBF1	C-promoter binding factor 1
cDNA	Complementary deoxyribonucleic acid
CGE	Caudal ganglionic eminence
CHGB	Chromogranin B / Secretogranin 1
CHL1	Close homolog of L1
cm^2	Centimetre-squared
CNTNAP2	Contactin-associated protein-like 2
CoP	Commissural plate
CouptfI/II	Chicken ovalbumin upstream promoter transcription factor I/II
CP	Cortical plate
CR	Calretinin
CREB	Cyclic adenosine monophosphate response element-binding

CS	Carnegie Stage
CSMN	Corticospinal motor neurones
CST	Corticospinal tract
Ct	Cycle threshold
Ctip2	Chicken ovalbumin upstream promoter transcription factor-interacting protein 2
Cux1/2	Cut-like homeobox 1/2
DAB	3, 3'-Diaminobenzidine
DAPI	4', 6-diamidino-2-phenylindole
DIG	Digoxigenin
DiI	1, 1-dioctadecyl-3, 3, 3', 3'-tetramethylindocarbocyanine perchlorate
DIV	Days *in-vitro*
dLGN	Dorsolateral geniculate nucleus
Dlx1/2	Distal-less homeobox 1/2
DPBS	Dulbecco's phosphate buffered saline
dTh	Dorsal-thalamic nuclei
DTT	Dithiothreitol
E(number)	Embryonic day
EDTA	Ethylene diamine tetra-acetic acid
Emx1/2	Empty spiracles homeobox 1/2
EphA2/4	Ephrin type-A receptor 2/4
Er81	E-twenty six (Ets) variant 1
ErbB4	Erythroblastic leukemia viral oncogene homolog 4
Erm	E-twenty six (Ets)-related molecule
EXOC4	Exocyst complex component 4
FACS	Fluorescence-activated cell sorting

FCS	Foetal calf serum
Fezf2	Forebrain embryonic zinc finger-like protein 2
Fgf2/8/15/17/18	Fibroblast growth factor 2/8/15/17/18
Fgfr1/2/3	Fibroblast growth factor receptor 1/2/3
Foxg1	Forkhead box G1
Foxp1/2	Forkhead box P1/2
FP	Forward primer
g	Gravitational force
GABA	Gamma-aminobutyric acid
Gad65	Glutamic acid decarboxylase 65 kDa isoform
GAP43	Growth-associated protein 43
GAPDH	Glyceraldehyde-3-phosphate dehydrogenase
GC-RMA	Gene Chip-Robust Multi-array Average
gDNA	Genomic deoxyribonucleic acid
GE	Ganglionic eminence
GFAP	Glial fibrillary acidic protein
GLAST	Astrocyte-specific glutamate transporter
GO	Gene Ontology
GRIA3	Glutamate receptor, ionotropic, AMPA 3
Grg1/4	Groucho-related gene 1/4
Gsh2	Glutathione synthetase homeobox 2
H & E	Haematoxylin and eosin
HASH1	Achaete-scute complex homolog 1 (Human)
HBSS	Hank’s balanced salt solution
HDBR	Human Developmental Biology Resource
HRP	Horseradish peroxidase
HSPGs	Heparin sulphate proteoglycans

ICC	Immunocytochemistry
IFL	Inner fibrous layer
Ig	Immunoglobulin
IGH	Immunoglobulin heavy chain variable region
IHC	Immunohistochemistry
INPs	Intermediate neuronal precursors
IPCs	Intermediate progenitor cells
ISH	*In-situ* hybridization
ISVZ	Inner subventricular zone
IZ	Intermediate zone
KCC2	K^+ Cl^- co-transporter 2
kDa	Kilodalton
KO	Knock-out
LDS	Lithium dodecyl sulfate
LGE	Lateral ganglionic eminence
Lhx6	LIM homeobox 6
LSD	Least significant difference
M	Molar
M1	Primary motor cortex
MAP2	Microtubule-associated protein 2
MAPK	Mitogen-activated protein kinase
MARs	Matrix attachment regions
Mash1	Achaete-scute complex homolog 1 (Murine)
MEM	Minimum essential medium
MGE	Medial ganglionic eminence
MTT	Methylthiazol tetrazolium
MZ	Marginal zone

n= (number)	Number of embryos/foetuses used
NAALADL2	N-acetylated alpha-linked acidic dipeptidase-like 2
NCBI	National Center for Biotechnology Information
NCOR2	Nuclear receptor co-repressor 2
NEK9	Never in mitosis gene A (NIMA)-related kinase 9
NeuroD	Neurogenic differentiation factor
Ngn1/2	Neurogenin 1/2
NIH	National Institute of Health
Nkx2.1	Nk2 homeobox 1
NPY	Neuropeptide Y
nr	Non-redundant protein sequences
NREC	Newcastle and North Tyneside Research Ethics Committee
Nrg1/3	Neuregulin 1/3
Nrp2	Neuropilin 2
NRQ	Normalized relative quantities
Nurr1	Nuclear receptor-related protein 1
Oct6/7	Octamer-binding transcription factor 6/7
OSVZ	Outer subventricular zone
Otx1	Orthodenticle homeobox 1
$p\leq$	Probability
P(number)	Postnatal day
Pax6	Paired-box 6
PBS-T	Triton X-100 / phosphate buffered saline
PCDH17	Protocadherin 17
PCW	Post-conceptional weeks
Pea3	Polyomavirus enhancer activator 3
PFA	Paraformaldehyde

PI3	Phosphatidylinositol-3
PKC	Protein kinase C
PLCγ	Phospholipase Cγ
PlxnB2	Plexin receptor B2
POA	Preoptic area
PP	Preplate
PSB	Pallial-subpallial boundary
PV	Parvalbumin
RC2	Radial glial cell marker 2
RGCs	Radial glial cells
RNF13	Ring finger protein 13
Robo1/2/3	Roundabout 1/2/3
RORβ	Retinoic acid-related orphan receptor beta
RP	Reverse primer
RREB1	Ras responsive element binding protein 1
rtPCR	Real-time polymerase chain reaction
S1	Primary somatosensory cortex
S100A10	S100 calcium binding protein A10
Satb2	Special AT-rich sequence-binding protein 2
SDHA	Succinate dehydrogenase complex subunit A
SDS-PAGE	Sodium dodecyl sulphate polyacrylamide gel electrophoresis
S.E.M.	Standard error of mean
Sema3F	Semaphorin 3F
Sfrp2	Secreted frizzled-related protein 2
SG	Subpial granular layer
Shh	Sonic hedgehog
siRNA	RNA interference

SNPs	Short neural precursors
Sox2/5	Sex determining region Y (SRY)-box 2/5
SP	Subplate
Sp8	Specificity protein 8
SPARC	Secreted protein acidic and rich in cysteine (Osteonectin)
Spry1/2	Sprouty 1/2
SRGAP1/2	SLIT-ROBO Rho GTPase activating protein 1/2
SSC	Sodium citrate
SST	Somatostatin
Svet1	Subventricular expressed transcript 1
SVZ	Subventricular zone
Tbr1/2	T-box brain 1/2
TBS	Tris-based buffer
Tgfα	Transforming Growth Factor alpha
Tle1/4	Transducin-like enhancer of split 1/4
Tlx	T-cell leukemia homeobox
TMS	Transcranial magnetic stimulation
U	Units
UTR	Untranslated region
V	Volt
vGlut1/2	Vesicular glutamate transporter 1-2
V1	Primary visual cortex
VB	Ventrobasal complex
VIP	Vasointestinal peptide
VL	Ventrolateral nucleus
VZ	Ventricular zone
WDR81	WD repeat domain 81

Wnt2b/3a/5b/7a/8b	Wingless 2b/3a/5b/7a/8b
ZFYVE1	Zinc finger FYVE domain-containing protein 1
µg	Microgram
µl	Microlitre
µm	Micrometer
µM	Micromolar
mA	Milliamps
ml	Millilitre
mM	Millimolar
mm	Millimetre
ng	Nanogram
nm	Nanometre
ρmol	Picomole

Gene Nomenclature

Species	Gene Symbol	Protein Symbol
Homo sapiens	*SATB2*	SATB2
Mus musculus *Rattus norvegicus*	*Satb2*	Satb2
Drosophila melanogaster *Xenopus laevis*	*satb2*	satb2

Table 0.1. Gene and protein symbol conventions.

Special AT-rich sequence-binding protein 2 (SATB2) is used as an example. Gene symbols are in italics and protein symbols are in normal fonts. Human (*Homo sapiens*) gene/protein symbols are capitalized. The first letter of rodent (*Mus musculus*, *Rattus norvegicus*) gene/protein symbols are capitalized followed by small letters. The gene/protein symbols for invertebrates described in this thesis (*Drosophila melanogaster*, *Xenopus laevis*) are all in small letters.

Chapter 1 Introduction

1.1 Corticogenesis in the Neocortex

The mammalian neocortex is a highly differentiated structure which arises from the dorsal telencephalon, and thus is also known as the dorsal pallium. Neocortical neurogenesis is initiated in anterolateral domains and it progresses posteromedially (McSherry and Smart, 1986), accounting for the uneven thickness of the neocortex along these tangential axes. During development, the neocortex differentiates radially from a morphologically uniform structure into a six-layered cortex, with neurones and glia arising at different developmental stages. Two main types of neurones are found in the mature neocortex: 20-30% are interneurones (non-pyramidal) and 70-80% are projection (pyramidal) neurones.

1.1.1 GABAergic Interneurones of the Neocortex

Classification of Neocortical Interneurones

The majority of the neocortical interneurones are inhibitory and utilize gamma-aminobutyric acid (GABA) as a neurotransmitter (Marin and Rubenstein, 2001). Neocortical interneurones can be subdivided on the basis of different properties, such as morphology, electrophysiology, ion channels composition and molecular profile (Markram et al., 2004). They are located in different layers and form multiple synaptic connections primarily with pyramidal projection neurones to strategically control their neuronal activities (Markram et al., 2004). A recent review has outlined the conservative grouping of mice neocortical interneurones into four major classes: i) fast-spiking, Parvalbumin (PV)-expressing basket and chandelier cells, ii) intrinsically burst-spiking or adapting non-fast-spiking, Somatostatin (SST)-expressing Martinotti cells with the majority of them extend their long axons into the neocortical Layer I (marginal zone, MZ), iii) rapidly adapting, Calretinin (CR)- and/or Vasointestinal peptide (VIP)-expressing bipolar or double-bouquet cells, and iv) rapidly adapting, Neuropeptide Y

(NPY)- and/or Reelin-expressing (but not SST) multipolar interneurones (Figure 1.1; (Gelman and Marin, 2010)). These neocortical interneurone subtypes are found to be largely in common between different mammalian species, however some subtypes in humans and non-human primates, such as the double bouquet cells (DeFelipe et al., 2006; Yanez et al., 2005) or interneurones of the preplate (PP)/MZ exhibit more elaborate morphology and distribution (Bystron et al., 2008; Meyer, 2007; Rakic and Zecevic, 2003).

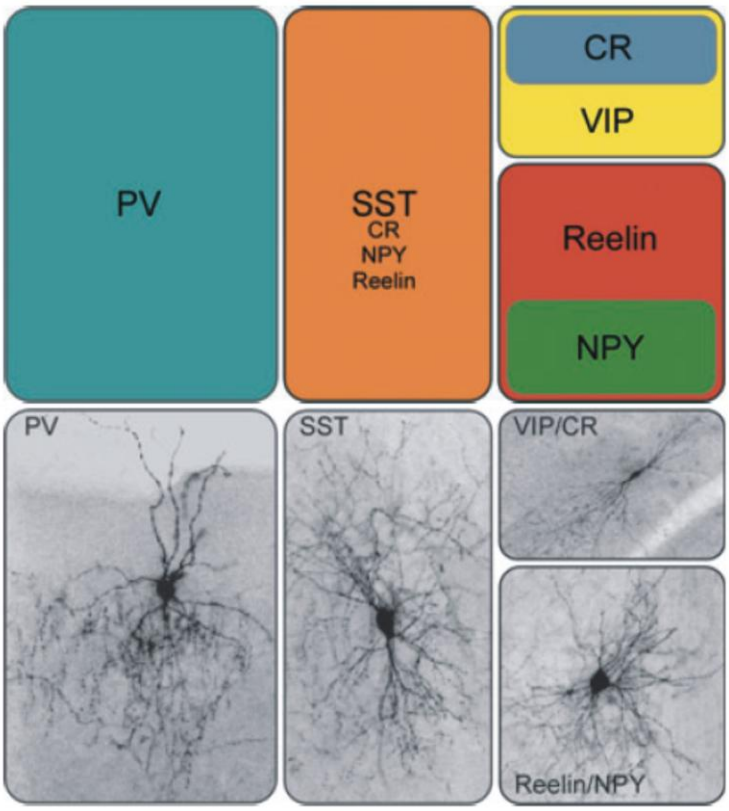

Figure 1.1. Cortical interneurone subtypes in mice neocortex.

There are four major groups of neocortical interneurones identified in the mouse neocortex: i) fast-spiking, Parvalbumin (PV)-expressing basket and chandelier cells; ii) intrinsically burst-spiking or adapting non-fast-spiking, Somatostatin (SST)-expressing Martinotti cells, which can be further subdivided by Reelin, Calretinin (CR) and/or Neuropeptide Y (NPY) expression; iii) rapidly adapting, CR- and/or Vasointestinal peptide (VIP)-expressing bipolar or double-bouquet cells; and iv) rapidly adapting, Reelin- and/or NPY-expressing (but not SST) multipolar interneurones. Adapted from (Gelman and Marin, 2010).

Origin and Migration of Neocortical Interneurones

In rodents, nearly all the neocortical interneurones are generated in the proliferative regions of the subpallial telencephalon, including the medial ganglionic eminence (MGE; 50-60%), caudal ganglionic eminence (CGE; 30-40%) and preoptic area (POA; 8-10%) predominantly, and to a lesser extent, the lateral ganglionic eminence (LGE), and septum (at E11 in mice), and migrate tangentially into different regions of the developing brain including the neocortex and olfactory bulb later in the development (at E13 and E15 in mice) (Gelman and Marin, 2010; Marin and Rubenstein, 2001). The interneurones migrate tangentially into the neocortex along different routes as neocortical layers are sequentially formed (described in Section 1.1.2): briefly, during early neurogenesis the interneurones enter the neocortex via the PP; while during mid stages of neurogenesis, they travel through the intermediate zone (IZ) and MZ; and during late stages they migrate mainly through the lower IZ/subventricular zone (SVZ), subplate (SP) and MZ (Metin et al., 2006).

In general, fate-mapping analyses in mice (Gelman and Marin, 2010; Miyoshi et al., 2010; Gelman et al., 2009; Wonders and Anderson, 2006) have shown that:

1) PV-containing neocortical interneurones are produced predominantly from the ventral MGE.
2) SST-containing neocortical interneurones are derived from the dorsal MGE with some of them also co-expressing Reelin, NPY and/or CR.
3) CGE on the other hand is the source of interneurones that express primarily CR (but not SST or PV) and/or VIP.
4) An additional population of interneurones derived from CGE express Reelin with some of them co-expressing NPY.
5) POA is recently identified as a source of neocortical interneurones, and is believed to generate interneurones with molecular profiles similar to MGE- (PV-, SST-expressing) and CGE- (NYP- and/or Reelin-expressing) derived interneurones.

6) The dorsal LGE generates interneurones that migrate towards the olfactory bulb expressing CR, while the ventral LGE and septum produce some unknown populations of neocortical interneurones.

However evolutionary changes have been observed in humans (Letinic et al., 2002) and in non-human primates (Petanjek et al., 2009b; Petanjek et al., 2009a). The major sources of neocortical interneurones are the germinal layers of the neocortex: ventricular zone (VZ) and SVZ, and the proportion of the subpallium-derived neocortical interneurones decreases (Figure 1.2; (Petanjek et al., 2008)). Ganglionic eminence (GE)-derived interneurones also migrate through the IZ and SVZ within the neocortex as observed in rodents, nevertheless both GE- and neocortical-derived interneurones eventually populate the neocortical layers II-VI arise from the cortical plate (CP) (Petanjek et al., 2009b; Petanjek et al., 2009a). A recent study has identified the origins of different interneurones subtypes in brain tissues obtained from human foetuses or infants suffered from holoprosencephaly with severe striatal hypoplasia and revealed changes of expression of neocortical GABAergic interneurone markers (Fertuzinhos et al., 2009). As a subset of NPY- and SST-expressing neocortical interneurones are shown to be significantly reduced or absent due to striatal hypoplasia, the authors suggest these neurones are of subpallial origin; whereas the unaffected interneurones containing CR are generated locally (Fertuzinhos et al., 2009).

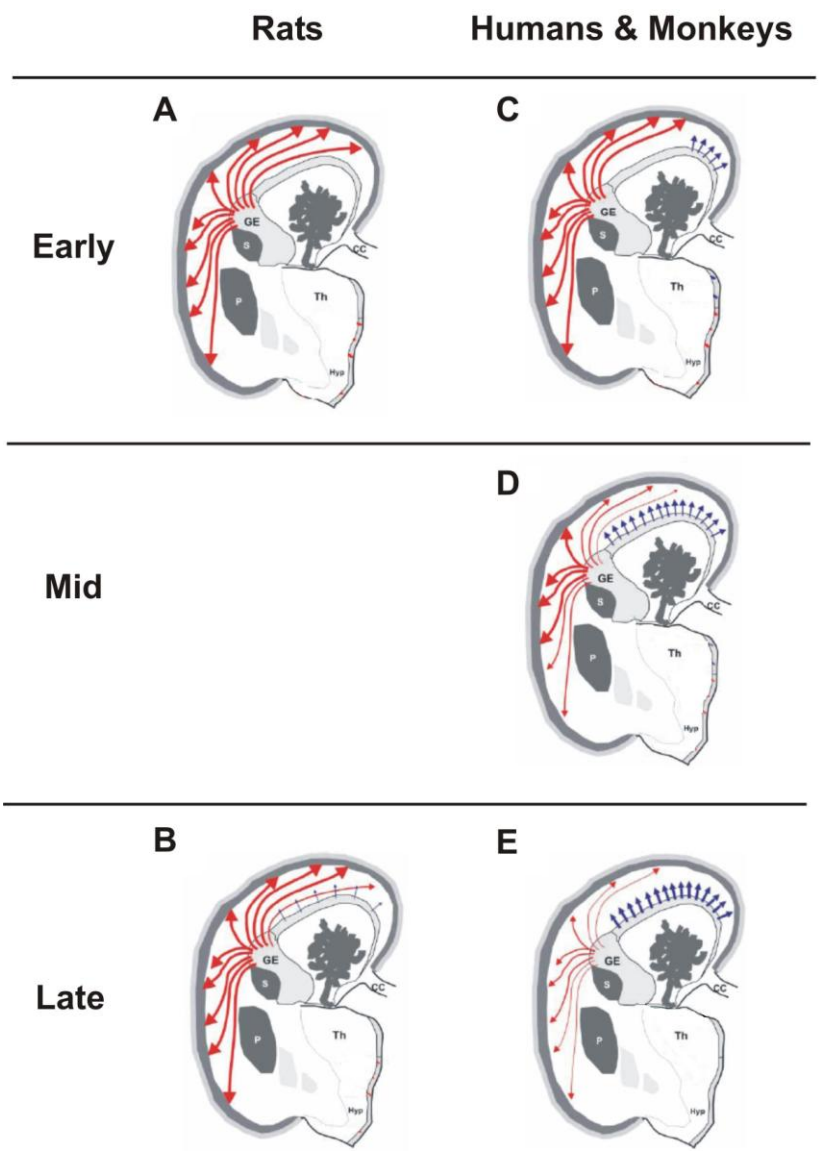

Figure 1.2. Origins of neocortical interneurones.

Schematic diagrams showing developmental changes of origins of rat, monkey and human neocortical interneurones presented on schematized coronal sections of human brains of 14 gestational weeks at an anterior level in the presence of ganglionic eminence (GE), thalamus (Th), hypothalamus (Hyp), caudate nucleus (S), putamen (P) and corpus callosum (CC). During early neurogenesis, nearly all neocortical interneurones are generated in the GE which have migrated tangentially into the developing rat neocortex (red arrows, A). In humans and monkeys, some radially migrating neocortical interneurones begin to be derived in the proliferative zones of the most dorsal part of the neocortex (blue arrows, C), and gradually increases throughout the developing neocortex as development progresses (blue arrows, D, E). Meanwhile, the proportion of GE-derived neocortical interneurones is decreasing (red arrows, D, E). During late stages of neurogenesis in rats, a small population of neocortical interneurones is also found to be produced locally in the proliferative zones of the neocortex (blue arrows, B). Adapted and modified from (Petanjek et al., 2008).

GABAergic interneurone fate and localization (pallium vs. subpallium; LGE vs. MGE vs. CGE) are regulated by various transcription factor genes expressed by their progenitors locating in these different domains. Briefly, studies in rodents have identified *Paired-box 6* (*Pax6*) and *Glutathione synthetase homeobox 2* (*Gsh2*) having opposing effects in order to specify progenitors in the pallium and subpallium into becoming projection neurones or interneurones respectively (Yun et al., 2001; Toresson et al., 2000). Together they are expressed in an over-lapping pattern by progenitors in the dorsal LGE during early neurogenesis, marking out the boundary between dorsal LGE and MGE (Yun et al., 2001; Stoykova et al., 2000; Toresson et al., 2000).

Within the MGE, *Nk2 homeobox 1* (*Nkx2.1*) specifies progenitors into adopting the MGE fate whereby their progenies migrate towards the globus pallidus (mantle zone of MGE), instead of adopting the LGE fate towards the striatum (mantle zone of LGE) (Sussel et al., 1999). A study which transplanted GFP-positive MGE cells into host embryos to map the fate of these cells postnatally from distinct domains of the MGE elegantly demonstrated that the two major neocortical (PV- and SST-expressing) interneurones are generated by progenitors residing in different MGE domains, thus providing evidence for the existence of distinct progenitor pools within the MGE (Flames et al., 2007).

The CGE is considered as the caudal extension of LGE and MGE that fuse together and is distinguishable on coronal sections in the presence of mid- to caudal-diencephalic structures. Thus the dorsal domain of CGE strongly expresses *Gsh2*, similar to the dorsal LGE, whereas the ventral domain of CGE expresses *Nkx2.1*, as observed in the MGE (Wonders and Anderson, 2006). Interestingly, recent transcriptomic analyses of the CGE have revealed progenitor domains with unique molecular profiles distinct from those found in the LGE and MGE (Willi-Monnerat et al., 2008). *Chicken ovalbumin upstream promoter transcription factor II* (*CouptfII*) is found to be highly expressed by progenitor cells within the CGE and involved in mediating the migration of interneurones into the neocortex via the caudal migratory stream (Kanatani et al., 2008).

In all the domains of the ganglionic eminence, GABAergic phenotypic specification of progenitors is controlled by *Achaete-scute complex homolog 1* (*Ascl1*/*Mash1*) and *Distal-less homeobox 1/2* gene (*Dlx1/2*) as they regulate the expression of the GABA synthesizing enzyme, Glutamic acid decarboxylase (Gad) (Stuhmer et al., 2002; Fode et al., 2000; Casarosa et al., 1999). As these progenitors exit the cell cycle, the post-mitotic interneurones either migrate towards the mantle zone of the subpallium or the neocortex. Semaphorin 3F (Sema3F)/Neuropilin 2 (Nrp2) (Marin et al., 2001) and Slit1 and -2/Roundabout 1 and -2 (Robo1 and -2) (Andrews et al., 2008; Andrews et al., 2007; Wichterle et al., 2003) are two repulsive mechanisms mediating the migration of MGE-derived neocortical interneurones to prevent them from entering the mantle zone of the subpallium; while Neuregulin 1 (Nrg1)/Erythroblastic leukemia viral oncogene homolog 4 (ErbB4) mediates the attraction of neocortical interneurones migrating towards the developing neocortex (Flames et al., 2004). During the migration towards the mantle zone of the subpallium or the neocortex, changes of gene expression are detected. One example is the expression of *LIM homeobox 6* (*Lhx6*), a downstream gene of *Nkx2.1*, by the MGE-derived post-mitotic interneurones in the mantle zone of MGE and the neocortex (Lavdas et al., 1999; Grigoriou et al., 1998). *Lhx6* is important for the differentiation and migration of MGE-derived interneurones, as these neurones do not express PV or SST and fail to migrate to their appropriate target layers in the neocortex in the absence of *Lhx6* (Zhao et al., 2008; Liodis et al., 2007). In contrast, *Nkx2.1* expression is down-regulated in post-mitotic interneurones before entering the neocortex (Marin et al., 2001). This down-regulation of *Nkx2.1* is paralleled by the up-regulation of *Nrp2* expression in neocortical, migrating interneurones in order to avoid the developing striatum (Nobrega-Pereira et al., 2008). On the contrary, *Nkx2.1* expression is maintained in post-mitotic interneurones entering the striatum, thus repressing *Nrp2* expression and rendering the interneurones insensitive to Sema3F (Nobrega-Pereira et al., 2008).

Changes in the molecular profiles of neocortical interneurones during development are also observed in humans as well as non-human primates. This may be useful to identify pallial vs. subpallial origins of neocortical interneurones. In humans, MASH1 is expressed by progenitors in the GE, but in both humans and rodents, MASH1/Mash1 is absent in DLX1/2/Dlx1/2-positive post-mitotic interneurones migrating away from the proliferative zone of GE (Figure 1.3; (Letinic et al., 2002)). On the other hand, MASH1

expression is maintained in post-mitotic interneurones derived from VZ/SVZ of the neocortex, and is probably involved in up-regulating the expression of *DLX* genes to induce the GABAergic phenotype (Figure 1.3; (Letinic et al., 2002)). Similar changes of gene expression were also observed in non-human primates in which *Mash1* expression is detected in *Gad65*-positive neurones originating from the pallial proliferative zones but not in those generated from the subpallium (Petanjek et al., 2009a). Another human-specific feature observed is the expression of *NKX2.1*/NKX2.1 mRNA and protein in the proliferative zones as well as the post-mitotic layers of the neocortex from 6-22 post-conceptional weeks (PCW), whereas in rodents *Nkx2.1* is not expressed in the neocortex (Rakic and Zecevic, 2003).

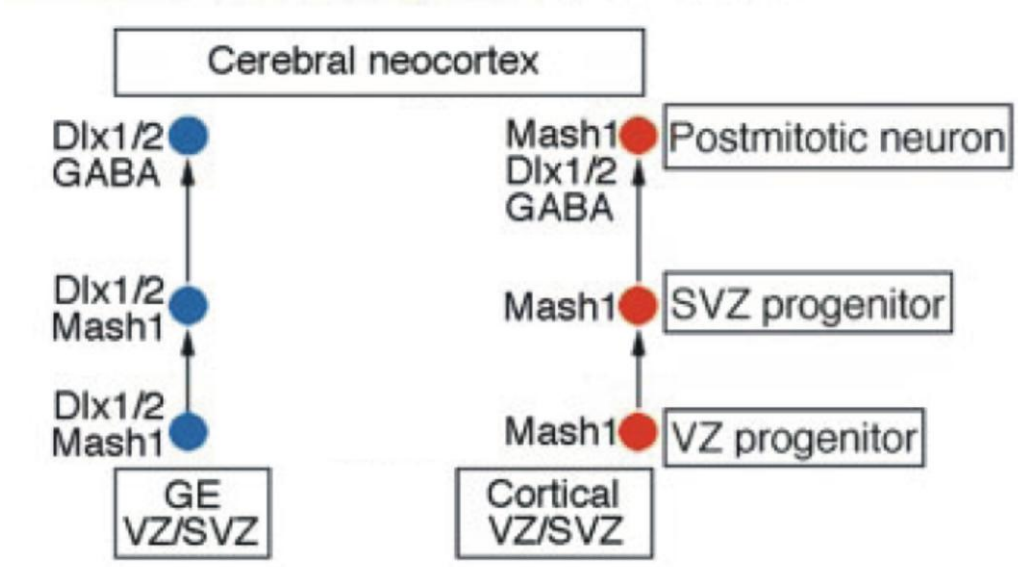

Figure 1.3. Neocortical GABAergic interneurones originating in the ganglionic eminence and neocortex.

The schematic diagram illustrates the molecular profiles of GABAergic interneurones that are generated from progenitors residing in either the ganglionic eminence (GE; blue), or the neocortical ventricular zone/subventricular zone (VZ/SVZ; red). The progenitors in the proliferative zones of the GE express MASH1 that induces the expression of DLX1/2 and then GABA in progenitors as well as post-mitotic interneurones as they migrate tangentially to reach the neocortex. MASH1 expression is down-regulated during differentiation and migration. The progenitors in the proliferative zones of the neocortex express MASH1, which continues to be expressed by migrating post-mitotic interneurones to induce the expression DLX1/2 and GABA. Adapted and modified from (Letinic et al., 2002).

1.1.2 Glutamatergic Projection Neurones of the Neocortex

Origin of Neocortical Projection Neurones

In contrast to neocortical interneurones, neocortical projection neurones are excitatory, utilizing glutamate as their neurotransmitter. Neocortical projection neurones are generated locally from progenitors in the neocortical proliferative zones (VZ/SVZ). As suggested by the radial unit hypothesis, "after progenitors have completed their proliferative cell divisions, post-mitotic projection neurones migrate along a common pathway radially to the developing CP to form ontogenetic columns" (Rakic et al., 2009). Each of the ontogenetic columns in the developing CP contains polyclonal post-mitotic neurones (i.e. they arise from different progenitors) and an inside-out generation sequence is observed (Rakic et al., 2009). Note that ontogenetic columns are different from functional columns which refer to groups of neurones subserving particular functions later e.g. neurones in barrel fields that respond to the same receptive field (Rakic et al., 2009). Nevertheless, each functional column comprises of several ontogenetic columns that originate from adjacent proliferative units in the VZ (Rakic et al., 2009).

The rodent and human VZ maintains its thickness and homogeneous appearance throughout corticogenesis, however it contains a heterogeneous population of progenitors. Two morphologically and molecularly distinctive neocortical progenitors have been identified in rodents, the radial glial cells (RGCs) (Pinto et al., 2008; Anthony et al., 2004; Noctor et al., 2002; Hartfuss et al., 2001; Miyata et al., 2001; Noctor et al., 2001) and short neural precursors (SNPs) (Mizutani et al., 2007; Gal et al., 2006), that divide at the apical surface and undertake interkinetic nuclear migration (the apical-basal movement of nuclei) during G1 and G2 phases of their cell cycles (Dehay and Kennedy, 2007). Recent study has discovered the importance of gap junctions/hemichannels in modulating the interkinetic nuclear migration, as gap junction/hemichannel-dependent calcium waves are detected in these progenitors in the VZ, and blockade of gap junctions/hemichannels affects the dynamics of the migration (Liu et al., 2010). Radial glial cell marker 2 (RC2)- and Astrocyte-specific glutamate transporter (GLAST)-expressing RGCs extend their basal fibres towards the pial

surface, spanning the entire thickness of the neocortex throughout mitotic division which is essential for proper radial migration of post-mitotic neurones (Gal et al., 2006). α-Tubulin 1-expressing SNPs on the other hand are anchored by ventricular end feet and have a short basal process that is retracted during mitotic division (Gal et al., 2006). Both RGCs and SNPs are confirmed as VZ progenitors as they express Pax6, which is important for neuronal fate specification, and confined to the VZ in rodents (Stancik et al., 2010; Heins et al., 2002). In contrast, they also reside in the human SVZ as revealed by presence of PAX6 expression in this layer during early corticogenesis, thus SVZ may be a source of additional PAX6-expressing progenitors (Fietz et al., 2010; Hansen et al., 2010; Bayatti et al., 2008a).

As corticogenesis progresses, mitotic activities take place at the basal surface of the VZ resulting in the gradual formation of the SVZ, where interkinetic nuclear migration is not detected (Dehay and Kennedy, 2007). Here in the SVZ, a third type of neocortical progenitor is found, known as basal progenitors or intermediate progenitor cells (IPCs) or intermediate neuronal precursors (INPs, to be used throughout the thesis), these cells are generated from RGCs (Englund et al., 2005; Noctor et al., 2004). INPs reside within the SVZ expressing T-box brain 2 (Tbr2) (Englund et al., 2005; Noctor et al., 2004) with a small proportion shown to divide at the ventricular surface (Kowalczyk et al., 2009; Noctor et al., 2008). Although these small number of Tbr2-positive cells dividing at the ventricular surface show similar morphologies to SNPs, they do not co-express α–Tubulin 1, indicating INPs are distinct from SNPs (Stancik et al., 2010). Unlike the thin rodent SVZ which constitutes only a few layers of cells (Martinez-Cerdeno et al., 2006), the human and non-human primate SVZ expands significantly and separate into an inner (ISVZ) and outer (OSVZ) layer by a cell-poor/fibre-rich inner fibrous layer (IFL) during the mid stage of gestation (Bayatti et al., 2008a; Smart et al., 2002). As observed in rodents, TBR2-expressing INPs are found in the ferret and human SVZ, mostly in the ISVZ and also diffusely in the OSVZ and VZ (Fietz et al., 2010; Hansen et al., 2010; Bayatti et al., 2008a). Recently, a fourth type of progenitor was identified via 1, 1-dioctadecyl-3, 3, 3', 3'-tetramethylindocarbocyanine perchlorate (DiI) tracing from the pial surface along their long basal processes into the elaborate human OSVZ as well as the ferret SVZ, namely the radial glia-like cells that express RGCs markers, Sex determining region Y (SRY)-box 2 (SOX2), PAX6 and Glial fibrillary acidic protein (GFAP) but lack apical contact with the ventricular surface (Fietz et al., 2010; Hansen et

al., 2010). In contrast to the interkinetic nuclear migration of VZ RGCs, the OSVZ radial glial-like cells exhibit mitotic somal translocation in which the nucleus moves rapidly up the basal fibre before cell division (Fietz et al., 2010; Hansen et al., 2010).

Different modes of division have been observed among the four types of progenitors: RGCs are able to divide symmetrically for self-renewal and asymmetrically for neurogenic differentiation to produce immature neurones as well as other neuronal precursor cells SNPs and INPs, thus contributing more extensively to laminar expansion by generating neurones for multiple layers over a longer period of time; SNPs are neuronal-committed precursor cells that undergo differentiative division to produce immature neurones, hence producing distinct neuronal populations over a shorter period of time as compared to RGCs; most INPs divide symmetrically to generate two immature neurones with a small population undergo asymmetrical division to produce one INP and one immature neurone (Stancik et al., 2010; Dehay and Kennedy, 2007); OSVZ radial glia-like cells often divide asymmetrically to produce two morphologically different daughter cells that both are able to proliferate before differentiation (Fietz et al., 2010; Hansen et al., 2010). The upper daughter cells that inherited the basal processes and some of the bipolar lower daughter cells continue to express SOX2 and are able to further proliferate, expanding the progenitor pool; other bipolar lower daughter cells are able to differentiate and become glutamatergic and GABAergic neuronal precursors expressing TBR2 or ASCL1 (also known as MASH1) (Hansen et al., 2010). Figure 1.4 summarizes the differential division of these neocortical progenitor cells during development (Fietz et al., 2010; Hansen et al., 2010; Stancik et al., 2010; Dehay and Kennedy, 2007).

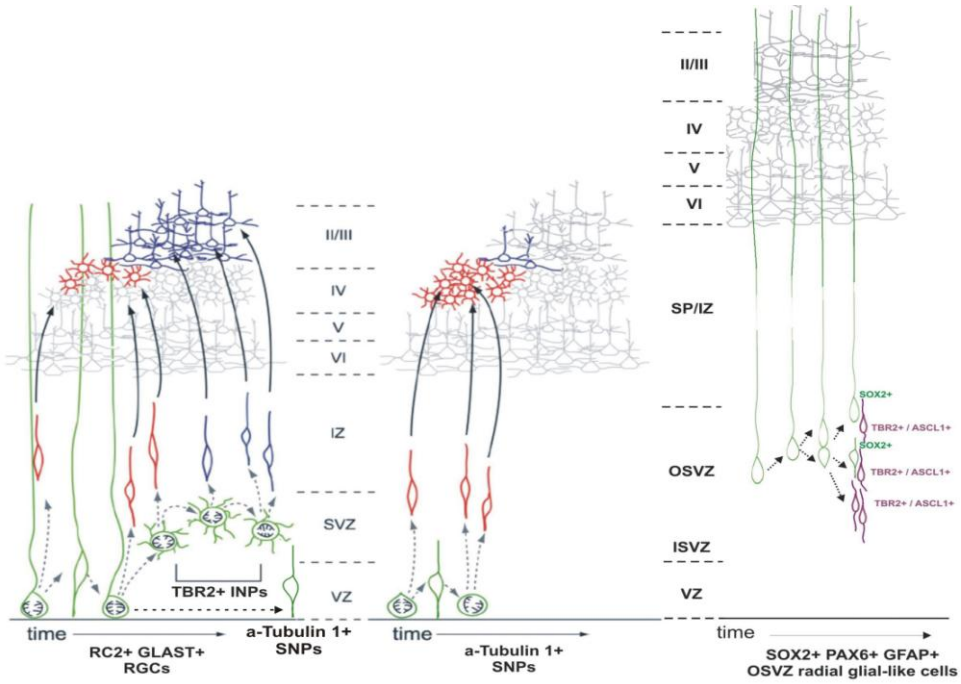

Figure 1.4. Differential division of neocortical progenitor cells during development.

Within the VZ, the RC- and GLAST-expressing radial glial cells (RGCs) extend long basal fibres towards the pial surface, undergo interkinetic nuclear migration and divide asymmetrically to produce immature neurones (red), TBR2-positive intermediate neuronal progenitors (INPs) and α–Tubulin 1-positive short neural precursors (SNPs), thus generating neurones for multiple laminae over an extended period of time. The SNPs possessing a short basal process and ventricular end foot also undergo interkinetic nuclear migration and give rise to immature neurones (red) primarily, thus supplying discrete neuronal population over a shorter period of time as compared to RGCs. Within the SVZ, INPs do not undergo interkinetic nuclear migration but divide symmetrically to produce two immature neurones (blue) primarily or asymmetrically to generate one INP and one immature neurone (red or blue). As development progresses, the human SVZ is segregated into inner and an elaborate outer compartment, namely the ISVZ and OSVZ respectively. The SOX2-, PAX6- and GFAP-expressing radial glia-like cells, which project their basal fibres towards the pial surface but lack the apical fibres, populate the OSVZ. They undergo mitotic somal translocation and produce upper and lower daughter cells. After each round of cell division, the upper daughter cells always adopt the basal fibres and maintain a proliferative potential by continually expressing SOX2. The lower daughter cells however become bipolar in morphology which are able to either divide asymmetrically to generate an upper proliferating SOX2-positive cell and an lower neuronal-committed TBR2-/ASCL1-positive cell (purple), or symmetrically to generate two neuronal-committed TBR2-/ASCL1-positive cells (purple). Adapted and modified from (Fietz et al., 2010; Hansen et al., 2010; Stancik et al., 2010; Dehay and Kennedy, 2007).

The determination of proliferative vs. differentiative divisions of RGCs and INPs is believed to be controlled through the length of G1 phase of cell cycles, in which a longer G1 phase would promote differentiative divisions, while a shorter G1 phase would result in self-renewing proliferative divisions (Pilaz et al., 2009; Dehay and Kennedy, 2007). RGCs and SNPs have remarkably different cell cycle kinetics in which SNPs have a longer G1 phase compared to RGCs (Stancik et al., 2010). RGCs and SNPs also differ in terms of the effects of Notch signal transduction pathways. While Notch signalling inhibits differentiation of both RGCs and SNPs, RGCs but not SNPs signal through the canonical Notch effector C-promoter binding factor 1 (CBF1) to maintain their proliferative state (Mizutani et al., 2007). OSVZ radial glia-like cells also rely on Notch signalling to retain their proliferative potential in order to expand their population (Hansen et al., 2010). β3-Integrin receptors are found to be expressed along the basal process of ferret OSVZ radial glia-like cells, and their blockade has led to a reduction of these OSVZ radial glia-like cells in ferret slice cultures, proving the importance of retention of the basal process for self-renewal via this type of receptors (Fietz et al., 2010). Furthermore, transgenic mice with a *fibroblast growth factor receptor 3* (*Fgfr3*) kinase domain mutation displayed increased proliferation in progenitors via activation of the mitogen-activated protein kinase (MAPK) pathway (Thomson et al., 2007; Inglis-Broadgate et al., 2005) and Fgfr1, -2 and -3 signalling is shown to inhibit the differentiation of RGCs to INPs (Kang et al., 2009), whereas cyclin D2 induces the transition from RGCs to INPs (Glickstein et al., 2009). Another gene deemed to be a key cell cycle regulator with differential effects temporally and regionally is *T-cell leukemia homeobox* (*Tlx*) (Li et al., 2008; Roy et al., 2004). In the absence of *Tlx*, expression of some cell cycle regulators such as p21 and cyclin D1 is affected (Li et al., 2008; Roy et al., 2004). Furthermore, the loss of *Tlx* has shortened the cell cycle length of early progenitor cells but prolonged the cell cycle length of late progenitor cells (temporal), eventually decreased the numbers of progenitor cells in the VZ posteriorly but throughout the entire anterior-posterior pole in the SVZ (regional) (Li et al., 2008; Roy et al., 2004). Tlx has also been shown recently to activate the canonical Wingless (Wnts)/β-catenin signalling pathway to stimulate adult mouse neural stem cell proliferation and self-renewal (Qu et al., 2010).

Before the onset of local neurogenesis, the first post-mitotic neurones that are believed to be unique to humans observed in the primordium of neocortex are known as the predecessor cells (Bystron et al., 2006). They have multiple origins including the basal telencephalon and migrate tangentially into the primordium of neocortex at around human Carnegie Stage (CS) 12, expressing β–Tubulin and TBR1 but not Reelin or DLX (Bystron et al., 2006). These cells have no axons but contain processes that project horizontally and attach to the pial surface of the neocortex, which potentially guide and trigger the commencement of local neurogenesis (Bystron et al., 2006). As neurogenesis begins, progenitor cells from VZ and SVZ migrate radially along radial glial fibres and differentiate into earlier born and later born projection neurones respectively in an inside-out fashion. The first neurones generated in the VZ start to aggregate superficially to form the PP (mouse E10.5-E12.5; human CS16-CS20), which subsequently segregates into the most superficial aspect of the neocortex, the MZ (Layer I) and SP, by the later-generated CP neurones (mouse E12.5-E13.5; human CS20-CS22) (O'Leary and Nakagawa, 2002; Meyer, 2001; Meyer et al., 2000). The PP neurones are also referred to as the pioneer neurones since they are the earliest neurones to be produced locally, and to differentiate into a heterogeneous population of neocortical cells including Cajal-Retzius cells, marginal zone cells and subplate cells, forming the earliest functional network via synaptic connections within the primitive neocortex (Super et al., 1998). However, other studies have argued that synaptic formation can only be detected after the formation of CP and cells in the PP communicate and show spontaneous oscillations (Kostovic and Judas, 2007). Tbr1 is expressed by PP neurones, regulating the partition of the PP, and is subsequently expressed in the SP and Layer VI of the developing CP (Hevner et al., 2001). The MZ (Layer I) contains several cell types, principally the Cajal-Retzius cells which secrete Reelin to guide the radial migration of post-mitotic neurones through the SP, displacing this layer away from the MZ and ensuring that neurones deposit gradually in an inside-out fashion in the CP (Rice and Curran, 2001). A smaller size of cell in the MZ is the marginal zone cell which is considered to be a local inhibitory interneurone expressing GABA (Super et al., 1998). Above the MZ, a transient layer of undifferentiated granular cells known as the subpial granular layer (SG) is a feature unique to human or non-human primate neocortex (Meyer, 2001). This layer is most prominent when maximal

neuronal migration into the CP occurs, during the mid-gestation period (Meyer, 2001). The migration of these cortical neurones requires guidance signals and defective migration and differentiation of Cajal-Retzius cells, GABAergic interneurones and projection neurones is observed in the absence the Plexin receptor B2 (PlxnB2) in mice (Hirschberg et al., 2010). In humans, a thin layer, termed pre-SP, is visible at 7-8 PCW (CS21-23) during the formation of the CP (Kostovic and Rakic, 1990). This layer begins to expand extensively after 13 PCW via detachment of the deep CP which merges with the pre-SP to form the proper SP, and contains branched neurites extended by immature pyramidal neurones at this age (Bayatti et al., 2008a; Kostovic and Rakic, 1990). During mid- to late-gestation, the elaborate SP contains GABAergic, glutamatergic and peptidergic neurones, synapses and thalamocortical afferents that are waiting and gathering in the superficial SP between 21 and 23 PCW before entering the CP after 22-24 PCW (Kostovic and Judas, 2007). A cell-sparse/fibre-rich layer termed the IZ is formed underneath the SP where axons of post-mitotic neurones are found during their migration to take up their laminar positions within the CP (O'Leary and Nakagawa, 2002). The formation of these transient layers of the developing neocortex in human is summarized in Figure 1.5 (Bystron et al., 2008).

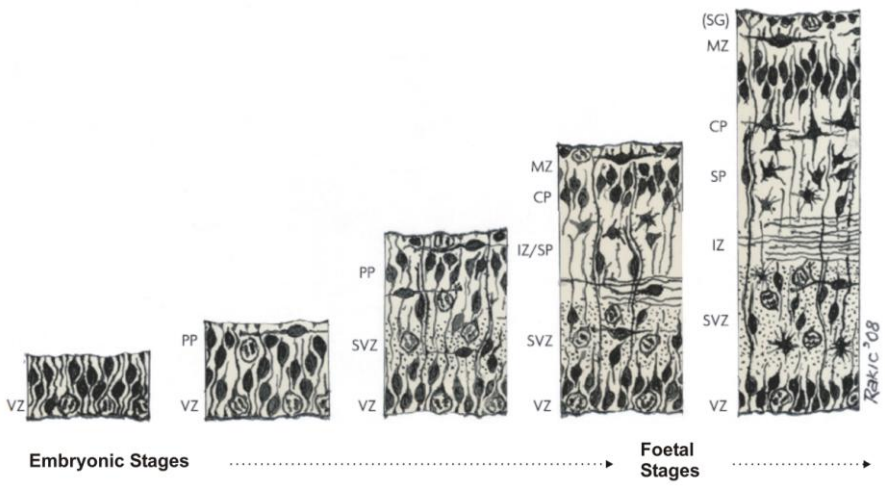

Figure 1.5. The formation of transient layers of the developing neocortex.

The Boulder Committee's summary diagram of neocortical development, revised in 2008 and depicting the sequential events during the formation of transient layers including the ventricular (VZ) and subventricular (SVZ), the preplate (PP), the intermediate zone (IZ), the subplate (SP) and the marginal zone (MZ). The human- or primate-specific subpial granular layer (SG) which forms part of the MZ is also illustrated in the diagram. Adapted and modified from (Bystron et al., 2008).

In summary, during different stages of neocortical development, progenitor cells originating from the neocortical proliferative zones have different cell cycle kinetics and unique molecule profiles contributing to the production of various populations of cortical neurones. Nevertheless, as they differentiate and migrate towards the post-mitotic layers radially, a sequential order of transcription factors expression across these transient layers of the developing neocortex is observed in rodents and in humans: *Pax6/PAX6* is expressed in the VZ by RGCs. Upon asymmetric division, a RGC directly produces an immature neurone at earlier stages. Alternatively, a RGC asymmetrically divides and indirectly produces immature neurones via generation and symmetric division of INPs at later stages that migrate away from the VZ into the SVZ. As the differentiation progresses *Pax6/PAX6* expression is lost and *Tbr2/TBR2* expression is detected in the SVZ. These cells continue to migrate through the IZ to the CP and differentiate into post-mitotic neurones, in which they sequentially express *neurogenic differentiation factor* (*NeuroD/NEUROD*) and *Tbr1/TBR1* in the IZ and CP. (Figure 1.6; (Bayatti et al., 2008b; Hevner et al., 2006)).

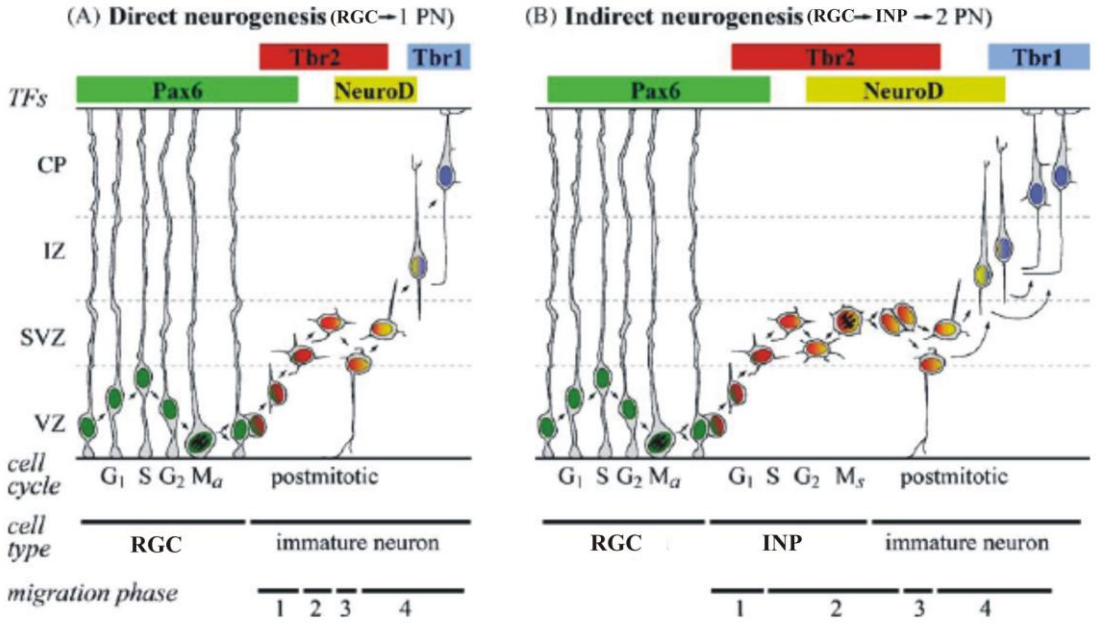

Figure 1.6. Production of cortical projection neurones and molecular profile of transient layers of the developing neocortex.

(A) During early stage of development, direct neurogenesis occurs in which a radial glia cell (RGC) divides asymmetrically to self-renew and produce one immature neurone directly that migrates towards the SVZ, IZ and eventually the developing CP. (B) During a later phase of development, indirect neurogenesis takes place whereby a RGC divides asymmetrically to self-replenish and produce one intermediate neuronal progenitor (INP) that migrate towards the SVZ. The INP undergoes symmetric division to differentiate into two immature neurones which migrate through the IZ until reaching the developing CP. (A, B) Nevertheless, a sequential order of gene expression was observed in these transient layers of the developing neocortex: Pax6 → Tbr2 → NeuroD → Tbr1, making them a useful molecular tool to mark out the different layers of the developing neocortex. Adapted and modified from (Hevner et al., 2006).

Classification of Neocortical Projection Neurones

Neocortical projection neurones are morphologically different and reside in different laminae of the six-layered neocortex that arise from the CP during development. Cellular staining of human mature neocortex has revealed some layer specific characteristics: Layer I, the outermost layer, contains the fewest cells; Layer II, the external granular layer, is highly populated by small granule cells; Layer III, the external pyramidal layer, harbours mostly medium-sized pyramidal cells; Layer IV, the internal granular layer, is compactly formed by small granule cells; Layer V, the internal pyramidal layer, houses pyramidal cells; and Layer VI, the multiform layer, is made up of various populations of cells (Kahle and Frotscher, 2002). As Layer IV is often referred as the granular layer, Layer II and III become collectively known as the supragranular layers, whereas Layer V and VI together are considered as the infragranular layers. These neurones in different laminae project their axons to different targets and in general: neurones in Layer II and III send axons to other neocortical areas ipsilaterally or contralaterally (callosally), forming corticocortical connections; whereas neurones in Layer V and VI extend axons to subcortical structures, forming ipsilateral corticostriatal, corticotectal, corticopontine and contralateral corticospinal projections from Layer V and corticothalamic projection from Layer VI (Molyneaux et al., 2007). Notice that within Layer V and VI, contralateral/callosal projection neurones are also found which are morphologically and electrophysiologically different from the subcerebral projection neurones residing in the Layer V and corticothalamic projection neurones in the Layer VI (Molyneaux et al., 2007; Molnar and Cheung, 2006). Neurones in Layer I and IV project axons intracortically, and in Layer IV neurones receive thalamocortical input (Molyneaux et al., 2007; Kahle and Frotscher, 2002). These major projection neurones subtypes are summarized in Figure 1.7 (Molyneaux et al., 2007). Their laminar identities and phenotypic projections are regulated by combinational expression of various transcription factors which will be described in the subsequent section.

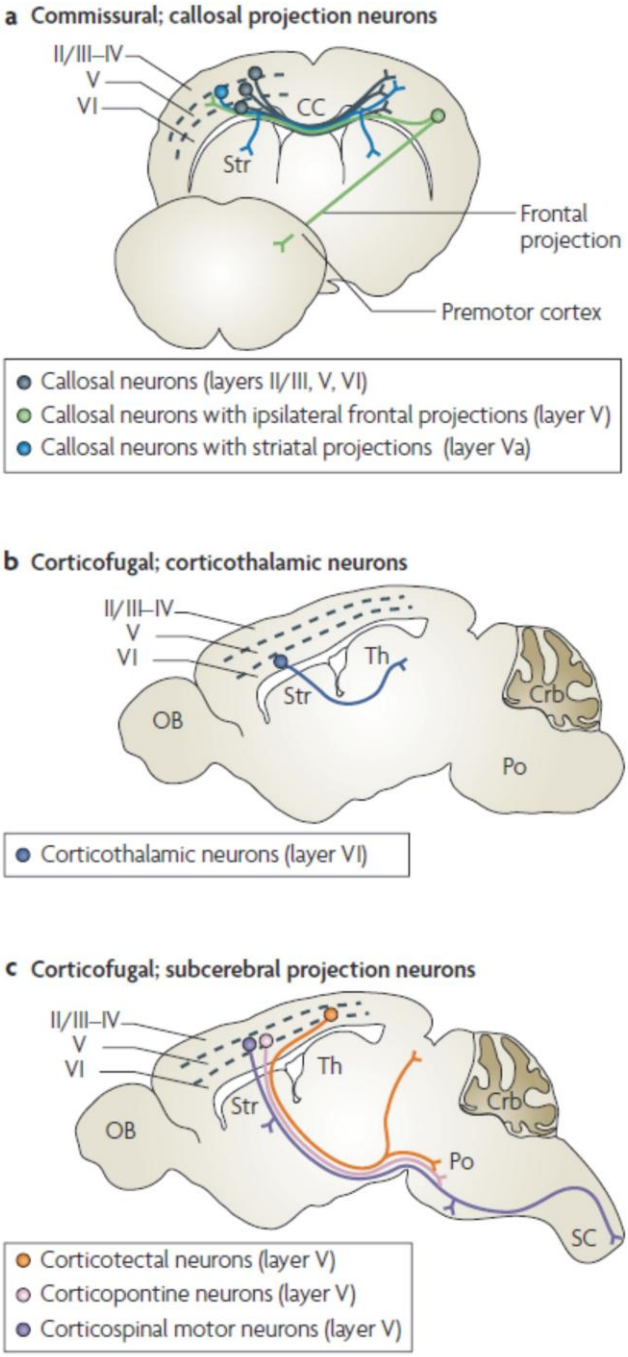

Figure 1.7. Major subtypes of projection neurones within the neocortex.

On the basis of their hodological properties, several principal subtypes of cortical projection neurones were classified: (a) The callosal projection neurones that send intracortical-interhemispheric axons are locating in Layer II/III, V and VI (grey). Within Layer V, there are two other callosal projection neurones: the contralateral corticocortical projections with ipsilateral/contralateral corticostriatal branches (blue); and contralateral corticocortical projections with ipsilateral frontal cortex branches (green). The corticothalamic neurones (b), a subtype of corticofugal projection neurones, are found in Layer VI (blue). Other Layer V corticofugal projection neurones (c) include corticotectal (orange), corticopontine (pink) and corticospinal motor (purple) neurones. Adapted from (Molyneaux et al., 2007).

The CP, which emerges at around CS22-CS23 in humans, has provided the neocortex with the six-layer characteristics, constituting different populations of projection neurones. The sequential production, distinct laminar and projection phenotypes of neocortical neurones are pre-determined by the intrinsic molecular profiles of their neocortical progenitors when they are born and can also be reflected in the post-mitotic projection neurones themselves. During the early stage of corticogenesis (mouse E12.5-E13.5) the glutamatergic code of early progenitors is programmed by two proneural genes, *Neurogenin 1* and *-2* (*Ngn1* and *-2*) that are expressed highly in the germinal zone of dorsal telencephalon and repressing the *Mash1*-regulating GABAergic programme (Fode et al., 2000). Furthermore, *Ngn2*$^{-/-}$ and *Ngn1*$^{-/-}$*2*$^{-/-}$ knock-out (KO) mice show abnormal glutamatergic phenotypes and molecular profiles of early born, deeper layer neurones in the CP (reduced expression of *Vesicular glutamate transporter 1, -2* (*vGlut1, -2*) and *Tbr1* in Layer VI and *E-twenty six (Ets) variant 1* (*Er81*) in Layer V) while late born, upper layer neurones (*Retinoic acid-related orphan receptor beta* (*RORβ)*-expressing Layer IV and *Octamer-binding transcription factor 6* (*Oct6*)- and *Cut-like homeobox 1* (*Cux1*)-expressing Layer II-IV) remain normal, thus suggesting *Ngn1* and *-2* are important in specifying glutamatergic fate of early born neocortical neurones (Schuurmans et al., 2004). On the other hand, the *Ngn*-independent mid and late phases of corticogenesis (E15.5 and E18.5) require *Pax6* and *Tlx* genes to function both independently and synergistically in the proliferative zone to specify the glutamatergic fate of late born, upper layer neurones (*RORβ*-expressing Layer IV and *Oct6*- and *Cux1*-expressing Layers II-IV) (Schuurmans et al., 2004).

The gene expression profiles of these upper and lower neocortical layers of the developing CP provide useful tools for marking out the boundaries between each layer. INPs within the SVZ generate post-mitotic neurones in superficial layers of the CP, and *Subventricular expressed transcript 1* (*Svet1*), *Cux1* and *-2* expression is initially observed in the SVZ and later in the upper layers II-IV from embryonic stages to adulthood (Cubelos et al., 2007; Nieto et al., 2004; Tarabykin et al., 2001). Transcriptional repressor gene *transducin-like enhancer of split 4* (*Tle4*) or *Groucho-related gene 4* (*Grg4*), a mammalian homologue of Drosophila *groucho 4* (*grg4*), is expressed in deeper layers while *Tle1 or Grg1* shows a complementary expression

pattern restricted to the superficial layers of the CP (Yao et al., 1998; Koop et al., 1996). Later on, *Forkhead box P2* (*Foxp2*) gene expression is observed restricted to Layer VI while the other family member, *Foxp1*, is expressing exclusively in the Layer III to V, although its expression seems to be increased in Layer VI postnatally (Ferland et al., 2003). In order to distinguish between Layer II, III and IV, expression of two POU domain transcription factor genes, *Oct6* and *Oct7* come into play since post-mitotic neurones of Layer III show co-expression of the two genes whereas post-mitotic neurones in Layer II and IV express either *Oct7* and *Oct6* genes respectively (Hevner et al., 2003). Two other transcription factors, *Er81* and *Orthodenticle homeobox 1* (*Otx1*), exhibit expression that is confined to Layer V. *Er81* expression is specific to deeper half of Layer V and *Otx1* is expressed superficially in Layer V (Hevner et al., 2003). More thorough and detailed lists of layer specific markers have been provided in reviews by Guillemot et al. (2006) and Molyneaux et al. (2007) (Molyneaux et al., 2007; Guillemot et al., 2006). Although molecular markers appear to be promising in mapping out different layers of the CP, one should be cautious when applying them and taking into account other factors that cause variation in gene expression such as species- and regional-specific differences within the neocortex.

As described previously, multiple types of projection neurones co-exist within each neocortical layer, particularly Layer V. On the other hand, certain types of projection neurone can be found in multiple layers, such as the callosal projection neurones. Nevertheless, with the use of retrograde labelling and fluorescence-activated cell sorting (FACS), these distinct projection neurone subtypes can be isolated for gene expression comparison at various stages of late embryonic and early postnatal murine development. This allows the identification of the combinatorial genetic codes potentially involved in the specification and/or differentiation of the corticospinal motor (CSMN)/callosal/corticotectal projection neurones by microarray analyses in various layers of the developing CP (Molyneaux et al., 2009; Arlotta et al., 2005).

Of the CSMN markers identified at various developmental stages, *Forebrain embryonic zinc finger-like protein 2* (*Fezf2*) and *Chicken ovalbumin upstream promoter transcription factor-interacting protein 2* (*Ctip2*) are found to be highly up-regulated in CSMN throughout their development and during early stages respectively (Arlotta et al., 2005) and have been studied the most. They are shown to be important in different

developmental aspects of subcerebral projection neurones including CSMN. *Fezf2* expression is initially detected in the developing neocortex as early as E8.5 in mice and gradually displays a low anterior to high posterior neocortical gradient by E10.5 (Hirata et al., 2004). By E15.5 in mice, *Fezf2* is expressed throughout the developing CP and its expression is enriched in Layer V and detected at lower level in Layer VI postnatally in mice and at 22 PCW in humans (Kwan et al., 2008; Arlotta et al., 2005; Molyneaux et al., 2005; Hirata et al., 2004). In the *Fezf2*$^{-/-}$ null mutant mice, subcerebral projection neurones including CSMN are not specified and are therefore lost in Layer V, as manifested by the absence of various CSMN markers despite normal migration and survival of Layer V neurones, while Layer VI appears to be expanded and disorganized with an abnormal molecular profile (Molyneaux et al., 2005). In addition, the differentiation of all subcerebral projection neurones including CSMN is defective as they have altered dendritic morphologies and fail to project their axons to appropriate subcortical targets beyond the thalamus, despite normal expression of major axon guidance molecules (Chen et al., 2008; Chen et al., 2005b; Chen et al., 2005a). *Fezf2* is shown to act as a cell fate switch between callosal and subcerebral projection neurones, evidently revealed by i) the transformation of most of the Layer V and VI neurones that normally express the CSMN marker Ctip2 into neurones expressing the callosal projection neurone marker special AT-rich sequence-binding protein 2 (Satb2) (genotype), and displaying electrophysiological profiles, morphologies and connections of callosal projection neurones (phenotype) in the absence of *Fezf2*; and ii) the induction of subcerebral projection neurone markers expression and phenotype in upper layer or heterotopic layer neurones where *Fezf2* is ectopically expressed (Chen et al., 2008; Chen et al., 2005b; Molyneaux et al., 2005).

Ctip2 is expressed predominantly by post-mitotic, subcortical projection neurones including CSMN in Layer V, at a lower level by corticothalamic projection neurones in Layer VI of the CP postnatally in mice (Lai et al., 2008; Arlotta et al., 2005) and in humans at 19 PCW (Johnson et al., 2009), regulating the post-mitotic differentiation of CSMN including axons outgrowth, pathfinding and/or survival (Arlotta et al., 2005). Additionally, ectopic expression of *Ctip2* in upper layer neurones induces subcerebral axonal targeting (Chen et al., 2008). Although both *Ctip2* and *Fezf2* are vital for subcerebral projection neurone development including CSMN as their null mutants are phenotypically similar, they are different in their mechanisms of function: *Fezf2* is

expressed at earlier stages during development in both cortical progenitors and post-mitotic subcerebral projection neurones to control their specification and differentiation, whereas Ctip2 is expressed later than Fezf2 and only in post-mitotic subcerebral projection neurones to control their differentiation primarily (Chen et al., 2008; Chen et al., 2005b; Chen et al., 2005a; Molyneaux et al., 2005). Hierarchically, Ctip2 is a major downstream effector of Fezf2 in regulating axonal targeting. This is because not only is Ctip2 expression abolished in *Fezf2*$^{-/-}$ mutants, electroporation of *Ctip2*-encoding transcript into *Fezf2*$^{-/-}$ null cortex is able to rescue the subcerebral projection phenotype of the electroporated neurones, restoring the projection of CSMN axons towards the spinal cord (Chen et al., 2008; Chen et al., 2005b; Chen et al., 2005a; Molyneaux et al., 2005). However, Ctip2 is not the solitary downstream effector of Fezf2, as i) the subcerebral projection phenotypic defect of *Fezf2*$^{-/-}$ is more severe as compared to *Ctip2*$^{-/-}$ mutants (failure in projecting beyond thalamus vs. pons) (Arlotta et al., 2005; Molyneaux et al., 2005); and ii) the electroporation of a *Fezf2*-encoding transcript into *Fezf2*$^{-/-}$ cortex during the period of subcerebral projection neurone production (E13.5 in mice) salvages development of the electroporated neurones and ectopic expression of *Fezf2* in upper layer neurones during their production period (E15.5 in mice) induces subcerebral axonal targeting, but does not always restore or induce their expression of Ctip2 (Chen et al., 2008).

Like *Ctip2*, another gene *Sox5* was also identified, by microarray analysis, to be highly up-regulated by CSMN during their early development (Arlotta et al., 2005). It is initially expressed by post-mitotic neurones in the PP but absent in the proliferative zones at E12.5 in mice. Gradually from E14.5-E16.5 in mice, its expression is detected in the Layer V, VI and SP neurones and by postnatal stages its expression is highly enriched in Layer VI and SP (Kwan et al., 2008; Lai et al., 2008). Two mechanisms of function for *Sox5* have been proposed: i) It is involved in controlling the sequential production and proper migration of SP neurones, Layer VI corticothalamic projection neurones and Layer V subcerebral projection neurones (Lai et al., 2008). Loss of *Sox5* function results in premature generation of Layer V subcerebral projection neurones in place of SP and Layer VI corticothalamic projection neurones due to premature induction of CSMN markers *Ctip2* and *Fezf2* (Lai et al., 2008). This proposal suggests the varying levels of *Sox5* act in concert with distinct levels of genes expressed in the SP and Layer VI such as Tbr1 and Ctip2 in Layer V in order to control the specification

of SP and deep layer neurones. SP neurones therefore can be characterized by combination of a high level of Tbr1, intermediate level of Sox5 and low level of Ctip2; Layer VI corticothalamic projection neurones express high levels of Sox5 and Tbr1 and a low level of Ctip2; and Layer V subcerebral projection neurones strongly express Ctip2, with intermediate and low levels of Sox5 and Tbr1 respectively (Lai et al., 2008; Leone et al., 2008). ii) In contrast to the prevention of premature induction mechanism, *Sox5* also controls the proper migration and post-migratory differentiation of SP, Layer V and VI neurones by down-regulation of the transient expression of CSMN-related genes *Ctip2* and *Fezf2* in SP and Layer VI corticothalamic neurones and thus restricting their expression predominantly to Layer V (Kwan et al., 2008). According to this proposal, the expression of Ctip2 and *Fezf2* is maintained in Layer VI and SP in the absence of *Sox5*, however this does not induce subcerebral projection phenotypes in Layer VI and SP neurones (axons are only misrouted towards hypothalamus; (Kwan et al., 2008)), contrary to the observation of the former proposal (Lai et al., 2008). Differences in *Sox5* function between these two proposals are further revealed by gain of *Sox5* function analyses in which the former study has shown an acquisition of earlier-born, subcerebral projection phenotype in later-born, callosal projection neurones when *Sox5* over-expression is occurring at the time when subcerebral projection neurone production has ceased (at E14.5) (Lai et al., 2008), whereas callosal projections are maintained when *Sox5* is over-expressed during the production of upper layer, callosal projection neurones (at E15.5) in the latter study (Kwan et al., 2008). Nevertheless, both studies have demonstrated the role of *Sox5* in repressing the expression of *Fezf2* and *Ctip2*, and a more direct relationship between Sox5 and Fezf2 has been identified by Kwan and co-authors, 2008 in which Sox5 is able to bind to a conserved enhancer element near *Fezf2* and suppress its transcription (Kwan et al., 2008; Lai et al., 2008).

As described previously, *Tbr1* is also highly expressed by deep layers, corticothalamic projection neurones. In the absence of *Tbr1 in-vivo*, the number of cells expressing Layer VI markers decreases while Layer V markers are ectopically expressed in earlier-born neurones, causing them to send axons into subcerebral targets instead of the thalamus (McKenna et al., 2011; Bedogni et al., 2010). Furthermore, Layer V neurones do not project their axons subcerebrally towards the brainstem and spinal cord when *Tbr1* is ectopically expressed in this layer (McKenna et al., 2011). Thus *Tbr1* promotes the fate specification of Layer VI corticothalamic projection neurones in the expenses of

Layer V subcerebral projection neurones and is found to achieve this by repressing the expression of *Fezf2* directly and activate/maintain the expression of *Sox5* (McKenna et al., 2011; Bedogni et al., 2010).

Satb2 is important in controlling the differentiation of some interhemispheric projection neurones, such as the callosal projection neurones, in Layer II-V of the neocortex by binding to and suppressing the expression of subcerebral projecting neuronal markers such as Ctip2 as well as regulating expression of axonal guidance molecules such as Ephrin type-A receptor 4 (EphA4) (Alcamo et al., 2008; Britanova et al., 2008), probably via interacting with chromatin-remodeling molecules histone deacetylases and binding directly to AT-rich matrix attachment regions (MARs) of target genes (Gyorgy et al., 2008; Szemes et al., 2006; Britanova et al., 2005). Bromodeoxyuridine (5-bromo-2-deoxyuridine; BrdU)-birthdating experiments indicate that early born SATB2-positive cells in the neocortex were generated before E11.5 in mice (Britanova et al., 2005). From E15.5-18.5 in mice, *Satb2* mRNA is detected in the CP and IZ of the neocortex, whereas its protein is predominantly expressed throughout Layer II-V above the TBR1-expressing lower CP (Alcamo et al., 2008; Britanova et al., 2008; Britanova et al., 2005). As *Satb2*-deficient neurones have altered genetic makeup, these conflicting molecular profiles cause defects in migration that lead to premature termination within the lower layers of the CP (Alcamo et al., 2008; Britanova et al., 2008). Moreover, these molecular profile changes also cause defects in post-mitotic differentiation such as axonal targeting. In the absence of *Satb2* functions, the callosal projecting axons are mis-routed towards subcortical targets such as cerebral peduncles despite an apparently intact adjoining callosal structure (Alcamo et al., 2008; Britanova et al., 2008). Alternatively, ectopic expression of *Satb2* in lower layers of the CP down-regulates Ctip2 expression and affects the development of corticospinal projection (Alcamo et al., 2008; Britanova et al., 2008). Various types of *SATB2* mutation in human patients as well as mouse models have been shown to be associated with defects in cleft palate formation, craniofacial patterning, osteoblast differentiation, jaw development and also cognition (Leoyklang et al., 2007; Britanova et al., 2006a; Britanova et al., 2006b; Dobreva et al., 2006).

Nuclear receptor-related protein 1 (Nurr1) is an orphan nuclear receptor transcription factor that is important for early differentiation and maintenance of dopamine neuronal

phenotypes in the midbrain through regulating genes involved in dopamine synthesis, transport, release and reuptake and continues to be expressed into adulthood (Kadkhodaei et al., 2009; Simon et al., 2003). Within the developing rodent neocortex, Nurr1 is found to be expressed predominantly by neurones in the SP of the dorsal neocortex and by both SP and lower layer CP neurones towards the lateral regions of the neocortex which are glutamatergic but not GABAergic (Hoerder-Suabedissen et al., 2009; Arimatsu et al., 2003). Retrograde tracing and immunostaining studies show that Nurr1-expressing neurones including those in the SP contribute predominantly to long-range intrahemispheric corticocortical projections, sparsely to interhemispheric corticocortical projections, and even more sparsely to the corticothalamic projections in developing rat neocortex (Arimatsu et al., 2003). This projection specificity is also shown to be conserved in monkeys (Watakabe et al., 2007). NURR1 may have a role to play in Parkinson disease and psychiatric disorders such as schizophrenia in which dopamine neurones are found to be degenerating. Many studies to-date have found correlations between *NURR1* mutations and Parkinson's disease (Sleiman et al., 2009; Jacobsen et al., 2008; Grimes et al., 2006; Huang et al., 2004), however there is not always a linkage between NURR1 mutations and the etiologies of psychiatric diseases such as schizophrenia (Feng et al., 2005; Ruano et al., 2004; Ishiguro et al., 2002; Chen et al., 2001; Buervenich et al., 2000). During development in rodents, there seems to be more neurones expressing Nurr1 in the lateral compared to the medial region of the neocortex persistently from embryonic to postnatal stages (Arimatsu et al., 2003) and predominant expression in the occipital cortex is observed from E14.5-18 ((Muhlfriedel et al., 2007); http://www.Genepaint.org).

A proposed model for the specification/differentiation of the major neocortical projection neurones during the development is illustrated in Figure 1.8 (adopted and modified from (Leone et al., 2008); with *Sox5* and *Tbr1* information incorporated based on (McKenna et al., 2011; Bedogni et al., 2010; Kwan et al., 2008; Lai et al., 2008)).

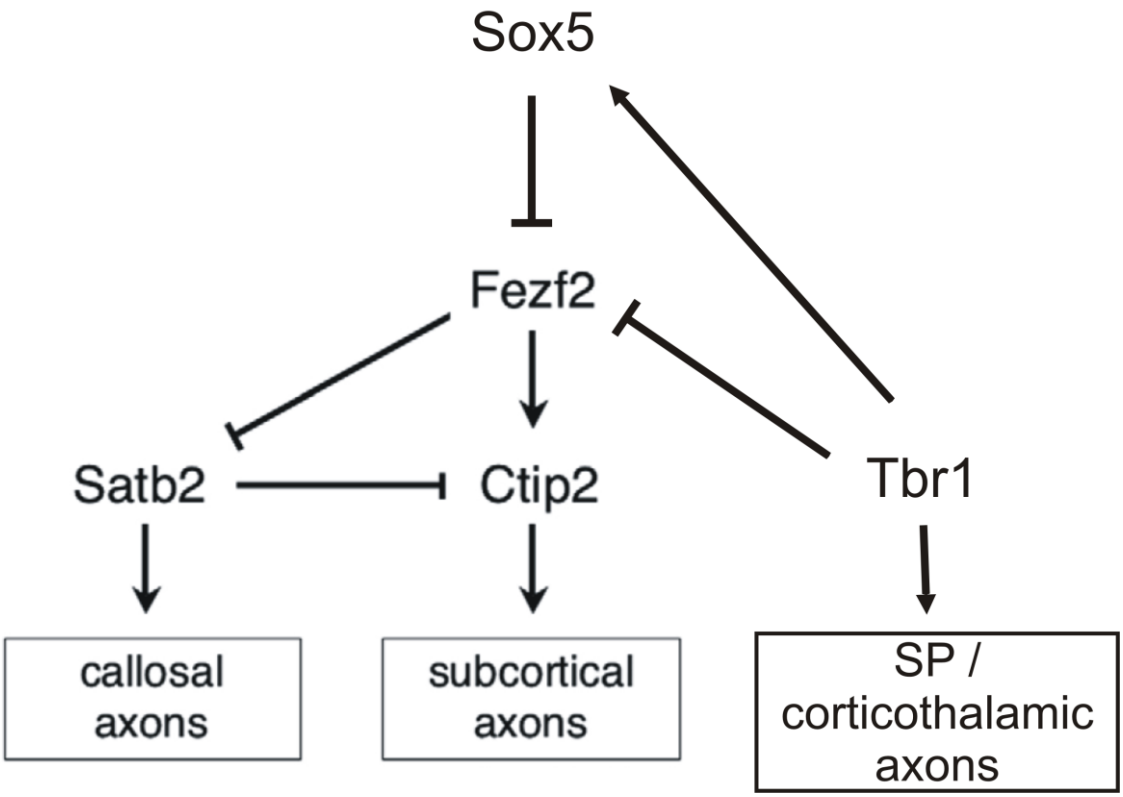

Figure 1.8. A proposed working model for the specification/differentiation of major neocortical projection neurones during development.

This model is based on the molecular profiles and genetic manipulation analyses of the above neocortical projection neurones. *Fezf2* acts upstream of *Satb2* and *Ctip2* to suppress callosal projection neurones fate via inhibition of *Satb2* expression and specify subcortical projection neurones fate via activation of *Ctip2* expression. *Satb2* is required for the development of callosal projection neurones and represses *Ctip2* expression in this neuronal subtype. Thus lack of *Satb2* would cause callosal projection neurones to extend their axons subcortically; while in the absence of *Fezf2*, *Ctip2* expression is repressed by *Satb2* expression and neurones would adopt callosal projection neurones fate. *Sox5* represses the expression of *Fezf2*, and together with *Tbr1* is known to be important in the development of SP and corticothalamic neurones. Adapted and modified from (Leone et al., 2008); with *Sox5* and *Tbr1* information incorporated based on (McKenna et al., 2011; Bedogni et al., 2010; Kwan et al., 2008; Lai et al., 2008).

1.2 Regionalisation across the Neocortex

Across the tangential dimension, the neocortex of the adult brain is subdivided into areas with clear sharp boundaries that are functionally unique and different from one another on the basis of cyto- and chemo-architecture, afferent/efferent connections and patterns of gene expression (O'Leary et al., 2007). In humans, functional division of neocortical areas indicates the primary motor area (Brodmann area 4 and 6) are located anterior to the central sulcus, the primary somatosensory (Brodmann area 1, 2 and 3) and visual areas (Brodmann area 17) are found posteriorly, and primary auditory area (Brodmann area 41 and 42) are bilaterally positioned in temporal lobe (Kahle and Frotscher, 2002). These areas display special features correlating to the functions they are serving. The primary somatosensory and auditory areas that receive inputs from ascending projection neurones contain thicker granular layers (Layer II and IV) that are densely packed with more cells as compared to the thinner pyramidal layers (Kahle and Frotscher, 2002). This feature is most prominent in the primary visual area, where Layer IV even appears to be duplicated (IVa and IVc) and separated by a cell-sparse layer (IVb) (Kahle and Frotscher, 2002). However, the pyramidal layers of the primary motor area which contain efferent projection neurones appears to be more elaborate in comparison to the granular layers (Kahle and Frotscher, 2002). (Figure 1.9; modified and adapted from (Kahle and Frotscher, 2002))

The process of areal differentiation of the neocortical primordium is frequently known as neocortical regionalisation and is believed to be regulated based on two mechanisms: the protomap (Rakic, 1988) and protocortex (O'Leary, 1989; Van der Loos and Woolsey, 1973) model (Mallamaci and Stoykova, 2006). The former model proposed an intrinsic mechanism for regulating early patterning of the neocortex by differential gene expression in progenitor cells, which is under the control of diffusible signalling molecules secreted from patterning centres and counter-gradient expression patterns of transcription factors. This model suggested heterogeneity of the cortical primordium in which the intrinsic molecular cues are carried forward to their progenies to impose their mature regional identities and is activity-independent. The later model, however, put forward a different theory by suggesting the neocortical primordium as a homogeneous structure with regionalisation directed by information conveying into the developing neocortex via external influences such as the thalamocortical afferents. This mechanism

is activity-dependent and established to refine the genetically pre-programmed regional specification processes, representing the later patterning of the neocortex (i.e. after the innervation of thalamocortical afferents).

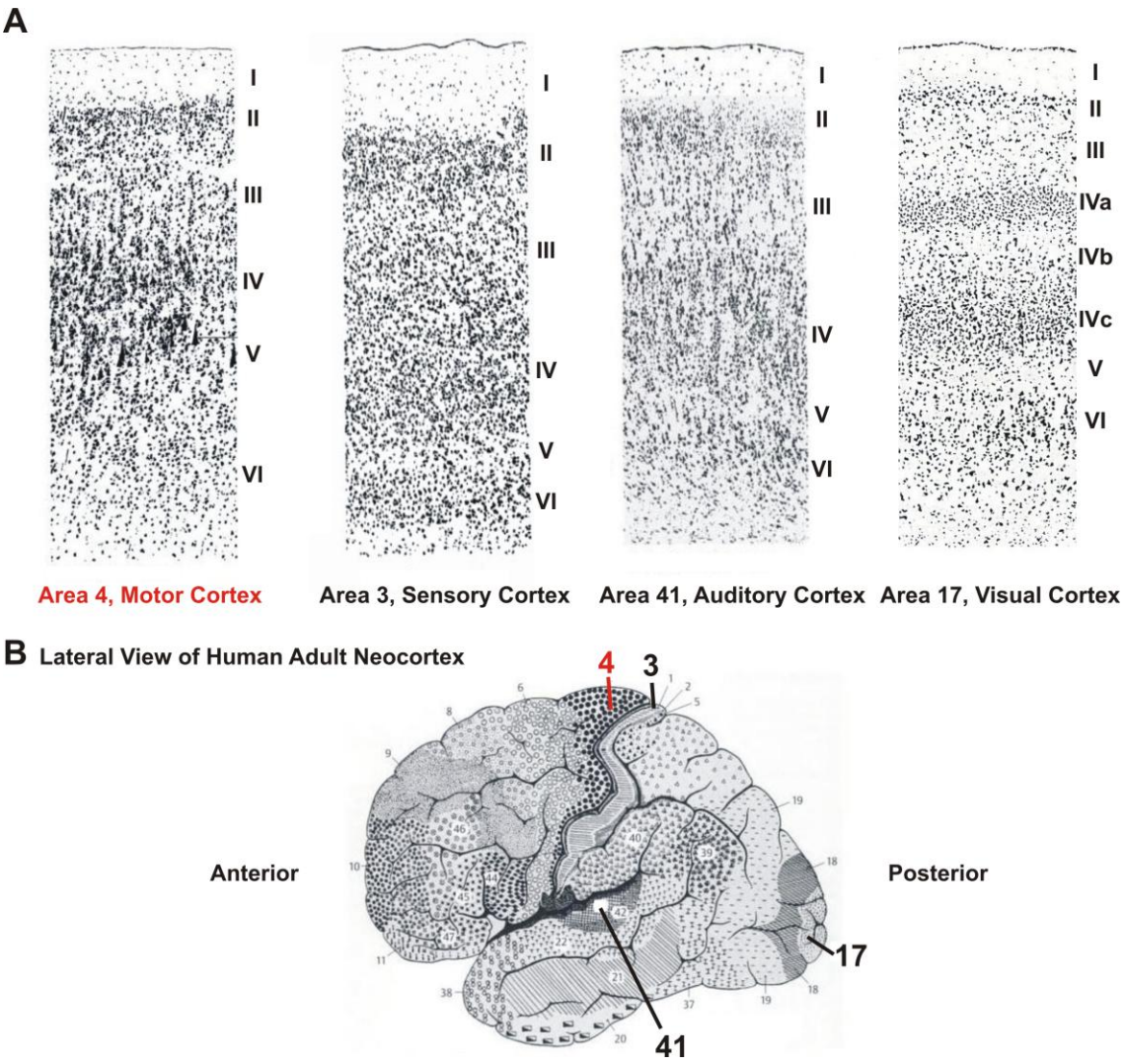

Figure 1.9. Cortical areas of the human adult neocortex.

(A) Primary areas of the human adult neocortex show cyto-architectural differences: area 4/motor cortex is characterized by a more elaborate Layer V; whereas Layer II and IV appears to be much thicker in area 3/sensory cortex and area 41/auditory cortex, and in the area 17/visual cortex Layer IV is even duplicated to become IVa and IVc which is separated by a cell-sparse layer (IVb). (B) Lateral view of the human adult neocortex illustrating various Brodmann areas, highlighting the location of area 4/motor cortex in the frontal lobe anterior to the central sulcus, area 3/sensory cortex in the parietal lobe posterior to the central sulcus, area 17/visual cortex in the occipital lobe lining the calcarine sulcus and area 41/auditory cortex in the temporal lobe on the transverse temporal gyri. Adapted and modified from (Kahle and Frotscher, 2002).

1.2.1 Protomap Theory

Two main classes of molecules presumed to be crucial for early regionalisation of the neocortical primordium are: i) signalling molecules, morphogens or secreted ligands (to be used throughout this section) and ii) transcription factors. The former molecules are discharged by surrounding borders of the cortical morphogenetic field that are often referred as the "patterning centres" or "signalling centres"; whereas the later ones are expressed by progenitor cells within the cortical morphogenetic fields. The secreted ligands are often capable of controlling the expression of transcription factors in a dose-dependent manner, thereby generating a gradient or transient expression of transcription factors by neocortical progenitors in the proliferative zones.

Secreted ligands and Patterning centres

Several patterning centres that are relevant for regionalisation have been discovered to secrete a set of ligands, locating at different regions of the brain and cooperate with each other in order to establish regional identities of the neocortex along the anterior-posterior and medial-lateral axes (Figure 1.11). Interfering with the expression of these ligands or their downstream signalling pathways has led to shifting of neocortical areas across the tangential dimension, thus allowing the deduction of their functional implications in regionalisation of the neocortex.

In general, during early stages of cortical neurogenesis (E10-E12.5), anterior cortical regionalisation is predominantly controlled by the anterior neural ridge (ANR), a region formed via the neural tube folding process and later become the commissural plate (CoP)/septum. Four members of the *Fibroblast Growth Factor* (*Fgf*) genes are expressed in discrete and partially overlapping domains of this anterior patterning centre: from E8-E12 in mice, *Fgf8* and *Fgf18* are expressed in the central domain of this anterior midline structure, whereas *Fgf17* expression extends more dorsally and *Fgf15* expression is much broader and extends ventrally but is absent in *Fgf8*-positive domain (Iwata and Hevner, 2009; Borello et al., 2008; Cholfin and Rubenstein, 2007; Gimeno and Martinez, 2007; Gimeno et al., 2003; Bachler and Neubuser, 2001; Crossley et al.,

2001; Xu et al., 1999; Hoshikawa et al., 1998; Maruoka et al., 1998; Crossley and Martin, 1995). *Fgf8* and *Fgf17* are known to specify the frontal-motor cortical area fates, as shown by anterior or posterior displacement of these area boundaries upon reduction of Fgf-signalling or over-expression of *Fgfs* (Cholfin and Rubenstein, 2007; Fukuchi-Shimogori and Grove, 2001). A more specific task of *Fgf17* in patterning the dorsal-frontal cortex has been revealed while the ventral-orbital frontal cortex specification appears to be *Fgf17*-independent (Cholfin and Rubenstein, 2007). Interestingly, *Fgf8* is shown to act positively upstream of *Fgf17* and *Fgf18*, but repress the expression *Fgf15* to cause their complementary expression pattern in the anterior patterning centre (Borello et al., 2008).

Additionally, the cortical hem, which is of medial pallial origin locating at the medial margin of the dorsal telencephalon, expresses multiple *Wnts* (*-2b, -3a, -5b, -7a, -8b*) and *Bone morphogenetic proteins* (*Bmp2, -4, -5, -7*) is important in the development of the adjacent hippocampus along the mediolateral axis of cortical neuroepithelium. Shimogori and co-authors (2004) have deduced interactions between the two signalling centres, suggesting that *Bmps* are able to suppress the anterior-pole patterning activities of *Fgf8* or *-17* to disinhibit *Wnts* signalling in order to promote the hippocampal fate (Shimogori et al., 2004). This conclusion is drawn based on the observation that inhibiting *Bmps* signalling dramatically increases expression of *Fgf8*, and with the expansion of *Fgf8* domain, expression of *Wnts* in the cortical hem is suppressed, as phenotypically manifested by a shrunken hippocampus (Shimogori et al., 2004).

An additional patterning centre in the ventral telencephalon and the hypothalamus of ventral diencephalon expresses *Sonic hedgehog* (*Shh*), which is involved in regional patterning of the forebrain to induce ventral fate via influencing factors from other patterning centres such as *Bmps* and *Fgf8* (O'Leary et al., 2007; Ohkubo et al., 2002; Crossley et al., 2001). Recently, *Forkhead box G1* (*Foxg1*) has been identified to integrate signals from the two patterning centres, the *Shh*-expressing ventral telencephalon/hypothalamus and the cortical hem, by acting downstream of Shh signalling pathway and directly repressing the transcription of *Wnts* during telencephalic dorsal-ventral patterning (Danesin et al., 2009).

During later stages of cortical neurogenesis (E12 onwards), a structure locating at the lateral edge of the cortex near the pallial-subpallial boundary (PSB), termed the cortical anti-hem, specifically expresses five genes for secreted ligands: *Transforming growth factor alpha* (*Tgfα*), *Nrg1 and -3*, *Fgf7* and *Secreted frizzled-related protein 2* (*Sfrp2*), which is a Wnt antagonist. However their function in regionalisation is less known (Subramanian et al., 2009). *Fgf15* is found to be also weakly expressed in the neuroepithelium of PSB, in addition to its expression in the ANR/CoP/septum (Borello et al., 2008).

Graded expression of transcription factors

A range of transcription factor genes are found to be expressed by neuronal progenitors in gradients along the anterior-posterior and medial-lateral pole of the neocortex and are important for imposing progenies with region-specific identities (Figure 1.10). In rodents, *Pax6* and *Empty spiracles homeobox 2* (*Emx2*) are shown to be expressed by progenitor cells in a reciprocal gradient throughout neurogenesis, i.e. *Pax6* is expressed higher in the anterolateral domains of the proliferative zone of the neocortex and lower in the posteromedial domains, on the other hand, *Emx2* expression appears to be higher posteromedially and lower anterolaterally in the neocortex (Bishop et al., 2002). Indeed, *Pax6* and *Emx2* preferentially impart anterolateral (e.g. motor and somatosensory) and posteromedial (e.g. visual) regional identities respectively by mutually suppressing expression of one another since *Pax6* loss-of-function experiments have shown an anterior shift of visual areal markers; while *Emx2* KO animals have displayed a posterior shift of motor and somatosensory areal markers (Bishop et al., 2003; Bishop et al., 2002; Lopez-Bendito et al., 2002; Muzio et al., 2002; Bishop et al., 2000). The contraction or expansion of cortical areas is in proportion to the alteration of cortical size and paralleled by misrouted (ventrally-displaced) thalamocortical and corticothalamic projections at the diencephalic-telencephalic boundary, indicating possible defects in early guidance (Bishop et al., 2003; Bishop et al., 2002; Jones et al., 2002; Lopez-Bendito et al., 2002; Muzio et al., 2002; Bishop et al., 2000). However, KO of *Pax6* and *Emx2* has detrimental effects which result in prominent reduction of cortical total surface areas thus compromising the comparison between mutants and wild type littermates. Furthermore, it causes animals to die at birth, limiting further analyses on area patterning postnatally. Therefore, later studies seek to investigate the

role of *Emx2* in controlling regionalisation of the neocortex have performed gain-of-function analyses and found disproportionate changes in size of primary somatosensory and motor areas shifting anterolaterally, whilst the cortical size, lamination, thalamic nuclei and thalamocortical projection development remain normal (Hamasaki et al., 2004). On the other hand, gain-of-function studies on *Pax6* seem to have resulted in minimal effects on regionalisation of the neocortex with a small though significant decrease in the size of primary somatosensory area, but more prominent alterations in the proliferation of late neocortical progenitors (Manuel et al., 2007). Additional evidence supporting the idea that *Pax6* has little direct importance in area patterning of the neocortex comes from a neocortical conditional KO of *Pax6* mutant, in which normal thalamocortical and corticofugal projections are developed normally despite anterior shift of positional specific molecular markers (Pinon et al., 2008).

The orphan nuclear receptor *CouptfI*, downstream of *Emx2*, is expressed highly by neocortical progenitors and post-mitotic neurones in the parietal and occipital lobe of the neocortex where sensory areas are located (Armentano et al., 2007). Its expression level is the lowest towards the frontal lobe of the neocortex constituting the motor areas (Armentano et al., 2007). Conditional KO of *CouptfI* (*Emx1*-Cre: *CouptfI*$^{loxP/loxP}$; *CouptfI*-cKO) in the neocortex causes enormous expansion of frontal/motor areas and significant compression of sensory areas towards the posterior occipital cortex, with altered axonal projections to maintain the area specific afferent and efferent connections, evidently supporting its role in repressing frontal-motor areal identities and specifying sensory-visual areal identities (Armentano et al., 2007). More specific functions of *CouptfI* in controlling the area-specific differentiation of distinct neuronal subtypes have been revealed by a recent study using conditional KO mice (Tomassy et al., 2010). *CouptfI* represses the differentiation of Layer VI corticothalamic neurones in sensory areas into Layer V corticofugal neurones by inhibiting expression of Ctip2 and *Fezf2*, such that, in the absence of *CouptfI* function, presumptive corticothalamic neurones abnormally display the molecular features and projection patterns of corticospinal neurones (Tomassy et al., 2010). Additionally, Layer V neurones in the sensorimotor cortex fail to develop into corticospinal neurones (Tomassy et al., 2010). *CouptfI* is also shown to be able to repress Fgf signalling by promoting the expression of the Fgf signalling inhibitors *Sprouty 1* and *-2* (*Spry1* and *-2*), and thereby advancing posterior fate (Faedo et al., 2010).

A member of the zinc-finger transcription factors family, *Specificity protein 8* (*Sp8*) is expressed strongly but transiently in the *Fgf8*-postive ANR/CoP at E8.0-8.5, and throughout the entire forebrain by neocortical progenitors with a high anteromedial to low posterolateral gradient across the VZ by E9.0 in mice (Sahara et al., 2007; Zembrzycki et al., 2007). Thereafter from E10.5 onwards, *Sp8* mRNA transcript level gradually decreases in neocortical VZ, but maintain strong expression levels throughout adulthood in other regions (Sahara et al., 2007; Zembrzycki et al., 2007). Like *Pax6* and *Emx2*, *Sp8* also plays a role in regionalisation. A study utilizing Cre-loxP conditional neocortical specific *Sp8* KO mutants (*Foxg1*-Cre: $Sp8^{loxP/loxP}$; *Sp8*-cKO) has revealed an anterior shift of neocortical areas at E12.5 paralleled by changes in thalamocortical innervation at E18.5 (Zembrzycki et al., 2007). Another study conducted by a separate group has electroporated *in-utero* a dominant negative expression construct of *Sp8* into the ANR/CoP at E11.5 in mice that also results in a considerable shift of cortical areas towards the anterior region of the neocortex accompanied by a decrease in sizes of primary sensory areas at P7, a phenotype observed when the endogenous Fgf8 secreted from the ANR/CoP is suppressed (Sahara et al., 2007). Additionally, expression of *Fgf8* and its downstream genes (e.g. *Polyomavirus enhancer activator 3* (*Pea3*), *Ets-related molecule* (*Erm*) and *Er81*) are strikingly reduced within ANR/CoP (Sahara et al., 2007). This provides evidence for the importance of *Sp8* in the maintenance of *Fgf8* and its targets' expression within the ANR/CoP by direct activation of *Fgf8* transcription (Sahara et al., 2007). This transcriptional activity is under the repression of *Emx2* in the neocortex thereby limiting *Fgf8* expression in the ANR/CoP but not in the neocortical proliferative zones (Sahara et al., 2007). However, *Sp8* seems to act upstream of *Emx2* by direct regulation as the loss of *Emx2* function does not alter the expression of *Sp8* (Zembrzycki et al., 2007). These studies have revealed some interactions between secreted ligands and transcription factors that are expressed in graded fashion. Furthermore, the shifting of neocortical areas and changes in thalamocortical inputs observed in these loss-of-function analyses suggest a role for *Sp8* in controlling the balance of regional patterning along the anterior-posterior axis of the neocortex.

The homeodomain transcription factor *Otx1* is expressed by subcerebral but not corticocortical projection neurones within Layer V and the progenitors that generate these neurones throughout the entire neocortex (Weimann et al., 1999). Yet when

knocking-out *Otx1*, aberrant subcerebral axonal projections are observed only from the visual cortex where exuberant connections from visual cortex to the spinal cord are not removed, thus associating *Otx1* with visual cortical fate specification and establishment of the visual area-specific Layer V subcerebral projections (Weimann et al., 1999). Recent evidence shows that *Otx1* is important in establishing the visual area identity, potentially via competing with sensorimotor area molecular determinants, as tract tracing of corticospinal projection neurones demonstrate a posterior shift of sensorimotor area in the slightly smaller *Otx1*$^{-/-}$ mice neocortices (Ando et al., 2008).

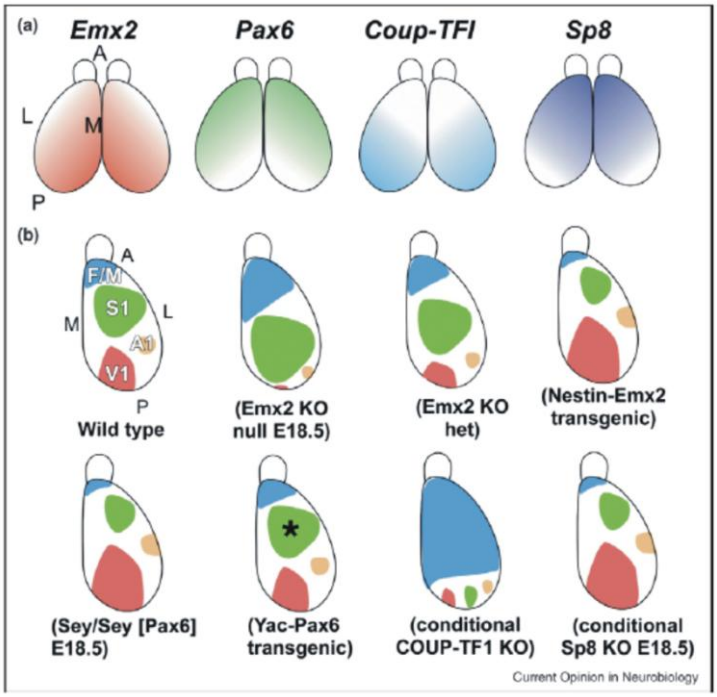

Figure 1.10. Role of graded expression of transcription factors in controlling regionalisation of the neocortex.

(a) Transcription factors *Emx2*, *Pax6*, *CouptfI*, and *Sp8* are expressed in a graded fashion along the anterior (A) - posterior (P) and lateral (L) - medial (M) axes of the neocortex. *Emx2* is expressed in high posteromedial to low anterolateral gradient, whereas *Pax6* showed opposite, counter-acting gradient as compared to *Emx2*. *CouptfI* is expressed in high posterolateral to low anteromedial gradient, whereas *Sp8* is expressed in an opposite manner to *CouptfI*.

(b) Results obtained via loss- or gain-of-function mutant mice of the above transcription factors as compared to wild-type littermates have revealed their importance in regionalisation of the neocortex. Analyses of homozygous *Emx2* KO (*Emx2* KO null) mice during late embryonic stage reveals a significant reduction in the size of posterior areas paralleled by an enlargement and posterior shift of anterior areas (F/M, frontal-motor; S1, somatosensory). A similar but less severe areal shifting is observed in heterozygous mutant mice (*Emx2* KO het) with reduced *Emx2* expression. Conversely, Nestin promoter-driven over-expression of *Emx2* (Nestin-*Emx2* transgenic) causes anterior shift of areas due to visual area (V1) expansion. *Pax6* KO mice (Sey/Sey [*Pax6*]) lack the functional Pax6 protein, display an anterior shift of areas as the posterior areas enlarge. However, over-expression of *Pax6* (YAC-*Pax6* transgenic) only causes a small, but significant, reduction in the size of S1 without obvious areal shift (asterisk). Neocortical deletion of *CouptfI* in mutant mice (conditional *CouptfI* KO) causes a substantial posterior shift of areas due to an enormous expansion of the F/M, paralleled by a significant reduction of the S1. Neocortical and commissural plate deletion of *Sp8* (conditional *Sp8* KO) causes a similar anterior areal shift during late developmental stages as observed in the *Fgf8* hypomorphic mutants. A1, auditory area. Adapted from (O'Leary and Sahara, 2008).

1.2.2 Protocortex Theory: role of thalamocortical axon projections

Most sensory inputs are transmitted to the according primary areas of neocortex through intermediate targets, the dorsal-thalamic nuclei (dTh), forming topographic projections from these functional modules in the thalamus to the neocortical primary areas: the dorsolateral geniculate nucleus (dLGN) projects to the visual cortex (V1); the ventrobasal complex (VB) to the somatosensory cortex (S1); and the ventrolateral nucleus (VL) to the motor cortex (M1) (Garel and Rubenstein, 2004). As described previously, secreted ligands and graded expression of transcription factors determine the relative size and location of these neocortical areas during early development. Since thalamocortical axon projections are the only supply of modality-specific information to the neocortex, further functional specifications of the primary areas are defined by and relied on the extrinsic influences via thalamocortical input at later stages of development. During development, the thalamocortical axons follow a long and complex trajectory: in general, they exit the dorsal thalamus (CS16-18) by turning abruptly at the diencephalic-telencephalic boundary and course anteriorly through the subpallial structures (CS20), then turn subsequently at the pallial-subpallial boundary through the internal capsule (Bystron et al., 2005; Garel and Rubenstein, 2004) to enter the neocortex via the SP from 13 PCW (Kostovic and Rakic, 1990), and stay in this zone for a period of time before further invading the CP (Layer IV) after 22-24 PCW (Kostovic and Judas, 2007). This prolonged period of axonal pathfinding and target selection requires proper guidance to lay down the route towards their final destination, potentially through cell adhesion molecules, while interference of the pathway has been shown to affect cortical map specification.

The guidance of thalamocortical projections is shown to be dependent on guidance cues expressed by other neuronal subtypes or in the environment where these neurones reside, which is detected by the transmembrane receptors/cell adhesion molecules expressed by thalamocortical axons. One example is via the subcortical “corridor cells” that are GABAergic neurones derived from LGE expressing Nrg1 (Lopez-Bendito et al., 2006). These “corridor cells” lay out a permissive route, which is superficial to the proliferative zones of the MGE and deep to the developing mantle zone where the globus pallidus is forming, for the tangential extension of thalamocortical axons expressing ErbB4 receptors (Lopez-Bendito et al., 2006). On the other hand, handshake

hypothesis suggests that local molecular cues are derived from SP neurones that send out early pioneer fibres to lay down a pathway and in the basal telencephalon intermingle with and guide the growing thalamocortical axons towards their neocortical target areas (Molnar and Blakemore, 1995). The radial unit hypothesis proposed to describe the generation of CP neurones (Rakic et al., 2009) can also be applied to the generation of SP neurones in which the spatial relationships and radial patterning of SP progenies are also maintained when they are generated from the VZ progenitors (O'Leary and Borngasser, 2006). Thus as proposed by the protomap hypothesis (Rakic, 1988), SP neurones in different regions of the neocortex may contain region specific molecular cues that guide the differential innervation of thalamocortical afferents to the appropriate neocortical areas.

The role of thalamocortical projection guidance cues in the patterning of developing neocortical areas has been illustrated by Dufour and co-authors (Dufour et al., 2003). The Eph family of receptor tyrosine kinases and their ligands, Ephrins, are implicated in the guidance of thalamocortical projections (Dufour et al., 2003). *EphA4* receptor and its ligand *EphrinA5* are expressed in similar medio^{HIGH}-lateral^{LOW} gradients in the rodent primary thalamic VB nuclei and in the primary cortical S1 (Layer IV), while double mutant *EphA4*$^{-/-}$E*phrinA5*$^{-/-}$ mice manifest aberrant thalamic VL motor nuclei projections to the cortical S1 area (Dufour et al., 2003). The design of a triple KO mutant *EphrinA2*$^{-/-}$*A3*$^{-/-}$*A5*$^{-/-}$, which severely disrupted the orderly patterns of thalamocortical projections from the dLGN to V1, have directly demonstrated a crucial role of thalamocortical patterning of neocortical areas along the tangential dimension, since V1 in these mutant mice is rotated and shifted medially and the internal organization of the visuotopic map also appears to be distorted (Cang et al., 2005). Furthermore, ectopic expression of *EphrinA5* in regions lateral to V1 shifts this cortical area medially, while ectopically expressing *EphrinA5* and -*A2* within V1 disrupts its topographic functional organization (Cang et al., 2005). A recent study has revealed the requirement for neural cell adhesion molecule L1 and Close homolog of L1 (CHL1) in eliciting the repellent responses to EphrinA5 to guide thalamocortical axons to the M1 (Demyanenko et al., 2010). Double KO of *CHL1*$^{-/-}$*/L1*$^{-/-}$ in mice has caused a significant posterior shift of thalamocortical projections from motor thalamic nuclei (VL) to the V1 (Demyanenko et al., 2010).

1.2.3 Summary

The protomap and protocortex mechanisms are important in specifying neocortical areas into distinctive functional modules and would certainly impose effects on one another (Figure 1.11; adapted from (O'Leary and Sahara, 2008)). Intrinsic molecular combinatorial codes within a cortical region act as notations for progenitor cells to play the tune of neuronal differentiation and migration accordingly in earlier stages of corticogenesis, forming a basic scaffold to guide any incoming axons. On the other hand, the later arrival of thalamocortical axon projections would conduct activity-based signals to their designated areas in order to orchestrate and shape the further differentiation of neurones within the cortical field at the later stage. Indeed, the thalamocortical influences on protomap have been demonstrated by Eph/Ephrin studies, whereas experiments performed by Shimogori and Grove (2005) have shed light onto the protomap influence on thalamocortical axon projections (Shimogori and Grove, 2005). In mice, ectopically expressing *Fgf8* in the posterior neocortex has rearranged the area map by duplicating the S1 field for which the thalamocortical axons are shown to be loyally tracking the changes in area position and innervate both S1 fields (Shimogori and Grove, 2005). Moreover, they have also shown Fgf8 can control the distribution of axon guidance molecules such as EphrinA5 in both the SP and CP along the anterior–posterior axis thereby offering laminar- as well as area-specific information for thalamocortical axon termination (Shimogori and Grove, 2005).

During development, corticogenesis and regionalisation are two closely associated processes as they shared similar molecular determinants. In addition to their importance in setting up the early neocortical map, secreted molecules such as Wnts and Fgf8 have been shown to regulate neocortical proliferation whereas Fgf15 plays a role in differentiation (Borello et al., 2008; Machon et al., 2007; Storm et al., 2006). Furthermore, the four transcription factors (Pax6, Emx2, CouptfI and Sp8) described previously are known to also control the proliferation of neocortical progenitors and/or their laminar destiny (Faedo et al., 2008; Mo and Zecevic, 2008; Zembrzycki et al., 2007; Heins et al., 2001; Warren et al., 1999).

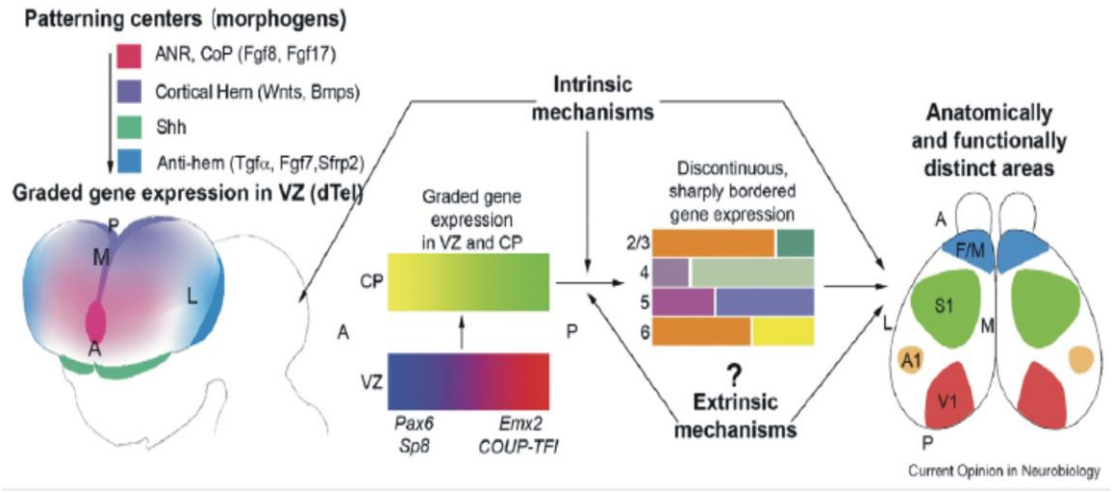

Figure 1.11. Mechanisms of regionalisation of the developing neocortex.

Four patterning centres are identified that secrete different ligands, termed morphogens (to be used in this figure legend) during early stages of development. The anterior midline domain, anterior neural ridge (ANR)/commissural plate (CoP) (red), produces Fgfs (such as -8 and -17); the cortical hem (purple) locating along the dorsal/posterior midline expresses Wnts and BMPs; the ventral telencephalon/hypothalamus in the ventral diencephalon (green) is a known source of Shh; whereas the anti-hem at pallial-subpallial boundary bilaterally, is a later patterning centre producing morphogens including Tgfα, Fgf7 and Sfrp2. These morphogens in turn control the expression of transcription factors (*Pax6*, *Emx2*, *CouptfI*, and *Sp8*) in the ventricular zone (VZ) of the dorsal telencephalon (dTel), establishing their graded expression patterns across the anterior-posterior (A-P) and medial-lateral (M-L) axes. These transcription factors are expressed by neocortical progenitors, thereby conveying regional or areal identities to the cells expressing them. Thus these genes can be referred to as the regionalisation genes. These genes are also able to regulate expression of other genes encoding transcription factors or cell adhesion molecules in the cortical plate (CP) that under the influence of extrinsic factors such as thalamocortical inputs, and are gradually transformed into distinct patterns with sharp boundaries. These downstream genes though with graded or restricted patterns of expression across the neocortex, they should be referred to as areal genes. As corticogenesis proceeds alongside with regionalisation, neocortical areas are eventually formed with unique anatomically distinctive neocortical layers (2-6), serving different functions. A1, primary auditory area; F/M, frontal/motor cortex; S1, primary somatosensory area; V1, primary visual area. Adapted from (O'Leary and Sahara, 2008).

1.3 Summary of Human-Rodent Differences in Neocortical Development

1.3.1 Cytoarchitectural Differences

During neocortical development of both humans and rodents, the neuroepithelial cells of the neocortical primordium proliferate and differentiate to become a complex multi-layered structure with regionally diverse cytoarchitecture. The sequential formation of neocortical transient layers is largely conserved between humans and rodents, however certain transient layers in humans become more complex and elaborate as neocortical development progresses, potentially accounting for the larger surface area with the formation of gyri and sulci and thicker neocortex in adult humans. During early embryonic development, prior to the segregation of the PP into MZ and SP, the human PP develops transiently into multiple layers namely the superficial Cajal-Retizus cell layer, the intermediate monolayer and the deep pioneer plate, in which such complexity is unique to humans (O'Leary and Nakagawa, 2002; Meyer, 2001; Meyer et al., 2000). During foetal development, the human SVZ is visibly divided into ISVZ and OSVZ by a cell-poor/fibre-rich IFL at around 12 PCW (Bayatti et al., 2008a), containing heterogeneous populations of progenitor cells giving rise to more diverse subtypes of glutamatergic projection neurones and also GABAergic interneurones (Fietz et al., 2010; Hansen et al., 2010); whereas the rodent SVZ only contains a few layers of cells and maintains its thickness throughout development (Martinez-Cerdeno et al., 2006). The human SP also starts to expand drastically during mid-gestation due to gradual accumulation of vast amount of fibre tracts and is about four times thicker than the CP at its maximal size (Kostovic and Rakic, 1990). The amount of fibre tracts accumulating in the SP correlates with the appearance of gyri as area with the largest number of fibre tracts in the SP causes bulging of the CP and is preferentially observed in regions where gyri become pronounced (Kostovic and Rakic, 1990). Thus the elaborate and complex SVZ and SP potentially underlie the neocortical thickness and surface area expansion in gyrencephalic humans. Furthermore, the MZ is another layer prominently different between the two species, in which a transient layer of undifferentiated granular cells are found above the human MZ, termed SG layer (Meyer, 2001). Figure 1.12 illustrates the histological comparison of sequential formation of neocortical transient layers between humans and rodents during development (Molnar et al., 2006).

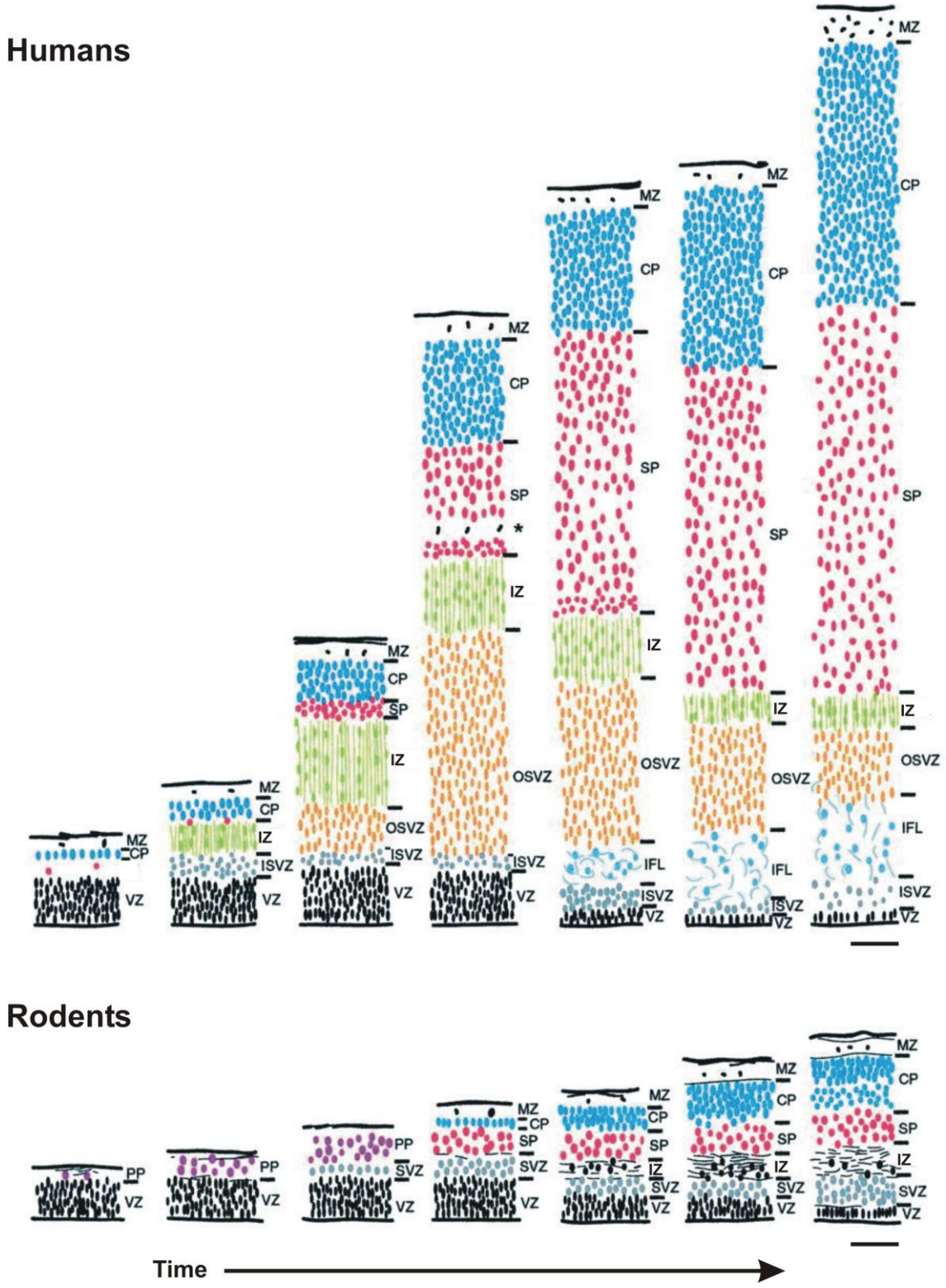

Figure 1.12. Comparison of neocortical layer formation in the developing human and rodent neocortices.

The top and bottom panels depict the sequential formation of various neocortical layers in humans and rodents respectively at comparable developmental stages. The internal detail of each layer reflects the orientation and shape of cells residing in each layer as well as its relative cell density. Notice a "clear-layer" indicated by an asterisk (*), is transiently present at E72 in non-human primates locating in the deep subplate (SP), which disappears during later stages of development (top panel). CP, cortical plate; IFL, inner fibrous layer; ISVZ, inner subventricular zone; IZ; intermediate zone; MZ, marginal zone; OSVZ, outer subventricular zone; PP, preplate; VZ, ventricular zone. Scale bars indicate 0.1 mm. Adapted and modified from (Molnar et al., 2006).

1.3.2 Molecular Differences

As described in previous section, Pax6 and Emx2 are the two best characterized transcription factors known to be involved in neocortex regionalisation with supporting evidence from mutant mice experiments to show they are expressed in counteracting gradients and control anterior and posterior neocortical area specification respectively (Muzio et al., 2002; Bishop et al., 2000). Spatial and temporal analysis of graded expression patterns of *PAX6* and *EMX2* by our group has previously revealed similarities and differences with previously published rodent data (Table 1.1; (Ip et al., 2010a; Bayatti et al., 2008b; O'Leary et al., 2007)). At 8 PCW they exhibited reciprocal gradients as described in rodents. However from 9 PCW, *PAX6* failed to exhibit the high anterolateral, low posteromedial gradient (seen at 8 PCW), while the *EMX2* gradient (high posteromedial, low anterolateral) persisted. Furthermore, *PAX6*/PAX6 expression is not limited to the VZ in humans but also detected in the SVZ (Bayatti et al., 2008b). On the other hand, expression of *EMX2*/EMX2 in humans is limited to the proliferative zones at 8 PCW, however, unlike rodents, the majority of its expression is shifted to the CP by 10 PCW while its expression in the proliferative zones maintained throughout all investigated stages (Bayatti et al., 2008b).

Thus although many mechanisms involved in corticogenesis and regionalisation are shared in common between rodents and humans, the human neocortex is composed of diverse and more complex local area identities reflecting differences in structure and function (Molnar and Cheung, 2006; Hill and Walsh, 2005; Monuki and Walsh, 2001). The differences observed between humans and rodents have highlighted the importance of utilizing human materials to investigate regionalisation further in order to identify some human-specific mechanisms.

Genes	Gradient (Humans)	Gradient (Rodents)	Laminar localization (Humans)	Laminar localization (Rodents)
PAX6	↑Anterior/Lateral ↓Posterior/Medial **at 8 GW, no gradient afterwards**	↑Anterior/Lateral ↓ Posterior/Medial	**SVZ**, VZ	VZ
EMX2	↑Posterior/Medial ↓Anterior/Lateral	↑Posterior/Medial ↓Anterior/Lateral	**CP**, **SVZ**, VZ	VZ

Table 1.1. Summary of the observed neocortical expression patterns of *EMX2* and *PAX6* (gradients and laminar localization) in the human brain as compared to previous studies in rodent.

Compiled by comparing studies reported in (Bayatti et al., 2008b; O'Leary et al., 2007). CP, cortical plate; SVZ; subventricular zone, VZ. Adapted from (Ip et al., 2010a).

1.4 Affymetrix Gene Chip Analysis

The observation of reciprocal gradients at early stages of human neocortical development implies that regionalisation events may be occurring relatively early in the developing human brains and that cells in the developing neocortex at this stage may exhibit a degree of intrinsic identity information (Rakic et al., 2009; Rakic, 1991). However, the loss of the *PAX6* (high anterolateral, low posteromedial) gradient at 9 PCW in humans is still early in neocortical development as CP starts to form at 7.5 PCW (Meyer et al., 2000) and even Layer VI has not formed completely (Bayatti et al., 2008a). Although in rodents *Pax6* has been found to be expressed in a gradient throughout neurogenesis (Manuel and Price, 2005), our observation supports recent evidence in rodents suggesting that *Pax6* is not directly involved in regional identity.

In order to identify other potential anterior markers during human neocortical development and assess whether any putative markers may be intrinsically regulated, our group has previously analyzed gene expression levels in developing neocortical tissue dissected anteriorly and posteriorly between 8-12.5 PCW using an Affymetrix whole genome chip array (U133 Plus 2.0, Affymetrix UK Ltd., High Wycombe, UK) (Ip et al., 2010a). In brief, GeneSpring GX 7.3 software (Agilent Technologies) was used for expression level analysis. Expression data for each probe set was background-corrected, normalized and summarized by Gene Chip-Robust Multi-array Average (GC-RMA), and gene expression levels between the two regions of the neocortex were calculated as fold changes. Using 1.75 as a threshold fold change (this threshold was arbitrary and chosen as *EMX2* was measured at 1.77-fold which had previously been confirmed to exhibit a gradient along the anterior-posterior axis by *in-situ* hybridization (ISH) in tissue sections; (Bayatti et al., 2008b)), the scatter plot in Figure 1.13A showed 383 Affymetrix probe sets that are more highly expressed anteriorly than posteriorly (marked by white) and 154 probe sets that exhibit higher expression posteriorly than anteriorly (marked by white) (Ip et al., 2010a). It is noteworthy that Affymetrix gene chip analysis is only one of the many applications to examine graded gene expression and the use of 1.75-fold as the threshold fold change does not preclude genes exhibiting <1.75-fold to be also expressed in gradients which could be significantly detected by

other methods such as quantitative real time-polymerase chain reaction (rtPCR) (Ip et al., 2010a).

Clustering study of all genes between different samples analyzed by condition tree analysis (Figure 1.13B) and principal component analysis (Figure 1.13C) by GeneSpring GX software indicated that gestational age was a variable affecting total gene expression between samples, as close clustering was observed at ages 9-11 PCW, while samples aged 8 and 12.5 PCW exhibited more variability (Ip et al., 2010a).

Gene ontologies were analyzed using the GO Ontology Browser within the GeneSpring GX analysis platform. This functional ontological analysis revealed expression profiles consistent with an enrichment of neural developmental processes occurring in both anterior- and posterior-derived neocortical tissue (Ip et al., 2010a). However genes classified within cell-signalling, adhesion, proliferation and cell death categories were up-regulated in anterior- compared to posterior-derived cells suggesting greater interactions between cells are taking place anteriorly than posteriorly (Ip et al., 2010a). Conversely posteriorly-derived samples tended to exhibit high expression levels of genes involved in ion transport, including ionotropic neurotransmitters and transporters (Ip et al., 2010a).

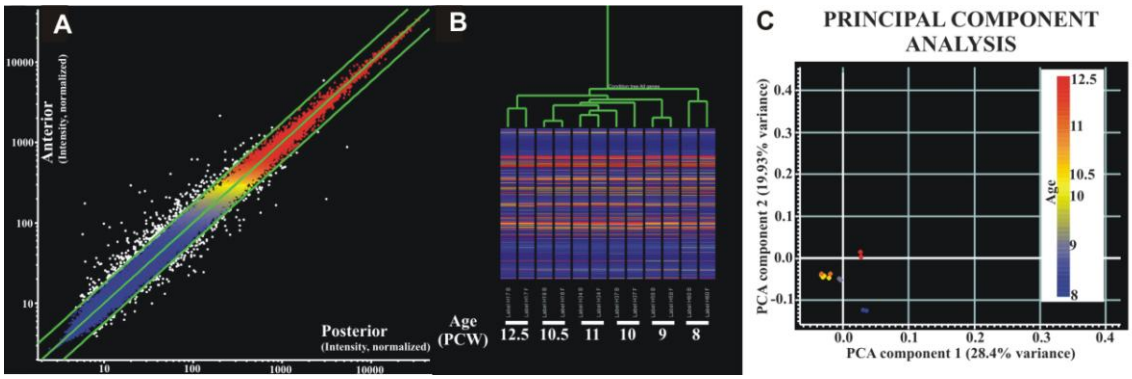

Figure 1.13. Affymetrix Chip Analysis of genes differentially expressed across the anterior-posterior axis of the developing human neocortex.

Scatter plot (A) showed expression levels of genes from posteriorly (X-axis) and anteriorly (Y-axis) plotted against each other. Genes marked in white correspond to those found to be differentially regulated along the anterior-posterior axis by at least 1.75-fold. Colours correspond to an arbitrary 'heatmap' indicating expression levels.

Condition tree (B), showing levels of all genes indicates that clustering of samples occurs in an age-dependent manner. At each indicated age 2 chips corresponding to levels of genes from anteriorly- and posteriorly-derived tissue are indicated.

Principal component analysis (C) revealed that age is one principal component variable in gene expression levels (principal component 2, Y-axis). The variance exhibited on the X-axis also highlights the differences between the closely clustering chips 9-11.5 PCW, and the two ages which cluster the least; 8 and 12.5 PCW. Chips are colour-labelled according to age (Blue 8 PCW, Grey 9 PCW, Yellow 10-10.5 PCW, Orange 11 PCW, and Red 12.5 PCW as indicated by the heatmap).

Performed by Dr. Nadhim Bayatti. Adapted from (Ip et al., 2010a).

1.5 Aims and Objectives

The development of anterior neocortical areas such as the motor cortex and the CSMN originating from this region in humans is of particular interest to our group since the potential anterior molecular determinants are yet to be identified in humans. Furthermore, the motor cortex and corticospinal tract is a common site of developmental brain damage leading to cerebral palsy (Eyre, 2007). In order to promote mechanisms that facilitate substitution or repair of these corticofugal neurones in the lesioned region, it is important to first localize their developmental origin. In addition, it is essential to identify genes that are related to these corticofugal neurones and investigate how these genes are regulated. Ultimately, the identification of regulatory mechanisms of corticofugal neurone- (especially CSMN-) related genes will facilitate potential future approaches aiming to promote population of endogenous stem cells or those from other source towards a corticospinal neurone phenotype.

The aim of the current project was to investigate graded gene expression in humans from the time when CP starts to emerge (8 PCW) to the innervation of thalamocortical afferents (around 12 PCW and above) in order to identify regulated genes that are related to the development of motor cortex and the associated corticofugal neurones. Additionally, in order to test the hypothesis that the anterior pole of the human neocortex may be an early site of the developing motor cortex harbouring corticofugal neurones including CSMN and to understand the development of this type of projection neurones, regulated candidate genes were then examined further to deduce the type and location of cells expressing them within the neocortex and/or along the axonal pathways of these subcerebral projection neurones. Furthermore, we sought to establish a human *in-vitro* regionalisation model in order to investigate the regulatory mechanisms of these candidate genes.

The objectives of this project were

1) to perform quantitative rtPCR to confirm the graded expression of a subset of genes identified previously by Affymetrix gene chip analysis between 8-12 PCW in humans, including a number of transcription factors, cell adhesion and axonal

guidance molecules and growth factors receptors, in which some are associated with corticospinal and other subcerebral projection neurones. (Chapter 3)

2) to verify laminar-enriched expression patterns of SATB2 and NURR1, which were to be used for demarcating various laminae in developing human neocortex, alongside with other laminar-enriched markers such as *ER81* and Growth-associated protein 43 (GAP43) by performing ISH and immunohistochemistry (IHC). (Chapter 4)

3) to investigate of the spatiotemporal expression patterns of the anteriorly-upregulated candidate genes that are associated with subcerebral projection neurones in the developing human brains by performing ISH and IHC. These anteriorly-upregulated candidate genes were the transcription factor *CTIP2;* axonal guidance molecule, *ROBO1* and its downstream signalling molecule, *Slit-Robo Rho GTPase activating protein 1* (*SRGAP1*). Other neuronal markers were also included for comparison as a) they are also known to be crucial for the development of subcerebral projection neurones in rodents but without obvious graded expression in developing human neocortex (*FEZF2* and *SOX5*); or b) they have laminar-enriched expression patterns in the rodent and/or human neocortex that aid the demarcation of various laminae (ER81, SATB2, NURR1, TBR1, GAP43 and Synaptophysin). (Chapter 5)

4) to establish a human *in-vitro* model of regionalisation by isolating cells from the anterior and posterior region of the neocortex and allowing them to grow separately in culture, and characterize this model by carrying out a) immunocytochemistry (ICC) with progenitor (Nestin), glial (GFAP), neuronal (CTIP2, MAP2, ROBO1 and SRGAP1) and some putative regionalisation markers (EMX2 and PAX6); and b) rtPCR with regulated genes as characterized *in-vivo*. Preliminary gene expression regulation study was initiated by stimulating cells with various treatments of FGFs and determined the changes in expression level of the anteriorly-upregulated candidate genes (*CTIP2*, *ROBO1* and *SRGAP1*) and the genes encoding receptors for FGFs (*FGFR1*, *-2* and *-3*) by rtPCR. (Chapter 6)

Chapter 2 Materials and Methods

2.1 Human Foetal Brains and Ethical Approval

Brains were dissected from human foetal and embryonic terminations of pregnancies obtained from the MRC-Wellcome Trust Human Developmental Biology Resource at Newcastle University (HDBR, http://www.hdbr.org). The HDBR has a license to act as a tissue bank from the Human Tissue Authority (license number 12534; Designated individual: Professor Andrew Hall) under Section 16 (2) (e) (ii) of the Human Tissue Act, 2004. The license authorizes "the storage of relevant material which has come from a human body for the use of a scheduled purpose". Ethical approval was obtained from the Newcastle and North Tyneside Research Ethics Committee (NREC, reference 08/H0906/21). The ethical approval covers the collection of the material for the HDBR tissue bank and all registered UK research projects including those of our group using material from the bank.

Tissue from ages between 8 and 17 PCW for tissue histological haematoxylin and eosin staining (H & E), ISH and IHC, quantitative rtPCR, dissociated cell cultures and Western blot were used. The number of samples used at each age in each study conducted in the current project was summarized in Table 2.1. Age was estimated from measurements of foot length and heel to knee length. These were compared with a standard growth chart (Hern, 1984).

	Studies	Experiments	Age (PCW)	Number of Samples (n=)
Ch.3	Confirmation of graded expression of subsets of genes identified by Affymetrix gene chip analysis	rtPCR	8	3
			10	4
			12	4
Ch.4	Verification of laminar-enriched expression patterns of *SATB2*/SATB2 and NURR1	H & E/ ISH/IHC	8	2
			9	2
			10	2
			12	2
			15	2
Ch.5	Analyses of spatial and temporal expression patterns of corticofugal projection neurone-associated genes and/or proteins	H & E ISH/IHC	8	3
			9	3
			10	3
			11	2
			12	1-2
			14	2
			15	2
			17	2
	Characterization of ROBO1 and SRGAP1 antibodies	WB	14	2
Ch.6	Characterization of *in-vitro* model of regionalisation (primary foetal brain cells culture)	rtPCR	11	4
		ICC (DAB)	11	4
		ICC (F)	11	1
	Preliminary gene expression regulation study: FGFs stimulation	rtPCR	10	1
			11	1
			12	1

Table 2.1. Number of samples used at each age for each study in the current project.

DAB, 3, 3'-Diaminobenzidine; F, fluorescence; H & E, haematoxylin and eosin staining; ICC, immunocytochemistry; IHC, immunohistochemistry; ISH, *in-situ* hybridization; rtPCR, real-time polymerase chain reaction; WB, Western blot.

2.2 Dissociated Cell Cultures

2.2.1 3-Day In-vitro Protocol

Both left and right neocortices were used for culture after removal of subcortical structures, temporal lobes and meninges of the brains. The neocortices were divided into three equal-sized slices along the anterior-posterior axis and cells were isolated from the anterior- and posterior-most slices and cultured separately. Short-term dissociated human foetal cell cultures were initiated according to an established rodent protocol with minor modifications (Figure 2.1; (Franke et al., 2000)). In brief, the anterior- and posterior-most neocortices were dissected under sterile conditions and briefly soaked in Ca^{2+}- and Mg^{2+}-free Dulbecco's phosphate buffered saline (DPBS, Invitrogen, Paisley, UK). The tissues were cut into small pieces trypsinized for 20 minutes in Ca^{2+}- and Mg^{2+}-free Hank's balanced salt solution (HBSS) containing 0.05% trypsin/ethylene diamine tetra-acetic acid (EDTA, Invitrogen). Trypsin action was terminated by transferring tissue pieces to HBSS supplemented with 10% heat-inactivated foetal calf serum (FCS, Invitrogen). The tissue was gently dissociated by trituration through a plastic pipette and passed through a 70 μm pore nitex mesh (Becton Dickinson, Oxford, UK). Cells were pelleted at 400 g for 5 minutes and re-suspended in minimum essential medium (MEM, Invitrogen) supplemented with 10% FCS. Cells were plated at 200,000 cells/cm^2 into 3.8 cm^2 12-well culture dishes (Falcon, Franklin Lakes, USA) and 1.3 cm^2 4-well SonicSeal Slides (Thermo Fisher Scientific, Thorn Business Park, UK) coated with poly-L-lysine (0.01% solution; molecular weight 70-150 kDa; Sigma-Aldrich, Poole, UK). After 24 hours (one day *in-vitro*, 1 DIV), cells were switched to serum-free MEM/1:1 F12 supplemented with 1:50 B27 (Invitrogen) for a further 48 hours (Figure 2.1). For characterization of this dissociated cell culture model, RNA was isolated from cells cultured under the above conditions after a total of 3 DIV and subjected to reverse transcription and rtPCR (see Section 2.3 and 2.4) or cells were fixed with 4% paraformaldehyde (PFA, Sigma-Aldrich)/PBS and subjected to immunocytochemistry (Section 2.9).

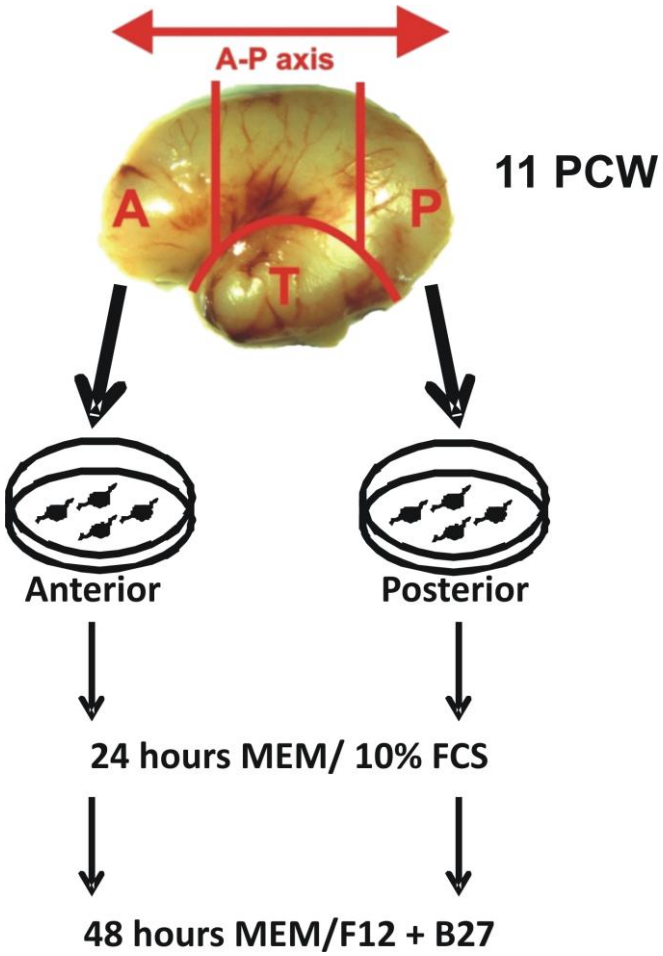

Figure 2.1 A schematic diagram showing method of dissecting brain slices for cell cultures.

After removal of meninges, temporal lobe (T), and subcortical material, tissue was dissected from the anterior (A) and posterior (P) neocortex, and subsequently dissociated and cultured separately. This example showed an 11 PCW brain (F3), which measured 30 mm along the anterior-posterior axis. FCS, foetal calf serum; MEM, minimum essential medium.

2.2.2 Treatment of Cell Cultures: Fibroblast Growth Factors Stimulation

After 1 DIV in 10% FCS/MEM, some cells isolated from the anteriorly- and posteriorly-derived tissues as above were treated with the fibroblast growth factors FGF2 (PeproTech, London, UK) or FGF8 (PeproTech) both at 20 ng/ml in serum-free 1:1 F12/1:50 B27/MEM for 24 hours (short-term) or 72 hours (long-term). Some cells were also treated with MEK inhibitor U0126 (10 μM; Merck, Feltham, UK) only or in addition to FGFs treatment for 24 hours (short-term) or 72 hours (long-term). For the 72-hour long-term stimulation, medium was changed every other day accordingly. The various treatments of anteriorly- and posteriorly-derived cells were summarized in Table 2.2. RNA was isolated from cells after completion of the treatments and subjected to reverse transcription and rtPCR (see Section 2.3 and 2.4).

Abbreviations	Treatments	Stimulation Time
C-24hr	Control – no treatment	24 hours
C-72hr		72 hours
C+U-24hr	U0126 alone (10 μM)	24 hours
C+U-72hr		72 hours
FGF2-24hr	FGF2 alone (20 ng/ml)	24 hours
FGF2-72hr		72 hours
FGF2+U-24hr	FGF2 (20 ng/ml) + U0126 (10 μM)	24 hours
FGF2+U-72hr		72 hours
FGF8-24hr	FGF8 alone (20 ng/ml)	24 hours
FGF8-72hr		72 hours
FGF8+U-24hr	FGF8 (20 ng/ml) + U0126 (10 μM)	24 hours
FGF8+U-72hr		72 hours

Table 2.2. Treatments of anteriorly- and posteriorly-derived cells.

2.3 RNA Isolation and Reverse Transcription

2.3.1 RNA Extraction and Reverse Transcription

For the production of digoxigenin (DIG)-labelled RNA probes, total RNA from a human foetal whole brain or neocortex aged between 8-12 PCW were isolated with Trizol/Chloroform (Invitrogen) according to the instructions of the manufacturer. For quantification of mRNA expression levels of target genes between the anterior and posterior part of the neocortex using rtPCR, right neocortices were used after removal of subcortical structures, temporal lobes and meninges of the brains and divided into 5 mm slices along the anterior-posterior axis (Figure 2.2). Total RNA was isolated from the anterior- and posterior-most of neocortical tissues and dissociated cell cultures using the PeqGOLD RNAPure reagent (Peqlab, Fareham, UK) according to the instructions of the manufacturer. Total RNA concentration was determined by spectrophotometric absorbance at 260 nm using NanoDrop 8000 (Fisher Scientific, Loughborough, UK). A total of 2 μg of RNA was reverse transcribed using 200 U/μl of SuperScript Reverse III Transcriptase Kit (Invitrogen) and 2 μg random hexadeoxynucleotides primers (Promega, Southampton Science Park, UK) in a final volume of 50 μl following the instructions of the manufacturers. The transcribed complementary (c)DNA template was used directly for the production of DIG-labelled RNA probes, whereas the concentration of the transcribed cDNA template was further diluted 2-fold prior rtPCR.

2.3.2 Genomic DNA Contamination Assessment

Genomic (g)DNA contamination of each cDNA sample used was assessed by standard PCR assay using *SDHA* primer sets (Table 2.3). The thermal cycle condition was 95˚C for 15 minutes; 40 cycles of 94˚C for 3 seconds, 60˚C for 40 seconds and 72˚C for 50 seconds, followed by 72˚C for 5 minutes. Positive control was incorporated by replacing cDNA sample with human gDNA sample. The amplified PCR products and 1kb Plus DNA ladder (10787-018; Invitrogen) were electrophorized on 1.5% agarose gel.

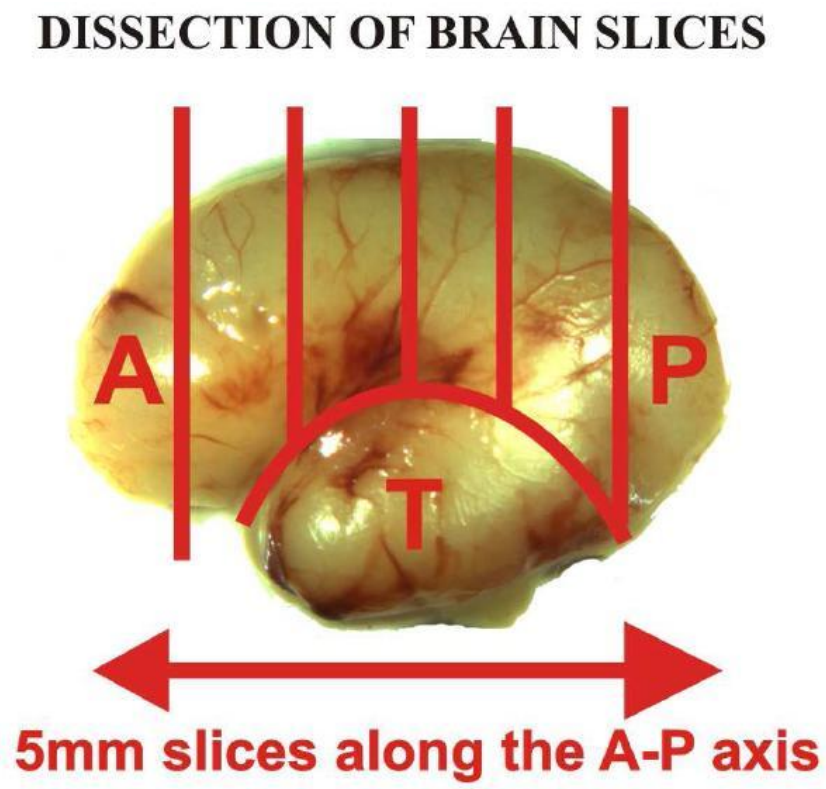

Figure 2.2. A schematic diagram showing method of dissecting brain slices for RNA extraction.

After removal of meninges, temporal lobe (T), and subcortical material, 5 mm coronal slices were cut coronally along the anterior-posterior axis. The most anterior (A) and posterior (P) slices were used in this study. This example showed an 11 PCW brain (F3), which measured 30 mm along the anterior-posterior axis. Adapted from (Ip et al., 2010a).

2.4 Quantitative real-time PCR (rtPCR)

The mRNA expression of various target genes in the anterior- and posterior-most of the neocortex and dissociated cultured cells were determined by rtPCR. The sequence-specific primer sets (Eurofins MWG Operon, Raynes Park, UK), designed using Primer3 (http://frodo.wi.mit.edu/primer3/) except *PAX6* (which was obtained from the PrimerBank, PrimerBank ID: 4505615a1, http://pga.mgh.harvard.edu/primerbank/), and amplicon sizes for all target genes were listed in Table 2.3.

Primer sets	5' to 3' Sequence		Amplicon size (bp)
	Forward Primers	Reverse Primers	
***β-ACTIN**	CTACAATGAGCTGCGTGTGGC	CAGGTCCAGACGCAGGATGGC	271
CNTNAP2	TGTCCTTCAGCCTTCATTCC	TGACATTCGCGAAACTTCC	110
COUPTFI	GAGCTGTTCGTGCTCAACG	ACCTGCTCCTGGAAGATGC	146
CTIP2	CAGAGCAGCAAGCTCACG	GGTGCTGTAGACGCTGAAGG	102
EMX2	TCCAAGGGAACGACACTAGC	TCTTCTCAAAGGCGTGTTCC	126
FEZF2	ACACGCATATCCGCATCC	AGGCCTTGTTGCAGATGG	147
FGFR1	CGTCTACAAGATGAAGAGTGG	GAGTCAGCAGACACTGTTACC	114
FGFR2	CTCTTCAACGGCAGACACC	CACTTGCCCAAAGCAACC	133
FGFR3	GTGCACAACCTCGACTACTAC	GATCATGTACAGGTCGTGTG	255
***GAPDH**	TGCACCACCAACTGCTTAGC	GGCATGGACTGTGGTCATGAG	86
MAP2	TTCCTCCATTCTCCCTCCTC	TCTGCGAATTGGCTCTGAC	121
PAX6	ATGTGTGAGTAAAATTCTGGGCA	GCTTACAACTTCTGGAGTCGCTA	103
PCDH17	GTTCCCAGAACTGGTCATCC	TGTCGTTGGAGTCAATCACC	143
ROBO1	TTGTGAGGGCAGCTAATGC	TCTCTGGACCTGCTTGTGG	116
ROBO2	AAAGAAGGCAGCCAGAACC	TCGGAACGTTGAATGTTGG	110
***SDHA**	TGGGAACAAGAGGGCATCTG	CCACCACTGCATCAAATTCATG	84
SOX5	ATGACCATGATGCTGTCACC	TTCACAACAGCCACCTTCC	103
SRGAP1	CCAACATTGATGCCTGTCC	TCTCATAAACAGGGCCATCC	139
S100A10	GGAACACGCCATGGAAAC	CCACAGCCAGAGGGTCTTT	143

Table 2.3. List of Primers for rtPCR.

Gene-specific primer sequences used for rtPCR. * indicates housekeeping genes. *CNTNAP2*, *Contactin-associated protein-like 2*; *GAPDH*, *Glyceraldehyde-3-phosphate dehydrogenase*; *MAP2*, *Microtubule-associate protein 2*; *SDHA*, *Succinate dehydrogenase complex subunit A*; *S100A10*, *S100 calcium binding protein A10*. Adapted from (Ip et al., 2010a).

2.4.1 Restriction Enzyme Digestion

The identities of amplified PCR products (PCR condition as described in Section 2.3.2) were confirmed using restriction enzyme digestion. The restriction enzymes used for each target gene were listed in Table 2.4. Single or double restriction sites in each sequence were identified by NEBcutter v2.0 (http://tools.neb.com/NEBcutter2/). 1 µg of amplified PCR product of each gene was used for the restriction digestion according to the instruction of the manufacturers and subsequently resolved by running the reaction mixture alongside with their undigested PCR products and 1 kb Plus DNA ladder (10787-018; Invitrogen) on 2% agarose gel. Upon failure of the reaction, the original amplified PCR products were gel extracted using Qiagen gel extraction kit (Qiagen, Crawley, UK) and 2 ng/µl of purified samples were sent off for direct sequencing with their forward primers (Eurofins MWG Operon Sequencing Service).

Target Genes	Restriction Enzymes	Cut position	Product size (bp)
CNTNAP2	DpnI (#R0176; New England BioLabs, Ipswich, UK)	50	50+60
COUPTFI	SphI (#R0182S; New England BioLabs)	75	75+71
CTIP2	DpnI	42	42+60
EMX2	HaeIII (#R6171; Promega)	50	50+76
FEZF2	HphI (#R0158S; New England BioLabs)	65	65+82
FGFR1	HaeIII	67	67+47
FGFR2	PpuMI (#R0506S; New England Biolabs)	57	57+76
FGFR3	DdeI (#R6291; Promega)	65	65+190
MAP2	DdeI	25, 33	25+8+88
PCDH17	HphI	49, 124	49+75+19
ROBO1	EcoRI (#R6011; Promega)	66	66+50
ROBO2	DdeI	60	60+50
SOX5	HphI	16	16+87
SRGAP1	HaeIII	124	124+15
S100A10	DdeI	77	77+66

Table 2.4. List of restriction enzymes for target genes.

Restriction enzymes used for confirmation of PCR products identities. Single or double cutting positions in each sequence and the size of the resulting fragments were also stated.

2.4.2 rtPCR

Three housekeeping genes, *β–ACTIN*, *GAPDH* and *SDHA* were used as internal reference to normalize the cDNA template between different samples. Negative control was incorporated by replacing the cDNA template with Molecular Biology grade water (VWR International, Lutterworth, UK). The SYBR Green-based rtPCR assay was performed in 7900HT Fast Real-Time PCR system (Applied Biosystems, Warrington, UK). A total volume of 10 µl rtPCR reaction was set up in triplicates, containing 5 µl of 2x SYBR Green rtPCR Master Mix (Invitrogen), 1 µl of the diluted cDNA template, 0.5 µl of each primer (10 ρmol/µl), and 3 µl of Molecular Biology grade water. The thermal cycle protocol for SYBR Green-based rtPCR assay was 95°C for 15 minutes followed by 40 cycles of 95°C for 15 seconds, 60°C for 30 seconds, 72°C for 30 seconds and 74°C for 10 seconds. Amplification of a single PCR product was confirmed by dissociation curve analysis of PCR products (68°C for 10 seconds followed by 99°C for 10 seconds) after completion of each rtPCR reaction. Baseline was set automatically by the machine and threshold was set manually above all the background signals. The data obtained were analyzed with the qBase software (Hellemans et al., 2007).

Normalized relative quantities (NRQ) of mRNA expression were calculated in qBase and NRQ data was presented with fold changes calculated for each gene comparing the two regions of the neocortex or cells ± standard error of mean (S.E.M.). A paired Student's *t*-test was performed to determine the significance of differences on expression levels from anteriorly- and posteriorly-derived neocortical tissue or cells of the same age ($p \leq 0.05$). Two-way analysis of variance (ANOVA) was performed to determine the significance of differences on expression levels from anteriorly- and posteriorly-derived neocortical tissues of different ages ($p \leq 0.05$), taking into account of the covariate of various sample ages. Factors causing significant differences on gene expression levels were subjected to post-hoc analysis (Least significant difference test, LSD test) to determine the effect of the factors on gene expression levels ($p \leq 0.05$). NRQ of mRNA expression for each gene of interest in anteriorly- or posteriorly-derived cells after various treatments were also calculated in qBase. Changes of their expression level were calculated and presented as fold changes ± S.E.M. between (1) FGFs-treated and control groups (FGFs/C) or (2) FGFs-, U0126-treated and U0126 alone-treated

groups (FGFs+U/C+U). A paired Student's *t*-test was performed to determine the significance of differences in expression levels in FGFs-treated and control groups as well as in FGFs-, U0126-treated and U0126 alone-treated groups ($p \leq 0.05$). Comparisons of fold changes between (1) and (2) were also made to examine the effects of the MEK inhibitor. A paired Student's *t*-test was performed to determine the significance of differences in fold changes between (1) and (2) ($p \leq 0.05$). The average of Ct values ± S.E.M. of the reference genes used from the 3 samples were also calculated to show if there was any effects of various treatments to their expression levels.

2.5 Tissue Processing and Sectioning

Tissue fixation and processing was performed by HDBR staffs after collection of samples. Prior to sectioning, brains were fixed for at least 24 hours at 4ºC in 0.1M PBS containing 4% PFA (Sigma Aldrich). Whole or half brains (divided sagittally) were transferred to 70% ethanol for storage at 4ºC prior to overnight tissue processing (70% ethanol for 15 minutes, 100% ethanol for 45 minutes, 100% ethanol for 1 hour twice, xylene for 45 minutes, xylene for 1 hour twice, wax for 1.5 hours, wax for 1 hour 45 minutes twice; Shandon Pathcentre Tissue Processor, Thermo Scientific, Epsom, UK) and paraffin embedding. 8 μm-thick paraffin sections were cut sagittally or coronally, mounted on slides, and used for tissue ISH and IHC. Brainstems subjected to frozen sectioning were cryoprotected in 30% sucrose/PBS after fixation in 4% PFA/PBS for at least 24 hours. 70 μm-thick sections were cut on freezing microtome and collected in PBS. These tissue sections were used for immunohistochemistry.

2.6 Haematoxylin and Eosin (H & E) Histological Staining

Paraffin sections were dewaxed in xylene for 5 minutes and rehydrated in serial dilution of ethanol with decreasing concentrations and then water for 3 minutes each. Dewaxed sections were initially stained with filtered Harris haematoxylin stain (Raymond A Lamb Ltd, Eastbourne, UK) for about 1 minute and rinsed in water. Sections were then treated briefly with acid alcohol (95% ethanol/1% concentrated hydrochloric acid (Sigma-Aldrich)) for 2 seconds to reduce the haematoxylin stain and rinsed in water. Nuclei of cells in sections became blue when treated with the weakly alkaline Scott's tap water substitute (3.5 grams sodium bicarbonate (Sigma-Aldrich), 20 grams magnesium sulphate (Sigma-Aldrich) in 1 litre of distilled water) for 10 seconds and then rinsed in water. The cytoplasmic components of cells in sections were stained pink when treated with filtered eosin stain (1% aqueous, Raymond A Lamb Ltd) for 30 seconds, and then rinsed in water. All H & E stained sections were dehydrated in increasing concentrations of ethanol, cleared in xylene and mounted in DPX mountant (Merck).

2.7 Tissue *in-situ* Hybridization (ISH)

2.7.1 Manufacturing of Probes

Primers (Eurofins MWG Operon) were designed using Primer3. The primers were designed with SP6 or T7 consensus sequences upstream to the forward (FP) and reverse (RP) gene-specific primer sequences respectively. The FP and RP sequences are listed in Table 2.5. DIG-labelled RNA probes were manufactured according to the protocol published previously (Bayatti et al., 2008b) with some modifications. In brief, gene-specific sequences were amplified by two rounds of PCR (95˚C for 15 minutes; 40 cycles of 94˚C for 3 seconds, 55-65˚C for 40 seconds and 72˚C for 50 seconds, followed by 72˚C for 5 minutes) and purified using Qiagen gel extraction kit (Qiagen). 75 ng of purified gene-specific cDNA was used for *in-vitro* transcription using DIG-RNA labelling kit (SP6/T7; Roche, Welwyn Garden City, UK). The concentration and quality of DIG-labelled RNA probes was assessed by spectrophotometric absorbance at 260 nm using NanoDrop 8000 (Fisher Scientific, Loughborough, UK), 1.5% agarose gel electrophoresis and dot blot.

Genes	GenBank accession numbers	Probe sequences	Primer sequences*	Product size
CTIP2	NM_138576.2	1892-2351	SP6 (FP) 5'-AATACGATTTAGGTGACACTATAGAATACAGGAGCTGCTACTGGAGAACGAA-3'	517 bp
	NM_022898.1	1679-2138	T7 (RP) 5'-TAAGTTAATACGACTCACTATAGGGCGATCCAGGTCCTTCTCCACCTTGAT-3'	
ER81	NM_004956.4	1609-2173	SP6 (FP) 5'-AATACGATTTAGGTGACACTATAGAATACTGACACCTGTGTTGTCCCAGAAA-3' T7 (RP) 5'-TAAGTTAATACGACTCACTATAGGGCGACCATGTCTGTCTTCAGCAGTGGA-3'	464 bp
	NM_001163147.1	1343-1907		
	NM_001163148.1	1151-1715		
	NM_001163149.1	1022-1586		
	NM_001163150.1	1088-1652		
	NM_001163151.1	1034-1598		
	NM_001163152.1	899-1463		
FEZF2	NM_018008.3	1120-1531	SP6 (FP) 5'-AATACGATTTAGGTGACACTATAGAATACAAACTTCACCTGCGAGGTGTGC-3' T7 (RP) 5'-TAAGTTAATACGACTCACTATAGGGCGAGTTGTGGGTGTGCATATGGAAGG-3'	469 bp
ROBO1	NM_002941.2	4013-4499	SP6 (FP) 5'-AATACGATTTAGGTGACACTATAGAATACTAGCCAAGATGCAAACCAGAAGG-3'	544 bp
	NM_133631.1	4859-5345	T7 (RP) 5'-TAAGTTAATACGACTCACTATAGGGCGATGTGTCTTGGATTGGGCAGTAGG-3'	
SATB2	NM_015265.2	711-1262	SP6 (FP) 5'-AATACGATTTAGGTGACACTATAGAATACTTAGCCAAAGAATGCCCTCTCTCC-3' T7 (FP) 5'-TAAGTTAATACGACTCACTATAGGGCGACCTCTTCAGCTCATCTCTGACTTGC-3'	552 bp
SOX5	NM_006940.4	1832-2257	SP6 (FP) 5-AATACGATTTAGGTGACACTATAGAATACCCTTTCCTGACATGCACAACTCC-3' T7 (RP) 5'-TAAGTTAATACGACTCACTATAGGGCGACCTCTCCTTTCACACCGTAAGTGC-3'	483 bp
	NM_152989.2	2062-2487		
	NM_178010.1	594-1019		

Table 2.5. List of primers for manufacturing of probes.

Gene-specific primer sequences used for the manufacturing of probes. Sequences underlined were gene-specific. FP, forward primer; RP, reverse primer.

2.7.2 Tissue ISH

Tissue ISH was performed with modifications from the previously published method (Bayatti et al., 2008b). Briefly, paraffin sections were dewaxed 3 times in xylene and in 1:1 xylene/ethanol, before rehydrated in serial dilutions of ethanol in Molecular Biology grade water. Sections were rinsed in diethypyrocarbonate-treated PBS and subsequently treated with 20 µl/ml proteinase K (Sigma-Aldrich) in PBS for 8 minutes at room temperature. Sections were post-fixed in 4% PFA/PBS buffer for 20 minutes at room temperature, washed in PBS, and treated with 0.1 M triethanolamine (Sigma-Aldrich, pH 8.0)/0.25% acetic anhydride (Sigma-Aldrich)/0.2% concentrated hydrochloric acid in PBS for 10 minutes at room temperature. Sections were dehydrated in increasing concentrations of ethanol and then air-dried by filtered air stream. DIG-labelled sense and antisense probes (300 ng) were used with 100 µl of DIG Easy Hyb mixture (Roche). Probe/Hyb mix (200 µl) was used per slide, covered with glass coverslips. Slides were incubated in a hybridization chamber overnight at 68ºC. Afterwards, sections were rinsed in 5x sodium citrate (SSC, pH 7.2) at 65ºC and subsequently washed twice in 2x SSC, then in 0.2x SSC at 50ºC and in 0.2x SSC at room temperature. Sections were rinsed in 0.1 M Tris (pH 7.6)/0.15 M NaCl (Buffer 1) and blocked with 10% FCS/Buffer 1 for 1 hour at room temperature. After blocking, sections were incubated with alkaline phosphatase-conjugated anti-DIG antibody (Roche; diluted 1:1000 in 2% FCS/Buffer 1) overnight at 4ºC. After antibody incubation, sections were washed 6 times in Buffer 1 at room temperature for 30 minutes each. Detection of probes was achieved by addition of NBT/BCIP solution (Roche; 20 µl/ml) in 0.1 M Tris (pH 9.5)/0.1 M NaCl (Buffer 2). The colour reaction was stopped by rinsing slides in Buffer 2 and distilled water. Sections were mounted in Aquamount (Merck).

2.8 Immunohistochemistry (IHC)

2.8.1 Immunoperoxidase-histochemistry

Paraffin sections were dewaxed twice in xylene for 10 minutes and rehydrated in decreasing concentration of ethanol. Subsequently, sections were treated with 3% hydrogen peroxide (Sigma-Aldrich) in methanol for 10 minutes to quench the endogenous hydrogen peroxidase activities, and boiled in 10 mM citrate buffer (pH 6.0) to unmask the epitopes. Sections were incubated with primary antibodies and 3% appropriate blocking serum (Vector Laboratory, Peterborough, UK) in 0.1% Triton X-100/PBS (PBS-T) in a moist chamber at 4˚C overnight. Frozen sections were incubated free floating with primary antibodies and 3% appropriate blocking serum in 0.1% PBS-T at 4˚C overnight with gentle agitation. Table 2.6 provides details of all the primary antibodies used. Negative control involving omission of primary antibodies was carried out to ensure the specificity of secondary antibodies and streptavidin-horseradish peroxidase (HRP) used. After washing 3 times in 0.1% PBS-T for 5 minutes each, sections were incubated with appropriate biotinylated-secondary antibodies (Table 2.7; Vector Laboratory, 1:200 in 0.1% PBS-T) at 4˚C for 2 hours. Subsequently, sections were washed 3 times in 0.1% PBS-T for 5 minutes each after they were incubated with streptavidin-HRP (Vector Laboratory, 1:200 in 0.1% PBS-T) at 4˚C for 1 hour. After incubation, sections were washed 3 times in 0.1% PBS-T for 5 minutes each then incubated with 3, 3'-Diaminobenzidine Enhanced Liquid Substrate System (DAB, Sigma-Aldrich) for up to 10 minutes before washing in PBS. Frozen sections were mounted on glass slides and air-dried overnight. All sections were dehydrated in increasing concentration of ethanol, cleared in xylene and mounted in DPX mountant (Merck).

Primary Antibodies	Host Species, Company	Working Concentration						References
			IHC		ICC		WB	
		DAB-P	F-P	DAB-Fr	DAB	F		
β-ACTIN	Goat polyclonal, Santa Cruz sc1616	---	---	---	---	---	1:500	(Zschocke et al., 2005)
CTIP2	Rat monoclonal, Abcam ab18465	1:1000	1:500	---	1:1000	1:500	---	(Kwan et al., 2008; Lai et al., 2008; Arlotta et al., 2005)
EMX2	Rabbit polyclonal, Sigma E6780	---	---	---	1:1000	---	---	(Bayatti et al., 2008b)
GAP43	Mouse monoclonal, Sigma G9264	1:1000	---	1:5000	---	---	---	(Bayatti et al., 2008a)
GFAP	Mouse monoclonal, Sigma G3893	---	---	---	1:400	1:400	---	(Bayatti et al., 2008a)
MAP2	Mouse monoclonal, Sigma M4403	---	---	---	1:1000	1:200	---	(Bayatti et al., 2008a)
NESTIN	Mouse monoclonal, Chemicon MAB5326	---	---	---	1:400	1:400	---	(Gu et al., 2002; Messam et al., 2002)
NURR1	Goat polyclonal, R & D Systems AF2156	1:200	---	---	---	---	---	(Hoerder-Suabedissen et al., 2009; Wang et al., 2010)
PAX6	Rabbit polyclonal, Covance PRB-278P	---	---	---	1:300	---	---	(Bayatti et al., 2008a)

ROBO1	Rabbit polyclonal, Abcam ab7279	1:4000	1:100	1:10000	---	1:100	1:1000	(Lindenmeyer et al., 2010; Marlow et al., 2010; Sheldon et al., 2009; Siegel et al., 2009)
SATB2	Mouse monoclonal, Abcam ab51502	1:400	1:100	---	---	---	---	(Azim et al., 2009; Alcamo et al., 2008; Britanova et al., 2008)
SOX5	Rabbit polyclonal, Sigma AV33323	1:200	1:100	---	---	---	---	(Kwan et al., 2008)
SRGAP1	Mouse monoclonal, Abcam ab57504	1:900	1:100	1:1000	---	1:100	1:200	---
TBR1	Rabbit Polyclonal, Abcam ab31940	1:500	1:500	---	---	---	---	(Bayatti et al., 2008a)
TBR2	Rabbit Polyclonal, Abcam ab23345	---	1:200	---	---	---	---	(Bayatti et al., 2008a)

Table 2.6. Details of primary antibodies used for fluorescence (F-) or chromogen-based (DAB-) immunohistochemistry (IHC) on paraffin (P) or frozen (Fr) sections, immunocytochemistry (ICC) and Western blot (WB).

Primary Antibody Species	Serum	Secondary Antibodies for IHC/ICC		Secondary Antibodies for WB
		DAB	F	
Goat	Horse	Biotinylated-Horse Anti-Goat IgG	---	HRP-Horse Anti-Goat IgG
Mouse	Horse	Biotinylated-Horse Anti-Mouse IgG	Cy3-Horse Anti Mouse IgG	HRP-Horse Anti-Mouse IgG
Rabbit	Goat/Sheep	Biotinylated-Goat Anti Rabbit IgG	Alexa Fluor 488 Goat Anti-Rabbit IgG Cy3-Sheep Anti-Rabbit IgG	HRP-Goat Anti-Rabbit IgG
Rat	Goat	Biotinylated-Goat Anti-Rat IgG	Alexa Flour 488 Goat Anti-Rat IgG	HRP-Goat Anti-Rat IgG

Table 2.7. Details of serum block and secondary antibodies used for fluorescence (F-) or chromogen-based (DAB-) immunochemistry (IHC), immunocytochemistry (ICC) and Western blot (WB).

HRP, horseradish peroxidase. Ig, Immunoglobulin.

2.8.2 Immunofluorescent-histochemistry

Paraffin sections were dewaxed twice in xylene for 10 minutes and rehydrated in decreasing concentration of ethanol. Sections were boiled in 10mM citrate buffer (pH 6.0) to break protein cross-links and unmask the epitopes in PFA-fixed tissue sections. Double-labelling was performed by incubating sections with primary antibodies in 3% appropriate blocking serum (Vector Laboratory) in 0.1% PBS-T on slide in a moist chamber at 4˚C overnight. Table 2.6 and Table 2.7 provide details of all the serum, primary and secondary antibodies used. After washing 3 times in 0.1% PBS-T for 5 minutes each, sections were incubated with appropriate fluorochromes-conjugated secondary antibodies (Invitrogen, Sigma-Aldrich, 1:200 in 0.1% PBS-T) at room temperature for 30 minutes in the dark. Sections were then incubated with 4',6-diamidino-2-phenylindole (DAPI) nucleic acid stain (Invitrogen, 1:10000 in 0.1% PBS-T) for 5 minutes at room temperature in the dark and washed twice in 0.1% PBS-T for 5 minutes each and rinse once in distilled water. Sections were mounted in Vectashield mounting medium (Vector Laboratory) and kept in the dark at 4˚C until examination.

2.9 Immunocytochemistry (ICC)

After fixation with 4% PFA/PBS, cells were washed 3 times with PBS and incubated with primary antibodies and 3% appropriate blocking serum (Vector Laboratory) in 0.1% PBS-T in a moist chamber at 4˚C overnight with gentle agitation. Table 2.6 provides details of all primary antibodies used. After washing 3 times in 0.1% PBS-T, cells cultured in 3.8 cm^2 12-well plates were incubated with appropriate biotinylated secondary antibodies (Table 2.7; Vector Laboratory, 1:200 in 0.1% PBS-T) at 4˚C for 2 hours. Alternatively, cells cultured in 1.3 cm^2 4-well SonicSeal slides were incubated with appropriate fluorochromes-conjugated secondary antibodies (Table 2.7; Invitrogen, Sigma-Aldrich, 1:200 in 0.1% PBS-T) at room temperature for 30 minutes in the dark. Subsequently, cells were washed 3 times in 0.1% PBS-T. Biotinylated-antibody-treated cells were then incubated with streptavidin-HRP (Vector Laboratory, 1:200 in 0.1% PBS-T) at 4˚C for 1 hour. After incubation, cells were washed 3 times in 0.1% PBS-T then incubated with DAB (Sigma-Aldrich) for up to 10 minutes before washing in PBS. All cells were then incubated with DAPI nucleic acid stain (Invitrogen, 1:10000 in 0.1% PBST) for 5 minutes at room temperature in the dark and subsequently washed 3 times in PBS. Cells in 12-well plates were kept in PBS at 4˚C in the dark until examination by light and fluorescent microscopy. The wells of the SonicSeal slides were snapped off and mounted in Vectashield mounting medium (Vector Laboratory). The slides were kept in the dark at 4˚C until examination by confocal microscopy.

2.10 Image Acquisition

2.10.1 Light Microscopy

DIG-RNA labelled, immunoperoxidase-stained sections and cells were examined using Axioplan 2 and Axiovert 200 microscope equipped with different objectives (Plan-NeoFluar, 1.25x /0.035, 2.5x /0.075, 5x /0.15, 10x /0.30, 20x /0.50, 40x /1.3 Oil). Both microscopes were coupled with Axiocam microscope digital camera (0.5x). Adobe Photoshop CS3 was used to convert images to grayscale with resolution set at 300 pixels/inches. Figures and labelling were made using CorelDRAW 11.

2.10.2 Fluorescent Microscopy

Epi-fluorescence microscopy was carried out on fluorescent dye-stained sections using a Zeiss Axio Imager Z1 microscope using the following objectives, EC Plan NeoFluar 2.5x /0.075, EC Plan NeoFluar 5x /0.15, EC Plan NeoFluar 10x /0.3, EC Plan NeoFluar 20x /0.5 and Plan Apochromat 40x /1.3 Oil. Sections were triple stained with DAPI, Alexa Fluor 488 and Cy3. The excitation source was a Mercury short arc lamp (HBO 100 W/2) and images were generated using the following filter sets, Zeiss filter set 49HE for DAPI, Zeiss filter set 38HE for Alexa Fluor 488 and Zeiss filter set 20HE for Cy3. Images were captured using an AxioCam HRm cooled monochrome digital camera in combination with the Axiovision 4.7 software package. Adobe Photoshop CS3 was used to merge images and impose false colours by assigning images into green, red and blue channels accordingly to show co-localization of expression.

2.10.3 Confocal Microscopy

Double-labelled cells were imaged using a Zeiss LSM 510 META confocal scan head mounted on a Zeiss Axiovert 200M platform, using a 20x /0.5 Plan NeoFluar objective. Sequential excitation at 488 nm and 543 nm was provided by Argon (5% power) and Helium-Neon (100% power) gas lasers, respectively. Emission filters BP 500-530 nm

and BP 565-615 nm were used for collecting Alexa Fluor 488 and Cy3 signal in channels 2 and 3 respectively. Images, with a frame size of 1024x1024 and a 4x line average, were captured using the Zeiss LSM 510 v.3.0 software**.**

2.11 Quantification

2.11.1 Densitometry

Quantification of expression levels of *ROBO1*, SRGAP1 and *CTIP2* was performed to confirm their tangential expression gradients, using the image processing program ImageJ (National Institute of Health, NIH; http://rsbweb.nih.gov/ij/). Photographs were taken from the anterior- and posterior-most extents of sagittal sections at 8, 9 and 10 PCW for comparison (n=2 for each stage and at least 3 sections for each embryo/foetus were used for statistical analysis). All photographs were taken with the same exposure time and cropped to similar widths. The average optical density of histological staining in the CP (expression detected in this layer throughout all investigated stages) and VZ (considered background staining throughout all investigated stages) were measured in rectangular boxes of equal widths, which spanned the thickness of the CP or the VZ, and were placed adjacently. To take into account of background staining, the ratio of mean grey values in the CP to the VZ was calculated. A paired Student's *t*-test was performed to determine the significance of expression level differences between the anterior and posterior regions ($p \leq 0.05$).

2.11.2 Cell Count

Quantification analysis was carried out with immunoperoxidase-stained cells which were counter-stained with DAPI nucleic acid stain. Images of four random fields of view were taken for each antibody stained. The same objective (Plan NeoFluar 20x /0.50) was used to take all images required for counting cells to ensure the surface area examined was constant for all samples (n=4). Adobe Photoshop CS3 was used to assign DAB staining to the red channel and DAPI to green. The percentage number of stained cells was calculated from counting numbers of specifically-labelled cells (red + yellow) and comparing with total number of cells (red + green + yellow). An example of PAX6/DAPI stained images together with the false-colour image was demonstrated in Figure 2.3. When comparing the expression levels between the anterior- and posterior-

derived cultures, a Student's paired *t*-test was performed and significance was set at $p \leq 0.05$.

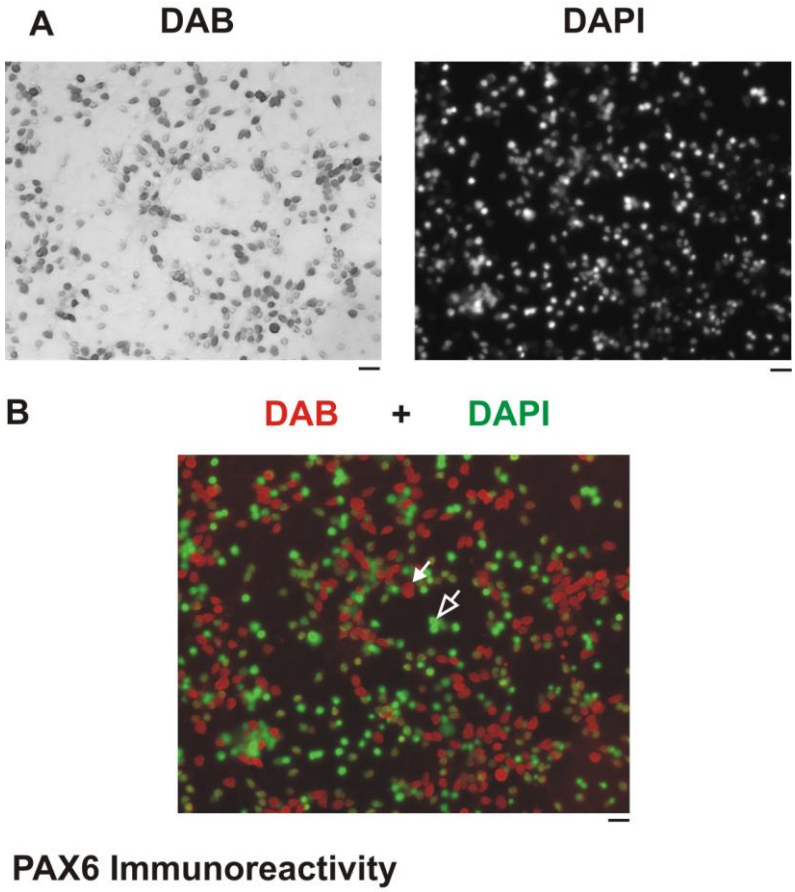

Figure 2.3. Immunocytochemistry Cell Counting Method.

(A) Cells immunoreactive for PAX6 were stained with DAB and counter-stained with DAPI. (B) For counting purpose, false-colour image was created by assigning DAB-staining to the red channel (filled arrowhead) and DAPI to green (empty arrow head). Scale bars indicate 20 µm.

2.12 Sodium Dodecyl Sulphate Polyacrylamide Gel Electrophoresis (SDS-PAGE) and Transfer

For characterization of some antibodies used in the studies, SDS-PAGE and Western blot was carried out. The procedures of SDS-PAGE electrophoresis and transfer were adapted from the Invitrogen NuPAGE Technical Manual and summarized below.

10 μg of protein sample was heated in 1x NuPAGE® lithium dodecyl sulfate (LDS) sample buffer (Invitrogen), 1x NuPAGE® reducing agent (Invitrogen) and distilled water. The boiling of sample at 70°C for 10 minutes accelerated the denaturation and unfolding of the proteins in the presence of the above ingredients. A discontinuous system for SDS-PAGE was performed using the NuPAGE® Novex Bis-Tris Gels with the 10-well, 4% polyacrylamide stacking gel which was placed above 4-12% polyacrylamide resolving gel of 1 mm thickness to separate proteins according to their molecular weights, which could be determined by running samples alongside with the Novex® Sharp unstained protein standards (LC5801; Invitrogen). NuPAGE® MOPS SDS Running Buffer with NuPAGE® Antioxidant (Invitrogen) was used. When an electric field (200 V, start: 100-115 mA/gel, end: 60-70 mA/gel, 50 minutes) is applied to SDS-denatured proteins in an SDS-PAGE gel matrix, the larger the denatured proteins, the more frequent the proteins were entangled in the gel matrix and thus the slower they moved through the gel.

NuPAGE® Transfer Buffer with NuPAGE® Antioxidant (Invitrogen) was used for transferring proteins from the gel onto pre-cut PVDF membrane (Invitrogen). Upon application of an electric field (30 V, 1 hour) separated proteins were transferred from the gel onto the membrane via hydrophilic and hydrophobic interactions between the membrane and proteins. After transfer, the membrane was equilibrated in distilled for 5 minutes. The efficiency of transfer was assessed by staining the membrane with 1x Ponceau (0.02% Ponceau, 0.3% trichloracetic acid, 0.3% sulphosalicylic acid).

2.13 Western Blot

1x Ponceau was removed by rinsing several times with distilled water. Blocking of non-specific binding was achieved by placing the membrane in the blocking buffer (5% non-fat dried milk, 0.05% Tween 20 (Sigma Aldrich) in 1x Tris-based buffer (TBS), pH 7.6) for 15 minutes twice at room temperature. The membrane was probed for the protein of interest with respective primary antibodies at 4°C overnight in antibody buffer (0.5% non-fat dried milk, 0.05% Tween 20 in 1x TBS buffer pH 7.6). β–ACTIN was used as a positive control. Optimal antibodies concentration was listed in Table 2.6.

The membrane was subjected to a 10-minute wash in wash buffer (0.05% Tween 20 in 1x TBS pH7.6) for 3 times before and after the secondary antibodies probing to rinse off any unbound antibodies. Appropriate species immunoglobulin HRP-linked secondary antibodies (Table 2.7; Vector Laboratory) in the antibody buffer were used at a final dilution of 1/1000 for 2 hours at room temperature. Immunoreactivity was detected using the SIGMAFAST DAB Tablet set (DAB tablet set in 5 ml distilled water) with developing time up to 20 minutes.

Chapter 3 Investigating Gradients of Gene Expression involved in Early Human Neocortical Development

3.1 Aim of Study

The aim of this chapter is to confirm the differential expression for a subset of genes identified by Affymetrix whole genome chip array and listed in Table 3.1 using rtPCR in neocortical tissue.

A number of known posterior markers were identified, including *FGFR3, COUPTFI* and *EMX2* (O'Leary and Nakagawa, 2002; Zhou et al., 1999; Simeone et al., 1992). Anteriorly, a number of potential markers of frontal and motor cortex as well as corticofugal neurones were observed including *CNTNAP2* (Abrahams et al., 2007), *PCDH17* (Kim et al., 2007), *S100A10*, *CTIP2* (Arlotta et al., 2005), *ROBO1* (Sundaresan et al., 2004) and its downstream signalling molecule *SRGAP1* (Wong et al., 2001). Some other genes were also included (Table 3.2) as they are expressed highly in the developing brains but exhibited no or small fold changes in expression when comparing levels in anteriorly- vs. posteriorly-derived tissue such as *FGFR* family members: *FGFR1* and *FGFR2* (Ford-Perriss et al., 2001), the transient anterior marker: *PAX6* (Bayatti et al., 2008b), a *ROBO* family member: *ROBO2* (Yue et al., 2006), the corticofugal neurone-related transcription factor: *FEZF2* (Chen et al., 2008; Chen et al., 2005a; Molyneaux et al., 2005), as well as the Layer VI/SP/corticothalamic neurone-associated transcription factor: *SOX5* (Kwan et al., 2008; Lai et al., 2008) and the pan-neuronal marker: *MAP2* (Bernhardt and Matus, 1984).

383 probe sets >1.75-fold in anterior compared to posterior neocortex			**154 probe sets >1.75-fold in posterior compared to anterior neocortex**		
Gene	**Fold**	**Function**	**Gene**	**Fold**	**Function**
PCDH17	2.84	Motor Cortex/Areal	***FGFR3***	15.57	Areal
S100A10	2.48	Layer V/Subcerebral	***COUPTFI***	5.97	Areal
ROBO1	2.15	Axon Guidance/Layer V/Subcerebral	***EMX2***	1.77	Areal
SRGAP1	2.15	Axon Guidance/ROBO-associated			
CNTNAP2	1.97	Frontal			
CTIP2	1.94	Layer V/Subcerebral			

Table 3.1. Selected genes up-regulated anteriorly or posteriorly in RNA extracted from human neocortex, hybridized to Affymetrix gene chip (U133plus2 human genome) and fold changes analyzed on GeneSpring GX software.

Performed by Dr. Nadhim Bayatti. Adapted from (Ip et al., 2010a).

Probe sets <1.75-fold anteriorly or posteriorly		
Gene	**Fold**	**Function**
FEZF2	1.67 (A<P)	Layer V/Subcerebral
FGFR1	1.59 (A>P)	FGFR Family
FGFR2	-	FGFR Family
MAP2	-	Pan-neuronal Marker
PAX6	-	Transient Anterior Marker
ROBO2	-	Axon Guidance
SOX5	-	Layer VI/SP/Corticothalamic Neurones

Table 3.2. Selected genes exhibited no or small fold changes of expression anteriorly or posteriorly in RNA extracted from human neocortex, hybridized to Affymetrix gene chip (U133plus2 human genome) and fold changes analyzed on GeneSpring GX software.

A, anterior; P, posterior; SP, subplate. Performed by Dr. Nadhim Bayatti. Adapted from (Ip et al., 2010a).

3.2 Results

3.2.1 Confirmation of gDNA-free cDNA Samples used for rtPCR

To ensure all cDNA samples from anterior and posterior neocortical tissues derived from human embryonic and foetal brains used for rtPCR were not contaminated by gDNA, standard PCR assay was employed with *SDHA* primer set.

The FP and RP of *SDHA* targeted sequences on exon 2 and exon 3 of *SDHA* respectively. Thus samples with gDNA would yield products containing intron sequence and of around 940 bp. A positive control was incorporated with a human gDNA sample instead of cDNA samples. Three bands between 850-1000 bp were amplified products of the gDNA positive control (filled arrows, Figure 3.1). All cDNA samples from 8-12 PCW neocortical tissues (white lines, Figure 3.1) gave rise only to bands below 100 bp which were equivalent to the size of *SDHA* cDNA (84 bp, Table 2.3). Thus these cDNA samples used for rtPCR were confirmed gDNA-free.

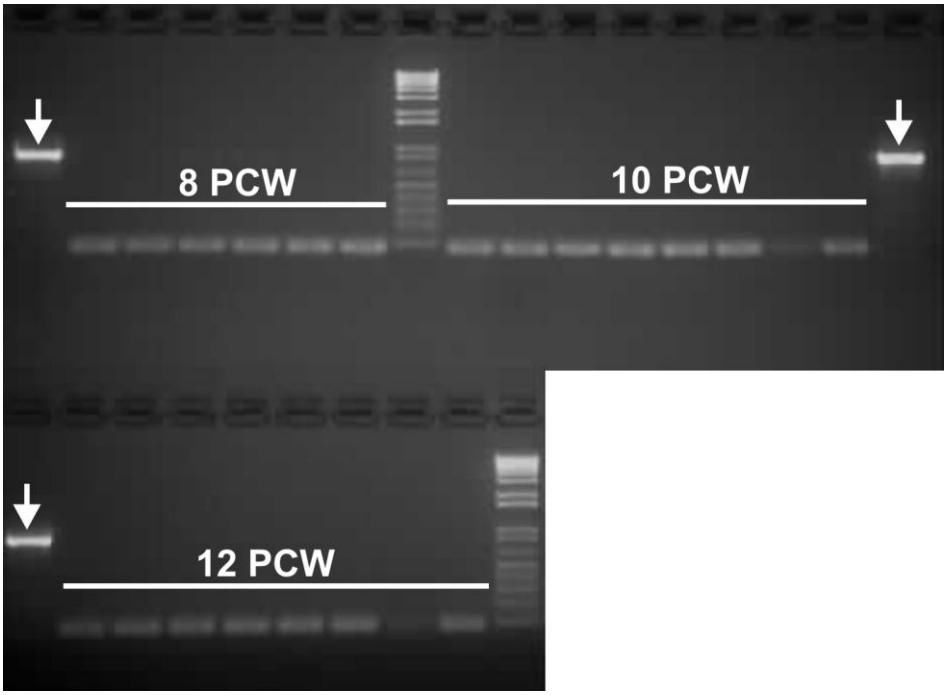

Figure 3.1. Confirmation of gDNA-free cDNA samples from neocortical tissues used for rtPCR.

Amplified products of *SDHA* using standard PCR assay. Products of positive control with human gDNA were indicated by filled arrows, whereas cDNA samples derived from anterior and posterior neocortical tissues used for rtPCR were indicated by white lines (8 PCW, n=3; 10 PCW, n=4; 12 PCW n=4). 1kb Plus DNA ladder was used to determine the size of bands.

3.2.2 Confirmation of Amplified PCR Products by Restriction Reaction and Direct Sequencing

To confirm the primer sets designed for rtPCR amplified the target genes of interest, restriction digestion was performed. Note that although two or three gene fragments should be produced after digestion, sometimes the smallest fragments either were too small to be resolved or they were of similar size with the larger fragments and thus appeared as single band but migrated further away from their original positions. Nevertheless, shift of bands further down the gel indicated reduction in size of the gene.

Identities of *COUPTFI, EMX2, FGFR1, FGFR3, ROBO2, SRGAP1* and *S100A10* were confirmed as digestion of their amplified PCR products was successful, indicated by shift of bands (arrows, Figure 3.2).

Absence of band or band-shifting after digestion was regarded as failure and purified samples were sent for direct sequencing with their forward primers, including *CTIP2, CNTNAP2, FEZF2, FGFR2, MAP2, PCDH17, ROBO1* and *SOX5*. Their identities were confirmed too as all sequences showed >96% identity to the respective target genes by the Basic Local Alignment Search Tool (BLAST) developed by National Center for Biotechnology Information (NCBI) and were listed in Table 3.3.

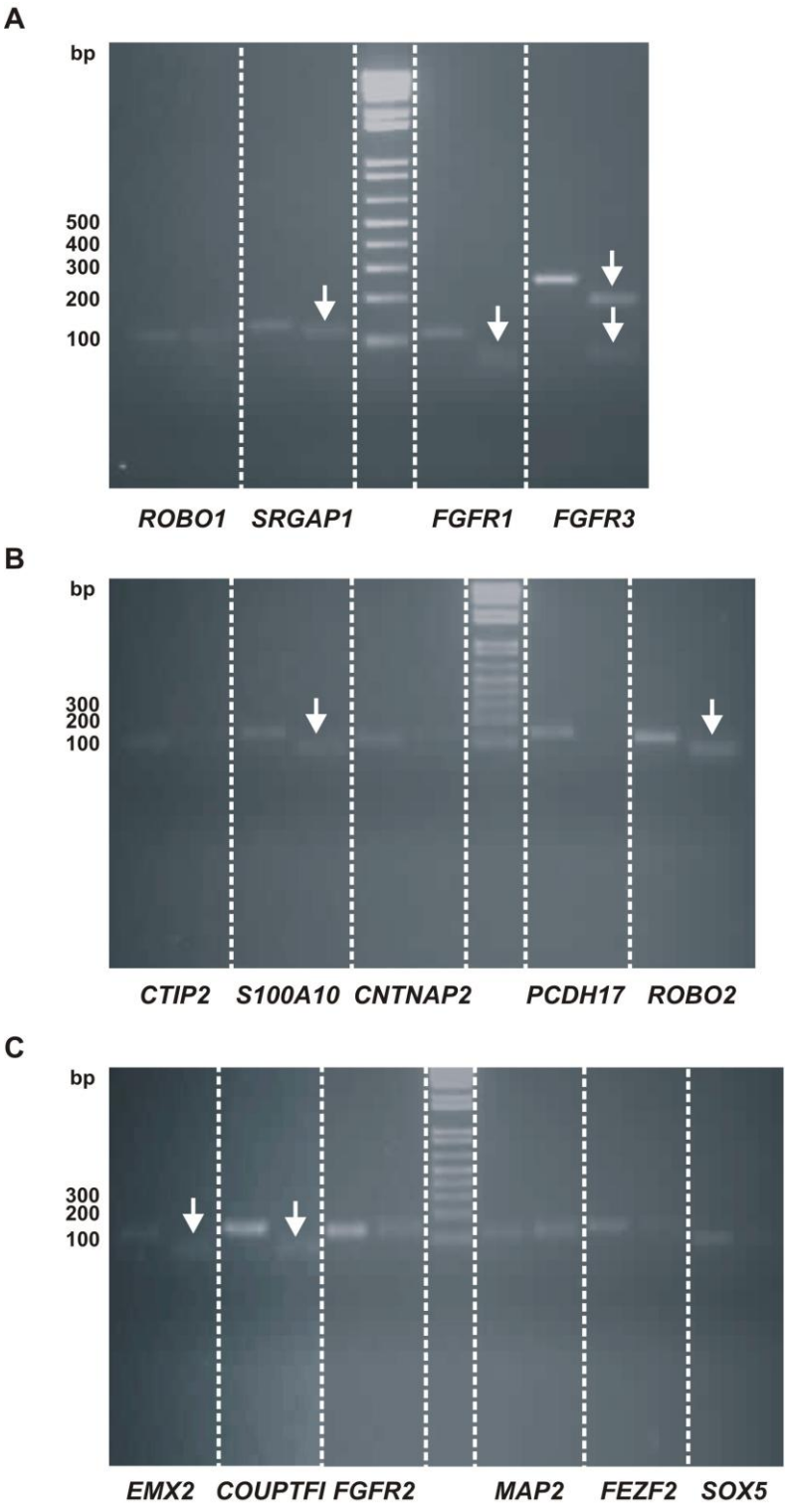

Figure 3.2. Confirmation of target genes identities by restriction digestion.

Amplified PCR products of *CNTNAP2, COUPTFI, CTIP2, EMX2, FGFR1, FGFR2, FGFR3, MAP2, PCDH17, ROBO1, SOX5, SRGAP1* and *S100A10* were digested by various restriction enzymes (Table 2.4). Undigested PCR products were loaded on the left lane of the demarcated areas (dotted white lines) and digested products on the right, successful restriction reactions were indicated by arrows. 1kb Plus DNA ladder was used to determine the size of bands.

Genes	GenBank accession numbers	Sequences of PCR products	Nucleotides of sequenced products
CTIP2	NM_138576.2	2809-2872	CAGATCGGCAGGAGGTGTACCGCTGCGACATCTGCCAGATGCCCTTCAGCGTCTACAGCA CCCATTT
	NM_022898.1	2596-2659	
CNTNAP2	NM_014141.4	2103-2158	CACTTGTAAATTTATACGAAGTGGCACAAAGGAAGCCGGGAAGTTTCGCGAATGTCAA
FEZF2	NM_018008.3	1387-1487	CGATTTTGCGGCAAGGCTTTCACCAAAAAGGGAACTACAAGAACCACAAGCTGACCCACA GCGGCGAGAAGCAGTACAAATGTACCATCTGCAACAAGGCCTGCAGG
FGFR2	NM_000141.4	2039-2132	CGAGTTGACTTCCAGAGGACCCAAAATGGGAGTTTCCAAGAGATAAGCTGACACTGGGCA AGCCCCTGGGAGAAGGTTGCTTTGGGCAAGTG
	NM_022970.3	2042-2135	
	NM_001144913.1	1545-1638	
	NM_001144914.1	1206-1299	
	NM_001144915.1	1444-1537	
	NM_001144916.1	1488-1581	
	NM_001144917.1	1691-1784	
	NM_001144918.1	1688-1781	
	NM_001144919.1	1775-1868	
MAP2	NM_002374.3	4924-5000	ATGAGATTCCTTCTCTCTCAACAGTTCTATCTCTTCTTCAGCACGGCGGACCACCAGGTCA GAGCCAATTCGCAGAAAGGGGGC
	NM_031845.2	856-932	
	NM_031847.2	856-932	
	NM_001039538.1	1230-1306	

PCDH17	NM_001040429.2	1519-1608	TACGCTCGTGCTGACTGCCCTGGACGGTGGCGAGCCTCCACGTTCCGCCACCGTACAGATCAACGTGAAGGTGATTGACTCCAACGACAA
ROBO1	NM_002941.2 NM_133631.1	1953-2013 2799-2859	AGTGAAACACAAGATGTCCTACCAACAAGTCAGGGGGTGGACCACAAGCAGGTCCAGAGAAAAGCACTTTT
SOX5	NM_006940.4 NM_152989.2 NM_178010.1	1502-1556 1732-1789 264-318	TGAGGAGCAACTCCGACGGGAACAACAGGTGCTTGATGGGAAGGTGGCTGTTGTGAAAGCCGGAGTCG

Table 3.3. Sequencing results of PCR products using forward primers for rtPCR.

3.2.3 Average Expression Levels between 8-12 PCW

After normalizing against expression levels of three housekeeping genes (*β-ACTIN*, *GAPDH* and *SHDA*) and averaged over 8-12 PCW, rtPCR confirmed most of the results of Affymetrix gene chip analysis (Figure 3.3). The putative anterior markers *CNTNAP2* (2.33-fold), *PCDH17* (4.59-fold) and corticofugal neurone-associated genes *CTIP2* (2.00-fold), *ROBO1* (2.14-fold), *S100A10* (2.24-fold) were found to be significantly higher in anteriorly- rather than posteriorly-dissected tissue. *SRGAP1* (1.28-fold), *FGFR1* (1.21-fold) and *MAP2* (1.18-fold) were also found to be expressed more highly anteriorly, with the differences being small but statistically significant. The previously identified rodent posterior markers *FGFR3* (61.36-fold), *COUPTFI* (18.98-fold) and *EMX2* (1.59-fold) exhibited significantly higher expression posteriorly than anteriorly. *FEZF2* (1.30-fold), *SOX5* (1.25-fold) and *FGFR2* (1.21-fold) were also found to be expressed more highly posteriorly, with the differences being small but statistically significant. *PAX6* and *ROBO2* exhibited no statistical significance either anteriorly and posteriorly. There were no significant differences in the normalized relative expression levels of all genes across all investigated ages except for *FGFR3* which was found to be significantly higher at 12 PCW than at 8 PCW.

A

Genes	Fold Changes	Gradient
PCDH17	4.59	A>P
CNTNAP2	2.33	A>P
S100A10	2.24	A>P
ROBO1	2.14	A>P
CTIP2	2.00	A>P
SRGAP1	1.28	A>P
FGFR1	1.21	A>P
MAP2	1.18	A>P
PAX6	1.11	n.d.
ROBO2	1.05	n.d.
FGFR3	61.36	A<P
COUPTFI	18.98	A<P
EMX2	1.59	A<P
FEZF2	1.30	A<P
SOX5	1.25	A<P
FGFR2	1.21	A<P

B

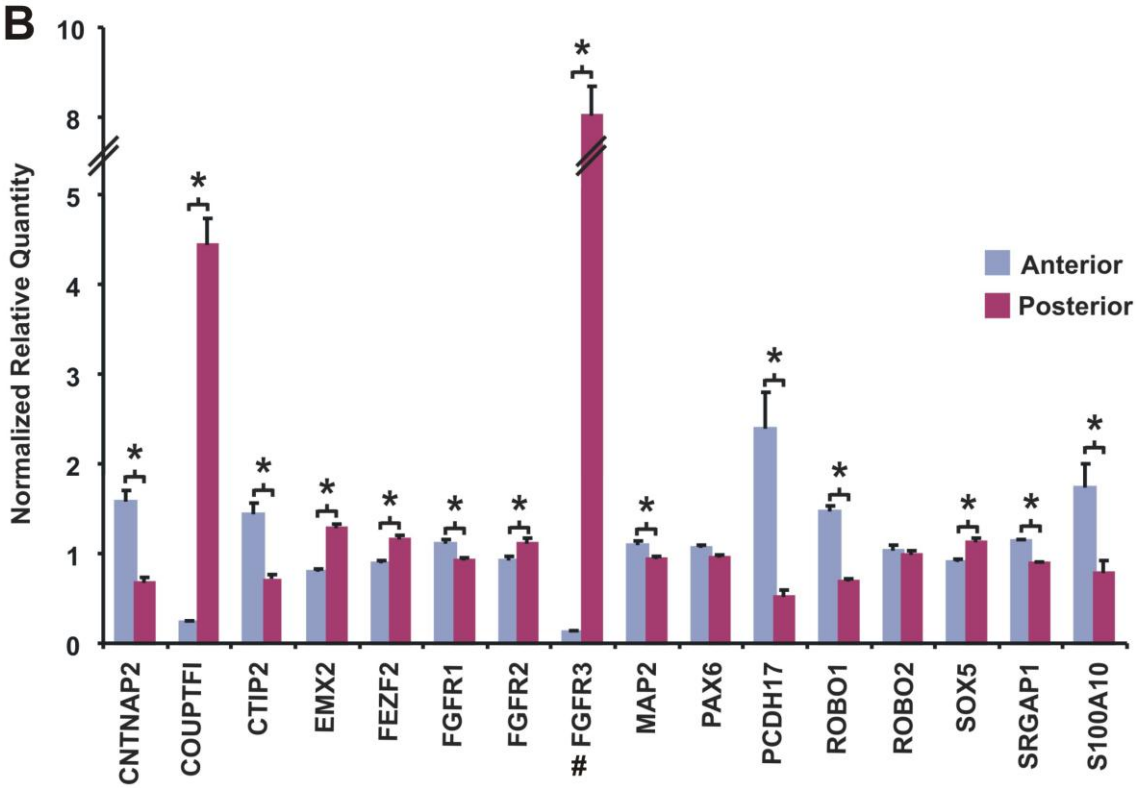

Figure 3.3. rtPCR confirmation of a subset of differentially regulated genes during early human neocortical development (8-12 PCW).

Table indicating fold changes (A) and graphical representation (B) of normalized relative quantity of a subset of genes determined by rtPCR from RNA extracted from anterior and posterior regions of developing human neocortex aged between 8-12 PCW (8 PCW, n=3; 10 PCW, n=4; 12 PCW, n=4). Genes exhibiting a high anterior to low posterior gradient include *CNTNAP2, CTIP2, PCDH17, ROBO1* and *S100A10*. Genes exhibiting a high posterior, low anterior gradient include *COUPTFI, EMX2* and *FGFR3*. No gradients were detected for *PAX6* and *ROBO2*. (Two-way ANOVA; *, $p \leq 0.05$ Anterior vs. Posterior). Normalized relative quantity of *FGFR3* at 8 PCW was found to be significantly lower than at 12 PCW (Two-way ANOVA, post-hoc LSD test; #, $p \leq 0.05$ marks the gene with this age-dependent effect), n.d., not detected; A, anterior, P, posterior. Adapted and modified from (Ip et al., 2010a).

3.2.4 Expression Levels at 8 PCW

At 8 PCW, after normalizing against expression levels of three housekeeping genes (*β-ACTIN, GAPDH* and *SHDA*), the level of fold changes was relatively smaller compared to the overall patterns observed between 8-12 PCW (Figure 3.4A). The putative anterior markers *CNTNAP2* (1.52-fold), *PAX6* (1.51-fold), *PCDH17* (1.60-fold) and corticofugal neurone-associated genes *CTIP2* (1.68-fold), *ROBO1* (1.75-fold) were found to be significantly higher in anteriorly- rather than posteriorly-dissected tissue. The previously identified rodent posterior markers *FGFR3* (32.72-fold) and *COUPTFI* (8.37-fold) exhibited significantly higher expression posteriorly than anteriorly. *EMX2* (1.22-fold) was also found to be expressed more highly posteriorly, with the difference being small but statistically significant. *FEZF2, FGFR1, FGFR2, MAP2, ROBO2, SOX5, SRGAP1* and *S100A10* exhibited no statistical significance either anteriorly and posteriorly.

Figure 3.4B shows NRQ of each selected gene. NRQ for posterior markers *COUPTFI* and *FGFR3* was high (3.14 and 5.72 respectively) in the posteriorly-dissected tissue at 8 PCW. The remaining selected genes displayed NRQ lower than 1.50 in both anteriorly- and posteriorly-dissected tissue.

A

Genes	Fold Changes	Gradient
ROBO1	1.75	A>P
CTIP2	1.68	A>P
PCDH17	1.60	A>P
CNTNAP2	1.52	A>P
PAX6	1.51	A>P
ROBO2	1.23	n.d.
MAP2	1.17	n.d.
S100A10	1.17	n.d.
SRGAP1	1.11	n.d.
FGFR1	1.10	n.d.
FGFR3	32.72	A<P
COUPTFI	8.37	A<P
EMX2	1.22	A<P
FEZF2	1.15	n.d.
FGFR2	1.06	n.d.
SOX5	1.00	n.d.

B

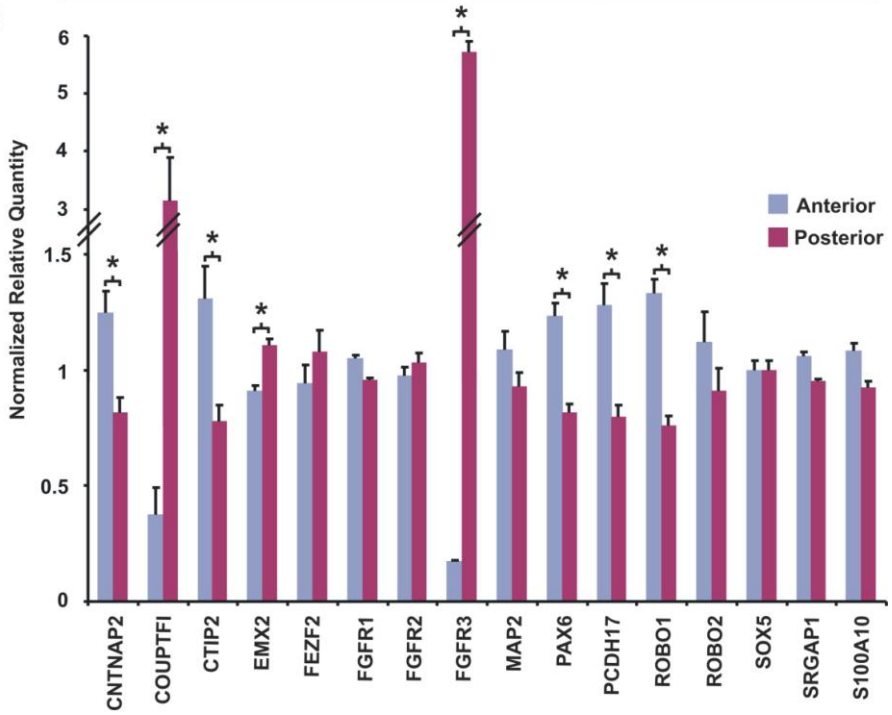

Figure 3.4. rtPCR confirmation of a subset of differentially regulated genes during early human neocortical development (8 PCW).

Table indicating fold changes (A) and graphical representation (B) of normalized relative quantity of a subset of genes determined by rtPCR from RNA extracted from anterior and posterior regions of developing human neocortex at 8 PCW (n=3). Genes exhibiting a high anterior to low posterior gradient include *CNTNAP2*, *CTIP2*, *PAX6*, *PCDH17* and *ROBO1*. Genes exhibiting a high posterior, low anterior gradient include *COUPTFI* and *FGFR3*. No gradients were detected for *FEZF2*, *FGFR1*, *FGFR2*, *MAP2*, *ROBO2*, *SOX5*, *SRGAP1* and *S100A10*. Normalized relative quantity >1.50 include *FGFR3* and *COUPTF1* in posteriorly-dissected tissue. (Student's paired *t-test*, *, $p \leq 0.05$), n.d., not detected; A, anterior, P, posterior.

3.2.5 Expression Levels at 10 PCW

At 10 PCW, after normalizing against expression levels of three housekeeping genes (*β-ACTIN, GAPDH* and *SHDA*), the level of fold changes followed most of the overall patterns observed between 8-12 PCW (Figure 3.5A). The putative anterior markers *CNTNAP2* (2.93-fold), *PCDH17* (4.05-fold) and corticofugal neurone-associated genes *CTIP2* (2.50-fold), *ROBO1* (2.29-fold), *S100A10* (3.47-fold) were found to be significantly higher in anteriorly- rather than posteriorly-dissected tissue. *FGFR1* (1.37-fold), *MAP2* (1.15-fold) and *SRGAP1* (1.22-fold) were found to be expressed more highly anteriorly, with the differences being small but statistically significant. The previously identified rodent posterior markers *EMX2* (1.90-fold), *FGFR3* (66.55-fold), *COUPTFI* (19.00-fold) together with *FGFR2* (1.50-fold) and *SOX5* (1.51-fold) exhibited significantly higher expression posteriorly than anteriorly. *FEZF2, PAX6* and *ROBO2* exhibited no statistical significance either anteriorly and posteriorly.

Figure 3.5B shows NRQ of each selected gene. NRQ for posterior markers *COUPTFI* and *FGFR3* continued to be high at 10 PCW (4.50 and 8.19 respectively) in the posteriorly-dissected tissue as compared to 8 PCW (Figure 3.4B). Anteriorly up-regulated genes *CNTNAP2* (1.74), *CTIP2* (1.63), *PCDH17* (2.07), *ROBO1* (1.52) and *S100A10* (2.05) exhibited higher NRQ in the anteriorly-dissected tissues when comparing to the observation at 8 PCW (Figure 3.4B). The remaining selected genes continued to display NRQ lower than 1.50 in both anteriorly- and posteriorly-dissected tissue.

A

Genes	Fold Changes	Gradient
PCDH17	4.05	A>P
S100A10	3.47	A>P
CNTNAP2	2.93	A>P
CTIP2	2.50	A>P
ROBO1	2.29	A>P
FGFR1	1.37	A>P
SRGAP1	1.22	A>P
MAP2	1.15	A>P
FGFR3	66.55	A<P
COUPTFI	19.00	A<P
EMX2	1.90	A<P
SOX5	1.51	A<P
FGFR2	1.50	A<P
ROBO2	1.22	n.d.
FEZF2	1.18	n.d.
PAX6	1.01	n.d.

B

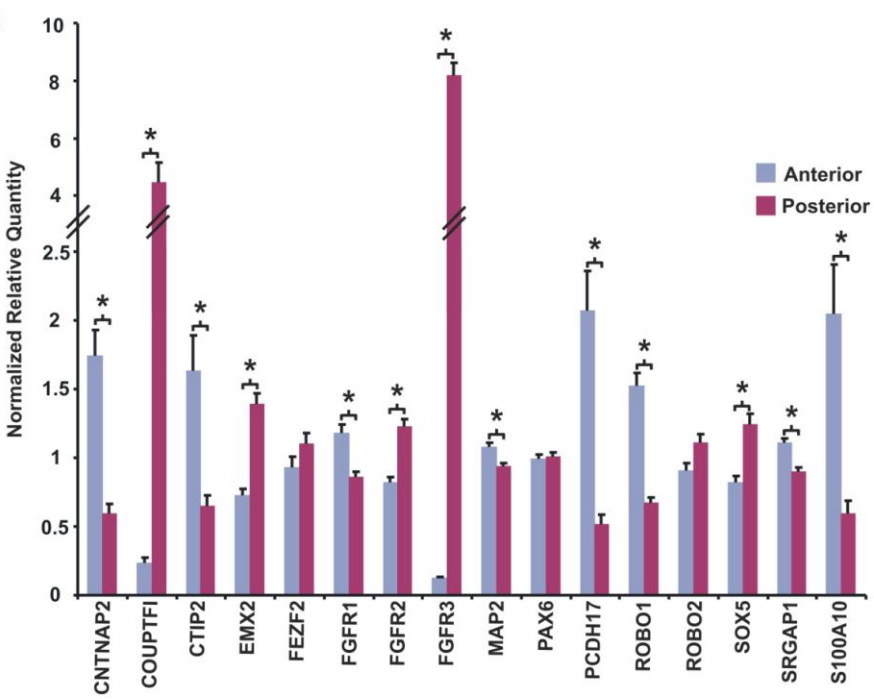

Figure 3.5. rtPCR confirmation of a subset of differentially regulated genes during early human neocortical development (10 PCW).

Table indicating fold changes (A) and graphical representation (B) of normalized relative quantity of a subset of genes determined by rtPCR from RNA extracted from anterior and posterior regions of developing human neocortex at 10 PCW (n=4). Genes exhibiting a high anterior to low posterior gradient include *CNTNAP2, CTIP2, PCDH17, ROBO1* and *S100A10*. Genes exhibiting a high posterior, low anterior gradient include *COUPTFI, EMX2, FGFR2, FGFR3* and *SOX5*. No gradients were detected for *FEZF2, PAX6* and *ROBO2*. Normalized relative quantity >1.50 include *FGFR3* and *COUPTF1* in posteriorly-dissected tissue and *CNTNAP2, CTIP2, PCDH17, ROBO1* and *S100A10* in anteriorly-dissected tissue. (Student's paired *t-test*, *, $p \leq 0.05$), n.d., not detected; A, anterior, P, posterior.

3.2.6 Expression Levels at 12 PCW

At 12 PCW, after normalizing against expression levels of three housekeeping genes (*β-ACTIN*, *GAPDH* and *SHDA*), the level of fold changes followed most of the overall patterns observed between 8-12 PCW (Figure 3.6A). The putative anterior markers *CNTNAP2* (3.08-fold), *PCDH17* (13.81-fold) and corticofugal neurone-associated genes *CTIP2* (1.86-fold), *ROBO1* (2.52-fold), S100A10 (3.62-fold) were found to be significantly higher in anteriorly- rather than posteriorly-dissected tissue. *ROBO2* (1.25-fold) and *SRGAP1* (1.44-fold) were also found to be expressed more highly anteriorly, with the differences being small but statistically significant. The previously identified rodent posterior markers *EMX2* (1.82-fold), *FGFR3* (97.97-fold), *COUPTFI* (22.22-fold) together with *FEZF2* (1.68-fold) exhibited significantly higher expression posteriorly than anteriorly. *SOX5* (1.21-fold) was found to be expressed more highly posteriorly, with the difference being small but statistically significant. *FGFR1*, *FGFR2*, *MAP2* and *PAX6* exhibited no statistical significance either anteriorly and posteriorly.

Figure 3.6B shows NRQ of each selected gene. NRQ for posterior markers *COUPTFI* and *FGFR3* continued to be high at 12 PCW (4.73 and 9.99 respectively) in the posteriorly-dissected tissue as compared to 8 PCW (Figure 3.4B). Anteriorly up-regulated genes *CNTNAP2* (1.77), *PCDH17* (3.88), *ROBO1* (1.59) and *S100A10* (1.96) exhibited higher NRQ in the anteriorly-dissected tissues when comparing to observation at 8 PCW (Figure 3.4B). The remaining selected genes continued to display NRQ lower than 1.50 in both anteriorly- and posteriorly-dissected tissue.

A

Genes	Fold Changes	Gradient
PCDH17	13.81	A>P
S100A10	3.62	A>P
CNTNAP2	3.08	A>P
ROBO1	2.52	A>P
CTIP2	1.86	A>P
SRGAP1	1.44	A>P
ROBO2	1.25	A>P
FGFR1	1.23	n.d.
MAP2	1.23	n.d.
FGFR2	1.09	n.d.
PAX6	1.01	n.d.
FGFR3	97.97	A<P
COUPTFI	22.22	A<P
EMX2	1.82	A<P
FEZF2	1.68	A<P
SOX5	1.21	A<P

B

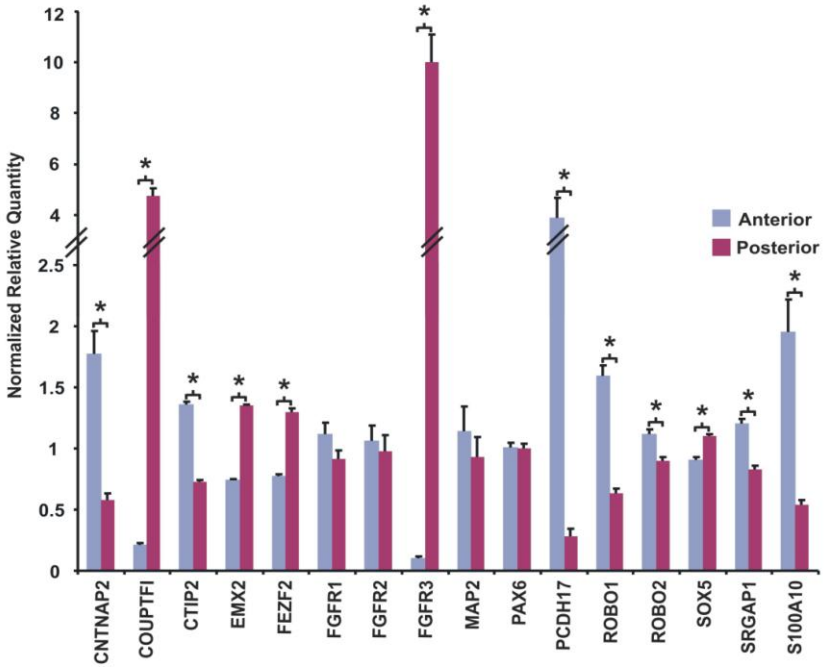

Figure 3.6. rtPCR confirmation of a subset of differentially regulated genes during early human neocortical development (12 PCW).

Table indicating fold changes (A) and graphical representation (B) of normalized relative quantity of a subset of genes determined by rtPCR from RNA extracted from anterior and posterior regions of developing human neocortex at 12 PCW (n=4). Genes exhibiting a high anterior to low posterior gradient include *CNTNAP2, CTIP2, PCDH17, ROBO1* and *S100A10*. Genes exhibiting a high posterior, low anterior gradient include *COUPTFI, EMX2, FEZF2* and *FGFR3*. No gradients were detected for *FGFR1, FGFR2, MAP2* and *PAX6*. Normalized relative quantity >1.50 include *FGFR3* and *COUPTF1* in posteriorly-dissected tissue and *CNTNAP2, PCDH17, ROBO1* and *S100A10* in anteriorly-dissected tissue. (Student's paired *t-test*, *, $p \leq 0.05$), n.d., not detected; A, anterior, P, posterior.

3.2.7 Summary of Gene Expression Gradients at 8, 10 and 12 PCW

In summary, anteriorly-upregulated genes *CNTNAP2*, *CTIP2*, *PCDH17* and *ROBO1* (highlighted in yellow, Table 3.4) and posteriorly-upregulated genes *COUPTFI*, *EMX2* and *FGFR3* (highlighted in green, Table 3.4) identified by Affymetrix gene chip analysis (>1.75-fold) were confirmed by rtPCR, displaying consistent and significant gradients of expression across the developing neocortex at 8, 10 and 12 PCW. Thus significant anterior-posterior expression gradients were also obtained when fold changes of expression levels were averaged across samples aged 8-12 PCW.

rtPCR showed some presumably non-regulated genes *FGFR1*, *FGFR2* and *MAP2* (<1.75-fold determined by Affymetrix gene chip analysis) showing no significant difference in expression levels between the anterior and posterior region of the neocortex at 8 and 12 PCW (highlighted in red, Table 3.4). Small but significant differences in expression levels were obtained at 10 PCW (highlighted in red, Table 3.4). Overall, these resulted in small but significant anterior-posterior expression gradients when fold changes of expression levels were averaged across samples aged 8-12 PCW (highlighted in red, Table 3.4).

Other anteriorly-upregulated genes identified by Affymetrix gene chip analysis (>1.75-fold) *S100A10* and *SRGAP1*, and presumably non-regulated genes *FEZF2*, *PAX6*, *ROBO2* and *SOX5* (<1.75-fold determined by Affymetrix gene chip analysis) did not illustrate consistent gradients of expression by rtPCR from 8 to 12 PCW (Table 3.4). Nevertheless the fold changes of *PAX6* expression resembled the patterns observed in tissue ISH with significantly high anterior, low posterior gradient at 8 PCW and is lost by 9 PCW (Bayatti et al., 2008b).

	8 PCW		10 PCW		12 PCW		8-12 PCW	
Gene	**Fold Change**	**Gradient**	**Fold Change**	**Gradient**	**Fold Change**	**Gradient**	**Fold Change**	**Gradient**
PCDH17	1.60*	A>P	4.05*	A>P	13.81*	A>P	4.59¥	A>P
S100A10	1.17	n.d.	3.47*	A>P	3.62*	A>P	2.24¥	A>P
CNTNAP2	1.52*	A>P	2.93*	A>P	3.08*	A>P	2.33¥	A>P
ROBO1	1.75*	A>P	2.29*	A>P	2.52*	A>P	2.14¥	A>P
CTIP2	1.68*	A>P	2.50*	A>P	1.86*	A>P	2.00¥	A>P
SRGAP1	1.11	n.d.	1.22*	A>P	1.44*	A>P	1.28¥	A>P
ROBO2	1.23	n.d.	1.22	n.d.	1.25*	A>P	1.05	n.d.
FGFR1	1.10	n.d.	1.37*	A>P	1.23	n.d.	1.21¥	A>P
MAP2	1.17	n.d.	1.15*	A>P	1.23	n.d.	1.18¥	A>P
FGFR2	1.06	n.d.	1.50*	A<P	1.09	n.d.	1.21¥	A>P
PAX6	1.51*	A>P	1.01	n.d.	1.01	n.d.	1.11	n.d.
#***FGFR3***	32.72*	A<P	66.55*	A<P	97.97*	A<P	61.36¥	A<P
COUPTFI	8.37*	A<P	19.00*	A<P	22.22*	A<P	18.98¥	A<P
EMX2	1.22*	A<P	1.90*	A<P	1.82*	A<P	1.59¥	A<P
FEZF2	1.15	n.d.	1.18	n.d.	1.68*	A<P	1.30¥	A<P
SOX5	1.00	n.d.	1.51*	A<P	1.21	A<P	1.25¥	A<P

Table 3.4. Summary of gene expression gradients at 8, 10 and 12 PCW confirmed by rtPCR.

Genes highlighted in yellow showed significantly consistent high anterior (A), low posterior (P) gradients at all investigated ages (8 PCW, n=3; 10 PCW, n=4; 12 PCW, n=4). Genes highlighted in green showed significantly consistent low anterior, high posterior gradients at all investigated ages. Genes highlighted in red displayed significant differential expression either anteriorly or posteriorly at 10 PCW only. The fold changes in relative expression levels of other genes showed variable trends across all investigated ages. Student's paired *t*-test was performed with relative expression level data sets yielded from samples of the same age between the anteriorly- and posteriorly-dissected tissue (*, $p \leq 0.05$). Two-way ANOVA was performed with relative expression level data set yield from samples of all ages between the anteriorly- and posteriorly-dissected tissue (¥, $p \leq 0.05$ Anterior vs. Posterior), and with post-hoc LSD test age-dependent effect was observed with *FGFR3* in which its relative expression level was significant lower at 8 PCW than at 12 PCW (#, $p \leq 0.05$).

3.3 Discussion

The current study has utilized rtPCR and confirmed some findings of the Affymetrix gene chip analysis by consistently showing a subset of genes regulated anteriorly and posteriorly in the neocortex during early stages of corticogenesis (8-12 PCW). These included *CTIP2*, *CNTNAP2*, *PCDH17* and *ROBO1* being highly upregulated anteriorly, and *COUPTFI*, *EMX2* and *FGFR3* and being highly upregulated posteriorly.

3.3.1 The Use of Affymetrix Gene Chip and rtPCR Analyses

Affymetrix gene chip arrays provide pixelated-fluorescent intensities data for each of the probe sets that hybridized with the biotin-labelled target in the neocortical tissue samples, reflecting a relative level of expression of the target genes after background correction, normalization and summarization procedures. Similarly, rtPCR in this study used fluorescent double-stranded DNA dye SYBR Green to provide NRQ of each target genes against several selected reference genes in neocortical tissue samples. Although they do not actually indicate absolute expression levels of target genes, both analyses are useful for comparison of expression levels in different tissues (i.e. anteriorly- vs. posteriorly-dissected neocortical tissues) processed in the same experiment, making rtPCR a suitable confirmatory tool for Affymetrix gene chip analysis. One limitation of gene chip arrays is that comparisons between genes for the same microarray are not appropriate as different RNA molecules may be amplified, labelled and hybridized differently in an experiment. Likewise, primer sets for different genes used in rtPCR do not perform equally, and without calculating the reaction efficiency, the actual amount of cDNA of each target genes in a sample cannot be determined and comparison should not be made between different genes in the same sample. Therefore, analyses in this study focused on the expression level differences (fold changes) between anteriorly- and posteriorly-dissected tissues and did not compare relative expression levels between selected subset of genes. However, comparison of relative expression levels of the same gene across all investigated ages is achievable.

Genes that control the establishment of the early cortical map in rodents are presumed to be expressed in gradients throughout the period when neurogenesis is occurring in the developing neocortex (Cecchi and Boncinelli, 2000). Affymetrix gene chip arrays have previously revealed robust consistent gradients of gene expression in human neocortical tissues aged 8-12.5 PCW (Figure 1.13; (Ip et al., 2010a)), an important time of neocorticogenesis. This corresponds to the period of development when the CP is forming (at 7.5 PCW) (Meyer et al., 2000) and during the early stages of neurogenesis (Bystron et al., 2008; ten Donkelaar, 2000) and regionalisation, well before innervation by thalamocortical fibres that may exert extrinsic influences on the differentiating progenitors (Kostovic and Rakic, 1990). Additionally, global functional information deduced by Gene Ontology (GO) categorizations identified some similar and different GO categories enrichment in anteriorly and posteriorly up-regulated probe sets (Ip et al., 2010a). Nevertheless, these functional classifications sometimes fail to identify specific groups of genes that may be inter-linked either due to specificity or due to unknown or as yet unassigned gene function (e.g. GO category cerebral cortex regionalisation GO:0021796 contains *EMX1* and *EMX2* but not *COUPTFI*). Therefore by searching manually through the gene list we were able to identify a number of anteriorly-regulated genes which are potentially involved in regionalisation at the anterior pole of the developing neocortex. These include cell-adhesion molecules (such as protocadherins) and transcription factors that are associated with motor cortex or corticofugal neurones, either at the site of origin of corticofugal neurones in Layer V or expressed in their outgrowing fibres (Molnar and Cheung, 2006).

3.3.2 Identification of Anteriorly Up-regulated Genes

A subset of these genes was chosen and patterns of gene expression were confirmed by rtPCR in dissected tissue. Of the anterior markers identified, *CNTNAP2* is a frontal cortex marker (Abrahams et al., 2007), *PCDH17*, an areal marker corresponding to the motor cortex in rodents (Kim et al., 2007), *CTIP2*, a gene highly expressed by early CSMN in Layer V in rodents (Arlotta et al., 2005), *ROBO1*, a gene encoding axon guidance molecule that is expressed in the corticospinal fibres before, during and after crossing the midline in the caudal medulla in rodents (Sundaresan et al., 2004), all exhibited robust and consistently higher levels in anteriorly-derived tissue at all

investigate ages (8, 10 and 12 PCW; Figure 3.3 - Figure 3.6, Table 3.4). However, *S100A10*, another gene highly expressed by early CSMN in Layer V in rodents (Arlotta et al., 2005) only exhibited significant high anterior, low posterior gradient at 10 (Figure 3.5, Table 3.4) and 12 PCW (Figure 3.6, Table 3.4), but not at 8 PCW (Figure 3.4, Table 3.4). Furthermore, *SRGAP1*, a gene encoding the downstream signalling molecule of ROBO1 (Wong et al., 2001) only exhibited a small but significant increase in anteriorly-derived tissue when fold changes in expression level were averaged between 8-12 PCW (Figure 3.3, Table 3.4). Nevertheless fold changes in expression level of *SRGAP1* correlated nicely with that of *ROBO1* from 8 to 12 PCW (Figure 3.4 - Figure 3.6, Table 3.4) and the small fold change in expression level of *ROBO1* observed at 8 PCW might have led to the small fold change in expression level observed with *SRGAP1* at the same age accordingly (Figure 3.4, Table 3.4). The BLAST developed by NCBI was employed to verify and compare the target sequence of primer set of *SRGAP1* used for rtPCR and that of Affymetrix probe set (1569269_s_at) that exhibited 2.15-fold higher expression anteriorly. Both target sequences were found to be within the coding sequence of *SRGAP1* mRNA (NM_020762.2, nucleotide 57-3314) albeit of different exons, i.e. target sequences of primer sets were within exon 17 and of probe set were within exon 21 to 22. The slight discrepancy observed between the two analyses is unlikely to be due to alternative splicing, as no alternative splicing variant has yet been identified for *SRGAP1*, or alternative polyadenylation at 3' untranslated region (UTR) of its mRNA, as target sequences were not within those regions. Although the *SRGAP1* primer set was not designed to span the exon-exon boundary, gDNA expression affecting the fold change detected by rtPCR was minimal, as acidic phenol (pH<4.0) was used during phenol/chloroform RNA extraction, retaining RNA in the aqueous phase but shifting DNA into the organic phase, and the gDNA-free condition was also proven by standard PCR assay with *SDHA* primer set (Figure 3.1). Nevertheless both analyses revealed the same pattern of regulation anteriorly.

3.3.3 Identification of Posteriorly Up-regulated Genes

EMX2 (Simeone et al., 1992), *COUPTFI* (Zhou et al., 1999) and *FGFR3* (O'Leary and Nakagawa, 2002) are reported regionalisation genes and exhibited higher expression in posteriorly-derived tissue at all investigated ages (8, 10 and 12 PCW; Figure 3.3 -

Figure 3.6, Table 3.4). Additional members of the *FGFR* family that are highly expressed in the brain (Ford-Perriss et al., 2001) exhibited small but significant gradients of expression. *FGFR1* exhibited higher expression anteriorly, while *FGFR2* was higher posteriorly when the fold changes of expression levels were averaged between 8-12 PCW (Figure 3.3, Table 3.4). However, they only exhibited significant differences in expression levels between the anteriorly- and posteriorly-derived neocortical tissues at 10 PCW only (Figure 3.5, Table 3.4), but not at 8 (Figure 3.4, Table 3.4) and 12 PCW (Figure 3.6, Table 3.4). Both the Layer V/corticofugal neurone-associated gene *FEZF2* (Chen et al., 2008; Chen et al., 2005a; Molyneaux et al., 2005) and the Layer VI/SP/corticothalamic neurone-related gene *SOX5* (Kwan et al., 2008; Lai et al., 2008) exhibited small but significant gradients of expression posteriorly on average (Figure 3.3, Table 3.4). *PAX6* and *ROBO* family member *ROBO2* (Yue et al., 2006) expression exhibited insignificant differences between anterior and posterior tissue on average (Figure 3.3, Table 3.4). The neuronal marker *MAP2* (Bernhardt and Matus, 1984) exhibited a small but significant increase in anteriorly-derived neocortical tissue on average (Figure 3.3, Table 3.4). Non-regulated as well as posteriorly up-regulated genes are good indications that developmental advancement in the anterior neocortex cannot simply account for the up-regulation of gene expression detected in the anteriorly-derived neocortical tissue.

3.3.4 Potential Human-specific Mechanisms of Regionalisation

As shown by our group previously, when carrying out hierarchical clustering by condition tree analysis including all genes, it was interesting to note that samples clustered according to their ages (Figure 1.13; (Ip et al., 2010a)). This was also confirmed by principal component analysis as age appears to be one major component of variance (Ip et al., 2010a). Samples derived from anterior and posterior neocortex at each age range clustered closest to each other, the samples between 9-11 PCW formed a closely clustered group, while samples from 8 and 12.5 PCW weeks were least related (Figure 1.13; (Ip et al., 2010a)). Results from rtPCR of the selected subset of genes revealed similar trends. Expression fold changes of most of the selected anteriorly and posteriorly up-regulated genes and their NRQ at 8 PCW (Figure 3.4) were comparatively smaller than those observed at 10 (Figure 3.5) and 12 PCW (Figure 3.6).

In particular, the NRQ of *FGFR3* was significant smaller at 8 PCW as compared to that detected at 12 PCW (Figure 3.3). These findings indicate that at 8 PCW, and probably before, different developmental mechanisms may be used, resulting in the differing gene expression profiles. This observation is supported by previous studies in humans that demonstrate a developmental switch may occur between 8 and 9 PCW that results in the deregulation of the *PAX6* (high anterolateral, low posteromedial) gradient (Table 1.1; (Bayatti et al., 2008b)) which is maintained in rodents throughout neocorticogenesis (Manuel and Price, 2005). The graded expression of *PAX6* observed at 8 PCW and loss from 9 PCW was also confirmed by rtPCR in this study (Figure 3.4 - Figure 3.6, Table 3.4). On the other hand, from 12 PCW onwards, extrinsic influences begin to be conveyed to the developing neocortex via the incoming thalamocortical afferents which potentially modify and refine the already established expression patterns and may cause larger fold changes we observed with a subset of genes at this age, supporting the protocortex theory of regionalisation (originally suggested by (Van der Loos and Woolsey, 1973) and subsequently developed by (O'Leary, 1989) as cited by (Mallamaci and Stoykova, 2006)).

Pax6/*PAX6* is expressed by neocortical progenitor cells within the proliferative zones in both rodents (Bishop et al., 2002) and humans (Bayatti et al., 2008b), and known to be controlling cell proliferation and differentiation in rodent KO studies (Warren et al., 1999). More notably, in addition to its role in the development of neocortical projection neurones, *PAX6* is found to be also involved in neurogenesis of neocortical interneurones, a function uniquely identified in human *in-vitro* neocortical progenitor-enriched culture (Mo and Zecevic, 2008). Thus the transient anteriorly-upregulated *PAX6* at 8 PCW might be regulating the mechanisms involved in generation of a subpopulation of neocortical interneurones originating from the anterior pole of the developing neocortex. The hypothesized anterior origin of a subpopulation of neocortical interneurones is currently under investigation by members of our group as a subset of genes associated with GABAergic interneurones is found to be highly upregulated anteriorly by Affymetrix gene chip arrays (Ip et al., 2010a). Recently, evidence has accumulated that the *Pax6* gradient in rodents is not directly involved in regionalisation processes (Pinon et al., 2008; Manuel et al., 2007), as neocortical identities indicated by distribution of area-specific thalamocortical and corticofugal projections are maintained in conditional *Pax6* KO mutants, while over-expression of

Pax6 in mutant mice does not alter the expression of Emx2 or other areal markers. Over-expression of *Emx2* however causes shifts in the position and increases the size of primary areas located posteriorly when compared to anterior structures (Hamasaki et al., 2004). Therefore there is a clear major regionalisation influence in the developing neocortex which comes posteriorly from genes such as *EMX2* and *COUPTFI*. Their expression is repressed by soluble factors such as FGF8, -15, -17 released from signalling centres located anteriorly (Rakic et al., 2009; O'Leary et al., 2007; O'Leary and Nakagawa, 2002).

There may be counter-gradients of, as yet, undiscovered regionalisation genes actively responsible for anterior specification, but these are yet to be identified. Numerous genes are known to be expressed in counter-gradients (Rakic et al., 2009), however a distinction must be made between whether these genes affect regionalisation *per se* or arise by being regulated by regionalisation genes which would induce a region-specific or areal expression pattern. Classically, regionalisation genes are expressed in the proliferative zones while areal genes are expressed downstream in specific layers of the developing CP (O'Leary et al., 2007). However, graded expression of regionalisation genes such as *EMX2* is translocated from the proliferative zones to the developing CP, potentially controlling expression of areal genes directly in this post-mitotic layer during early stages of corticogenesis in humans (Bayatti et al., 2008b). Although Affymetrix gene chip analysis and rtPCR are useful in identifying genes that are expressed differentially along the tangential axis of the developing neocortex, more thorough investigation is therefore required to localize their expression on human neocortical tissues spatially and temporally via tissue *in-situ* hybridization and immunohistochemistry. Of the identified anteriorly up-regulated genes, we have decided to further examine some corticofugal neurone-associated genes such as *ROBO1*, *SRGAP1* and *CTIP2* (Chapter 5), as their early anterior spatial clustering implies that cells may have information imparted to them at an early developmental stage, possibly as cortical progenitors. This evidence also suggests that the anterior neocortex at this stage may be the site of origin of the later developing motor cortex and corticofugal neurones in a similar manner to the anterior location of the motor cortex in rodents (O'Leary and Nakagawa, 2002). Prior to the investigation of expression patterns of corticofugal neurone-associated genes, verification of expression patterns of some other neuronal genes or proteins (NURR1 and SATB2) is carried out on human

embryonic and foetal tissue (Chapter 4). This is because they are believed to be highly expressed in certain layers of the rodent neocortex and therefore after confirming their expression patterns in the human neocortex, different laminae of the human neocortex can be marked out.

Chapter 4 Verification of SATB2 and NURR1 Expression Patterns in Early Human Neocortical Development

4.1 Aim of Study

The aim of this chapter is to test the suitability of using *SATB2*/SATB2 and NURR1 as laminar-enriched markers to help to delineating different laminae of the neocortex especially within the developing CP.

Although both Satb2 (Layer V at early stages and eventually Layer II-V; (Alcamo et al., 2008; Britanova et al., 2008)) and Nurr1 (Layer VI and SP; (Hoerder-Suabedissen et al., 2009)) are highly expressed in certain layers of the neocortex during development in rodents, their expression patterns have not yet been reported in humans at our investigated ages (8-15 PCW). Therefore tissue ISH and immunoperoxidase- and immunofluorescent-histochemistry was performed to verify *SATB2*/SATB2 and NURR1 expression patterns on human embryonic and foetal tissues between 8-15 PCW.

As previously reported by our group, the SP begins to become visible underneath the TBR1-positive developing CP and is GAP43-positive by 12 PCW, while Layer V of the developing CP can be marked by ER81 expression by 16 PCW (Bayatti et al., 2008a), Therefore, the objective of the present study was to compare the expression patterns for *ER81*, GAP43 and TBR1 with those of *SATB2*/SATB2 and NURR1 in human embryonic and foetal tissues aged between 8-15 PCW. In addition, expression of SATB2 and NURR1 across the tangential dimension of the human neocortex was also reported.

4.2 Results

4.2.1 Negative Controls for Tissue ISH

To confirm the specificity of anti-sense probes of *ER81* and *SATB2* for tissue ISH, the negative sense probes of each gene were used alongside during the experiment. All sections hybridized with sense probes showed no signal, and representative sections were presented in Figure 4.1.

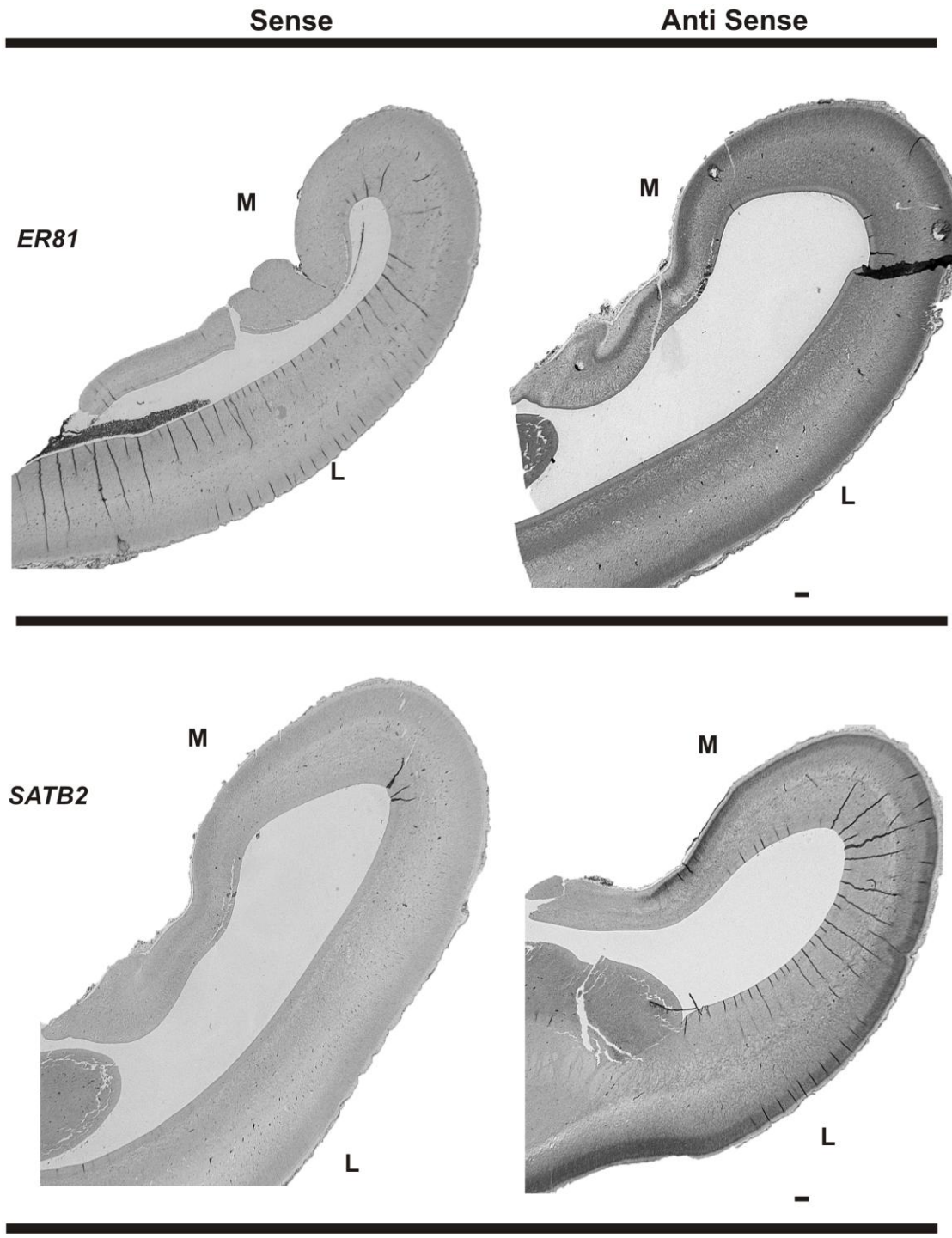

Figure 4.1. Detection of anti-sense and sense probes for *ER81* and *SATB2*.

Specificity test for the anti-sense probes was carried for *ER81* and *SATB2*. Representative images were captured with coronal sections of 12 PCW (n=2). The lateral (L) and medial (M) part of the neocortex was labelled for orientation purposes. Scale bars indicated 500 µm.

4.2.2 Negative Controls for Immunoperoxidase-histochemistry

To confirm the specificity of biotinylated-secondary antibodies used throughout the project, immunoperoxidase staining was performed in the absence of primary antibodies and applied biotinylated anti-goat IgG, anti-mouse IgG, anti-rabbit IgG or anti-rat IgG on each section. All sections immunostained with secondary antibodies showed no staining (Figure 4.2).

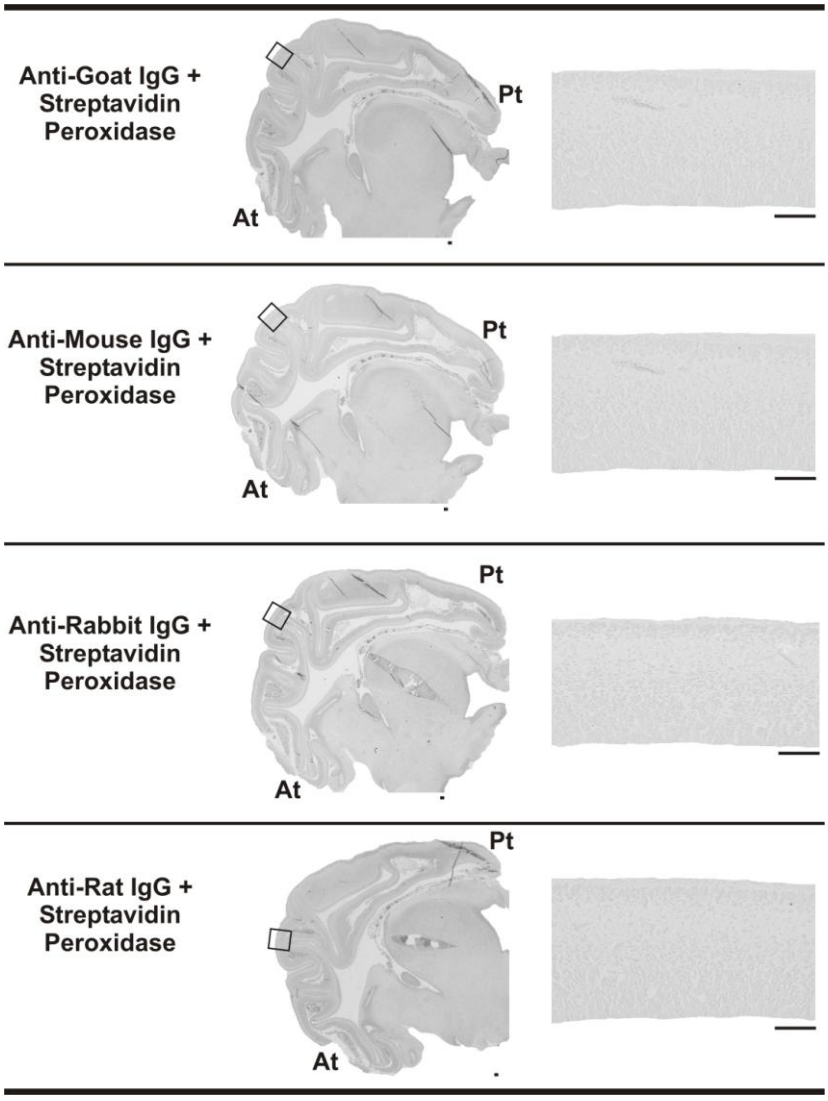

Figure 4.2. Omission of primary antibodies.

Specificity test for the biotinylated-secondary antibodies was carried out on sagittal sections of brain aged 10 PCW (n=1) for anti-goat IgG, anti-mouse IgG, anti-rabbit IgG and anti-rat IgG. Higher magnification photos were taken at the boxed regions. The anterior (At) and posterior (Pt) part of the neocortex was labelled for orientation purposes. Scale bars indicated 200 μm.

*4.2.3 Laminar Expression of SATB2/*SATB2 *during Early Human Neocortical Development*

To investigate the laminar expression of *SATB2*/SATB2, tissue ISH and immunoperoxidase- and immunofluorescent-histochemistry was performed. Images were taken from the dorsolateral anterior neocortex for comparison between sections stained with H & E for anatomical references, *ER81* and *SATB2* sense and anti-sense probes and GAP43 and SATB2 antibodies as well as examination of doubled-labelled sections with SATB2/TBR1 and SATB2/SOX5 antibodies (Figure 4.3). Adjacent sections were selected for each gene/protein between 8-12 PCW.

From 8-9 PCW, *SATB2* mRNA expression was almost absent or of very low level as the staining between sense and anti-sense probes of *SATB2* was of similar intensities (Figure 4.3A, B).

At the protein level, SATB2 expression was strongly observed in a few cells scattering in the VZ, SVZ, IZ and CP (black double arrowheads, Figure 4.3A), and weakly in cells dispersing within the SVZ and IZ (black empty arrowhead, Figure 4.3A) of the dorsolateral anterior neocortex at 8 PCW. Within the IZ, some SATB2-expressing cells displayed a horizontal orientation (black filled arrow, Figure 4.3A) and thus may be migrating along the tangential dimension of the neocortex.

By 9 PCW, a denser layer of cells strongly expressing SATB2 was detected in the lower CP and individual SATB2-positive cells of similar intensity were also found to be scattered within the VZ, SVZ and IZ of the dorsolateral anterior neocortex (black double arrowheads, Figure 4.3B). Cells expressing a lower level of SATB2 remained present predominantly in the SVZ and CP at 9 PCW (black empty arrowhead, Figure 4.3B). Within the CP, some SATB2-expressing cells exhibit a vertically-elongated orientation (black empty arrow, Figure 4.3B), which might potentially be migrating radially.

At 12 PCW, the CP was delineated by the absence of GAP43 immunoreactivity underneath the MZ. Cells in the upper CP, presumably the developing Layer V, were *ER81*-positive (strong *ER81* anti-sense signal in comparison to the clear sense probe staining) and strongly expressed both *SATB2* mRNA (strong *SATB2* anti-sense signal in comparison to the clear sense probe staining) and SATB2 protein (Figure 4.3C). Notice the strong and intense anti-sense signal of *SATB2* observed at 12 PCW (Figure 4.3C) further confirmed the almost absent or very low level of *SATB2* mRNA expressed at 8-9 PCW (Figure 4.3A, B). Within the developing Layer V towards the upper part, cells were discreetly expressing either SATB2 or SOX5 (Figure 4.3C''), however in the lower Layer V, some cells were found to be co-expressing SATB2 and SOX5 (white filled arrow, Figure 4.3C''). A relatively lower level of *SATB2*/SATB2 mRNA and protein expression was detected throughout the lower CP, presumably Layer VI that is strongly immunoreactive for TBR1 (Figure 4.3C'), the SP and IZ (Figure 4.3C). Very few or no *SATB2*/SATB2-expressing cells were detected within the VZ, ISVZ and OSVZ (Figure 4.3C).

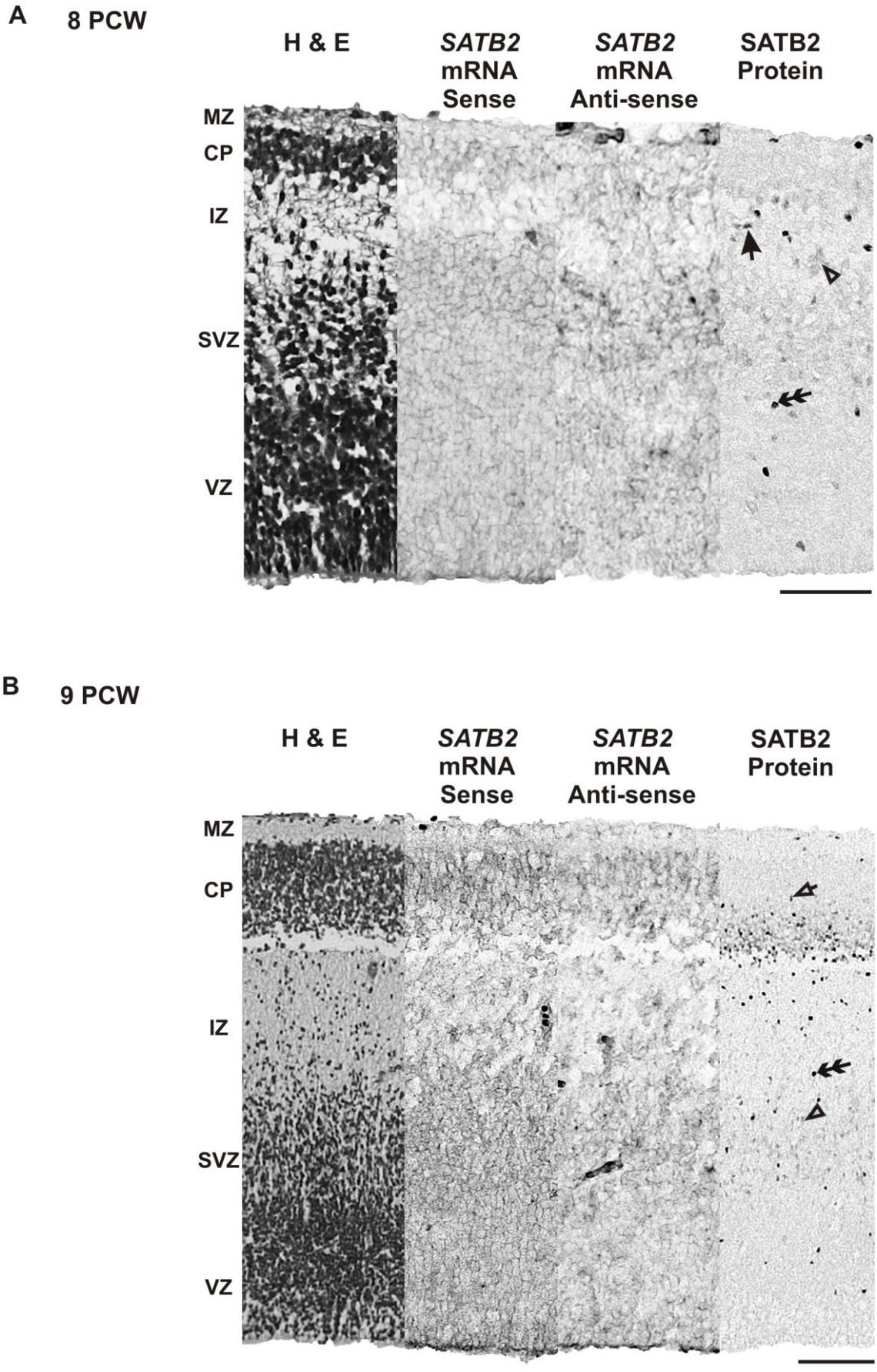
A
8 PCW
H & E
SATB2 mRNA Sense
SATB2 mRNA Anti-sense
SATB2 Protein
MZ
CP
IZ
SVZ
VZ
B
9 PCW
H & E
SATB2 mRNA Sense
SATB2 mRNA Anti-sense
SATB2 Protein
MZ
CP
IZ
SVZ
VZ

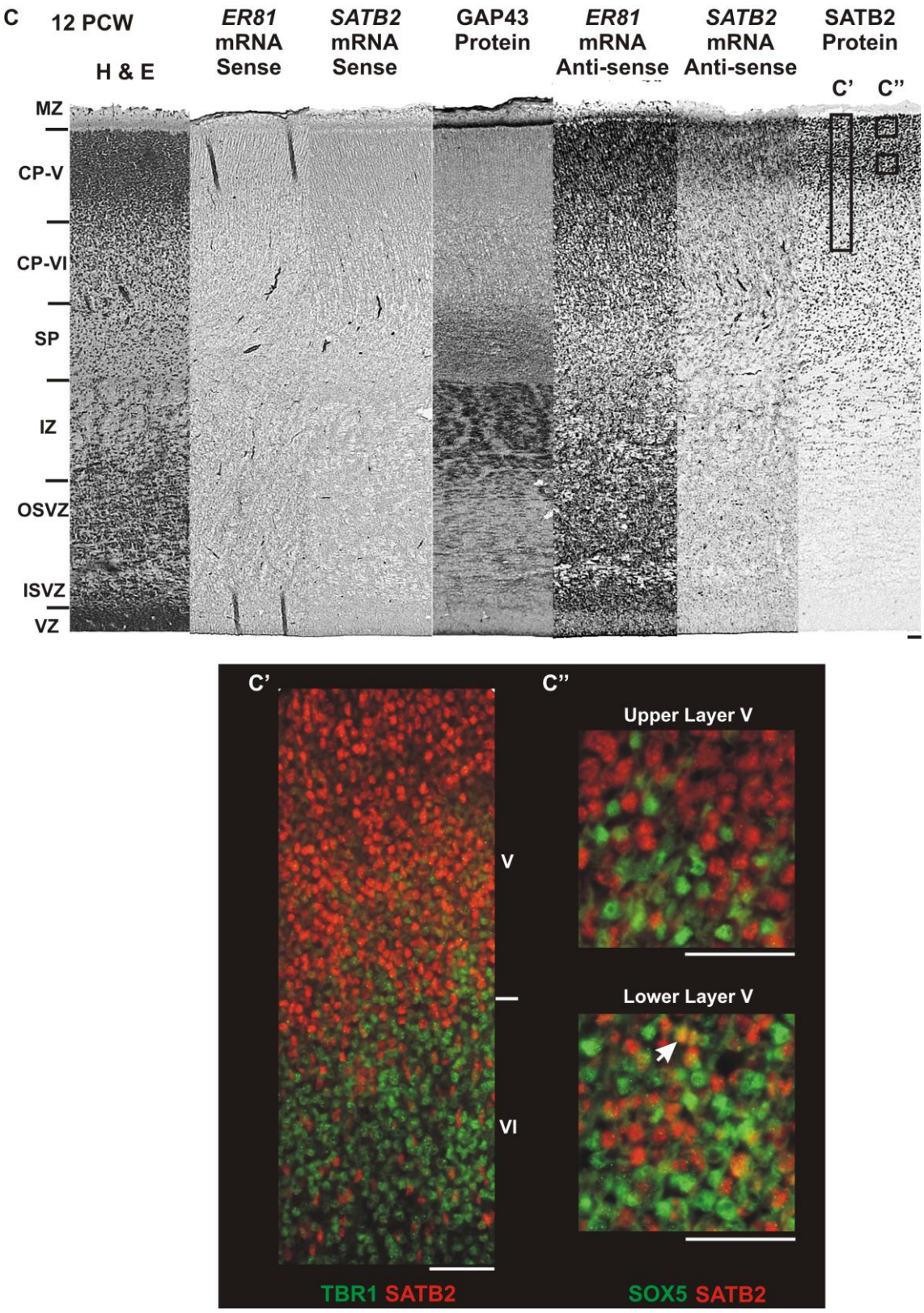

Figure 4.3. Laminar localization of *SATB2*/SATB2 during early human neocortical development (8-12 PCW).

Tissue ISH and IHC was performed to determine the laminar expression pattern of *SATB2*/SATB2 in comparison to histological H & E staining, *ER81* anti-sense signal and GAP43, SOX5 and TBR1 immunoreactivities.

At 8-9 PCW, *SATB2* mRNA expression was minimal or almost absent as sense and anti-sense probes of *SATB2* yielded similar intensity of staining (A, B). A few individual cells strongly immunoreactive for SATB2 were observed in the ventricular zone (VZ), subventricular zone (SVZ), intermediate zone (IZ) and cortical plate (CP) at 8 PCW (n=2) (black double arrowheads, A). Cells expressing SATB2 at lower level were predominantly dispersed in the SVZ and IZ at 8 PCW (black empty arrowhead, A). The number of strongly SATB2-positive cells increased by 9 PCW (n=2), accumulating in the lower CP and was also observed scattering in the VZ, SVZ and IZ (black double arrowheads, B). Cells expressing lower level of SATB2 remained present predominantly in the SVZ and CP at 9 PCW (black empty arrowhead, B).

At 12 PCW (n=2), absence of GAP43 immunoreactivity revealed the developing CP underneath the MZ (C). *SATB2*/SATB2 mRNA and protein expression increased drastically within the presumptive *ER81*-positive Layer V of the CP (C). Predominant expression of SATB2 is in Layer V above the TBR1-positive Layer VI of the CP (C'). No co-localization of SATB2 and SOX5 was observed in the upper Layer V, but some cells co-expressed SATB2 and SOX5 in the lower Layer V (white filled arrow, C'').

Black filled arrow indicates tangentially migrating cells (A); black empty arrow indicates radially migrating cells (B). Scale bars indicate 100 μm.

4.2.4 Tangential Expression Gradient of **SATB2** *during Early Human Neocortical Development*

To investigate the expression of SATB2 across the tangential axis of the neocortex, immunoperoxidase-histochemistry was performed and images were taken separately from the anterior and posterior regions of sagittal sections of the neocortex aged 8 and 9 PCW for comparison. The sagittal sections were taken from a relatively lateral position in which the diencephalic origin of the choroid plexus was visible. H & E stained sections from nearby regions were presented alongside for anatomical references (Figure 4.4).

From 8 PCW, SATB2-immunoreactive cells were mostly observed within the SVZ and CP of the neocortex anteriorly and posteriorly (Figure 4.4A). Within the SVZ, there were more cells expressing SATB2 in the anterior neocortex, despite having varying levels of expression among cells in the same layer, as compared to the posterior region of the neocortex (filled arrows indicates strongly SATB2-expressing cells; empty arrows indicates weakly SATB2-expressing cells, Figure 4.4A red boxed region, A', A''). This pattern of expression became more distinctive at 9 PCW, with more strongly and weakly SATB2-positive cells being detected within the SVZ in the anterior as compared to the posterior neocortex (filled arrows indicates strongly SATB2-expressing cells; empty arrows indicates weaker SATB2-expressing cells, Figure 4.4B red boxed region, B', B''). A few individual strongly SATB2-immunostained cells were also observed scattering within the VZ and IZ of both the anterior and posterior neocortex (Figure 4.4A, B, filled arrows). Thus these observations indicated that SATB2 is expressed in a high anterior, low posterior fashion in the neocortex from 8-9 PCW, and the differences were more noticeable within the SVZ.

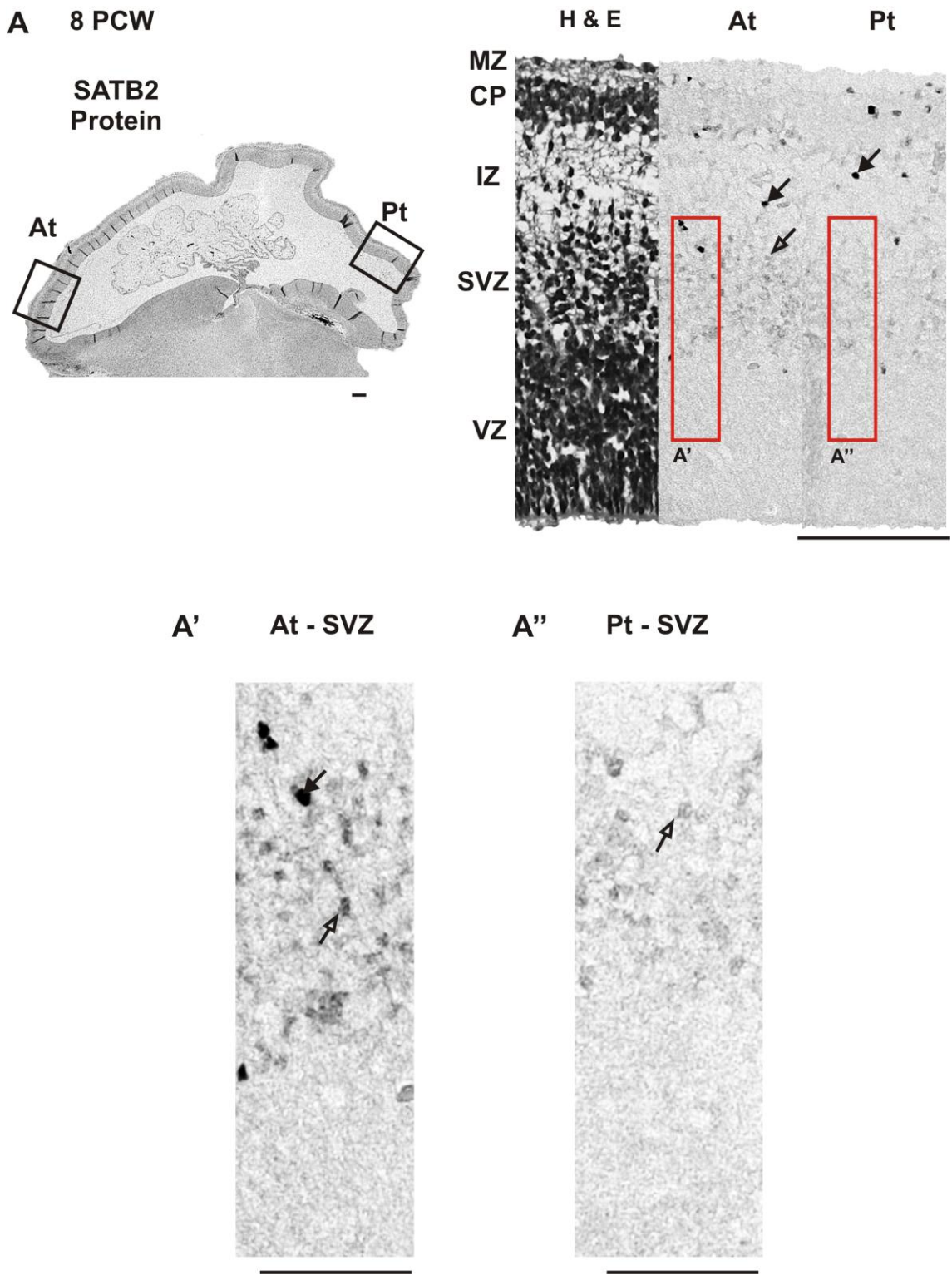
A
8 PCW
SATB2
Protein
At
Pt
H & E
At
Pt
MZ
CP
IZ
SVZ
VZ
A'
A''
A'
At - SVZ
A''
Pt - SVZ

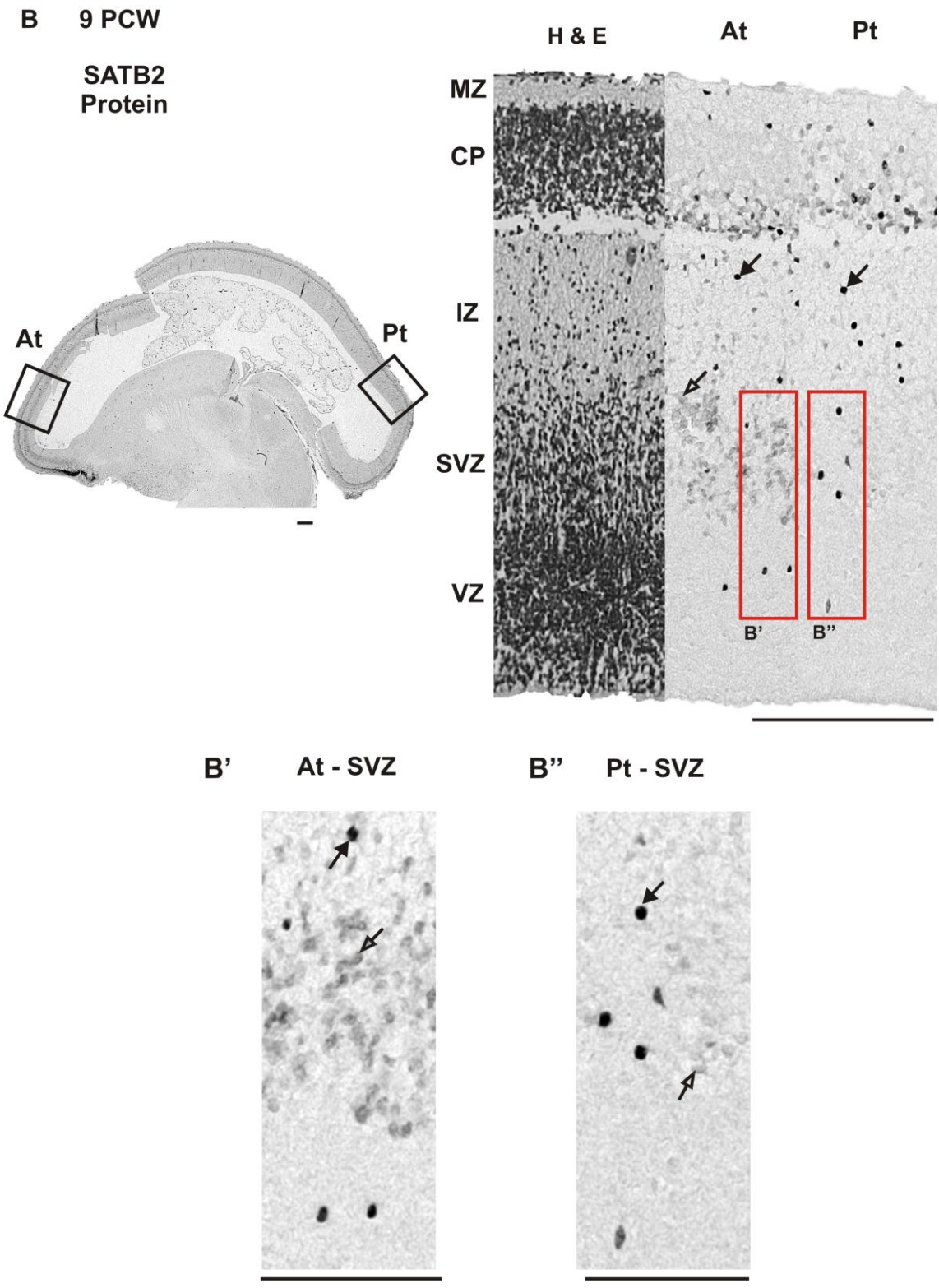

Figure 4.4. Expression gradient of SATB2 during early human neocortical development (8-9 PCW).

IHC was performed to determine the tangential expression pattern of SATB2 along the anterior-posterior axis of the developing human neocortex in conjunction with the histological H & E staining. Representative sagittal sections of human brains at 8 (n=2, A) and 9 PCW (n=2, B) were selected at a lateral level in which the diencephalic origin of the choroid plexus was visible and higher magnification pictures were taken at the indicated black boxed regions (A and B) of the anterior (At) and posterior (Pt) neocortex. Higher magnification images were also captured at the indicated red boxed regions within the VZ/SVZ (A and B) and presented in A', A'', B' and B''.

Two populations of SATB2-expressing cells were identified at both ages, i.e. the strongly SATB2-immunoreactive cells (filled arrows) and the weaker SATB2-positive cells (empty arrows; A, B). At both ages, more SATB2-immunoreactive cells (strongly and weakly expressing) were detected anteriorly (A', B') within the SVZ as compared to the posterior region of the neocortex (A'', B''). A few individual strongly SATB2-immunostained cells were also sparsely distributed within the VZ and IZ of both the anterior and posterior neocortex (A, B). Scale bars indicate 200 μm.

4.2.5. Tangential and Laminar Expression of **NURR1** *during Early Human Neocortical Development*

Expression patterns of NURR1 between 8-10 PCW

To investigate the expression of NURR1 across the tangential axis of the neocortex, immunoperoxidase-histochemistry was performed and images were taken separately from the anterior, dorsal and posterior regions of sagittal sections of the neocortex aged 8-10 PCW for comparison. The sagittal sections were taken from a relatively lateral position in which the diencephalic origin of the choroid plexus was visible. H & E stained sections from nearby regions were presented alongside for anatomical references (Figure 4.5).

At 8 PCW, no NURR1 expression was detected throughout the neocortex along its anterior-posterior axis (Figure 4.5A). NURR1-immunoreactive cells were only observed at the ventral surface of the pons, the pontine flexure and the upper medulla (Figure 4.5A).

At 9 PCW, small numbers of NURR1-expressing cells were found to be aggregating at the lower layer of the CP of the dorsal part of the neocortex, but not in any layer of the anterior or posterior region of the neocortex (Figure 4.5B).

By 10 PCW, cells immunostained for NURR1 were detected throughout the neocortex along its anterior-posterior axis, but remained restricted to the lower CP (Figure 4.5C).

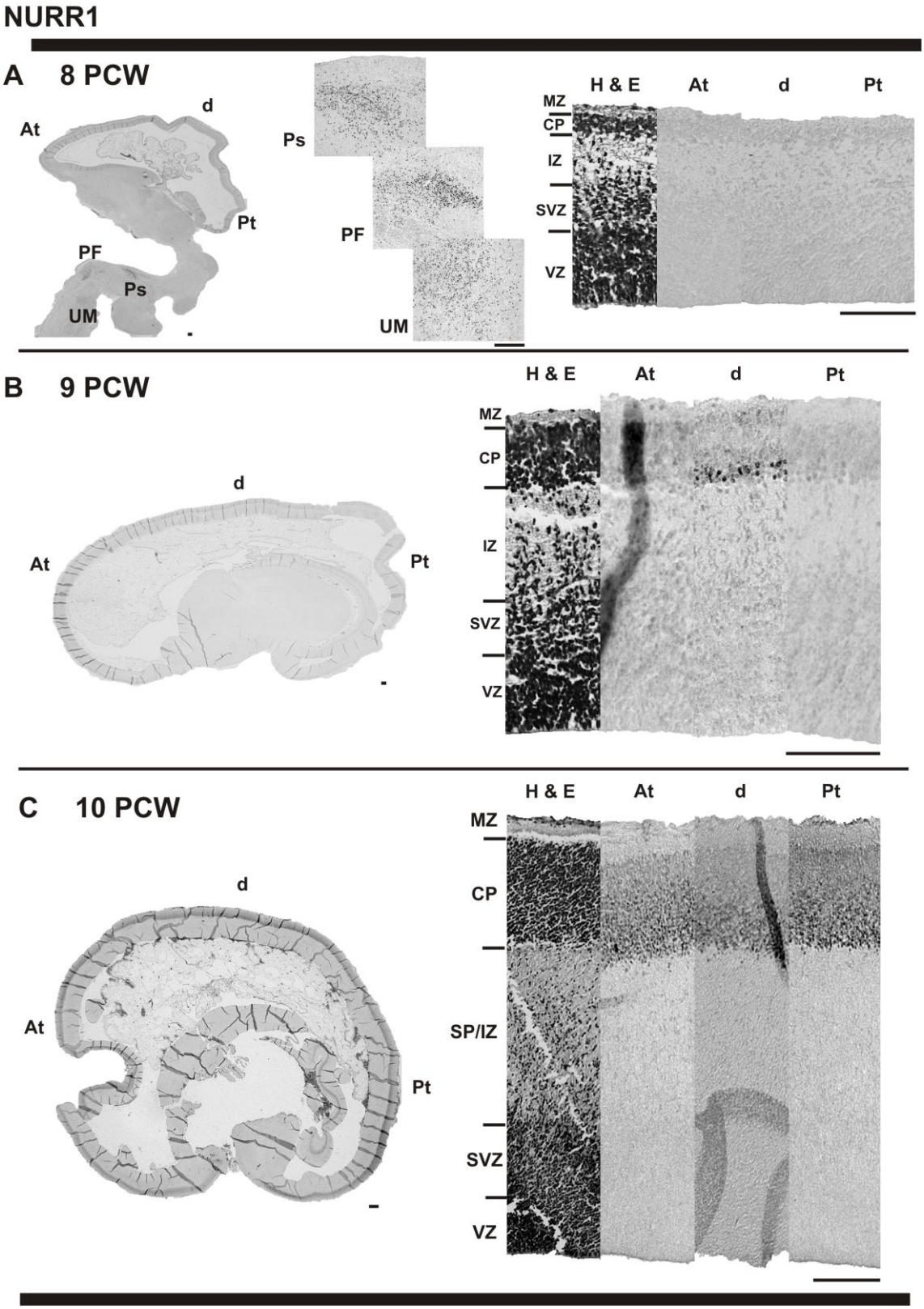

Figure 4.5. Tangential and laminar expression of NURR1 during early human neocortical development (8-10 PCW).

IHC was performed to determine the tangential expression pattern of NURR1 along the anterior-posterior axis of the developing human neocortex in conjunction with the histological H & E staining. Representative sagittal sections of human brains at 8 (n=2, A), 9 (n=2, B) and 10 PCW (n=10, C) were selected at a lateral level in which the diencephalic origin of the choroid plexus was visible and higher magnification pictures were taken at the indicated regions of the anterior (At), dorsal (d) and posterior (Pt) neocortex.

At 8 PCW, NURR1 was not expressed by cells in the neocortex along its tangential dimension, but by cells locating in the pons (Ps), pontine flexure (PF) and the upper medulla (UM) (A). At 9 PCW, NURR1 immunoreactivity was detected in the lower cortical plate (CP) of the dorsal part of the neocortex, but not in any layer of the anterior or posterior part of the neocortex (B). At 10 PCW, NURR1 was expressed by cells within the lower part of the CP throughout the entire neocortex along its anterior-posterior axis (C).

Higher magnification images were also taken at the pons, pontine flexure and the upper medulla. Scale bars indicate 200 μm.

Expression patterns of NURR1 at 12 and 15 PCW

To investigate the laminar expression patterns of NURR1 along the tangential axes of the neocortex aged 12 and 15 PCW, immunoperoxidase-histochemistry with NURR1 and GAP43 antibodies was performed on coronal sections selected at three different levels based on the presence or absence of some anatomical landmarks: i) the most anterior sections indicated by the absence of any basal telencephalic structures, the ganglionic eminences (LGE and MGE); followed by ii) sections with the presence of the LGE/MGE; and further posteriorly iii) sections with the presence of the CGE (Figure 4.6). Within each of these sections, three regions of the neocortex were examined: medial (m), dorsal (d) and lateral (l) (black solid lines, Figure 4.6).

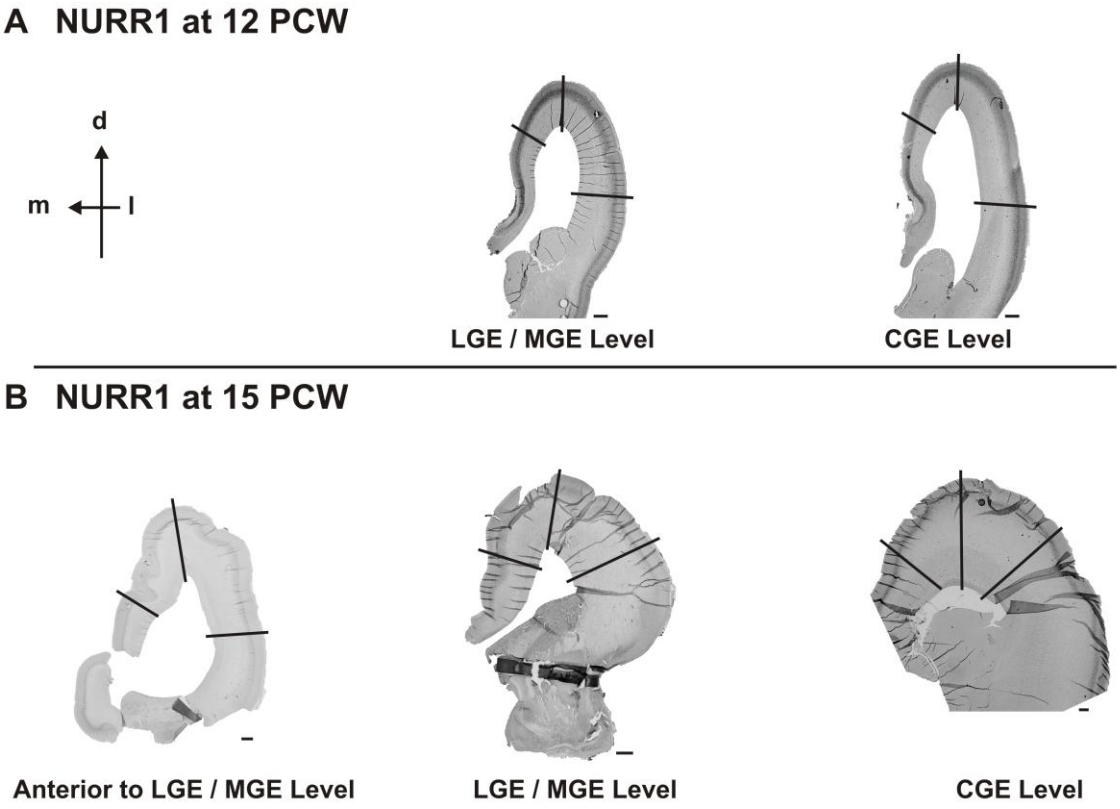

Figure 4.6. Anatomical orientation of coronal sections selected for the study of NURR1 laminar expression patters at 12 and 15 PCW.

Three levels of sections aged 12 (n=2, A) and 15 PCW (n=2, B) were selected along the anterior–posterior axis of the neocortex based on the presence or absence of some anatomical landmarks: anterior to the lateral ganglionic eminence (LGE)/medial ganglionic eminence (MGE) indicated by the absence of these subcortical structures, presence of the LGE/MGE and presence of the caudal ganglionic eminence (CGE). Black solid lines indicate regions where high magnification images were captured within each of these sections, namely the medial (m), dorsal (d) and lateral (l) domains of the neocortex. Scale bars indicate 200 μm.

From 12-15 PCW, when comparing the laminar expression patterns of GAP43, which predominantly expressed in the fibre-rich layers MZ, SP and IZ in humans, different NURR1 laminar immunoreactive patterns were observed along the two tangential axes of the neocortex: anterior-posterior and medio-dorso-lateral axes. Sections stained with H & E at the corresponding levels were also presented alongside with the NURR1- and GAP43-immunostained sections to provide additional histological information (Figure 4.7 and Figure 4.8).

At 12 PCW, at the anterior level with the presence of LGE/MGE as well as the posterior level with the presence of CGE, NURR1-expressing cells were found in the lower CP, presumably Layer VI, above the GAP43-immunoreactive SP in the medial and lateral part of the neocortex, but in both Layer VI of the CP and SP in the dorsal part of the neocortex (Figure 4.7A, B). It was found that that Layer VI was packed with more NURR1-expressing cells than the SP in the dorsal region of the neocortex. In the dorsal SP, NURR1-positive cells were more sparsely distributed (Figure 4.7A, B).

At 15 PCW, at the level anterior to the LGE/MGE, a dense layer of cells expressing NURR1 was observed in Layer VI of the CP, with a subset of them also found in the GAP43-positive SP in the medial region of the neocortex (Figure 4.8A). However, within the dorsal and lateral region of the neocortex, NURR1 immunoreactivity was only detected in Layer VI of the CP (Figure 4.8A).

At the relatively posterior levels with the presence of LGE/MGE and CGE at 15 PCW, changes of NURR1 laminar expression patterns were observed. In the medial region of the neocortex, NURR1 was densely expressed by cells in the upper part of the SP, with a few individual NURR1-positive cells scattering towards the lower part of the SP (Figure 4.8B, C). Dorsally, a denser layer of NURR1-expressing cells were found in the lower layer of the CP, presumably the Layer VI, and fewer cells immunoreactive for NURR1 were also detected in the upper part of the SP (Figure 4.8B, C). Laterally at the LGE/MGE level, NURR1-immunoreactive cells were predominantly observed in the Layer VI of the CP (Figure 4.8B), whereas at the CGE level, cells expressing NURR1 were found to be aggregating in the upper part of the SP (Figure 4.8C).

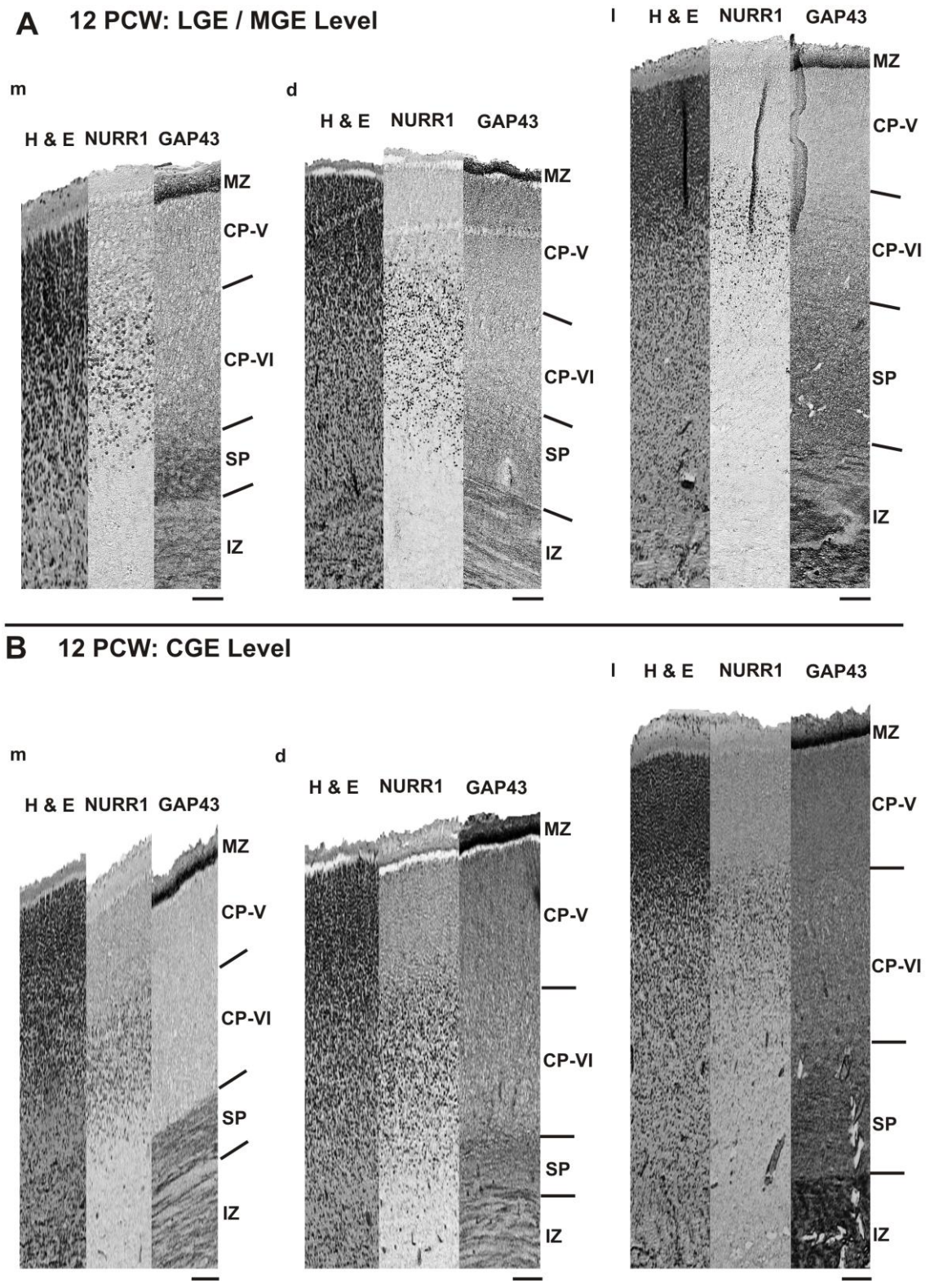

Figure 4.7. Tangential and laminar expression of NURR1 at 12 PCW.

IHC on paraffin sections revealed NURR1 expression in comparison to GAP43 expression and alongside with histological H & E staining at 12 PCW (n=2). Coronal sections of brains were selected at two levels: relatively anterior with the presence of lateral ganglionic eminence (LGE)/medial ganglionic eminence (MGE) (A) and relatively posterior with the presence of caudal ganglionic eminence (CGE) (B). GAP43 immunostained the marginal zone (MZ), subplate (SP) and intermediate zone (IZ) at all levels (A, B). At the levels of LGE/MGE and CGE, NURR1-immunoreactive cells were found predominantly in Layer VI of the cortical plate (CP) medially (m), dorsally (d) and laterally (l) (A, B). Fewer cells expressing NURR1 were also observed in the SP solely in the dorsal part (d) of the neocortex (A, B). Scale bars indicate 100 μm.

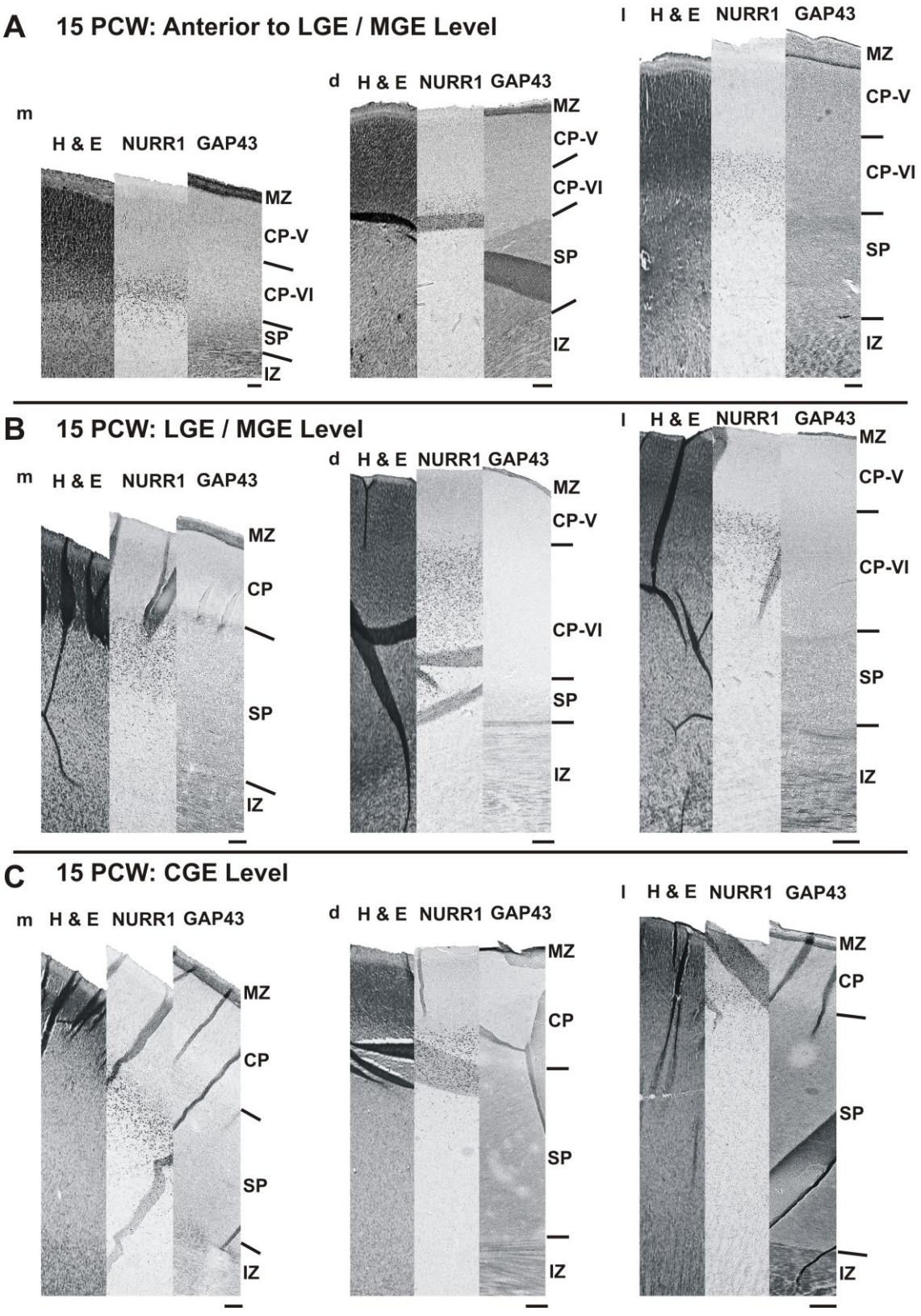

Figure 4.8. Tangential and laminar expression of NURR1 at 15 PCW.

IHC on paraffin sections revealed NURR1 expression in comparison to GAP43 expression and alongside with histological H & E staining at 15 PCW (n=2). Coronal sections of brains were selected at: (A) most anteriorly with the absence of lateral ganglionic eminence (LGE)/medial ganglionic eminence (MGE), (B) relatively mid-level with the presence of LGE/MGE and (C) most posteriorly with the presence of caudal ganglionic eminence (CGE). GAP43 immunostained the marginal zone (MZ), subplate (SP) and intermediate zone (IZ) at all levels (A-C). In (A), NURR1-immunoreactive cells were found predominantly in Layer VI of the cortical plate (CP) medially (m), dorsally (d) and laterally (l), with fewer cells expressing NURR1 were also detected in the SP of the medial part (m) of the neocortex. In (B), pronounced NURR1 expression was observed in the upper part of the SP medially. However, within the dorsal and lateral region, NURR1 immunoreactivity was mostly found in the Layer VI of the CP, and to a lesser extent also in the upper SP of dorsal neocortex. In (C), prominent NURR1 expression was observed in the upper part of the SP medially and laterally. However, within the dorsal region, NURR1 immunoreactivity was mostly found in the Layer VI of the CP, and to a lesser extent also in the upper SP. Scale bars indicate 200 μm.

Overall, NURR1 only started to be expressed by cells in the lower CP of the neocortex dorsally from 9 PCW and then the entire lower CP of the neocortex by 10 PCW (Figure 4.5). By 12 PCW when Layer V was forming, NURR1 appeared to be predominantly expressed by cells in Layer VI of the CP in humans (Figure 4.7 and Table 4.1). As development progresses, NURR1 expression gradually shifted from the Layer VI of the CP towards the upper part of the SP when examining sections from the anterior to posterior region of the developing neocortex aged 15 PCW (Figure 4.8 and Table 4.1).

	Anterior to LGE/MGE			**LGE/MGE**			**CGE**		
12 PCW	**m**	**d**	**l**	**m**	**d**	**l**	**m**	**d**	**l**
CP (VI)				++	++	++	++	++	++
SP					+			+	
15 PCW									
CP (VI)	++	++	++		++	++		++	
USP	+			++	+		++	+	++

Table 4.1. Summary of NURR1 laminar expression between 12-15 PCW.

+ and ++ indicate relatively lower and higher expression of NURR1 respectively in the Layer VI of the cortical plate (CP) and/or subplate (SP), particularly within its upper compartment (USP) at 12 (n=2) and 15 PCW (n=2). Medial (m), dorsal (d) and lateral (l) regions of the neocortex were examined at three levels along its anterior-posterior axis: anterior to the lateral (LGE)/medial ganglionic eminence (MGE), at the level of LGE/MGE and posteriorly at the CGE.

4.3 Discussion

4.3.1 Verification of SATB2 and NURR1 Expression Patterns during Early Human Neocortical Development

The brains of humans and rodents differ not only in terms of their sizes, the cytoarchitecture and connectivity of neuronal networks also appear to be more complex in humans after evolutionary development (Hill and Walsh, 2005). On the molecular basis, genes that are known to play a vital role in corticogenesis and regionalisation in rodents are found to be expressed in different patterns in humans too. Therefore although the use of various rodent layer-enriched markers could potentially help to distinguish between different laminae in the developing neocortex in humans, one should be cautious and verify their patterns of expression in humans prior to extrapolating data from rodent studies and applying them directly onto human studies. The studies in this chapter sought to validate the use of *SATB2*/SATB2 and NURR1 as laminar-enriched markers in humans by comparing their expression patterns with some already established markers in humans such as *ER81* (Layer V) and GAP43 (MZ, SP and IZ) during early human neocortical development.

Previous molecular neuroanatomical studies by our group have shown that by 16 PCW Layer V can be visualized by ER81 immunoreactivity in the human neocortex (Bayatti et al., 2008a) which is expressed by a subpopulation of neurones in the neocortical Layer V of rodents and non-human primates (Yoneshima et al., 2006). The current observation of *ER81* expression has provided evidence that Layer V in the human neocortex is already formed by 12 PCW (Figure 4.3). In addition, the *ER81*-positive Layer V also strongly expressed *SATB2*/SATB2 (Figure 4.3). Although other transient layers of the neocortex also showed a weaker expression of *SATB2*/SATB2, its predominant expression correlating with that of *ER81* and above the TBR1-positive Layer VI (Figure 4.3) has proven the suitability of employing *SATB2*/SATB2 as a Layer V marker at 12 PCW. However as neocortical development progress, one should not exclude the possibility of detecting *SATB2*/SATB2 expression in upper layers of the human CP, as observed in rodents (Alcamo et al., 2008; Britanova et al., 2008). The current study was limited by quality of tissue sections at older ages in which tissue ISH

was not suitable for tissue sections aged 15 PCW and above. In addition, the ER81 antibody (obtained from Dr. Jessell) used in previous study (Bayatti et al., 2008a) could not be applied on paraffin-embedded tissues which have been used in the current study. Therefore, comparison of expression patterns between *SATB2*/SATB2 and *ER81*/ER81 cannot be carried out beyond 15 PCW. Nevertheless, results obtained in the current study have validated *SATB2*/SATB2 as a Layer V marker in the human developing neocortex at least at around 12 PCW.

Previous molecular neuroanatomical studies by our group have shown that by 12 PCW the SP can be visualized by GAP43 immunoreactivity in the human neocortex (Bayatti et al., 2008a). Here, by comparing with the expression pattern of GAP43 from 12 PCW onwards, NURR1 was found to be predominantly expressed by neurones in Layer VI of the CP in humans, above the GAP43-positive SP, while in some regions it was also expressed in the upper SP, overlapping partially with the GAP43 immunoreactivity, depending on the developmental stages (Figure 4.7, Figure 4.8, Table 4.1). This spatial difference is also observed in rodents, but with different expression patterns such that Nurr1 is predominantly a SP marker in the dorsal region of the neocortex, but more widely expressed in Layer V, VI and SP towards the lateral part of the neocortex in mice from embryonic stage to adulthood (Hoerder-Suabedissen et al., 2009; Arimatsu et al., 2003). Therefore using NURR1 solely as a Layer VI or SP marker is not adequate. In any case, one should not rely on one marker but always use a combination to demarcate boundaries between different layers of the neocortex. For this reason, when examining the laminar expression patterns of the corticofugal neurone-associated genes in the next chapter (Chapter 5), a range of markers would be included for confirmation and better illustration.

4.3.2 Expression Patterns of SATB2 and its Implications

Satb2 is expressed predominantly by post-mitotic, callosal projecting neurones in Layer V as well as upper layers of the CP in rodents during corticogenesis (Alcamo et al., 2008; Britanova et al., 2008). Unlike absence of Satb2 expression in the rodent VZ/SVZ (Britanova et al., 2005), strong and weak SATB2-immunoreactive cells are present in the heterogeneous proliferative zones in humans (Figure 4.3, Figure 4.4). Whether these

cells are proliferative or post-mitotic would require further analyses such as co-localization studies of SATB2 with INPs or post-mitotic neuronal markers. It has been reported in rodents a subset of projection neurones derived from *Emx1*-positive neocortical progenitors expressing SATB2 would migrate tangentially within the rodent developing neocortex (Britanova et al., 2006a). We have also observed some horizontally elongated SATB2-immunoreactive cells that are potentially migrating along the tangential axis. It would be interesting to test if these neurones also co-express EMX1 to confirm their neocortical origin.

By 12 PCW, similar to the observation in rodents (Alcamo et al., 2008), the majority of SATB2-expressing neurones occupy the *ER81*-positive Layer V of the CP, above the TBR1-positive neurones dominating Layer VI, though TBR1 expression is also detected in the lower Layer V in humans (Figure 4.3). Additionally, our findings are consistent with a recent study that has reported the observation in human foetal brains at 29 PCW that the small numbers of SATB2-expressing neurones observed in Layer VI do not express TBR1 (Saito et al., 2010). In contrast, with the use of retrograde tract tracing of callosal axons together with microarray analyses and SOX5 immunostaining, it is reported that SOX5 is not expressed by callosally projecting neurones in rodents from embryonic to postnatal stages investigated (Lai et al., 2008). Within Layer V, corticofugal neurones are also found which project their axons towards subcortical structures of the brain. This type of neurones will be described and investigated further in Chapter 5. Briefly, they express markers such as *Fezf2* in proliferative states (Chen et al., 2008; Chen et al., 2005b; Chen et al., 2005a; Molyneaux et al., 2005) and *Fezf2* as well as Ctip2 when they become post-mitotic in rodent studies (Arlotta et al., 2005). SOX5 has been shown to down-regulate *Fezf2* and Ctip2 in mice and refine their expression within Layer V of the CP (Kwan et al., 2008). Additionally, *Fezf2* is known to act upstream of Satb2 and Ctip2 to repress the callosal- and promote the subcerebral-projecting phenotypes respectively (Chen et al., 2008). Thus neurones in the lower Layer V co-expressing SATB2 and SOX5 (Figure 4.3) are likely to be undergoing transitional state between callosal- and subcerebral-projecting phenotypes at post-mitotic level in which SOX5 is repressing FEZF2 expression to release the inhibition of SATB2 thus inducing the differentiation of callosal projecting neurones. (Chapter 1, Figure 1.8)

Interestingly, our Affymetrix gene chips analysis have shown that *SATB2* probe set (235147_at) was highly up-regulated by 3.13-fold in the anterior compared to the posterior region of the neocortex between 8-12 PCW (Ip et al., 2010a). The graded expression of SATB2 has not been reported in rodent studies, yet we have detected a high anterior – low posterior expression gradient (3.13-fold) across the developing neocortex between 8-12 PCW in Affymetrix gene chips analysis (probe set 235147_at) (Ip et al., 2010a) and observed more strongly and weakly SATB2-positive cells primarily in the SVZ of the anterior as compared to the posterior neocortex at early stages of neocorticogenesis prior to the innervation of any thalamocortical afferents (Figure 4.4). However, quantification of these strongly and weakly SATB2-immunoreactive cells at in both regions with more samples to carry out statistical analyses and rtPCR is required to further confirm this expression gradient at protein and RNA level respectively in the developing human neocortex. In rodents, loss- and gain-of *Pax6* function studies show reduced and increased *Satb2* expression in the developing neocortex respectively (Holm et al., 2007). Thus like *TBR2*, this high anterior – low posterior expression gradient of SATB2 in the SVZ is probably regulated by *PAX6* before its expression gradient is lost by 9 PCW in humans (Bayatti et al., 2008b).

4.3.3 Expression Patterns of NURR1 *and its Implications*

Nurr1 expression is restricted to the SP in the dorsal region of the neocortex, visible as a thin band underneath the Layer VI of CP, but widely expressed in Layer V, VI and SP towards the lateral part of the neocortex in mice from embryonic stage to adulthood (Hoerder-Suabedissen et al., 2009; Arimatsu et al., 2003). Here we have observed NURR1 expression varies from region to region and between different developmental stages, predominantly expressed in Layer VI of the CP at 12 PCW (Figure 4.7, Table 4.1) and gradually shifted from Layer VI of the CP to the SP when examining sections from anterior to posterior regions of the neocortex at 15 PCW (Figure 4.8, Table 4.1). As reported previously in our group, a GAP43-positive human SP begins to form visibly underneath Layer VI of the CP from 12 PCW (Bayatti et al., 2008a). However, NURR1 expression starts to be detectable from 9 PCW onwards, emerging from lower layer of the developing CP in the dorsal region of the neocortex (Figure 4.5).

Nevertheless, this dorsal region of the neocortex might correspond to the future somatosensory area where the SP begins to form first as compared to the posteriorly-locating visual area (Kostovic and Rakic, 1990). Thereafter from 12 PCW NURR1 is predominantly expressed in the Layer VI of the CP in most regions of the neocortex with some in the upper SP of the dorsal neocortex (Figure 4.7, Table 4.1), which may correspond to the condensation of parts of Layer VI with the pre-subplate to form the SP proper, as proposed by Kostovic and Rakic (1990) (Kostovic and Rakic, 1990). FOXP2, a marker delineating Layer VI of the CP in mice, non-human primates and humans (Hisaoka et al., 2010; Wang et al., 2010; Takahashi et al., 2008; Vargha-Khadem et al., 2005), also confirmed the expression of NURR1 spanning the lower Layer VI and upper SP of the dorsal cortex at 15 PCW (Wang et al., 2010). In addition to the expression of *Nurr1* by glutamatergic, pyramidal neurones (Arimatsu et al., 2003), a recent report has shown that in the sensorimotor cortex of young mice (P18), *Nurr1* is also expressed by *vGlut1*- and *cholecystokinin*-positive, multipolar neurones with spiny dendrites, which can be found in the lower Layer VI adjacent to the white matter (Andjelic et al., 2009). It would be interesting to probe the various neuronal subtypes expressing NURR1 in human foetal neocortex during development. By 16 PCW, the SP can be divided into the upper SP with more NPY-expressing neurones and the lower SP with more K^+ Cl^- co-transporter 2 (KCC2)-immunoreactive neurones (Wang et al., 2010; Bayatti et al., 2008a). Here, we have shown that SP could potentially be divided into upper and lower SP by 15 PCW in which NURR1 expression was predominantly found in the upper part (Figure 4.8, Table 4.1).

Although the low anterior – high posterior expression gradient (1.87-1.92-fold) of *NURR1* detected between 8-12 PCW by Affymetrix gene chip analysis in humans (probe sets 2.16248_s_at, 204621_s_at and 204622_x_at) (Ip et al., 2010a) was not observed at the protein level in this study, NURR1 began to be expressed by neurones in the neocortex in a regionalised fashion at 9 PCW (Figure 4.5). In rodents, there seems to be more neurones expressing Nurr1 in the lateral region compared to the medial region of the neocortex persistently from embryonic to postnatal stages (Arimatsu et al., 2003) and predominant expression in the occipital cortex is observed from E14.5-18 ((Muhlfriedel et al., 2007); http://www.Genepaint.org). In adult rats, expression profiling in the neocortex has revealed cortical maps of Layer IV, V and VI that are characterized by the differential expression of *RORβ*, *Er81* and *Nurr1* (Hirokawa et al.,

2008). *Nurr1* is found to be highly expressed in Layer V of the entorhinal cortex and Layer VI of some somatosensory areas in the parietal cortex (Area 2 and the ventral area of parietal cortex) (Hirokawa et al., 2008). It is worth looking further into the expression pattern of *NURR1*/NURR1 in the human developing neocortex to determine whether its expression begins in a graded or regionalised pattern.

4.3.4 Potential Interaction between SATB2 and NURR1

Although there is no direct biochemical evidence to show interactions between Satb2 and Nurr1, Satb2 is probably repressing the expression of Nurr1, directly or indirectly, since Nurr1 expression is expanded towards the upper layers of the CP in the absence of *Satb2* expression in mice (Britanova et al., 2008). In humans, the inhibitory effects of SATB2 on NURR1 expression probably also exist in order to control the differentiation of some projection neurones in Layer V and above to send axons contralaterally between the two hemispheres instead of ipsilaterally. Additionally, this inhibitory effect probably occurs across the tangential dimension of the neocortex and contributes to the potential complementary graded/regionalised expression of SATB2 and NURR1.

Nevertheless, the data we have obtained to-date for SATB2 and NURR1 is preliminary and would require more thorough examination, which includes:

1) rtPCR confirmation of tangential graded expression of *SATB2* and *NURR1*, using neocortical tissues from anterior, posterior and possibly dorsal regions of 8, 10 and 12 PCW.

2) Repetition of immunoperoxidase-histochemistry for SATB2 with Toluidine Blue counter-stain on sagittal brain sections from 8-10 PCW, quantification of SATB2-positive cells in the different layers of the anterior region compared to the posterior region of the neocortex and determination of statistical significant differences between different layers in different regions.

3) Co-localization studies of SATB2 with TBR2 (INP markers) or TBR1 (early post-mitotic neuronal markers) to confirm the types of cells expressing SATB2 within the heterogeneous SVZ from 8 PCW onwards.

4) Co-localization studies of SATB2 with EMX1 to confirm the neocortical origin of SATB2-positive, tangentially migrating neurones within the developing neocortex.

5) Repetition of immunoperoxidase-histochemistry for NURR1 with more sagittal brain sections at various levels (medial vs. lateral) from 8-10 PCW to precisely identify the regions in the neocortex where it starts to be expressed.

6) Investigation of the mechanisms that regulate the expression of SATB2 and NURR1 *in-vitro* in human neocortical cell cultures.

Chapter 5 Investigating Expression of Corticofugal Neurone-associated Genes *ROBO1*, *SRGAP1* and *CTIP2* in Early Human Neocortical Development

5.1 Introduction

5.1.1 The Descending Fibre Tracts: Corticofugal Projections

The descending fibre tracts in mammals are collectively known as corticofugal projections which originate from diverse neocortical areas and terminate at different regions of the central nervous system. These include corticothalamic, corticostriatal, corticopontine, corticotectal, corticospinal and corticobulbar projections. During development, these fibre tracts exit the neocortex and course through the internal capsule to reach the telencephalic-diencephalic boundary. At the transition to the mesencephalon, the corticospinal axons advance towards the ventral surface and together with the corticopontine and corticobulbar axons forming the cerebral peduncles (Kahle and Frotscher, 2002). Within each of the cerebral peduncles, the corticospinal axons take up the central part and are topographically arranged according to their terminations at different levels of the spinal cord (Kahle and Frotscher, 2002). In the medulla oblongata, the corticobulbar axons terminate on the cranial nerve nuclei, while most of the corticospinal axons travel further towards the spinal cord after crossing over to the opposite side in the pyramidal decussation (70-90%), forming the lateral corticospinal tract (CST) (Kahle and Frotscher, 2002). The remaining uncrossed fibres that stay projecting ipsilaterally towards the spinal cord are known as the anterior CST (Kahle and Frotscher, 2002). There are about 19 million axons present in the human cerebral peduncle prior to the entry of the pons, and around one million of axons are found in the medullary pyramids (Brodal, 1978; Tomasch, 1969). The long trajectories of these corticofugal projections require proper guidance to avoid any deviation and ensure correct axonal pathfinding and target selection at each point from its origin to its destination, and this is believed to be achieved by the interactions of various cell adhesion/axon guidance molecules (Faulkner et al., 2008; Runker et al., 2008).

5.1.2 Development and Plasticity of the Origin of the Corticofugal Neurones

The motor cortex is an important site of origin for the corticospinal projection neurones, whose tract (CST) is the major descending pathway to control voluntary and skilled movements of distal musculature. In addition, the motor cortex also houses the majority of corticobulbar neurones projecting to cranial motor nuclei, and corticopontine neurones projecting to the ventral surface of the pons, as revealed by horseradish peroxidase injections in the pontine nuclei of macaque monkeys (Glickstein et al., 1985). In humans, imaging techniques have revealed a comparatively larger contribution of the prefrontal areas to the corticopontine tract as compared to macaque monkeys (Ramnani et al., 2006). The CST together with the corticobulbar fibres convey commands from the neocortical motor centres to refine and modify the mechanical and stereotyped motions controlled by the subcortical motor centres thereby producing specific, fine-tuned movements (Kahle and Frotscher, 2002).

The development of CST is the most studied of the descending corticofugal projections. In rodents, the corticospinal projection originates from Layer Vb throughout the whole developing neocortex postnatally, and is eventually restricted to its adult location including posterior frontal/anterior parietal cortex via pruning of collateral projections (Oudega et al., 1994; O'Leary and Koester, 1993; O'Leary, 1992; Stanfield and O'Leary, 1985; Bates and Killackey, 1984). Macaque monkeys at birth have regional cortical projections patterns resembling that of the mature macaque (Galea and Darian-Smith, 1995; Galea and Darian-Smith, 1994). However, the patterns are further refined during maturation that areas of cortical origins and targets of projections are reduced through collateral elimination, thus resulting in approximately 60% of CST fibres arising from the primary, premotor and supplementary motor cortices in the frontal lobe with a further 15% arising from the prefrontal, cingulate and insular cortices and 25% from the parietal cortex in the mature macaque monkeys (Galea and Darian-Smith, 1995; Galea and Darian-Smith, 1994). Similarly in humans, the fibres of the CST originate in the primary motor cortex (area 4), premotor and supplementary motor cortices (area 6) in the frontal lobe, primary somatosensory cortex (area 1, 2 and 3) as well as the second sensorimotor area (area 40) in the parietal lobe (Kahle and Frotscher, 2002). However, the proportion of CST fibres arising from the frontal lobe may be even higher in humans

as compared to non-human primates due to the increased importance of direct neocortico-moto-neuronal connections from the primary motor cortex for human-specific sensorimotor behaviour including skilled use of the hand and digits (Lemon, 2008). The origin of the CST appeared to show some degree of variation between different species such as rodents (Oudega et al., 1994; O'Leary and Koester, 1993; O'Leary, 1992; Stanfield and O'Leary, 1985; Bates and Killackey, 1984), non-human primates (Galea and Darian-Smith, 1995; Galea and Darian-Smith, 1994) and humans (Lemon, 2008) whereby the proportion of different neocortical areas giving rise to the CST varies. This is probably reflecting some species-specific functions that the tract subserves and these ontological differences probably arise through species-specific developmental mechanisms of corticogenesis and regionalisation, thus highlighting the importance of utilizing human materials to study the corticospinal as well as other corticofugal systems as compared to other species.

The motor cortex harbouring the above important corticofugal neurones is a common site of developmental brain damage leading to cerebral palsy that occurs in one in four hundred live births (Eyre, 2007). The corticospinal system is plastic during development and perinatal injuries would alter the final patterns of the origin and termination of the CST. In cats, unilateral corticospinal inactivation or prevention of limb use results in retention of larger number of ipsilateral corticospinal fibres from the more active neocortex and causes abnormal visually-guided movements (Martin et al., 2007). Similarly, transcranial magnetic stimulation (TMS) of the affected motor cortex though fail to elicit responses in the paretic upper limbs of patients with hemiplegic cerebral palsy, abnormal responses were evoked when TMS was applied to the unaffected ipsilateral motor cortex (Eyre, 2007). A more recent study suggests that lesions at early stages of human development may lead to subsequent substantial re-organization of the origins of the corticospinal output such that an electromyographic response of the ipsilateral biceps was recorded when TMS was applied to the visual area of the infarcted side of the neocortex (Basu et al., 2010). Therefore, the present study set out to explore how the cortical map is established and the processes preceding motor cortex differentiation in order to understand the mechanisms of re-organization and improve outcome after such lesions.

5.1.3 Corticofugal Neurone-associated Markers

Chapter 3 has discussed the work using Affymetrix gene chips to probe mRNA expression in human foetal neocortical tissues between 8-12.5 PCW identified gene probe sets related to motor cortex and corticofugal axon development that were highly up-regulated at the anterior pole of the neocortex compared to the posterior pole (Table 3.2; (Ip et al., 2010a)). These included *CTIP2*, *ROBO1* and *SRGAP1*, genes whose expression is not exclusive to corticospinal neurones but crucial to their development. In rodents, the transcription factor Ctip2 is expressed by subcerebral projecting neurones in Layer V and is important for post-mitotic differentiation of corticospinal neurones including fasciculation, outgrowth and pathfinding of their axons but not early specification, since its expression is not observed in the proliferative zones (Arlotta et al., 2005). Robo protein expression has been demonstrated throughout the developing corticofugal pathways including the CST (Sundaresan et al., 2004) and has been shown to be involved in human CST development (Jen et al., 2004). E18.5 *Robo1*$^{-/-}$*Robo2*$^{-/-}$ double mutants showed severe mis-projection and crossing over of corticospinal axons from the internal capsule towards the midline at the telencephalic level and a complete absence of cerebral peduncles in the mesencephalon (Lopez-Bendito et al., 2007). Along with their downstream signalling molecule srGAP1, they play a role in axonal growth guidance by regulating actin polymerization (Wong et al., 2001). Other important functions of srGAPs have been proposed such as regulating transcription factor activity or protein transcription as highly regulated shuttling of srGAPs between the nucleus and the cytoplasm has been observed throughout neurogenesis (Yao et al., 2008).

Another corticofugal-related transcription factor *Fezf2* is expressed by progenitors and post-mitotic Layer V subcerebral projecting neurones in rodents, but is more important in earlier specification and differentiation of corticofugal neurones as it acts upstream of Ctip2 during development (Chen et al., 2008; Chen et al., 2005b; Chen et al., 2005a; Molyneaux et al., 2005). Sox5, a transcription factor acting further upstream of *Fezf2* and Ctip2, is expressed by post-mitotic corticothalamic projecting neurones in Layer VI and SP in rodents and is proposed to be responsible for determining the generation

sequence and the molecular/laminar identity of corticofugal projection neurones (Kwan et al., 2008; Lai et al., 2008).

5.2 Aim of Study

In order to test the hypothesis that the anterior pole of the neocortex may be an early site of origin of corticospinal neurones and other corticofugal projections, the present study aims to study the localized genes/proteins expression of CTIP2, ROBO1 and SRGAP1 utilizing human neocortical and brainstem tissue from 8-17 PCW, a period of time when the CP first starts to form (7.5 PCW, (Meyer et al., 2000)), to when the thalamocortical innervation of the SP occurs (13 PCW, (Kostovic and Rakic, 1990)) and the appearance of distinct layers in the CP by 16 PCW (Bayatti et al., 2008a).

Objectives of this chapter were:

1) to confirmation of the high anterior to low posterior expression gradients of *ROBO1* and *CTIP2* by ISH and SRGAP1 by IHC, in comparison with *FEZF2* and *SOX5*.

2) to analysis of the laminar and cellular mRNA/protein expression patterns of these genes in comparison to other laminar-specific markers, i.e. SATB2 (Layer V at early stages) (Alcamo et al., 2008), ER81 (Layer V) (Yoneshima et al., 2006), NURR1 (Layer VI, SP) (Wang et al., 2010; Hoerder-Suabedissen et al., 2009), TBR1 (Layer VI, SP) (Bayatti et al., 2008a; Hevner et al., 2001), Synaptophysin and GAP43 (MZ, SP) (Bayatti et al., 2008a) in order to identify and localize these genes/proteins to the emerging Layer V.

3) to demonstration of ROBO1 and SRGAP1 as corticofugal neurone-associated markers in humans by showing their expression in Layer V of the CP and along the subcerebral projecting fibres in the brainstem.

5.3 Results

5.3.1 Negative Controls for Tissue ISH

To confirm the specificity of anti-sense probes of *CTIP2*, *FEZF2*, *ROBO1* and *SOX5* for tissue ISH, the negative sense probes of each gene were used alongside during the experiment. All sections hybridized with sense probes showed no signal, and representative sections were presented in Figure 5.1.

Comparison of sense and anti-sense probes of *ER81* and *SATB2* was presented in Figure 4.1.

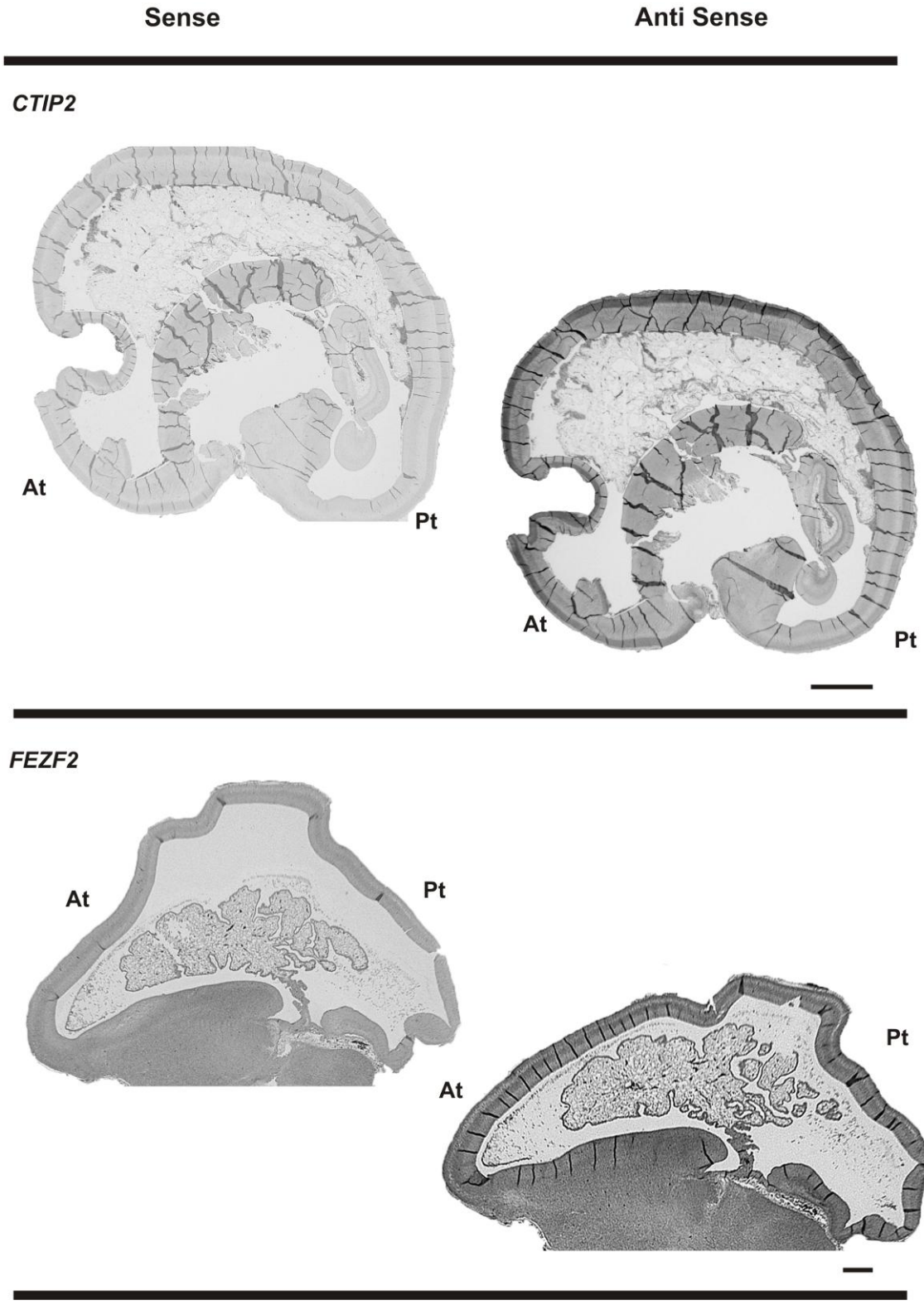
Sense
Anti Sense
CTIP2
At
Pt
At
Pt
FEZF2
At
Pt
At
Pt

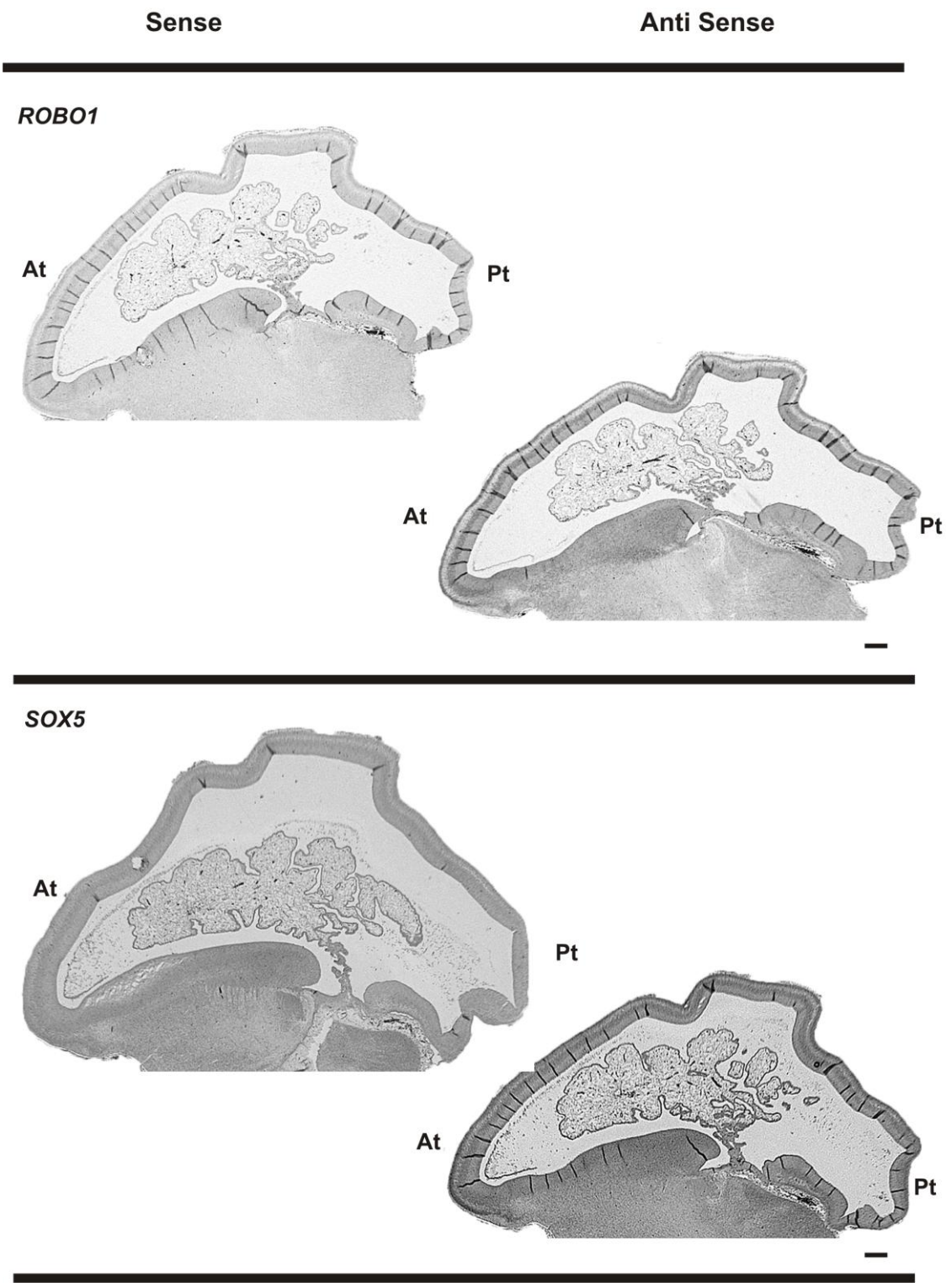

Figure 5.1. Detection of anti-sense and sense probes for *CTIP2, FEZF2, ROBO1* and *SOX5*.

Specificity test for the anti-sense probes was carried for *CTIP2, FEZF2, ROBO1* and *SOX5*. Representative images were captured with sagittal sections of 8 PCW (n=3) for *FEZF2*, *ROBO1* and *SOX5* and of 10 PCW (n=3) for *CTIP2*. The anterior (At), lateral (L), medial (M) and posterior (Pt) part of the neocortex was labelled for orientation purposes. Scale bars indicated 500 µm.

5.3.2 Characterization of Primary Antibodies

Primary antibodies used in this study were obtained commercially and staining patterns observed by other research groups were published (Table 2.6) except SRGAP1. Of the publication-used antibodies, ROBO1 has not been used on any brain or neocortical tissues.

Therefore SDS-PAGE and Western blot was performed to characterize ROBO1 and SRGAP1 antibodies, using protein samples obtained from the anterior and posterior regions of the human foetal neocortical tissues aged 14 PCW. Positive control was included using β–ACTIN antibody, revealing a band slightly above 40 kDa (actual size 44 kDa) (Figure 5.2). A strong single band between 110-160 kDa was observed with SRGAP1 antibody (actual size 124 kDa), proving its specificity (Figure 5.2).

For ROBO1 antibody, multiple bands were observed including the ones of correct size (175-181 kDa, arrows, Figure 5.2). The immunogen used to manufacture this antibody was a synthetic peptide: -VLGGYERGEDNNE conjugated to KLH, corresponding to amino acids 1632-1644 of human ROBO1 (Abcam datasheet; http://www.abcam.com/Robo1-antibody-ab7279.html). This sequence was blast with Blastp of NCBI against the non-redundant protein sequences (nr) of the *Homo sapiens* database. The blast results showing proteins with size ranging from 10-260 kDa were summarized in Table A.1 in Appendix. Briefly, the immunogen was 100% identical to all isoforms of human ROBO1 protein with molecular weight ranging from 175-181 kDa. 61% or less of the immunogen sequence was similar to other protein segments including, Ankyrin 2 (ANK2; 63 kDa), Arrestin domain-containing 3 (ARRDC3; 46 kDa), Chromogranin B/Secretogranin 1 (CHGB; 78 kDa), Exocyst complex component 4 (EXOC4; 110 kDa), Glutamate receptor, ionotropic, AMPA 3 (GRIA3; 101 kDa), Immunoglobulin heavy chain variable region (IGH; 13 kDa), N-acetylated alpha-linked acidic dipeptidase-like 2 (NAALADL2; 36-89 kDa), Never in mitosis gene A (NIMA)-related kinase 9 (NEK9; 107 kDa), Nuclear receptor co-repressor 2 (NCOR2), Ras responsive element binding protein 1 (RREB1; 52-188 kDa), Rho GTPase-activating protein 4 (ARHGAP4; 28 kDa), Ring finger protein 13 (RNF13; 43 kDa), SLIT-ROBO1 Rho GTPase-activating protein 2 (SRGAP2; 121 kDa), Secreted protein acidic

and rich in cysteine/Osteonectin (SPARC; 35 kDa), WD repeat domain 81 (WDR81; 63 kDa), Zinc finger FYVE domain-containing protein 1 (ZFYVE1; 40-87 kDa). The mRNA transcripts of the above proteins were expressed in the developing human neocortex aged 8-12.5 PCW as confirmed by Affymetrix gene chip analysis. This could account for the multiple bands observed with Western blot, as the secondary and territory structures of proteins were destroyed during denaturation of samples and antibody was more likely to recognize the primary sequence with less homology.

Nevertheless, this ROBO1 antibody should not cross react with other members of the ROBO family such as ROBO2 and -3 as there is no similarity between the immunogen sequence and the sequences of human ROBO2 or -3 proteins. ROBO1 antibody adsorption could not be performed as peptide with this particular immunogen sequence was not available. Although this commercial ROBO1 antibody did not seem to have the best specificity, it nonetheless was able to recognize all isoforms of the human ROBO1 protein and its immunostaining patterns were comparable to its mRNA expression patterns revealed by ISH (Figure 5.5).

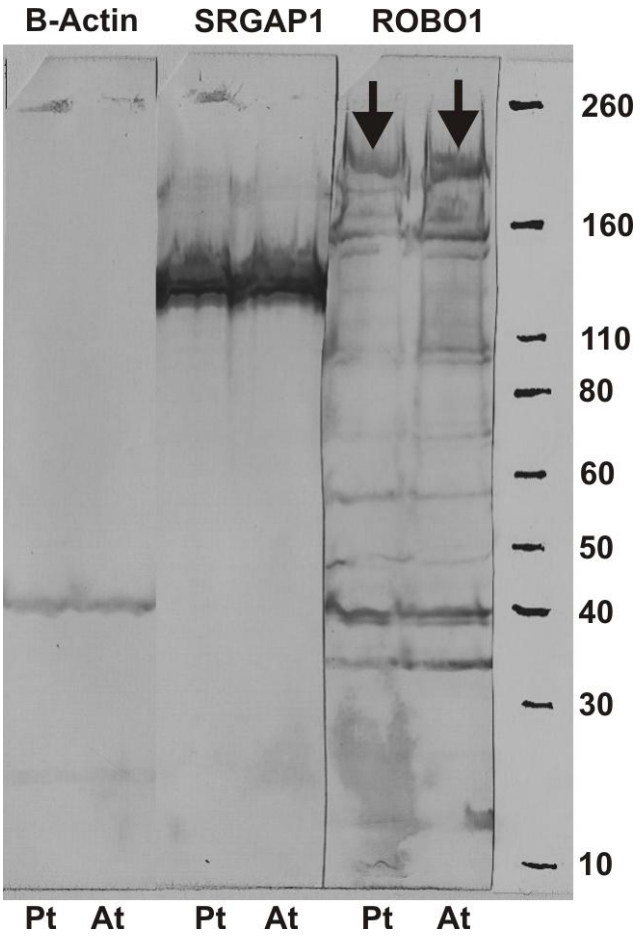

Figure 5.2. Characterization of ROBO1 and SRGAP1 antibodies.

SDS-PAGE and Western blot using protein samples obtained from the anterior (At) and posterior (Pt) human neocortical tissues at 14 PCW (n=2) revealed a single band with anti-SRGAP1 antibody of approximately 124 kDa. However, multiple bands were obtained with anti-ROBO1 antibody with the correct band of approximately 175-181 kDa (arrows). Anti-β–ACTIN antibody was used as positive control which revealed a single band of approximately 44 kDa. Novex® Sharp Unstained Protein Standard was used to determine the size of each band.

5.3.3 ISH/IHC Confirmation of ROBO1, SRGAP1 *and CTIP2 Tangential Gradients*

ISH carried out for *ROBO1* and *CTIP2* and IHC for SRGAP1 at 8, 9 and 10 PCW was performed on sagittal sections to determine their tangential expression gradients. Expression of all three appeared consistently higher in anterior compared to posterior regions of the neocortex at all ages studied (Figure 5.3A, B). The expression levels observed were quantified by measuring the relative optical densities of histological staining and confirmed significant differences between the anterior and posterior poles in expression levels for all three genes at all stages investigated (Figure 5.3C). In addition, a statistically significant high posterior to low anterior gradient for *FEZF2* was detected by ISH at 9 and 10 PCW but not 8 PCW, but *SOX5* exhibited no statistical significant difference in intensity of expression either anteriorly or posteriorly at all investigated stages (Figure 5.3).

Expression patterns of *CTIP2*, *ROBO1*, *FEZF2* and *SOX5* at mRNA level and SRGAP1 at protein level in coronal sections at 8 and 12 PCW were examined. Laminar staining patterns resembled those seen in sagittal sections, but no lateral to medial gradients of expression were observed (Figure 5.4).

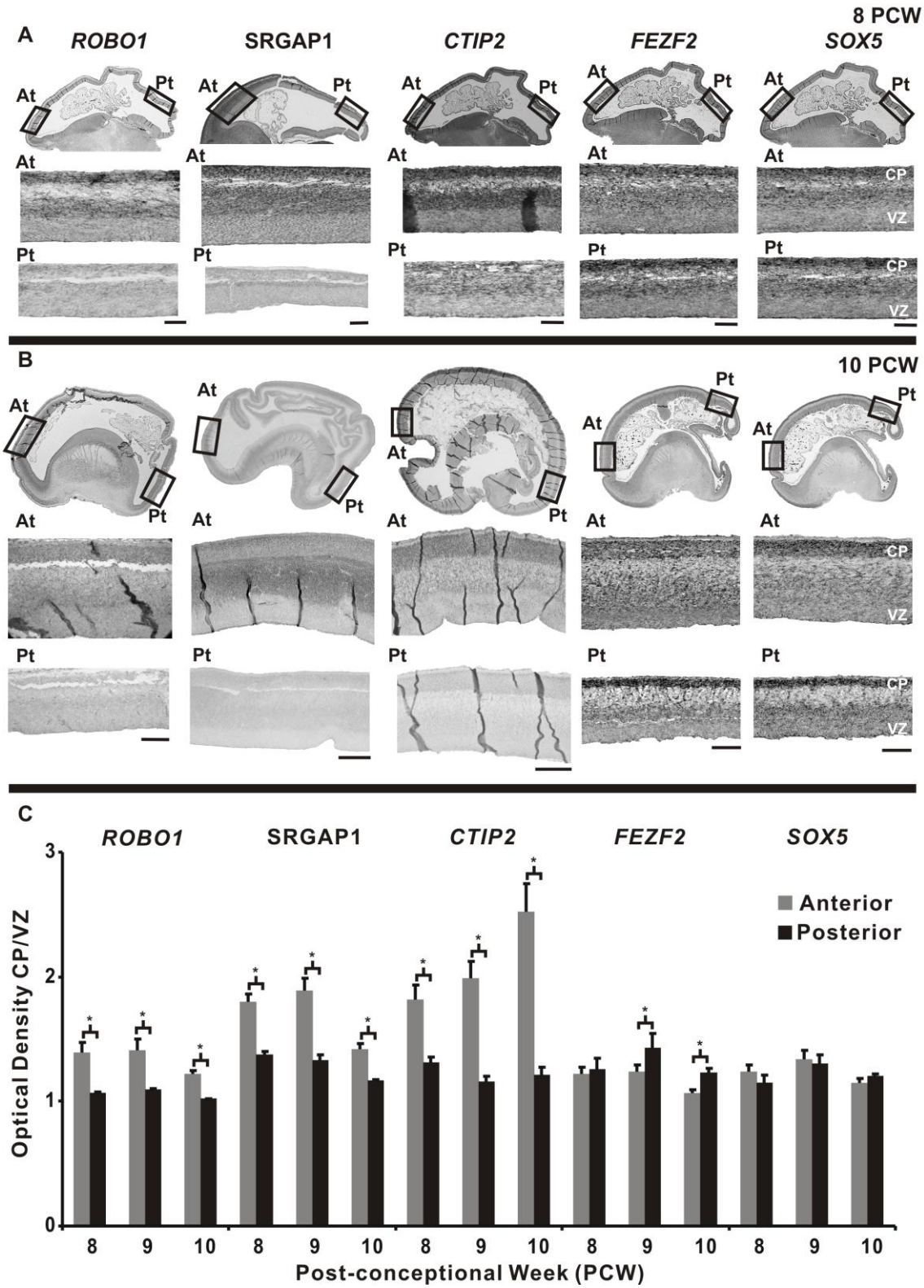

Figure 5.3. ***ROBO1*****, SRGAP1 and** ***CTIP2*** **anterior-posterior expression gradients in sections from the developing human neocortex.**

ISH of sagittal sections for *ROBO1*, *CTIP2*, *FEZF2* and *SOX5* and IHC for SRGAP1 (A, B) revealed that *ROBO1*, SRGAP1 and *CTIP2* were expressed at high levels anteriorly within the subventricular zone, intermediate zone and cortical plate (CP) between 8-10 PCW. A high posterior, low anterior expression of *FEZF2* was detected but at 9 and 10 PCW only. No gradient was detected for *SOX5* at any stage investigated. Higher magnification images, outlined with boxes, were taken at the anterior (At) and posterior (Pt) regions of the neocortex. (C) The optical density of histological staining for *ROBO1*, *CTIP2*, *FEZF2*, *SOX5* mRNA and SRGAP1-immunoreactivity at the anterior pole of the neocortex (grey bars) was measured in the CP and expressed relative to background staining in the ventricular zone (VZ) (see Section 2.11.1) and compared to the same ratios measured at the posterior pole (black bars). *, $p \leq 0.05$ (paired Student's *t*-test; 8 PCW, n=3; 9 PCW, n=3; 10 PCW, n=3). Scale bars indicate 200 μm. Adapted from (Ip et al., 2010b).

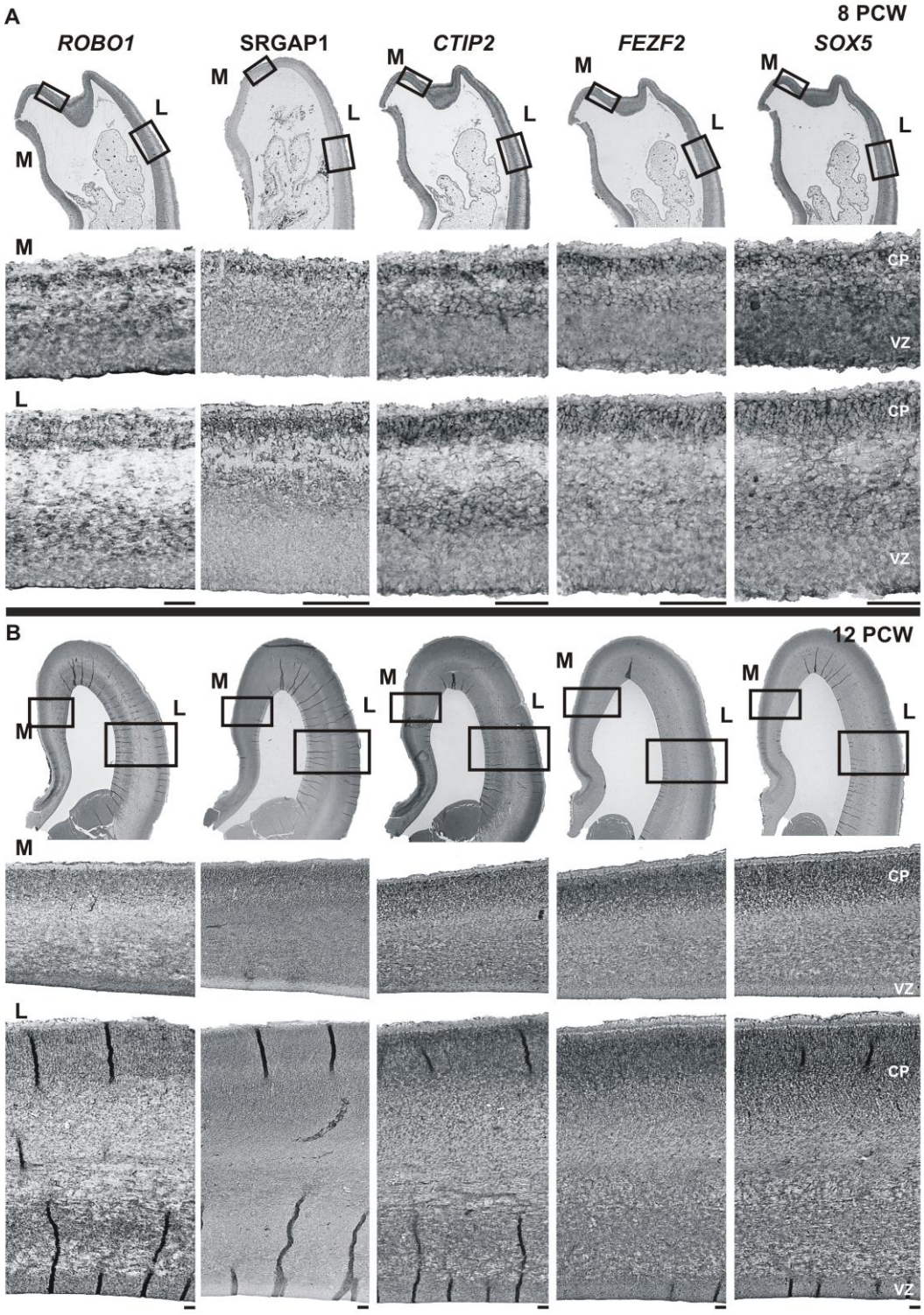

Figure 5.4. *ROBO1*, SRGAP1 and *CTIP2* medial-lateral expression gradients in sections from the developing human neocortex.

ISH of coronal sections for *ROBO1*, *CTIP2*, *FEZF2* and *SOX5* and IHC for SRGAP1 revealed no difference in expression level between medial (M) and lateral (L) regions of the neocortex at 8 PCW (A; n=2) and 12 PCW (B; n=2). Areas outlined with boxes are shown at higher magnification. CP, cortical plate; VZ, ventricular zone. Scale bars indicate 200 μm. Adapted from (Ip et al., 2010b).

5.3.4 Laminar and Cellular Expression of ROBO1*/ROBO1, SRGAP1 and* CTIP2*/CTIP2*

To investigate the laminar expression of *ROBO1*/ROBO1, SRGAP1 and *CTIP2*/CTIP2, tissue ISH and immunoperoxidase-histochemistry was performed. Images were taken from the dorsolateral anterior neocortex for comparison between sections stained with H & E for anatomical references, *ROBO1* and *CTIP2* anti-sense probes as well as ROBO1, SRGAP1 and CTIP2 antibodies (Figure 5.5). To investigate the cellular expression of ROBO1, SRGAP1 and CTIP2, immunofluorescent-histochemistry was performed and sections were doubled-labelled with CTIP2/TBR1, CTIP2/TBR2, CTIP2/ROBO1, CTIP2/SRGAP1 and ROBO1/SRGAP1 antibodies (Figure 5.6). Adjacent sections were selected for each gene/protein between 8-10 PCW.

From 8-10 PCW, the majority of expression of *ROBO1* and *CTIP2*/CTIP2 was found in cell bodies in the CP and the SVZ. To a lesser extent, they were also expressed in the migrating neurones passing through the IZ of the dorsolateral anterior neocortex. (Figure 5.5A, B). At 10 PCW although the IZ and SP contained few *ROBO1*-positive cell bodies, immunoreactivity for ROBO1 and SRGAP1 protein was high in these regions showing that receptor complexes containing these proteins were highly expressed on growing axons passing through these regions (Figure 5.5B).

The human SVZ, constituting a heterogeneous population of cells including radial glia-like cells, intermediate neuronal precursors (INPs) and early post-mitotic, immature neurones (Fietz et al., 2010; Hansen et al., 2010; Bayatti et al., 2008a) is profoundly different from the thin rodent SVZ, (Martinez-Cerdeno et al., 2006) at comparable developmental stages. At 10 PCW, double-labelling of CTIP2 with INPs marker, TBR2 (Hevner et al., 2006) showed that although CTIP2 expression was detected in the SVZ, it was not expressed by INPs (Figure 5.6A), but TBR1-positive immature neurones (Figure 5.6B, arrow; (Bayatti et al., 2008a)). Similarly within the CP, a subset of post-mitotic neurones also co-expressed CTIP2 and TBR1 (Figure 5.6B, arrow). In addition, double-labelling of CTIP2/ROBO1, CTIP2/SRGAP1 and ROBO1/SRGAP1 showed that a substantial subpopulation of post-mitotic neurones co-expressed CTIP2, ROBO1 and SRGAP1 (Figure 5.6C-E, arrows). Note that the intracellular location of CTIP2 was

distinct from those of ROBO1 and SRGAP1 in which CTIP2 was predominantly expressed within the nuclei and ROBO1 and SRGAP1 showed cytoplasmic and/or cell surface localization (Figure 5.6C-E).

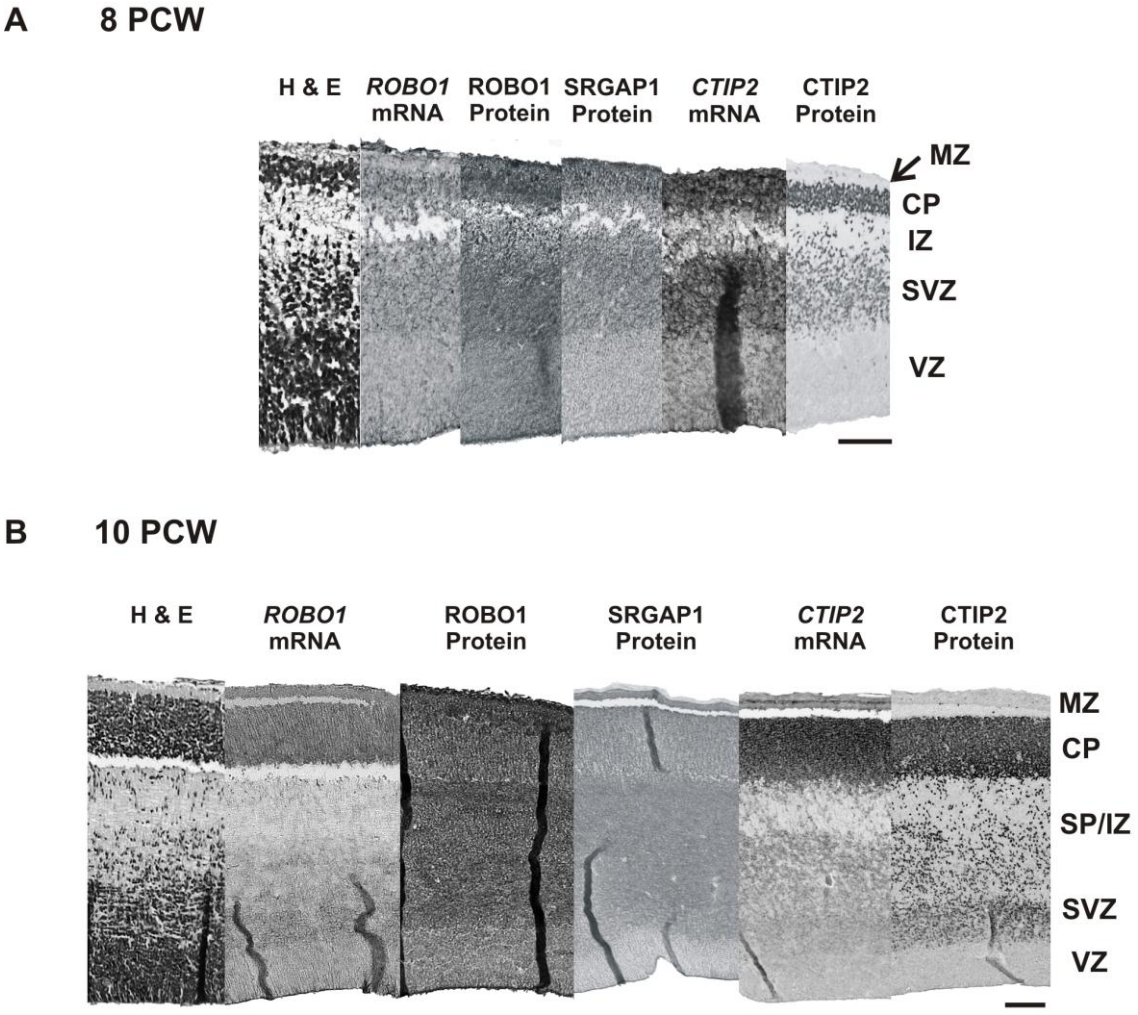

Figure 5.5. Laminar localization of ROBO1, SRGAP1 and CITP2 during early human neocortical development (8-10 PCW).

ISH and IHC on paraffin sections revealed expression of ROBO1 mRNA and protein, SRGAP1 protein and CTIP2 mRNA and protein in the subventricular zone (SVZ), intermediate zone/subplate (IZ/SP) and cortical plate (CP) at 8 (n=3) and 10 PCW (n=3) (A, B). All sections were taken from the dorsolateral region of the neocortex and adjacent sections were selected for each gene/protein at each stage. Note the higher expression of ROBO1 and SRGAP1 protein in the IZ and SP compared to *ROBO1* mRNA, which was more highly expressed in the CP. This revealed the predominant localization of the proteins to receptor complexes in axons compared to the predominant localization of mRNA in the cell body. CTIP2, a transcription factor, was predominantly localized to the nucleus of positive cells. Histological H & E stained sections of the corresponding level were included for anatomical references. Scale bars indicate 200 μm. Adapted and modified from (Ip et al., 2010b).

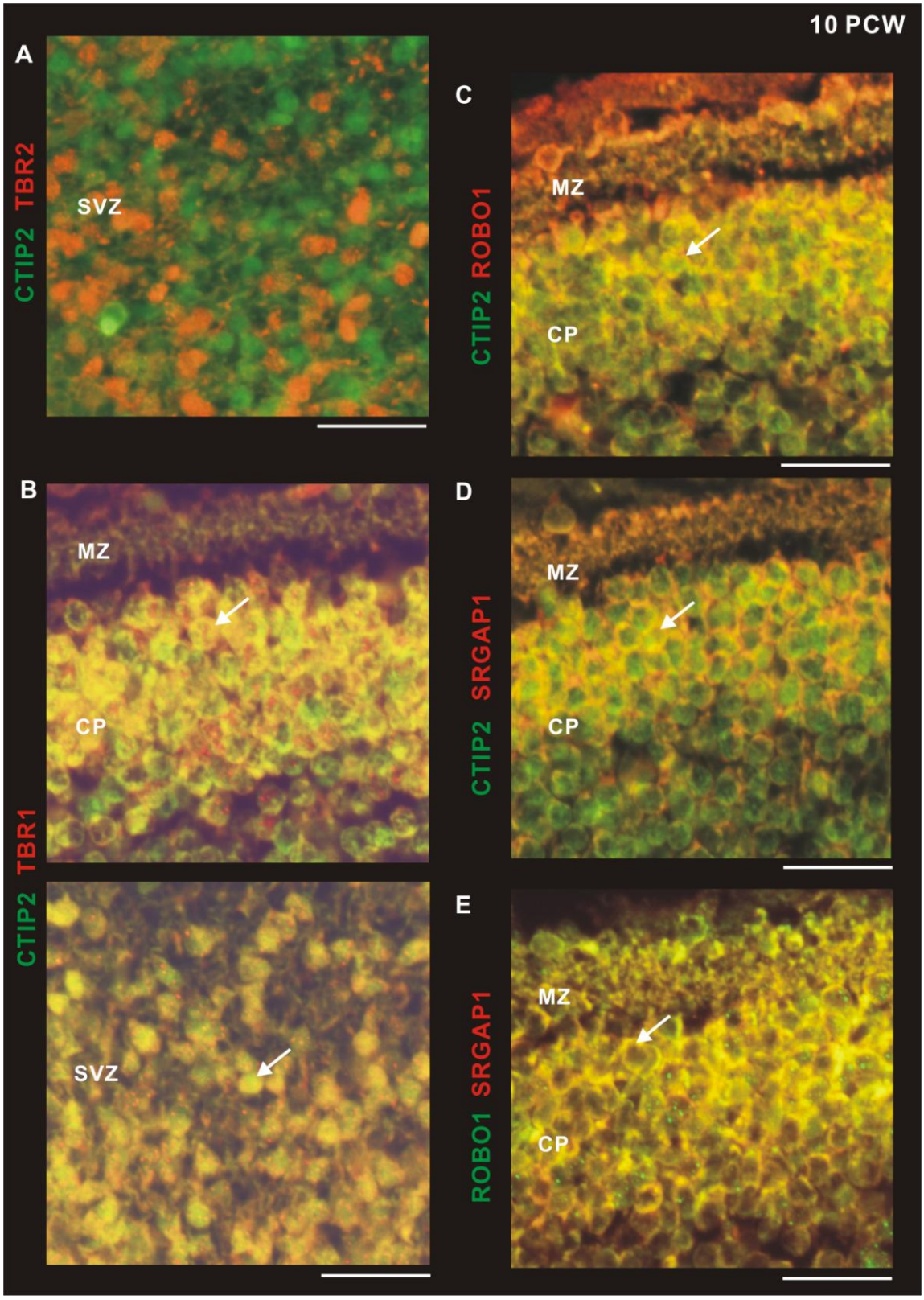

Figure 5.6. Cellular localization of ROBO1, SRGAP1 and CTIP2 at 10 PCW.

(A-B) At 10 PCW (n=2), within the subventricular zone (SVZ), most CTIP2-positive cells (green) did not express TBR2 (red) a marker for INPs, but co-expressed with post-mitotic marker TBR1 (yellow, arrow), indicating that CTIP2 positive cells are predominantly post-mitotic neurones. (B) Within the CP, CTIP2 and TBR1 were also co-expressed by a subpopulation of post-mitotic neurones within the nuclei (yellow, arrow) (C-E) A subset of post-mitotic neurones co-expressed CTIP2 (nucleic localization), ROBO1 and SRGAP1 (cytoplasmic and/or cell surface localization) (arrows). Scale bars indicate 100 μm. Adapted and modified from (Ip et al., 2010b).

5.3.5 Laminar and Cellular Expression of ROBO1*/ROBO1, SRGAP1 and* CTIP2*/CTIP2 during the Emergence of Layer V*

The expression patterns of *ER81*, *SATB2*, TBR1, NURR1, GAP43 and Synaptophysin observed at 12 PCW led us to propose that Layer V of the CP was formed at around this time point (Figure 5.7A). The CP was found to be delineated by the absence of GAP43 and Synaptophysin expression, which were prominently detected in the SP, IZ and MZ (Figure 5.7A). The segregation of layers in the CP was revealed by strong *ER81* and *SATB2* expression in the upper CP (Figure 5.7A), presumably Layer V and strong TBR1 and NURR1 expression in the lower CP (Figure 5.7A), presumably Layer VI. *ROBO1*, SRGAP1 and CTIP2 together with *FEZF2* and SOX5 were expressed by neocortical neurones in both layers of the CP (Figure 5.7A). In the upper CP, discrete populations of CTIP2-positive and SATB2-positive cells were observed with only a small number of them co-expressing both markers (arrow, Figure 5.7A'). However, a larger proportion of cells in the upper CP co-expressed both ROBO1 and SATB2 (arrow, Figure 5.7A''). Notice the cytoplasmic and/or cell surface localization of ROBO1 resulted in punctate staining observed in individual cells, in comparison to CTIP2 and SATB2 which were localized to the nuclei of cells (Figure 5.7A', A'').

At 15 PCW, a similar expression pattern was observed with some refinements (Figure 5.7B). SATB2 remained strongly expressed by neocortical neurones located in the upper CP (Layer V) (Figure 5.7B). Layer VI neurones continued to express TBR1 and NURR1, however a subset of NURR1-expressing cells were observed in the GAP43-positive SP. CTIP2 and SOX5 continued to be expressed by neocortical neurones in both Layer V and VI of the CP (Figure 5.7B). ROBO1 and SRGAP1 were expressed strongly by neocortical neurones in Layer V of the CP (Figure 5.7B), however, ROBO1 and SRGAP1 expression in the SP was weaker between 12-15 PCW (Figure 5.7) than at earlier stages. This suggested that axon growth cones expressing the ROBO1 receptor complex were not present in the SP at this stage.

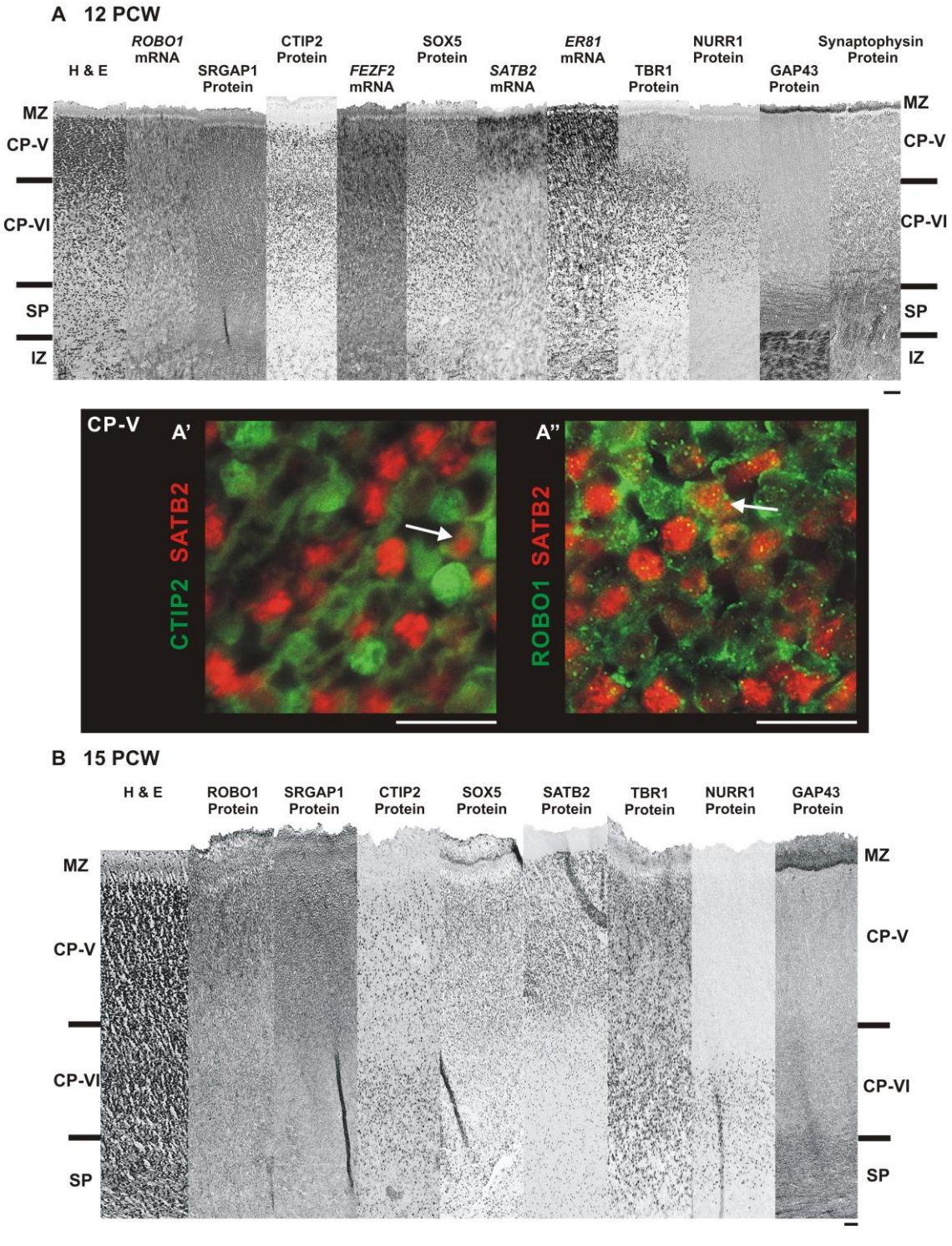

Figure 5.7. Laminar and cellular localization of ROBO1, SRGAP1 and CTIP2 at 12 and 15 PCW.

(A) Comparison of expression of *ROBO1*, SRGAP1 and CTIP2 with various laminar-specific markers (*SATB2, ER81*, TBR1, NURR1, GAP43 and Synaptophysin) revealed the emergence of Layer V by 12 PCW (n=2). The cortical plate (CP) was identified by GAP43- and Synaptophysin-negative immunoreactivity, proximal to the marginal zone (MZ). Within the CP, strong *SATB2* expression was detected in the Layer V above the TBR1- and NURR1-expressing Layer VI. *ROBO1*, SRGAP1 and CTIP2 together with *FEZF2* and SOX5 expression were observed throughout the CP (Layer V and VI). (A') At 12 PCW, within Layer V of the CP, post-mitotic neurones predominantly expressed either CTIP2 (green) or SATB2 (red), and very few co-expressed both markers (arrow). (A'') However, there were many more ROBO1 and SATB2 co-expressing cells (arrow).

(B) At 15 PCW (n=2), NURR1-expressing cells were observed in Layer VI and also in the upper parts of the GAP43-positive subplate (SP). Expression of CTIP2 together with SOX5, SATB2 and TBR1 were detected in both Layer V and VI with different intensities, whereas intense immunostaining of ROBO1 and SRGAP1 were observed mostly in the Layer V. All sections were taken from the dorsolateral region of the neocortex and adjacent sections were selected for each gene/protein at each foetal stage.

IZ, intermediate zone; Scale bars represent 50 μm. Adapted and modified from (Ip et al., 2010b).

5.3.6 ROBO1 and SRGAP1 Expression in Corticofugal Axons

At 12 PCW, GAP43 immunoreactivity revealed growing axons of all corticofugal projections such as corticothalamic, corticostriatal, corticopontine, corticotectal, corticobulbar and corticospinal axons through the internal capsule at the LGE, MGE levels of the telencephalon (white arrows, Figure 5.8A). However, ROBO1 and SRGAP1 expression in the internal capsule appeared to be complementary to the expression pattern of GAP43 (white arrows, Figure 5.8A). Additionally, cells in the developing striatum including the caudate nucleus and putamen also expressed ROBO1 and SRGAP1 (Figure 5.8A). Note that the pattern of *ROBO1* mRNA expression was similar to its protein expression (small insert, Figure 5.8A). These observations indicated that *ROBO1*/ROBO1 and SRGAP1 were likely to be produced by cells locating in the developing striatum and that the ROBO1/SRGAP1 receptor complexes were not expressed by fibre segments travelling through the internal capsule at this stage.

At the mesencephalic level, fibres such as corticopontine, corticobulbar and corticospinal axons projecting through the ventral surface formed the cerebral peduncle were strongly immunoreactive for GAP43, but weaker for ROBO1 and SRGAP1 (Figure 5.8B). Nevertheless, their expression patterns were similar. At the level of pons, corticofugal fibres including corticospinal, corticobulbar and corticopontine axons travelled longitudinally and were found in large distinct bundles at a relatively ventrolateral position of the pontine bulb, which were revealed by GAP43 immunoreactivity (arrow, Figure 5.8C). These longitudinally projecting corticofugal axons were also immunoreactive for both ROBO1 and more strongly SRGAP1 (filled arrows, Figure 5.8C). The pontine bulb also housed another type of fibres which were projecting transversely from the pons towards the cerebellum (pontocerebellar axons) which were locating near the midline and dorsomedial to the corticofugal bundles. However, due to the damage of the tissue sections during sectioning, only one half of the pontine bulb towards the lateral side was preserved and thus expression of GAP43, ROBO1 and SRGAP1 in the pontocerebellar fibres could not be determined. The tissue in and around the corticofugal fibres consisted of pontine grey neurones which were negative for GAP43, ROBO1 and SRGAP1 immunoreactivity (empty arrows).

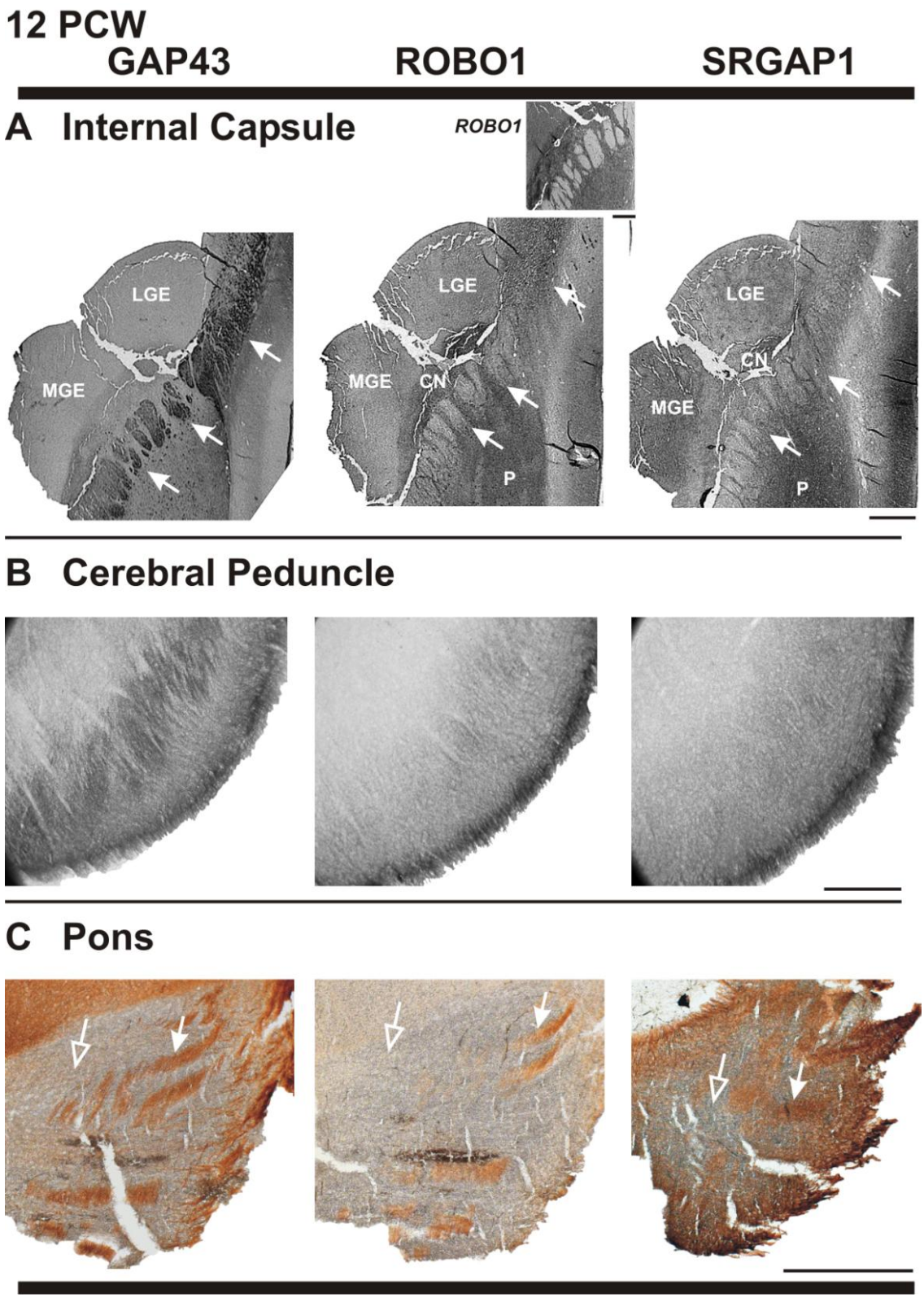

Figure 5.8. ROBO1 and SRGAP1 expression along the corticofugal projections.

(A) Coronal sections of the human brain at telencephalic level revealing the LGE, MGE, developing striatum (CN, caudate nucleus; P, putamen) and internal capsule at 12 PCW (n=2). GAP43 expression was detected in all growing axons of different pathways through the internal capsule (white arrows). However, the patterns of *ROBO1*/ROBO1 mRNA (small insert) as well as protein and SRGAP1 protein expression were found to be complementary to that of GAP43 within the internal capsule (white arrows). *ROBO1*/ROBO1 and SRGAP1 expression was also observed in the developing striatum. (B) Transverse mesencephalic sections of the human brain revealing the cerebral peduncle at 12 PCW (n=1). Strong GAP43 expression was detected in all growing axons of different pathways through the cerebral peduncle. Weaker but similar patterns of ROBO1 and SRGAP1 immunoreactivity were observed. (C) Transverse human brainstem sections revealing the pons at 12 PCW (n=1). GAP43, ROBO1 and SRGAP1 immunoreactivity was observed in the longitudinally projecting corticofugal axons which included corticopontine and corticospinal projections (filled arrows). The pontine grey neurones found in and around the corticofugal fibres did not express all three markers (empty arrows). Scale bars indicate 0.1 cm.

At 11 PCW, GAP43 immunoreactivity revealed growing axons in multiple pathways through the medulla at the level of olives (Figure 5.9A), whereas both ROBO1 and SRGAP1 immunoreactivity were restricted to the two small regions at the ventral surface of the medulla (arrow, Figure 5.9B, C). When examining sections at the level of decussation of corticospinal axons, small numbers of fibres immunoreactive for GAP43 were found extending from the ventral surface of the medulla crossing over the decussation (Figure 5.9D). However, expression of ROBO1 and SRGAP1 was not detected in fibres crossing over the decussation but was present in fibres on the ventral surface at this level (arrows, Figure 5.9E, F).

ROBO1- (Figure 5.9G) and SRGAP1- (Figure 5.9H) immunoreactive pyramidal fibres were first detected at the decussation at around 14 PCW. By 17 PCW, prominent pyramids were present on the ventral surface of the medulla and these were strongly immunoreactive for both ROBO1 (Figure 5.9I) and SRGAP1 (Figure 5.9J) as fibres have extended to the decussation and beyond. It was noteworthy that expression of ROBO1 and SRGAP1 was stronger in pyramidal fibres in the caudal medulla (Figure 5.9) as compared to the corticofugal axons in the mesencephalon and the pons (Figure 5.8 B, C).

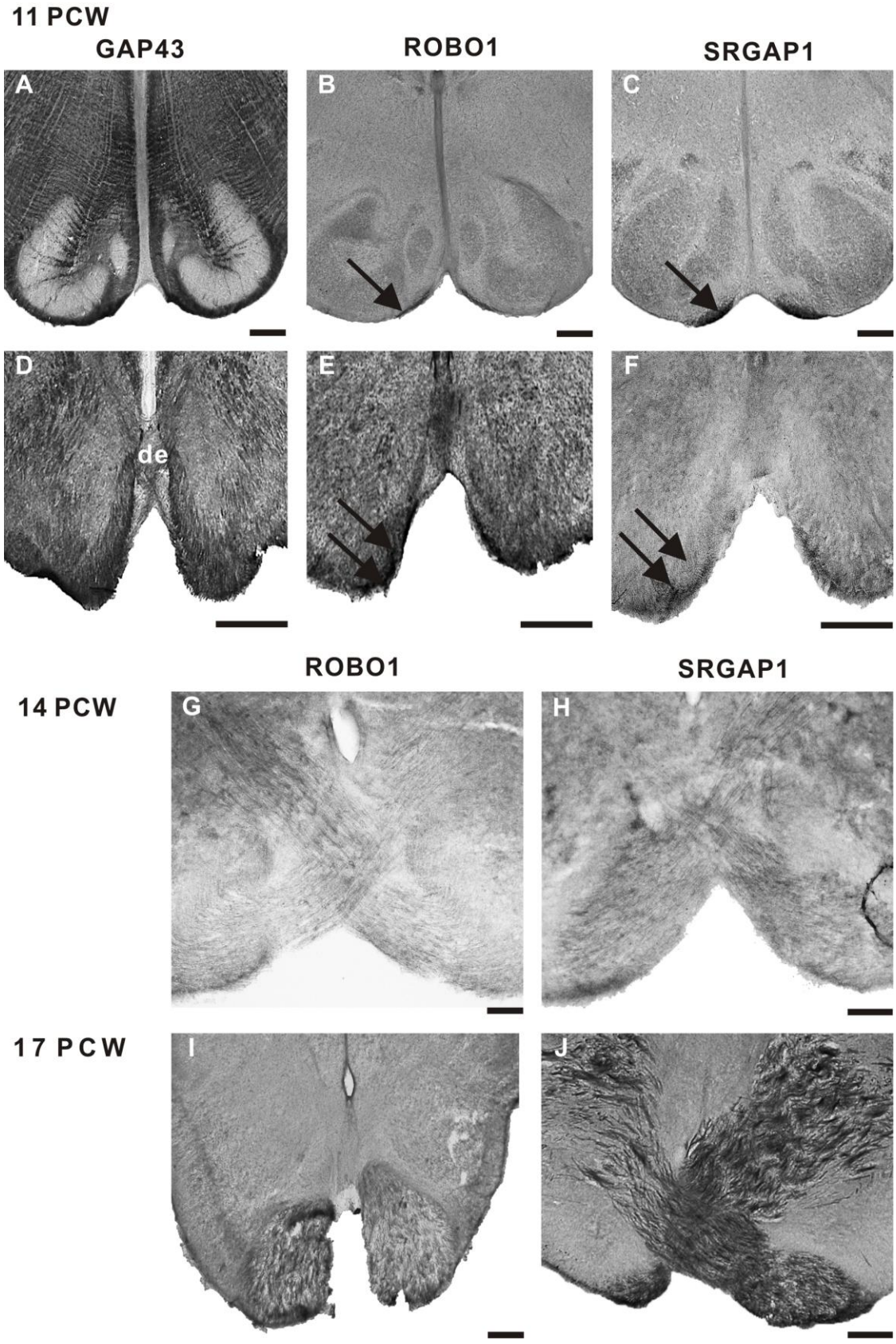

Figure 5.9. ROBO1 and SRGAP1 are corticospinal tract markers in the caudal medulla.

(A-C) Caudal medulla sections at the level of olives at 11 PCW (n=2). GAP43 expression was detected in all growing axons of different pathways revealed in this section (A). However, ROBO1- (B) and SRGAP1- (C) immunoreactive fibres were observed only in the two small regions at the ventral surface of the medulla, presumably where the future medullary pyramids are formed. (D-F) show caudal medulla sections at the level of decussation at 11 PCW. Small numbers of fibres crossing over the midline in the medulla were immunoreactive for GAP43 (D), but negative for ROBO1 (E) and SRGAP1 (F). (G-J) Caudal medulla sections at the level of decussation at 14 (n=2) and 17 PCW (n=2). Both ROBO1 (G, I) and SRGAP1 (H, J) showed strong expression in fibres crossing over at the decussation. Scale bars represent 0.5 mm. Adapted from (Ip et al., 2010b).

5.4 Discussion

In order to understand the origins and formation of the human corticofugal projections, we have examined the expression patterns of three corticofugal neurone-related genes and/or proteins *ROBO1*/ROBO1, SRGAP1 and *CTIP2*/CTIP2 using ISH and IHC during the early stages of corticogenesis. Prominent ROBO1 and SRGAP1 immunoreactivity was seen in corticofugal axons from and beyond mesencephalic level at around 12 PCW (Figure 5.8) and pyramidal fibres in the medulla from 11–17 PCW (Figure 5.9), confirming their role in the development of corticofugal projections. All three genes showed graded expression at the early stages of CP formation being highly at the anterior pole of the neocortex (Figure 5.3), providing evidence that this region might be an early site of the developing motor cortex where corticofugal projection neurones were generated. Furthermore, two transcription factors deemed key to the development of Layer V subcortical projection neurones, *FEZF2* (Chen et al., 2008; Chen et al., 2005b; Chen et al., 2005a; Molyneaux et al., 2005) and *SOX5* (Kwan et al., 2008; Lai et al., 2008), showed no gradients or small posterior to anterior gradients depending on age and method of study (Figure 5.3), indicating that anterior to posterior expression gradients are not universal to Layer V-related genes at this stage of development. *ROBO1*/ROBO1, SRGAP1 and *CTIP2*/CTIP2 were all persistently expressed in both the SVZ and CP of the neocortex from 8-15 PCW (Figure 5.5, Figure 5.7). However, expression in the SVZ was in post-mitotic neurones only and not in INPs (Figure 5.6). By 15 PCW, expression of *ROBO1* and SRGAP1 was concentrated in Layer V of the CP (Figure 5.7), the origin of subcerebral projection neurones.

5.4.1 Ontogeny of Corticofugal Projections Development Revealed by Expression of ROBO1 and SRGAP1 along the Corticofugal Axons

The corticofugal projections such as corticospinal and corticopontine axons are the major descending pathways that predominantly originate from Layer V of the frontal motor areas in primates (Lemon, 2008; Glickstein et al., 1985; Porter, 1985). These long distance projections require proper guidance for correct axonal pathfinding and target selection at each point from its origin to its destination, potentially through cell adhesion molecules (Faulkner et al., 2008; Runker et al., 2008). Here, we show that the

cell adhesion/axon guidance molecule ROBO1 and its downstream signalling molecule SRGAP1 were expressed along the corticofugal axons at various foetal stages during their formation (Figure 5.8, Figure 5.9), potentially playing a role in guiding axons towards different targets at least from the mesencephalon up to the caudal medulla that have been investigated.

Although multiple GAP43-positive axon pathways were present in the medulla at 11 PCW, ROBO1 and SRGAP1 were solely expressed by fibres located at the future sites of the CST pyramids on the ventral surface of the medulla (Figure 5.9). Thus these ROBO1- and SRGAP1-positive fibres probably represent the earliest arriving corticospinal axons at the level of the olives. In more caudal sections, small numbers of GAP43-positive but ROBO1- and SRGAP1-negative fibres crossed the decussation (Figure 5.9). Perhaps these decussating fibres are not corticospinal axons but pioneer fibres in the CST serving as scaffolds or temporary targets for the developing corticospinal axons, in the same way as the establishment of subcortical projections is dependent on the guidance of pioneer axons from subplate cells projecting towards the internal capsule (McConnell et al., 1994; Kim et al., 1991; McConnell et al., 1989). It is noteworthy that these GAP43-immunoreactive fibres crossing over at the decussation at 11 PCW were of small amount (Figure 5.9) and probably only detectable in a few thick sections cut at 70 µm. Thus double immunofluorescent labelling of all the sections with GAP43/ROBO1 antibodies would be useful to confirm whether these fibres are truly pioneer (GAP43-positive, ROBO1-negative) or corticospinal axons (GAP43-positive, ROBO1-positive). However, one should be cautious with the application of ROBO1 antibodies due to relatively poor specificity based on the results of Western blot and NCBI protein BLAST analysis (Figure 5.2). SRGAP1 antibody would probably be a better option as it is a monoclonal antibody and has shown better specificity (Figure 5.2). However both GAP43 and SRGAP1 antibodies were raised in mice, limiting their uses in combination. One way to overcome this limitation is by labelling these antibodies directly with fluorescent dyes of different absorbance and emission profiles (labelling kits available commercially), thus the use of species-specific, fluorescent dye-conjugated secondary antibodies could be avoided. Alternatively, CST growth cones may not express the ROBO1 receptor complex as they cross the decussation to avoid repulsive interaction with SLIT expressed in the extracellular matrix at the midline (Long et al., 2004; Kidd et al., 1998). However in mice, Robo (1 and 2) are strongly

expressed in corticospinal fibres before, during and after crossing the midline in the caudal medulla from P2 onwards and may be involved in axon fasciculation as well as guidance (Sundaresan et al., 2004).

By 12 PCW, corticofugal fibres including corticopontine, corticospinal and corticobulbar axons travelling through the cerebral peduncle and pons expressed both ROBO1 and SRGAP1 (Figure 5.8), however fewer or no expression was detected along the fibre segment projecting through the internal capsule (Figure 5.8) or the fibre-rich IZ of the neocortex (Figure 5.7). This observation might suggest that corticofugal fibres express ROBO1 and SRGAP1 only in their growing regions, i.e. their growth cones, and thus indicating these corticofugal axons might still be actively elongating and branching in the cerebral peduncle and pons at this stage of development. It is noteworthy that similar ROBO1 and SRGAP1 expression patterns were observed in the developing dorsal striatum which forms the future caudate nucleus and putamen (Figure 5.8). This expression pattern is also observed in the rodents during the course of interneurones migration and known to be playing a role in their guidance (Andrews et al., 2008; Andrews et al., 2007). Therefore, it is likely that the 35% of interneurones originating from the basal telencephalon in humans (Letinic et al., 2002) also require the guidance of ROBO1/SRGAP1 complexes to reach the neocortex. Within each of the cerebral peduncle, the mature CST and corticobulbar axons occupies the central part with corticopontine axons flanking either side of them (Kahle and Frotscher, 2002). ROBO1, SRGAP1 and GAP43 expression showed no clear segregation between these corticofugal fibre subtypes (Figure 5.8) raises possibilities that these axons might be projecting through the entire cerebral peduncle during development. Axonal pruning, a mechanism shown in rodents to selectively eliminate collateral axons from inappropriate targets (Low et al., 2008; O'Leary and Koester, 1993), might also occur at later stages in the cerebral peduncle to further refine the patterns to its mature form. However, until now there is no evidence that axonal pruning take place in humans. In the ventral pontine bulb, the more strongly and diverse SRGAP1 expression in the longitudinally projecting corticofugal axons as compared to the expression of ROBO1 (Figure 5.8) probably suggests that other members of the ROBO family proteins e.g. ROBO2 is also involved in guiding these axonal tracts through associating with SRGAP1.

By 14-17 PCW, prominent pyramids were present which are strongly immunoreactive for both ROBO1 and SRGAP1, as were fibres extending to the decussation and beyond (Figure 5.9). The decussation of ROBO1- and SRGAP1-positive fibres was observed around the time when a distinct ROBO1- and SRGAP1-positive Layer V emerges in the neocortex (Figure 5.7).

5.4.2 Expression of Corticofugal Neurone-associated Genes/Proteins in the SVZ and IZ

The expression of *CTIP2*/CTIP2 in the human SVZ is an intriguing discovery since its expression is absent in the mouse VZ or SVZ from E12 to P6 (Arlotta et al., 2005). The human SVZ, however, is relatively larger and divided into two layers, the inner and outer SVZ, by the IFL from 11 PCW onwards and contains post-mitotic markers such as TBR1 (Bayatti et al., 2008a; Bystron et al., 2008). By comparison, the thin rodent SVZ constitutes only a few layers of cells at a comparable developmental stage (Martinez-Cerdeno et al., 2006) and is Tbr1-negative (Hevner et al., 2006; Hevner et al., 2003). In the present study, CTIP2-positive cells were not found to express the INPs marker TBR2 (Hevner et al., 2006; Hevner et al., 2003) but early post-mitotic marker TBR1 (Hevner et al., 2006; Hevner et al., 2003) (Figure 5.6). Therefore Arlotta and others' (2005) proposal that Ctip2 is not involved in early specification of neocortical progenitors in mice due to the lack of its expression in the VZ or SVZ (Arlotta et al., 2005) is likely to hold true in humans also, despite its expression in the SVZ. Instead, CTIP2 may control the expression of ROBO1 and SRGAP1 which are related to corticofugal neurones and could be required from the earliest stages of development, for instance, in guiding the outgrowth of their axons towards the internal capsule whilst the immature neurones are still migrating towards the CP. In contrast to the sparsely distributed SATB2-positive cells observed in the SVZ at 8 and 9 PCW (Figure 4.3, Figure 4.4), *CTIP2*/CTIP2 expression was already abundant in the SVZ and CP at 8 PCW (Figure 5.5). This might suggest that despite some SATB2-expressing neurones designated to occupy with CTIP2-expressing neurones in Layer V, the callosal projecting neurones are probably generated later than the subcerebral projecting neurones. Alternatively, it might be due to some differential regulatory machineries causing SATB2 expression to be switched on later than CTIP2.

Our observation of ROBO1 and SRGAP1 expression in the human SVZ and IZ (Figure 5.5-Figure 5.7) was largely in agreement with the expression patterns in mice. Robo1 protein expression was detected in the axons transversing the lower IZ/SVZ from E15.5 while *srGAP1* mRNA expression was observed in the proliferative zone at E16.5 in mice (Bacon et al., 2009; Andrews et al., 2008; Andrews et al., 2007; Andrews et al., 2006). Our observation of a gradual loss of *ROBO1* and *CTIP2* mRNA expression within SP/IZ from 10 PCW onwards (Figure 5.5, Figure 5.7) suggests the occurrence of radial somal translocation of ROBO1+/CTIP2+ subcerebral projecting neurones through the SP/IZ towards the CP is potentially guided by ROBO1/SRGAP1 receptor complexes.

5.4.3 Emergence of Laminar Specific Expression of Corticofugal Neurone-associated Genes/Proteins in the CP

Expression of *ROBO1* mRNA, SRGAP1 protein and *CTIP2*/CTIP2 mRNA and protein within the human CP (Figure 5.5-Figure 5.7) was largely consistent with the expression patterns observed in rodents (Bacon et al., 2009; Lopez-Bendito et al., 2007; Arlotta et al., 2005; Bagri et al., 2002; Whitford et al., 2002). An exception is ROBO1 protein which is weakly expressed in the CP of mice (Andrews et al., 2007; Andrews et al., 2006). The expression of these genes and proteins in the human CP (Figure 5.5-Figure 5.7), which constitutes post-mitotic neurones, suggest that *ROBO1*/ROBO1, SRGAP1 and *CTIP2*/CTIP2 are likely to play a role in mediating processes involved in the differentiation of subcerebral projecting neurones such as axonal projection fasciculation, outgrowth and pathfinding. Note that SRGAP1 cytoplasmic expression was observed at all stages investigated in our study (Figure 5.5-Figure 5.7) which differs from the reported nucleus-cytoplasm shuttling phenomenon occurring from P1 to adult in mice (Yao et al., 2008). Nuclear expression of SRGAP1 might be observed at later stages in human neocortical development not studied here. Alternatively, the lack of nucleus-cytoplasmic shuttling observation is probably due to the use of post-mortem human tissue instead of experimental mouse tissue in which optimal preservation is achievable.

In humans, previous work has shown both Layer V and VI can be distinguished within the CP by 16 PCW (Bayatti et al., 2008a). Our new observations suggest that Layer V is probably formed slightly earlier, from 12-15 PCW. Layer V was easily distinguishable by the restricted expression of *SATB2*/SATB2 and concentrated expression of *ER81* in this layer and the absence of expression of NURR1 (Figure 4.3, Figure 4.7, Figure 4.8). However, ROBO1 and SRGAP1 expression was not restricted to the putative Layer V at 12 PCW, but only at 15 PCW (Figure 5.7). Thus, the present study in humans only finds ROBO1-, SRGAP1- and CTIP2-positive neurones that are restricted to Layer V (Figure 5.7) by the time that presumptive ROBO1- and SRGAP1-positive corticospinal fibres are crossing the decussation in large numbers (Figure 5.9).

The expression of *ROBO1* and SRGAP1 in Layer V of the CP (Figure 5.7) is consistent with the findings in rodents, in which *Robo1* was expressed at Layer V in P7 mice (Schuurmans et al., 2004; Sundaresan et al., 2004) and Layer II and V in P10 rats (Whitford et al., 2002), while *srGAP1* was primarily expressed at Layer II to V in P7 mice (Bacon et al., 2009). Expression of ROBO1 and SRGAP1 in superficial layers of the CP might also be observed at later stages in human neocortical development not studied here. In addition to guiding subcerebral projection neurones, Robo protein was found to be responsible for establishing various forebrain commissures in rodents (Andrews et al., 2006; Sundaresan et al., 2004; Jones et al., 2002). That a sub-population of SATB2+ callosal projecting neurones (Alcamo et al., 2008; Britanova et al., 2008) co-expressed ROBO1 (Figure 5.7) might suggest its involvement in directing this neuronal subtype in Layer V.

Although CTIP2 expression is seen in both Layer V and VI at 15 PCW (Figure 5.7), it has been shown to be predominantly expressed in Layer V at 19 PCW in humans (Johnson et al., 2009). The change in laminar expression pattern is likely to be under the control of two genes; *Fezf2*, an upstream gene that promotes Ctip2 expression (Chen et al., 2008; Leone et al., 2008; Chen et al., 2005a; Molyneaux et al., 2005) and *Sox5*, which was found to regulate and restrict the expression of *Fezf2* and Ctip2 from a domain spanning the SP, Layer VI and V at E14.5 to only Layer V by P0 in mice (Kwan et al., 2008). Similarly, *FEZF2* expression is restricted to Layer V in the human neocortex at 22 PCW (Kwan et al., 2008) but was shown to be expressed throughout the CP in our study at 12 PCW (Figure 5.7). Despite the lack of *CTIP2*/CTIP2/*FEZF2*

enrichment in Layer V at this stage, the molecular identities of neurones within this layer were already specified, including SATB2+/ROBO1+/CTIP2- or SATB2+/ROBO1-/CTIP2- callosal projecting neurones and CTIP2+/ROBO1+/SATB2- subcerebral projecting neurones (Figure 5.7).

5.4.4 Is the Anterior Neocortex the Potential Site of Origin of the Motor Cortex during the Early Stages of Human Cortical Plate Development?

This chapter provides further extensive evidence for high anterior to low posterior expression gradients for *ROBO1*, SRGAP1 and *CTIP2* (Figure 5.3), in addition to our previously published evidence for similar gradients for other genes, including *S100A10* and *ER81* (Ip et al., 2010a) associated with the development of corticospinal neurones but also with all subcerebral projection neurones (Yoneshima et al., 2006; Arlotta et al., 2005; Hevner et al., 2003). *FEZF2* and *SOX5*, acting upstream to promote and repress expression of transcription factors such as CTIP2 in subcerebral projection neurones and SP/Layer VI/corticothalamic neurones respectively (Chen et al., 2008; Kwan et al., 2008; Leone et al., 2008; Chen et al., 2005a; Molyneaux et al., 2005), were not expressed in this gradient (Figure 5.3). Why should it be that, as development unfolds, gene expression associated with corticofugal axon projections is relatively higher at the anterior pole of the neocortex?

It may be that a much higher number of Layer V neurones from frontal cortex are corticofugal neurones compared with Layer V neurones at the occipital pole. Retrograde tracing has demonstrated that the various motor areas of the frontal lobe make the predominant contribution to both corticospinal (Galea and Darian-Smith, 1995; Galea and Darian-Smith, 1994) and corticopontine (Glickstein et al., 1985) pathways in the adult macaque monkeys, whereas retrograde labelling from the superior colliculus results in a patchy distribution of labelled neurones in the visual cortex sometimes present at a relatively low density (Lock et al., 2003). This disparity could be reflected in relatively higher expression of some corticofugal neurone-related genes anteriorly compared to posteriorly. The motor cortex is not found predominantly towards the anterior pole of the neocortex in the adult human brain as it is in the rodent. This may be because the prefrontal cortex, a much larger structure in the human compared to rodent

brain, starts to expand during later stages of development (Fuster, 2002) such that the motor cortex location would then begin to shift posteriorly to its adult position anterior to the central sulcus.

In order to ensure that the required larger numbers of corticofugal neurones are initially specified at anterior pole of the neocortex, regionalisation mechanisms may interact with the specification of corticofugal identity by genes such as *SOX5* and *FEZF2*, accounting for the observed anterior to posterior expression gradients of *ROBO1*/SRGAP1 and *CTIP2* (Figure 5.3). It is known that the conditional KO of the transcription factor *Sp8*, expressed in a high anteromedial to low posterolateral gradient across the VZ in mice (Sahara et al., 2007), results in a reduction of *Robo1* expression in deep layers of the CP at E18.5 (Zembrzycki et al., 2007). Another transcription factor *PAX6* is expressed in a high anterolateral to low posteromedial gradient in humans at 8 PCW (Bayatti et al., 2008b) and in mice throughout neocortical development (Bishop et al., 2000). Similar phenotypes, in which thalamocortical and corticofugal fibres were ventrally misprojected at the diencephalic level in mice at E18.5, have been observed in *Pax6*$^{-/-}$ mutant mice (Jones et al., 2002) and *robo1*$^{-/-}$*robo2*$^{-/-}$ double mutants (Lopez-Bendito et al., 2007). Recently, a more direct relationship between *Pax6* and *Robo1* has been demonstrated in which the expression of *Robo1* and *-2* in the thalamus is markedly reduced in the *Pax6*$^{-/-}$ mutant mice, which potentially accounts for the misrouted thalamocortical projections observed in their previous study (Clegg et al., 2010). In addition, *Robo2* expression disappears from the neocortical epithelium in the homozygous *Pax6* mutant at E13 (Jimenez et al., 2002). In humans the *PAX6* gradient has disappeared by 9 PCW, so although the *ROBO1* expression may also be under the regulation of *PAX6*, this may be indirect or under the control of genes downstream of *PAX6* which exhibit gradients at later stages (Bayatti et al., 2008b). It is noteworthy that an isoform of ROBO1 (DUTT1/ROBO1b) was also found to be highly enriched in the prefrontal region of the neocortex during late mid-foetal stages in humans (Johnson et al., 2009).

A recent study in KO mice (Tomassy et al., 2010) has revealed that the transcription factor *CouptfI*, expressed in a high posterior to low anterior gradient across the neocortex in both mice (Armentano et al., 2007) and humans (Ip et al., 2010a), represses the differentiation of Layer VI corticothalamic neurones in sensory areas into Layer V

corticofugal neurones by inhibiting expression of Ctip2 and *Fezf2*, such that, in the absence of CouptfI function, presumptive corticothalamic neurones abnormally display the molecular features and projection patterns of corticospinal neurones. At the same time, Layer V neurones in the sensorimotor cortex fail to develop into corticospinal neurones. Therefore, the observation of a high anterior to low posterior gradient in *CTIP2* expression between 8-12 PCW (Figure 5.3) may reflect necessary suppression of *CTIP2* expression by *COUPTFI* in Layer VI of the posterior, sensory cortex.

Elevated expression of ROBO1, SRGAP1 and CTIP2 by corticospinal neurones compared to other corticofugal projection neurones may be required for growth and maintenance of the CST beyond the pons and across the medullary decussation (Lopez-Bendito et al., 2007; Arlotta et al., 2005), whereas the other major neocortical subcerebral projections terminate, in maturity, predominantly ipsilaterally in the mesencephalon and pons. In the rodent early neocortical development, all of the Layer V neurones of the neocortex project to the spinal cord but subsequently selective axon pruning reduces the origins of the CST to the sensorimotor cortex (Oudega et al., 1994). There is no direct evidence that this is also the case in humans, however a recent study found that an early lesion to the frontal and parietal cortex resulted in the formation of direct connections from occipital cortex to spinal cord motoneurones from the same hemisphere (Basu et al., 2010). This could represent retention of a pathway normally removed during development. Regionalised expression of specific cell-cell signalling molecules such as ROBO1/SRGAP1 (Figure 5.3) may protect corticospinal axons from retraction from the spinal cord and promote their removal from inappropriate target areas, in the same way as regionalised expression of Plexin 3A and -4A in the rodent visual cortex that promotes pruning of their corticospinal projections and protection of appropriate projections to the superior colliculus (Low et al., 2008). However, the plasticity of corticospinal development under pathological or experimental conditions (Basu et al., 2010; Li et al., 1995; Sharkey et al., 1986) suggests that genetically specified regionalisation mechanisms can be overridden by epigenetic influences.

Defining the temporal and spatial expression patterns of genes that specify the phenotype of corticofugal neurones especially the corticospinal neurones will be invaluable in understanding how lesions and infections can perturb the protomap during

neocortical development, and how to produce corticospinal neurones from stem cells for the repair of brain following neonatal hypoxia or adult stroke. The chapter provides evidence for the localized expression of genes associated with corticofugal neurones in the early stages of human neocortical development. The next step will be to probe the mechanisms that regulate the expression of these genes *in-vitro* in human neocortical cell cultures.

Chapter 6 Characterization of Human *in-vitro* Regionalisation Model and its Application

6.1 Introduction

6.1.1 Fibroblast Growth Factor System

The FGF signalling is intriguing due to the differential molecular and biochemical properties, spatiotemporal distribution, affinities/specificities of the ligands (FGFs) and their receptors (FGFRs) across the developing neocortex as well as the diverse downstream signalling pathways.

There are 22 members of FGFs (*FGF1-23*; human *FGF19* and mouse *Fgf15* are orthologous genes) in mice and humans which can be grouped on the basis of the evolutionary relatedness of their sequences into 7 subfamilies via phylogenetic analysis, or 6 subfamilies via analysis of the location of genes on chromosomes, or 4 subfamilies based on their mechanisms of release from cells (Itoh, 2007; Stachowiak et al., 2007; Itoh and Ornitz, 2004). The genes encode proteins that contain about 150-300 amino acids (aa), accounting for their size differences. The proteins have a 120-aa conserved domain with 30-70% aa sequence identity (Itoh, 2007; Itoh and Ornitz, 2004). Among them, *Fgf2* and *Fgf8* play a vital role in early stages of corticogenesis such as proliferation, differentiation and patterning. Their expression is detected at high level early in the developing rodent brains, with *Fgf2* expression more widespread throughout the developing neural tube by both proliferating and differentiating cells and *Fgf8* expression more confined to specific regions of the developing CNS by proliferating cells (Ford-Perriss et al., 2001). *In-vitro* studies have shown that Fgf2 stimulates the proliferation of neural crest cells directly in the presence of serum (Murphy et al., 1994) and controls the proliferative and differentiative division of neocortical neural precursor cells in a dose-dependent manner, in which low Fgf2 concentrations result in proliferation and high Fgf2 concentrations cause cells to differentiate, expressing markers for neurones and astrocytes (Murphy et al., 1990a). In addition, the lineage differentiation of neocortical progenitors is also regulated by different dosages of Fgf2:

lower Fgf2 concentrations lead to neuronal differentiation predominantly, whereas higher, threshold level of Fgf2 stimulates oligodendroglial production (Qian et al., 1997). *In-vivo* studies of Fgf2 micro-injection and *Fgf2*$^{-/-}$ null mice demonstrate that the number of rounds, but not the cell cycle length of division, of neocortical progenitors is regulated by this factor during early neurogenesis (Raballo et al., 2000; Vaccarino et al., 1999). However, a later *in-vitro* study suggested otherwise that Fgf2 also regulates cell cycle pro- and anti-mitogenic regulators such as cyclin D1 and p27 to achieve proliferation of neocortical precursor cells in rat (Li and DiCicco-Bloom, 2004). Fgf2 is thought to also regulate post-mitotic differentiation such as axonal growth (Kawamata et al., 1997). More recently, a study has shown in rat that Fgf2 is able to induce functional recovery from neonatal motor cortex injury, possibly via restoration of the corticospinal connectivity from the refilled but non-stratified lesioned region of the motor cortex to the cervical spinal cord with the re-grown fibre projection (Monfils et al., 2008). As described in Chapter 1, Fgf8 is an important secreted ligand that is highly expressed in the anterior patterning centre (ANR/CoP) and involved in the patterning of the brain during early corticogenesis (Crossley et al., 2001; Fukuchi-Shimogori and Grove, 2001). A recent study, in another patterning centre situated at the mesencephalic-rhombencephalic boundary, has shown that Fgf8 can regulate the anteriorly-directed growth of midbrain dopaminergic axons, by inducing expression of axon guidance molecules such as sema3F (Yamauchi et al., 2009).

The receptors for FGFs are known as FGFRs and have three immunoglobulin-like (Ig) loops flanking an acidic box extracellularly, a single transmembrane domain, and intracellular tyrosine kinase domains (Eswarakumar et al., 2005). In contrast to the vast amount of ligand subtypes, there are only four subtypes of FGFRs (FGFR1-4) identified in mice and humans that are encoded by four genes independently (Itoh and Ornitz, 2004). Among them, only FGFR1-3 are present in the mammalian forebrain during development and each of the FGFR1-3 has an isoform which arises from alternative splicing of the exon corresponding to the third of the Ig domain (Ig-III), generating receptor isoforms IIIb or IIIc of each FGFR1-3 (Iwata and Hevner, 2009; Itoh and Ornitz, 2004). Other proteins have been identified to bind FGFs or FGFRs including: heparin sulphate proteoglycans (HSPGs), that act as co-receptors (Allen and Rapraeger, 2003; Ford-Perriss et al., 2002); Klotho proteins, which are novel transmembrane proteins acting as co-receptors for binding of endocrine FGFs to FGFRs (Kuro-o, 2008);

and cell adhesion molecules (CAMs)/cadherins, interacting with the acidic box of FGFRs (Sanchez-Heras et al., 2006; Cavallaro and Christofori, 2004). Across the mammalian developing neocortex, FGFRs (1-3) are expressed by progenitor cells with some of them being differentially regulated. In both rodents and humans, *Fgfr3/FGFR3* expression is detected at higher level in the posterolateral region of the developing neocortex (Ip et al., 2010a; Iwata and Hevner, 2009; Fukuchi-Shimogori and Grove, 2003). No graded expression of *Fgfr1* and higher expression of *Fgfr2* is only detected in the lateral region of the rodent developing neocortex (Iwata and Hevner, 2009; Hebert et al., 2003; Vaccarino et al., 1999). However in humans, we have reported small but significant differences of *FGFR1* and *-2* expression between the anterior and posterior poles of the developing neocortex: *FGFR1* expression being higher anteriorly while *FGFR2* expression being higher posteriorly (Chapter 3; (Ip et al., 2010a)). *Fgfr3* was originally thought to play a role in regionalisation due to its graded expression pattern across the rodent developing neocortex, but rather it is shown to be involved in regulating the proliferation of neocortical progenitors during embryonic development in rodents as illustrated by a remarkable enlargement of the brain which is due to an increased rate of proliferation paralleled by a decreased rate of developmental apoptosis in mutants with *Ffgr3* kinase domain mutation (Thomson et al., 2007; Inglis-Broadgate et al., 2005). Recently, a study using *Xenopus laevis* has shown the importance of the Fgfr in maintenance of axon guidance cues during development since broad inhibition of the Fgfr function causes the expression of *xsema3A* and *xslit1* to decrease, which is accompanied by a failure of the axons of retinal ganglion cells to project beyond the mid-diencephalon (Atkinson-Leadbeater et al., 2010).

Upon binding of FGFs, FGFRs undergo homodimerization and autophosphorylation that activates a range of downstream signalling pathways differentially. i) The mitogen-activated protein kinase (MAPK) cascade is one of the major downstream pathways which regulate proliferation/differentiation and expression of a number of genes downstream of Fgfs (Iwata and Hevner, 2009; Mason, 2007; Thomson et al., 2007; Eswarakumar et al., 2005). Furthermore, some interesting studies have shown the inhibition of Fgf2-induced MAPK downstream signalling pathway via MEK inhibitor or elevation of intracellular cyclic adenosine monophosphate (cAMP) levels would drive the glial cells from proliferation to functional differentiation and up-regulate expression of glutamate transporters in neocortical astroglial culture *in-vitro*, a potential

mechanism of neuroprotection in the case of neuroexcitotoxicity (Figiel et al., 2003; Bayatti and Engele, 2001). ii) phosphatidylinositol-3 (PI3) kinase-Akt pathway promotes the survival and proliferation of cells (Brader and Eccles, 2004); iii) Phospholipase Cγ (PLCγ) pathway activates protein kinase C (PKC) and triggers calcium signalling (Iwata and Hevner, 2009); and iv) Rac-cdc42-Rho pathway mediates cell adhesion and migration via cytoskeletal remodelling (Iwata and Hevner, 2009).

6.2 Aim of Study

6.2.1 Characterization of Human in-vitro Regionalisation Model

Previous work using an Affymetrix whole genome chip array (Figure 1.13; (Ip et al., 2010a) and rtPCR (Figure 3.3; (Ip et al., 2010a)) to analyze the gradients of gene expression in developing neocortical tissue between 8 and 12.5 PCW has identified and confirmed some potential anterior and posterior markers during human neocortical development, supporting the protomap theory (Rakic et al., 2009; Rakic, 1991). The aim of the first half of this chapter was to assess whether these intrinsically-regulated putative markers would exhibit similar expression profile outside their normal physiological environment.

The objectives were:

1) to establish an *in-vitro* human cell culture model of regionalisation by dissecting tissue from anterior and posterior neocortex aged 11 PCW, dissociating and culturing in isolation.

2) to characterize this cell culture model by IHC of cells for various characteristic proteins: GFAP for astrocytes, Nestin for neural progenitors and MAP2 for neurones.

3) to confirm the maintenance of intrinsic molecular identities of cells isolated from the anterior neocortex by double-immunofluorescent labelling for CTIP2, ROBO1 and SRGAP1 which are known to be associated with corticofugal neurones (Chapter 5), together with the above markers used.

4) to confirm the maintenance of intrinsic regional identities of cells out of their environment by rtPCR and IHC for the examination of expression levels of a subset of genes/proteins for which graded expression patterns had been previously confirmed by rtPCR in neocortical tissue (Chapter 3).

Once the cell culture model was successfully establishes and characterized, it could then be utilized for the study of gene regulation, in order to identify potential mechanisms

controlling the expression of some putative anterior and posterior markers in the developing human neocortex.

6.2.2 Preliminary study: Application of Human in-vitro Regionalisation Model

The specificities/affinities of different FGFs binding to their FGFRs is intriguing as they are not identical, for example Fgf2 preferentially binds to Fgfr1, whereas Fgf8 binds with stronger affinity to Fgfr3 (Iwata and Hevner, 2009). As *FGFR1* and *-3* showed differential expression across the developing neocortex in humans (Chapter 3; (Ip et al., 2010a)), cultured cells isolated from the anterior and posterior poles of the developing human neocortex, if they had maintained their intrinsic regional identities, would express these FGFRs at different levels. Thus, when stimulating these cells with FGF2 or -8, differential activation of FGFR1 or -3 would result and potentially initiate different downstream signalling cascades in the anteriorly- and posteriorly-derived cells (Fortin et al., 2005).

Since FGFs system is shown to be important in the guidance of various axonal projections during neocortical development, we initiated a preliminary investigation into the potential of FGF signalling in regulating the expression of some corticofugal neurone-associated genes that were expressed highly in the anterior neocortical tissues (*CTIP2*, *ROBO1* and *SRGAP1*). We hypothesized that FGFs is potentially regulating the expression of these corticofugal neurone-associated genes, and tested the involvement of MAPK downstream signalling pathway. Furthermore, given the differences in biochemical properties and spatiotemporal expression patterns of FGFs/FGFRs within the developing neocortex, we sought to test the hypothesis that FGFs regulate these corticofugal neurone-associated genes differentially in the anterior and posterior region of the neocortex. Finally, the effects of FGFs on the expression of genes encoding their cognate receptors, *FGFRs* were also investigated.

The objectives of the second half of this chapter were to use our established human *in-vitro* regionalisation model in order to:

1) investigate the changes in expression levels of the corticofugal neurone-associated genes and genes encoding receptors of FGFs in the anteriorly- and posteriorly-derived cells by rtPCR after FGF2 or -8 treatments for 24 hours and 72 hours in comparison to the non-treated cells that has been cultured for the same period of time.

2) look into the effect of blocking the MAPK pathway on the expression levels of the corticofugal neurone-associated genes and genes encoding receptors of FGFs in the anteriorly- and posteriorly-derived cells by rtPCR after administration of the MEK inhibitor, U0126, together with FGF2 or -8 treatments for 24 hours and 72 hours in comparison to cells treated with U0126 only and has been cultured for the same period of time.

6.3 Results

6.3.1 Characterization of Human Neocortical Dissociated Cultures

Immunoperoxidase-histochemistry

A putative *in-vitro* model of human regionalization was established by initiating human neocortical cultures using dissected and dissociated anterior and posterior slices of human neocortex aged 11 PCW (Figure 6.1A). Cell cultures were maintained in MEM:10% FCS for 24 h followed by 3 DIV in serum-free MEM:F12 medium supplemented with B27. Cell cultures were initially characterized by testing immunoreactivity for GFAP, Nestin, and MAP2, markers of astrocytes, neural progenitors and neurones, respectively (Figure 6.1A). Cell counts were also carried out and indicate that MAP2-positive neurones account for the majority of cells cultured (75.1 ± 6.1%), while presumably overlapping populations of Nestin- and GFAP-positive cells accounted for 26.6 ± 4.8% and 19.2 ± 2.75%, respectively. There were no observable differences in the levels of these genes when comparing anteriorly- and posteriorly-derived cultures (Figure 6.1C).

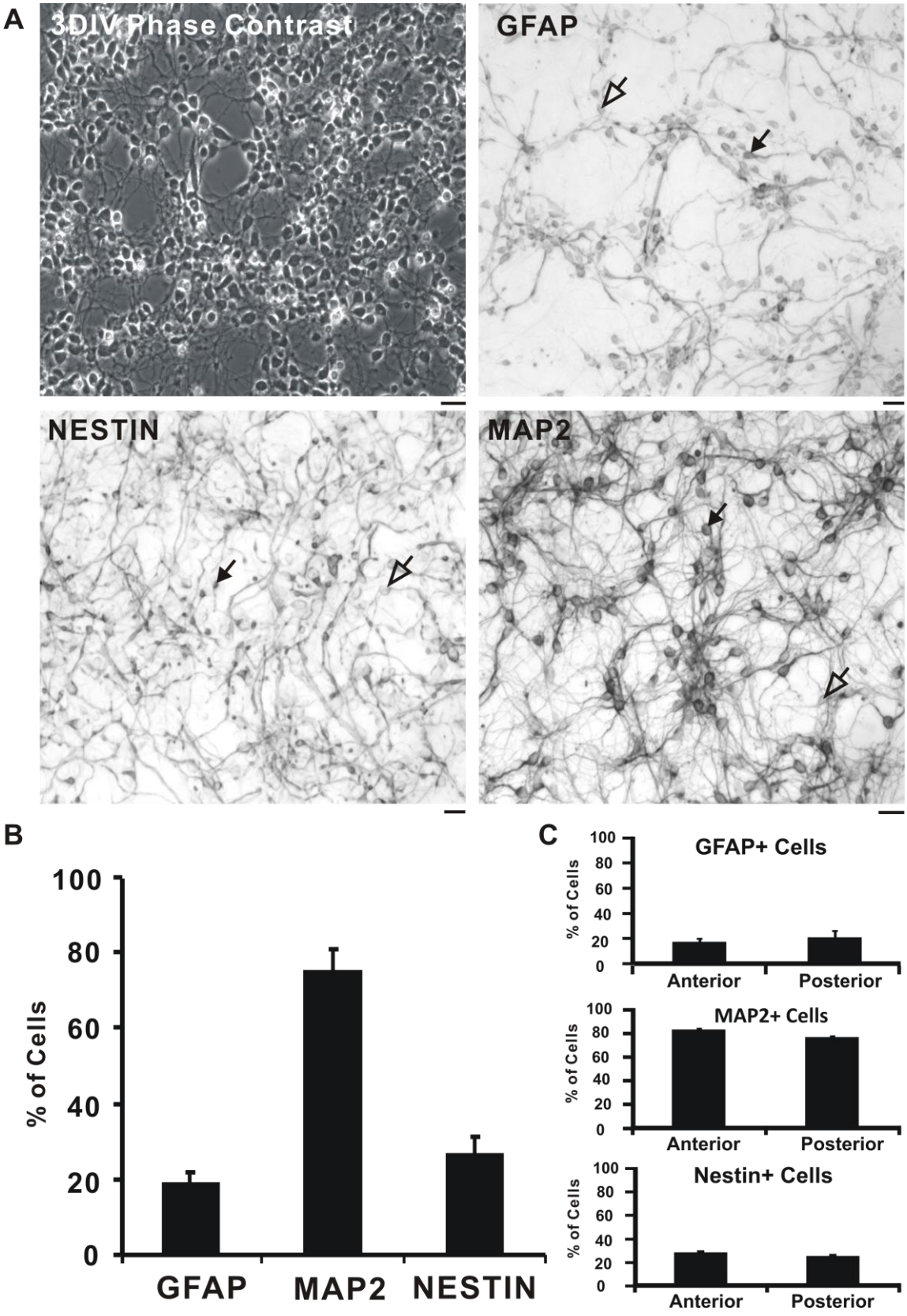

Figure 6.1. Characterization of human neocortical cultures.

Neuronal cell cultures were initiated from 11 PCW (n=4) human neocortex and maintained for 3 DIV. Panels in (A) depicts cells under phase contrast, and stained with antibodies for GFAP, NESTIN and MAP2. (B) Cell counts from random fields of vision (n=4) indicate that MAP2-positive neurones account for most of the cells in culture (75.1 ± 6.1%), while GFAP- and Nestin-positive cells account for 19.2 ± 2.75% and 26.6 ± 4.8%, respectively. In each case, immunopositive cells are indicated by filled arrowheads, and examples of negatively stained cells are indicated by empty arrowheads. (C) Cell counts from random fields of vision (n=4) indicate that cultures derived from anterior and posterior region of the neocortex contained similar number of GFAP-, MAP2- and Nestin-positive cells. Scale bars: 20 µm. Adapted from (Ip et al., 2010a).

Immunofluorescent-histochemistry

To confirm the maintenance of intrinsic molecular identities of cells in *in-vitro* condition, the dissociated cultures initiated from the anterior neocortex were then further characterized by double-labelling of CTIP2, that is associated with corticofugal neurones, with neural progenitor marker Nestin and astrocytic marker GFAP (Figure 6.2A, B). The post-mitotic corticofugal neurone-associated marker CTIP2 was not expressed by neural progenitors or astrocytes as cells expressing CTIP2 did not co-express Nestin (Figure 6.2A) nor GFAP (Figure 6.2B) respectively. Note that double-labelling was also carried out with CTIP2 and MAP2 antibodies. However, immunostaining of MAP2 did not yield a satisfactory fluorescent signal and only one sample was available, so there is no data regarding the co-localization of CTIP2 and MAP2.

On the other hand, a subpopulation of cells co-expressed some corticofugal neurone-associated markers: CTIP2 (nucleic localization) with ROBO1 (cytoplasmic localization, filled arrow, Figure 6.2C) and CTIP2 (nucleic localization) with SRGAP1 (cytoplasmic localization, filled arrow, Figure 6.2D), mimicking the immunoreactivity patterns observed in tissue sections (Figure 5.6C and D).

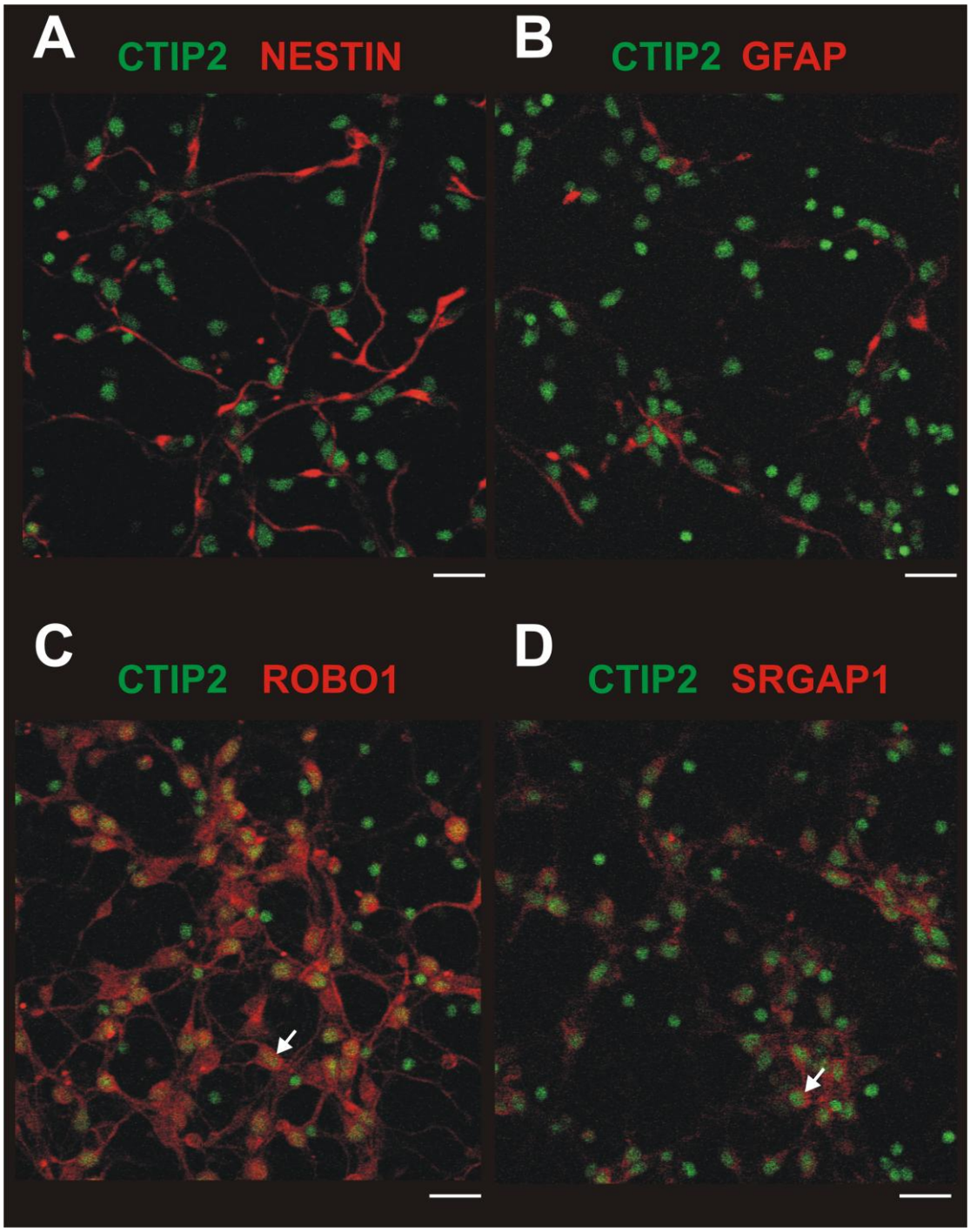

Figure 6.2. Confirmation of intrinsic molecular identities of cells derived from human neocortical cultures.

Double immunofluorescence was carried out for corticofugal neurone-associated markers with Nestin and GFAP on cultures derived from tissue dissected from the anterior poles of 11 PCW aged neocortex (n=1). CTIP2 did not co-localize with Nestin (A) nor with GFAP (B) in these cells. On the other hand, some cells were co-expressing the corticofugal neurone-associated markers CTIP2 (nucleic localization)/ROBO1 (cytoplasmic localization, arrow, C), as well as CTIP2 (nucleic localization)/SRGAP1 (cytoplasmic localization, arrow, D). Scale bars: 20 µm.

6.3.2 Confirmation of a Subset of Regulated Markers in Human Neocortical Dissociated Culture by Immunocytochemistry

To analyze whether neocortical cells maintain their genetic / regional identities when removed from their natural physiological and anatomical environment, cultures were analyzed for immunoreactivity to EMX2 and PAX6, putative regionalization markers, as well as CTIP2, the anteriorly up-regulated corticofugal neurone-associated marker (Figure 6.3A). Cell counts from random fields of view (n=4 for each) indicated differences in levels of EMX2 and CTIP2 but not PAX6 when comparing anteriorly- and posteriorly-derived cultures (Figure 6.3B). The percentage of cells immunoreactive for EMX2 was significantly higher in cell cultures derived from the posterior neocortex (80.7 ± 3.0%) as compared with cultures initiated from the anterior neocortex (37.9 ± 18.3%) indicating a 2.13-fold increase (posterior vs. anterior) between the two cultures. The percentage of cells immunoreactive for CTIP2 was slightly but significantly higher in cell cultures derived from the anterior neocortex (71.2 ± 5.1%) as compared with cultures initiated from the posterior neocortex (53.4 ± 4.7%) indicating a 1.33-fold increase (anterior vs. posterior) between the two cultures. PAX6, however, exhibited no significant differences between cultures (anterior, 49.37 ± 3.6%; posterior, 57.4 ± 0.9%, 0.86-fold, anterior vs. posterior).

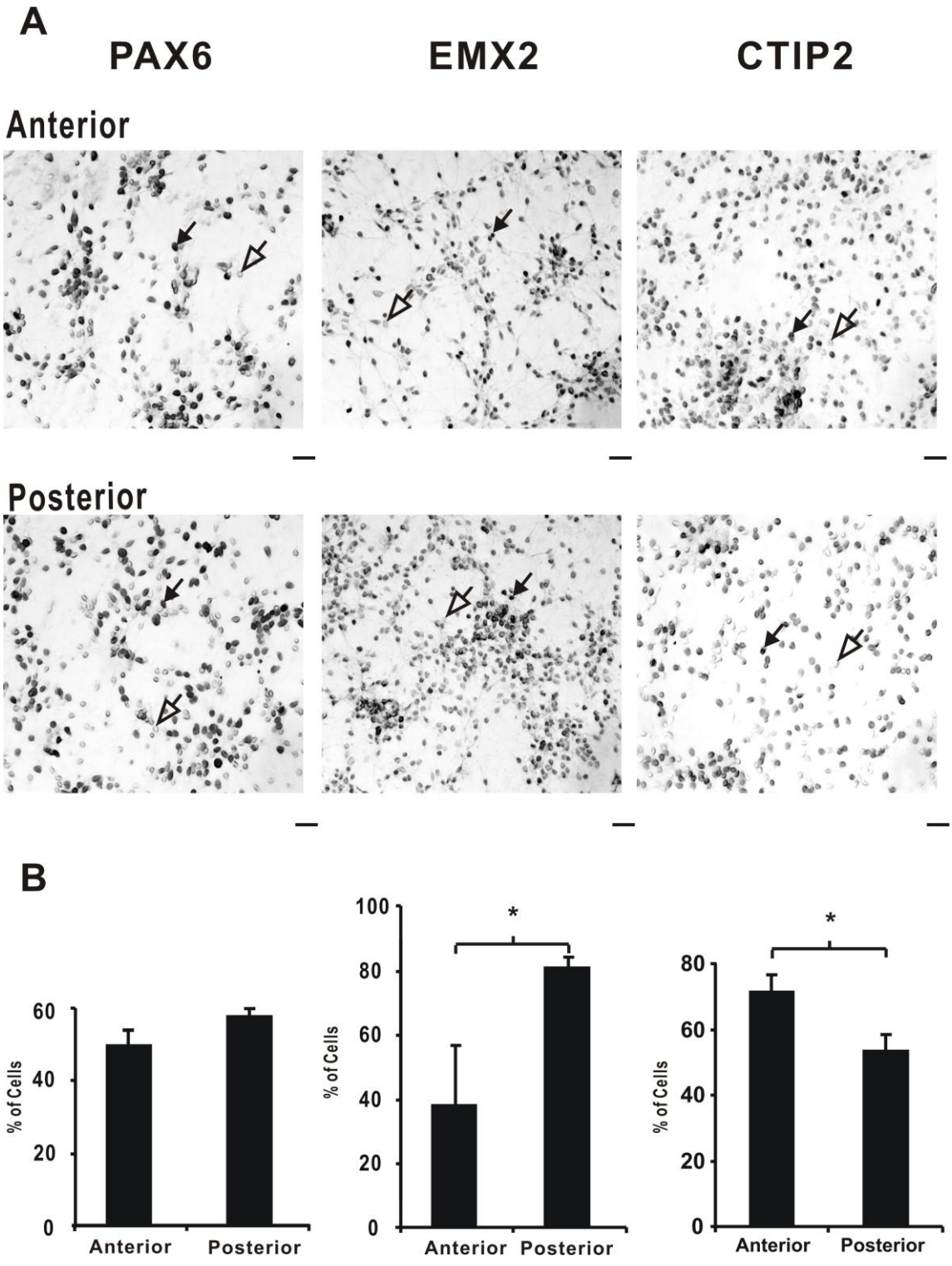

Figure 6.3. Anteriorly- and posteriorly-derived human neocortical cultures exhibit differences in EMX2 and CTIP2 but not in PAX6 expression.

Immunohistochemistry was carried out for EMX2, PAX6 and CTIP2 on cultures derived from tissue dissected from the anterior and posterior poles of 11 PCW aged neocortex (n=4) (A). (B) Cell counts carried from random fields of vision (n=4 per anterior and posterior) show a significant increase in numbers of cells expressing EMX2 (filled arrowheads in A) posteriorly than anteriorly whereas the numbers of CTIP2-positive cells (filled arrowheads in A) were slightly but significantly highly in anteriorly- than posteriorly-derived culture. However, PAX6 (filled arrowheads in A) showed no differences between cultures. EMX2-, PAX6- or CTIP2-negative cells are indicated by empty arrowheads in A. Scale bar: 20 µm. Student's paired *t*-test, $*p \leq 0.05$. Adapted and modified from (Ip et al., 2010a).

6.3.3 Confirmation of gDNA-free cDNA Samples used for rtPCR in Characterization of Human in-vitro Regionalisation Model

To ensure all cDNA samples from cells derived from anterior and posterior human neocortex aged 11 PCW used for rtPCR were not contaminated by gDNA, standard PCR assay was employed with *SDHA* primer set. The FP and RP of *SDHA* targeted sequences on exon 2 and exon 3 of *SDHA* respectively. Thus samples with gDNA would yield products containing intron sequence and of around 940 bp. A positive control was incorporated with a human gDNA sample instead of cDNA samples. A band between 850-1000 bp indicated the amplified product of the gDNA positive control (filled arrow, Figure 6.4). The majority of cDNA samples (white line, Figure 6.4) gave rise only to bands below 100 bp (except the sample indicated by an empty arrow, Figure 6.4) which were equivalent to the size of *SDHA* cDNA (84 bp, Table 2.3). Thus these cDNA samples used for rtPCR were gDNA-free. The sample containing gDNA (empty arrow, Figure 6.4) was subjected to re-extraction until complete elimination of gDNA prior to rtPCR.

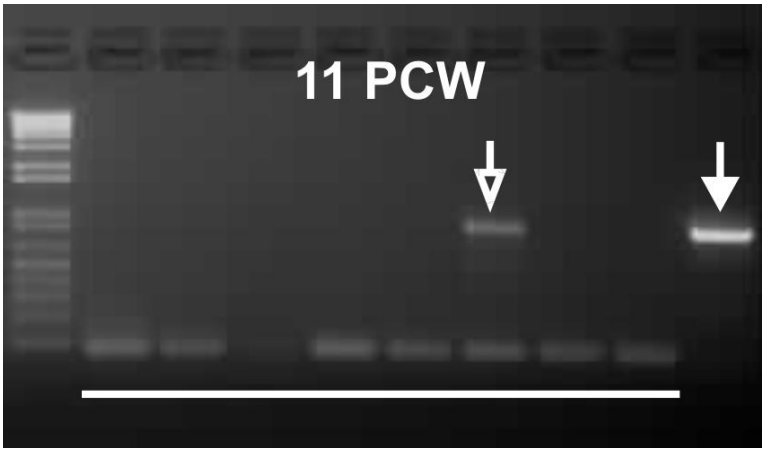

Figure 6.4. Confirmation of gDNA-free cDNA samples from characterized cultured cells used for rtPCR.

Amplified products of *SDHA* using standard PCR assay. Product of positive control with human gDNA was indicated by filled arrow, whereas cDNA samples from cells derived from anterior and posterior neocortex aged 11 PCW (n=4) used for rtPCR were indicated by white lines. The sample derived from cells containing gDNA was indicated by empty arrow. 1kb Plus DNA ladder was used to determine the size of bands.

6.3.4 Confirmation of a Subset of Regulated Markers in Human Neocortical Dissociated Culture by rtPCR

At mRNA level, rtPCR was performed on reverse transcribed RNA extracted from cell cultures initiated from 11 PCW aged neocortex and maintained for 3 DIV (Figure 6.5). Examining some of the genes as characterized *in-vivo*, a similar pattern of results to that of tissue was obtained when comparing expression levels in anteriorly- and posteriorly-derived cultures. *CNTNAP2* (2.67-fold), *CTIP2* (2.78-fold), *PCDH17* (3.92-fold), *ROBO1* (2.01-fold) and *S100A10* (2.76-fold) were found to be significantly higher in anteriorly- than posteriorly-derived cultures. *FGFR1* (1.32-fold) was found to be marginally but significantly expressed at higher levels anteriorly (Figure 6.5B). The posterior markers *COUPTFI* (10.18-fold), *EMX2* (1.73-fold) and *FGFR3* (59.28-fold) exhibited significantly higher expression when compared to anteriorly-derived cultures (Figure 6.5A, B). Six of the genes, *FEZF2, FGFR2, MAP2, PAX6, SOX5* and *SRGAP1* exhibited no statistically significant difference in expression either anteriorly or posteriorly.

A

Genes	Fold Changes	Gradient
PCDH17	3.92	A>P
CTIP2	2.78	A>P
S100A10	2.76	A>P
CNTNAP2	2.67	A>P
ROBO1	2.01	A>P
FGFR1	1.32	A>P
PAX6	1.13	n.d.
FGFR3	59.28	A<P
COUPTFI	10.18	A<P
EMX2	1.73	A<P
SOX5	1.62	n.d.
FEZF2	1.47	n.d.
MAP2	1.37	n.d.
FGFR2	1.34	n.d.
SRGAP1	1.12	n.d.

B

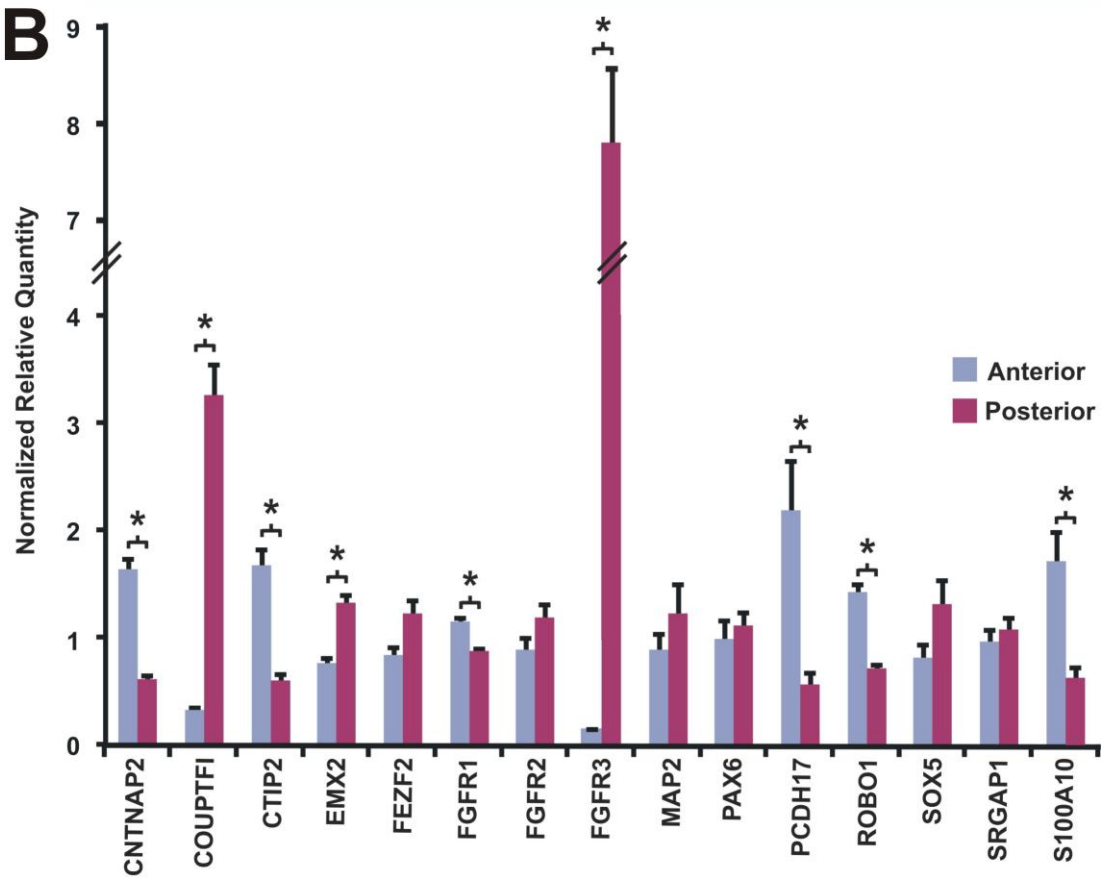

Figure 6.5. rtPCR confirmation for a subset of differentially regulated genes during early human neocortical development in cultures derived from 11 PCW human neocortex.

Table indicating fold changes (A), and graphical representation (B) of NRQ of a subset of genes determined by rtPCR from RNA extracted from anteriorly- and posteriorly-derived cultures of human neocortex aged 11 PCW (n=4). *CNTNAP2*, *CTIP2*, *PCDH17*, *ROBO1* and *S100A10* exhibited a high anterior to low posterior gradient. *COUPTFI*, *EMX2* and *FGFR3* exhibited a high posterior, low anterior gradient. No gradients were detected for *FEZF2*, *FGFR2*, *MAP2*, *PAX6*, *SOX5* and *SRGAP1*. Student's *t*-test, *p≤ 0.05, n.d., not detected; A, anterior; P, posterior. . Adapted and modified from (Ip et al., 2010a).

6.3.5 Confirmation of gDNA-free cDNA Samples used for rtPCR in Gene Regulation Study

To ensure all cDNA samples from stimulated cells derived from anterior and posterior human foetal neocortex used for rtPCR were not contaminated by gDNA, standard PCR assay was employed with *SDHA* primer set. The FP and RP of *SDHA* targeted sequences on exon 2 and exon 3 of *SDHA* respectively. Thus samples with gDNA would yield products containing intron sequence and of around 940 bp. The majority of cDNA samples from stimulated cells derived from anterior and posterior neocortex aged 10-12 PCW (white lines, Figure 6.6) gave rise only to bands below 100 bp (except the sample indicated by empty arrow, Figure 6.6) which were equivalent to the size of *SDHA* cDNA (84 bp, Table 2.3). Thus these cDNA samples used for rtPCR were gDNA-free. The sample containing gDNA (empty arrow, Figure 6.6) was subjected to re-extraction until complete elimination of gDNA prior to rtPCR.

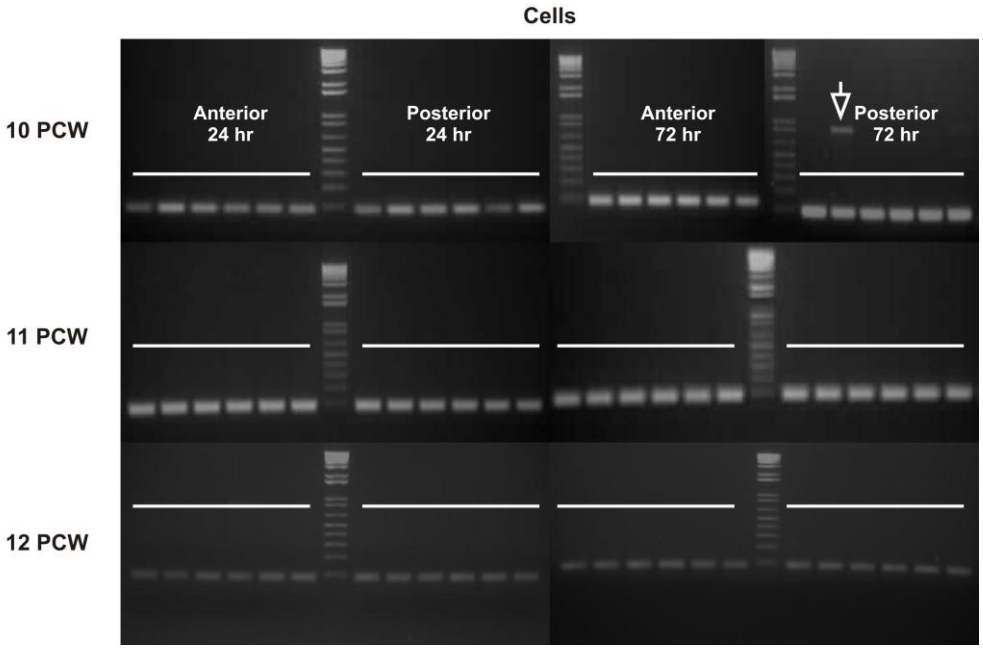

Figure 6.6. Confirmation of gDNA-free cDNA samples from treated cells used for rtPCR.

Amplified products of *SDHA* using standard PCR assay. cDNA samples from anteriorly- and posteriorly-derived cells treated variously for 24 or 72 hours (hr) were indicated by white lines (10 PCW, n=1; 11 PCW, n=1; 12 PCW, n=1). The sample derived from cells containing gDNA was indicated by empty arrow. 1kb Plus DNA ladder was used to determine the size of bands.

6.3.6 Effects of FGFs and/or MEK Inhibitor on Expression of Reference Genes

To confirm the expression of the three reference genes, *β-ACTIN, GAPDH* and *SDHA*, in cultured neocortical cells was not influenced by the addition of FGFs and/or the MEK inhibitor, U0126, their cycle threshold (Ct) values obtained after rtPCR were compared between different treatment groups. Ct value was inversely proportional to the expression level of a gene.

After different treatments to cells derived anteriorly (for 24 and 72 hours, Figure 6.7A and B) and posteriorly (for 24 and 72 hours, Figure 6.7C and D), the averaged Ct values of each reference genes from the 3 samples aged 10, 11 and 12 PCW were consistent, indicating there was no change in the expression of reference genes in cells subjected to various treatments as compared to the non-treated control groups.

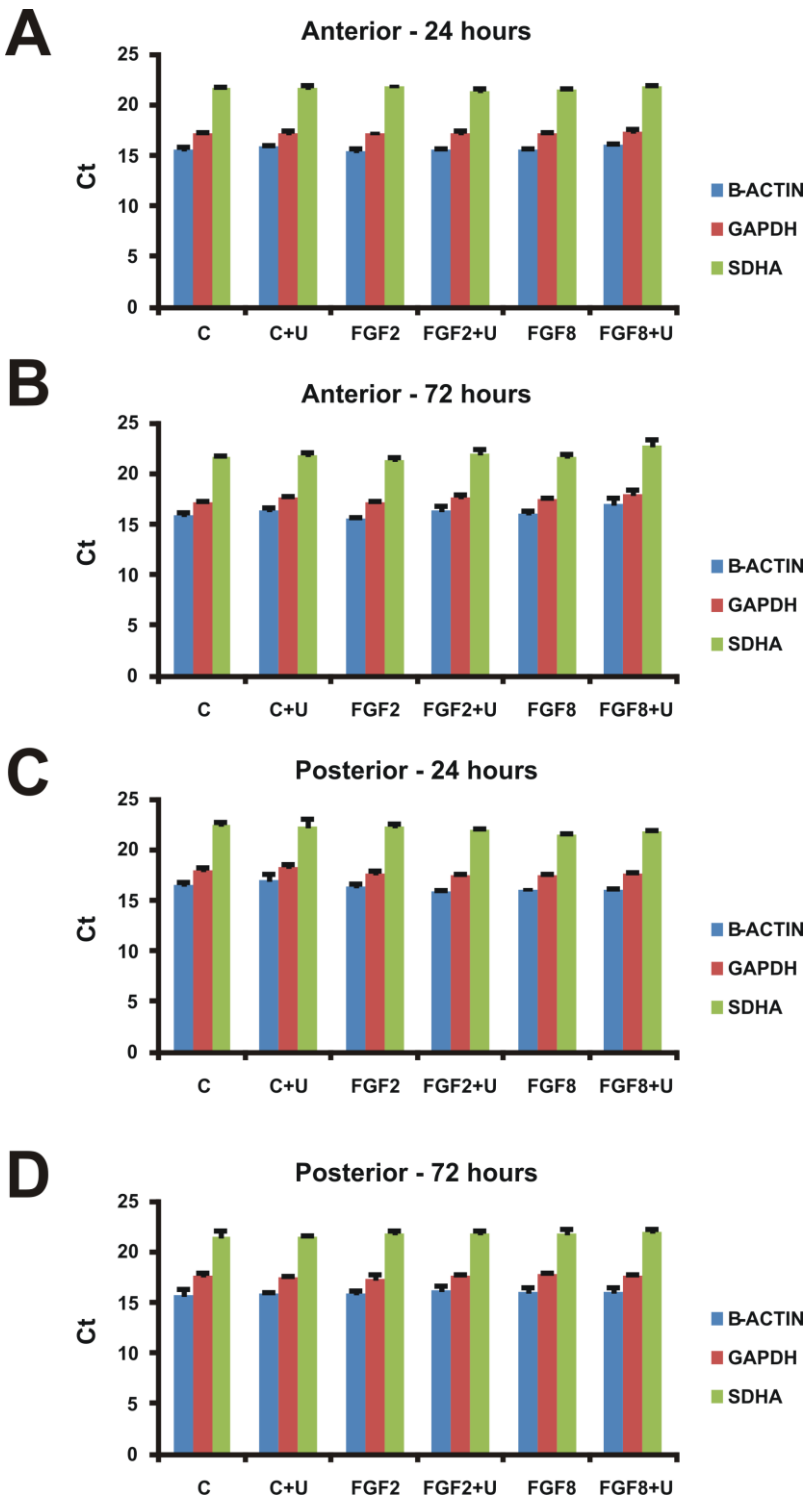

Figure 6.7. Ct values of reference genes in different groups of cultured cell.

Graphical representation of cycle threshold (Ct) values of reference genes *β–ACTIN* (blue), *GAPDH* (pink) and *SDHA* (green) determined by rtPCR from RNA extracted from anteriorly- (A, B) and posteriorly- (C, D) derived cultures of human neocortex aged 10 (n=1), 11 (n=1) and 12 (n=1) PCW for 24 and 72 hours. C, non-treated control groups; C+U, U0126-treated alone groups; FGF2, FGF2-treated groups; FGF2+U, FGF2 and U0126-treated groups; FGF8, FGF8-treated groups; FGF8+U, FGF8 and U0126-treated groups.

6.3.7 Regulation of Corticofugal Neurone-associated Genes and Fibroblast Growth Factor Receptor Genes Expression by FGF Signalling

rtPCR was performed on reverse transcribed RNA extracted from cell cultures initiated from the anterior and posterior neocortex aged 10-12 PCW, which were treated with FGF2 (20 ng/ml) or FGF8 (20 ng/ml) in the presence or absence of U0126 (10 μM), a MEK inhibitor, for 24 or 72 hours and used for the preliminary studies of gene expression regulation (Table 2.2).

The effects of FGFs treatment on gene expression were determined by calculating the fold changes of expression level of each gene in FGFs-treated groups in comparison to the control groups (i.e. FGFs/C). The trend and magnitude of fold changes in gene expression were graphically presented in which significant and/or ≤ -1.5-/≥ 1.5-fold changes indicated the down- and up-regulation of gene expression after stimulation with FGF2 or FGF8. Similarly, the effects of blocking FGFs-induced MAPK signalling pathways on gene expression were determined by calculating the fold changes of expression level of each gene following stimulation with FGFs in the presence of U0126 in comparison to control groups which were treated with U0126 alone (i.e. FGFs+U/C+U).

Comparisons of fold changes between FGFs/C and FGFs+U/C+U were carried out to determine if the changes in gene expression induced by FGFs were MAPK signalling-dependent or -independent. Any inhibition of putative FGFs-induced up- or down-regulation of gene expression by U0126 would indicate a dependence on the MAPK intracellular signalling pathway. This was carried out by comparison of fold changes between FGFs/C and FGFs+U/C+U groups and indicated by statistical significant differences and/or ≥ 0.5 in fold change differences between the two groups.

Effects of FGF2 Signalling on Expression of *CTIP2*, *ROBO1* and *SRGAP1*

After 24 hours of FGF2 stimulation, expression of *CTIP2* was down-regulated by 1.63- and 1.72-fold in the anteriorly- and posteriorly-derived cells respectively (Figure 6.8A). Prolonged FGF2 stimulation (72 hours) down-regulated the expression of *CTIP2* by 2.22- and 4.72-fold in the anteriorly- and posteriorly-derived cells respectively (Figure 6.8A). The FGF2-induced down-regulation of *CTIP2* expression appeared to be inhibited by U0126 in the anteriorly-derived cells after 24-hour treatment and was significantly inhibited after 72 hours (Figure 6.8A). However, the inhibition by U0126 was only observed in the posteriorly-derived cells after 72 hours (Figure 6.8A). Thus the down-regulation of *CTIP2* expression induced by FGF2 occurred at all time points anteriorly and posteriorly, and the down-regulation of *CTIP2* expression was potentially dependent on MAPK signalling.

Expression of *ROBO1* in the anteriorly-derived cells was not influenced by short- and long-term FGF2 stimulation (Figure 6.8B). Whereas in the posteriorly-derived cells, *ROBO1* expression was up-regulated marginally but significantly by 1.39-fold after 24-hour stimulation of FGF2, and prolonged FGF2 stimulation (72 hours) up-regulated *ROBO1* expression significantly by 2.02-fold (Figure 6.8B). The FGF2-induced up-regulation of *ROBO1* expression was inhibited by U0126 after 72 hours only in the posteriorly-derived cells (Figure 6.8B). Thus the up-regulation of *ROBO1* expression induced by FGF2 only occurred posteriorly, and the substantial up-regulation of *ROBO1* expression observed after the long-term FGF2 stimulation was potentially dependent on MAPK signalling.

In the anteriorly-derived cells, expression of *SRGAP1* was significantly down-regulated by 1.56-fold only after a prolonged FGF2 stimulation (72 hours) (Figure 6.8C). Whereas in the posteriorly-derived cells, *SRGAP1* expression was already down-regulated by 1.50-fold after stimulation of FGF2 for 24 hours, and by 2.38-fold after an extended treatment of FGF2 for 72 hours (Figure 6.8C). The FGF2-induced down-regulation of *SRGAP1* expression was all inhibited by U0126 in the anteriorly- and posteriorly-derived cells after 72 hours and significantly in the posteriorly-derived cells after 24 hours (Figure 6.8C). Thus the down-regulation of *SRGAP1* expression induced

by FGF2 occurred anteriorly and primarily in the posteriorly-derived cells, and the observed down-regulation of *SRGAP1* expression was potentially dependent on MAPK signalling.

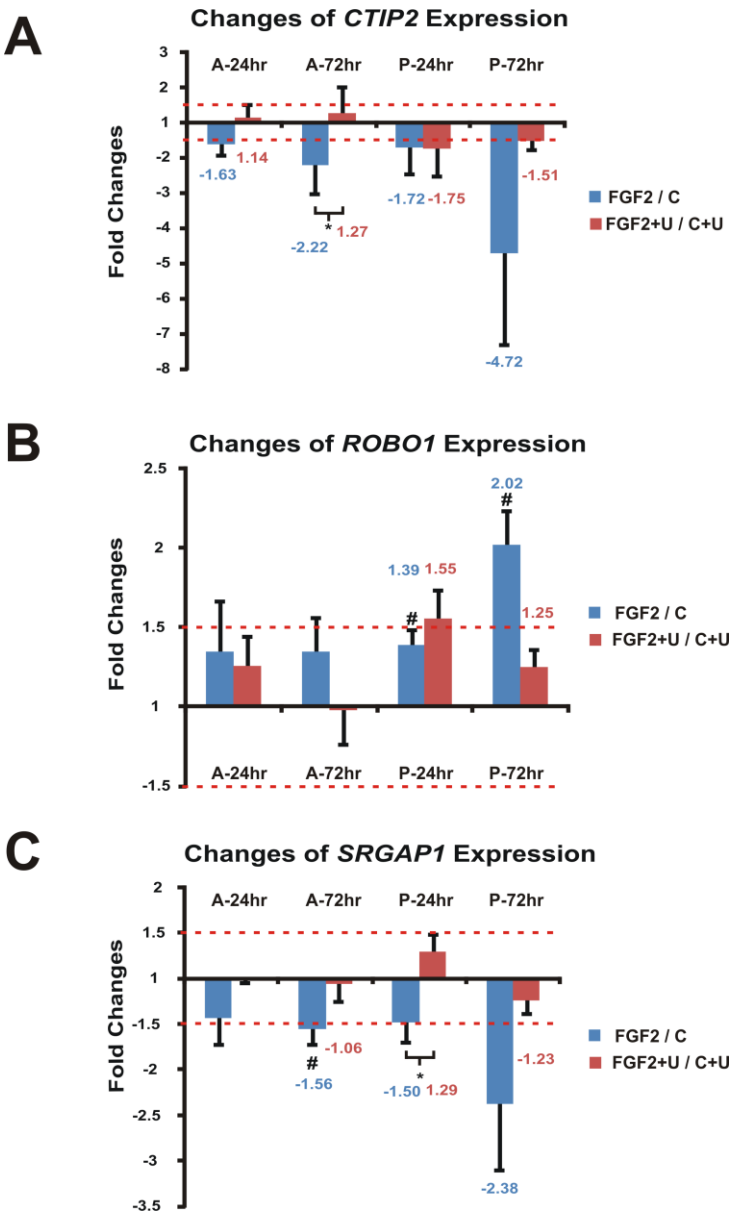

Figure 6.8. Spatiotemporal effects of FGF2 signalling on *CTIP2*, *ROBO1* and *SRGAP1* expression.

Graphical representation of fold changes of *CTIP2* (A), *ROBO1* (B) and *SRGAP1* (C) expression determined by rtPCR from RNA extracted from anteriorly- and posteriorly-derived cultures of human neocortex aged 10 (n=1), 11 (n=1) and 12 (n=1) PCW, which have been treated with FGF2 in the presence or absence of U0126 for 24 and 72 hours (24hr/72hr). Blue bars represented the fold changes in gene expression after FGF2 stimulation in comparison to non-treated control groups (FGF2/C). Pink bars represented the fold changes in gene expression after FGF2 stimulation in the presence of U0126 in comparison to U0126-treated alone groups (FGF2+U/C+U). Red dotted lines indicated 1.5-fold increase or decrease of expression level. # indicated significant differences of expression level between FGF2 and control groups or FGF2+U and C+U groups ($p \leq 0.05$). * indicated significant differences of fold changes between FGF2/C and FGF2+U/C+U ($p \leq 0.05$). A, anterior; P, posterior.

Effects of FGF8 Signalling on Expression of *CTIP2*, *ROBO1* and *SRGAP1*

After 24 hours of FGF8 stimulation, expression of *CTIP2* was down-regulated by 1.57-fold in the anteriorly-derived cells and a prolonged FGF8 stimulation (72 hours) down-regulated expression of *CTIP2* by 1.91-fold in these cells (Figure 6.9A). Whereas in the posteriorly-derived cells, *CTIP2* expression was down-regulated by 2.13-fold only after 72 hours of FGF8 stimulation (Figure 6.9A). The FGF8-induced down-regulation of *CTIP2* expression was inhibited by U0126 only in the anteriorly-derived cells after 24 hours (Figure 6.9A). Note that the expression of *CTIP2* was significantly down-regulated by 1.86-fold when the anteriorly-derived cells were treated with both FGF8 and U0126 for 72 hours (Figure 6.9A). Thus the down-regulation of *CTIP2* expression induced by FGF8 occurred both anteriorly and posteriorly, and the down-regulation of *CTIP2* expression anteriorly after 24 hours was potentially dependent on MAPK signalling.

Expression of *ROBO1* in the anteriorly- and posteriorly-derived cells was not influenced by short- and long-term FGF8 stimulation alone (Figure 6.9B). However *ROBO1* expression was marginally but significantly up-regulated by 1.47-fold when the anteriorly-derived cells were treated with both FGF8 and U0126 for 24 hours (Figure 6.9B). Thus the up-regulation of *ROBO1* expression was induced by FGF8, however the intracellular signalling pathways involved were potentially under the repression of MAPK signalling.

In the anteriorly-derived cells, expression of *SRGAP1* was slightly but significantly down-regulated by 1.27-fold only after a prolonged FGF8 stimulation (72 hours) (Figure 6.9C). Similarly in the posteriorly-derived cells, *SRGAP1* expression was down-regulated by 1.58-fold after an extended stimulation of FGF8 for 72 hours (Figure 6.9C). The addition of U0126 did not inhibit the FGF8-induced down-regulation of *SRGAP1* expression anteriorly or posteriorly (Figure 6.9C). Thus the down-regulation of *SRGAP1* expression induced by the long-term stimulation of FGF8 occurred both anteriorly and posteriorly, however the down-regulation was independent of MAPK signalling.

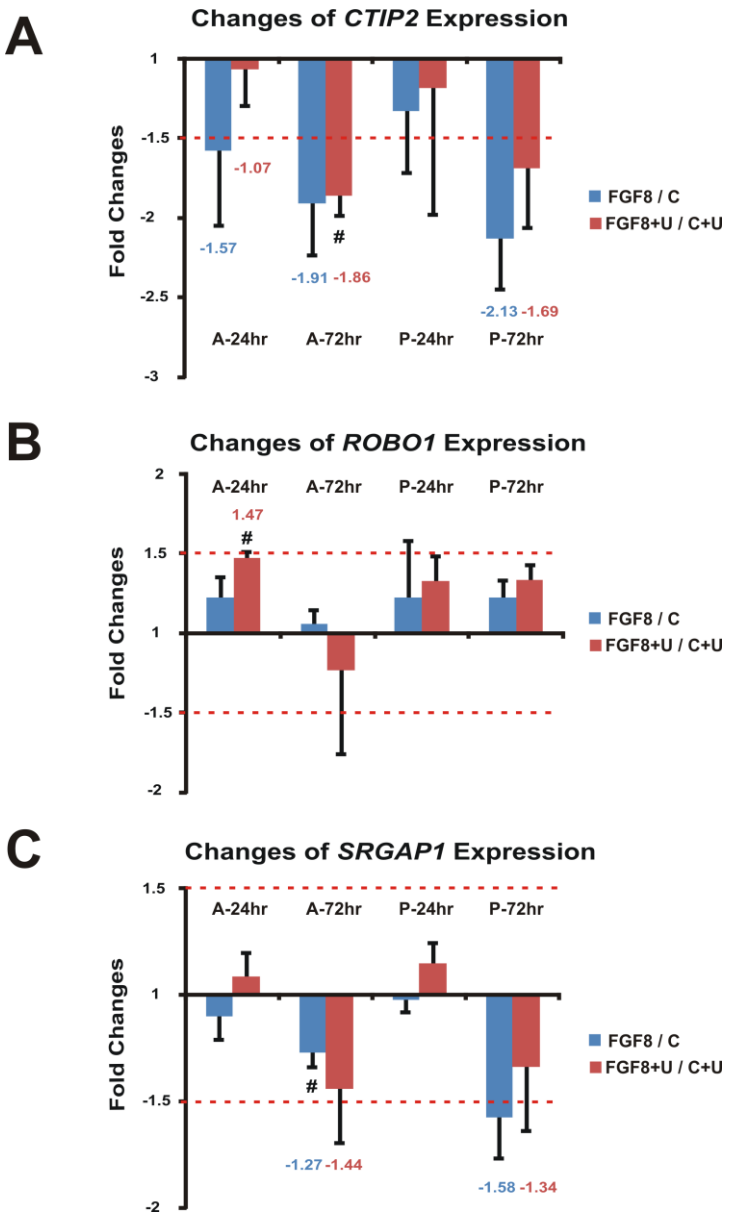

Figure 6.9. Spatiotemporal effects of FGF8 signalling on *CTIP2*, *ROBO1* and *SRGAP1* expression.

Graphical representation of fold changes of *CTIP2* (A), *ROBO1* (B) and *SRGAP1* (C) expression determined by rtPCR from RNA extracted from anteriorly- and posteriorly-derived cultures of human neocortex aged 10 (n=1), 11 (n=1) and 12 (n=1) PCW, which have been treated with FGF8 in the presence or absence of U0126 for 24 and 72 hours (24hr/72hr). Blue bars represented the fold changes in gene expression after FGF8 stimulation in comparison to non-treated control groups (FGF8/C). Pink bars represented the fold changes in gene expression after FGF8 stimulation in the presence of U0126 in comparison to U0126-treated alone groups (FGF8+U/C+U). Red dotted lines indicated 1.5-fold increase or decrease of expression level. # indicated significant differences of expression level between FGF8 and control groups or FGF8+U and C+U groups ($p \leq 0.05$). * indicated significant differences of fold changes between FGF8/C and FGF8+U/C+U ($p \leq 0.05$). A, anterior; P, posterior.

Effects of FGF2 Signalling on Expression of *FGFR1*, *FGFR2* and *FGFR3*

After 24 hours of FGF2 stimulation, expression of *FGFR1* was up-regulated by 1.94- and 2.29-fold in the anteriorly- and posteriorly-derived cells respectively (Figure 6.10A). Prolonged FGF2 stimulation (72 hours) up-regulated the expression of *FGFR1* by 5.97- and 4.25-fold in the anteriorly- and posteriorly-derived cells respectively (Figure 6.10A). The FGF2-induced up-regulation of *FGFR1* expression was inhibited by U0126 in the anteriorly- and posteriorly-derived cells only after 72 hours (Figure 6.10A). Thus the up-regulation of *FGFR1* expression induced by FGF2 occurred at all time points anteriorly and posteriorly, however only the substantial up-regulation of *FGFR1* expression after the prolonged FGF2 stimulation was potentially dependent on MAPK signalling.

Expression of *FGFR2* in the anteriorly-derived cells was down-regulated by 2.80- and 4.46-fold after 24 and 72 hours of FGF2 stimulation (Figure 6.10B). Whereas in the posteriorly-derived cells, *FGFR2* expression was down-regulated by 3.36-fold only after 72-hour stimulation of FGF2 (Figure 6.10B). The FGF2-induced down-regulation of *FGFR2* expression was all inhibited by U0126 anteriorly and posteriorly (Figure 6.10B). Thus the down-regulation of *FGFR2* expression induced by FGF2 occurred both anteriorly and posteriorly, and was potentially dependent on MAPK signalling.

Expression of *FGFR3* was down-regulated by 3.21-fold in the posteriorly-derived cells after a prolonged FGF2 stimulation (72 hours) only (Figure 6.10C). This FGF2-induced down-regulation of *FGFR3* expression was significantly inhibited by U0126 (Figure 6.10C). Note that the expression of *FGFR3* was down-regulated by 1.84-fold when the anteriorly-derived cells were treated with both FGF8 and U0126 for 72 hours (Figure 6.10C). Similarly, the expression of *FGFR3* was down-regulated slightly but significantly by 1.18-fold when the posteriorly-derived cells were treated with both FGF8 and U0126 for 24 hours (Figure 6.10C). Thus the down-regulation of *FGFR3* expression induced by FGF2 occurred in the anteriorly- and posteriorly-derived cells after FGF2 stimulation, and the prolonged down-regulation of *FGFR3* expression posteriorly was potentially dependent on MAPK signalling. However, the intracellular

signalling pathways involved anteriorly after 72 hours and posteriorly after 24 hours were potentially under the repression of MAPK signalling.

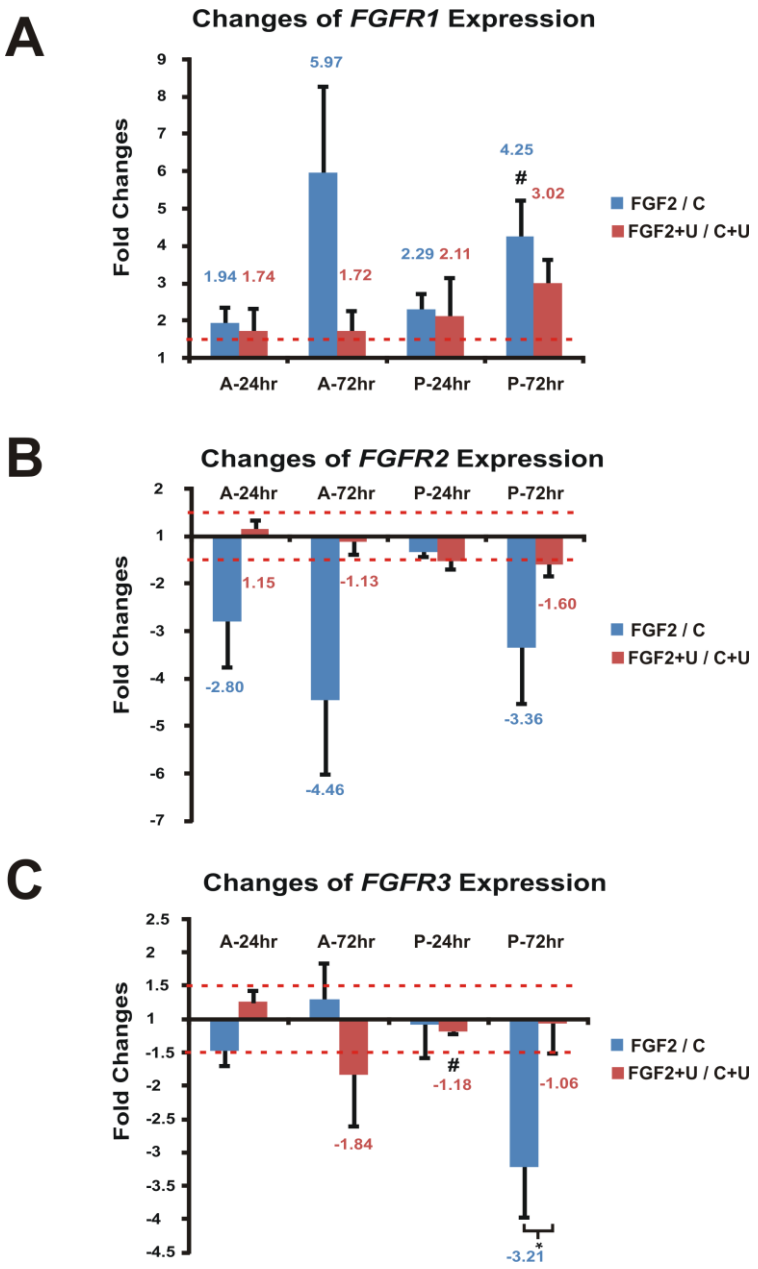

Figure 6.10. Spatiotemporal effects of FGF2 signalling on *FGFR1-3* expression.

Graphical representation of fold changes of *FGFR1* (A), *FGFR2* (B) and *FGFR3* (C) expression determined by rtPCR from RNA extracted from anteriorly- and posteriorly-derived cultures of human neocortex aged 10 (n=1), 11 (n=1) and 12 (n=1) PCW, which have been treated with FGF2 in the presence or absence of U0126 for 24 and 72 hours (24hr/72hr). Blue bars represented the fold changes in gene expression after FGF2 stimulation in comparison to non-treated control groups (FGF2/C). Pink bars represented the fold changes in gene expression after FGF2 stimulation in the presence of U0126 in comparison to U0126-treated alone groups (FGF2+U/C+U). Red dotted lines indicated 1.5-fold increase or decrease of expression level. # indicated significant differences of expression level between FGF2 and control groups or FGF2+U and C+U groups ($p \leq 0.05$). * indicated significant differences of fold changes between FGF2/C and FGF2+U/C+U ($p \leq 0.05$). A, anterior; P, posterior.

Effects of FGF8 Signalling on Expression of *FGFR1*, *FGFR2* and *FGFR3*

After 24 hours of FGF8 stimulation, expression of *FGFR1* was up-regulated by 1.61-fold in the anteriorly-derived cells and a prolonged FGF8 stimulation (72 hours) up-regulated its expression by 2.98-fold in these cells (Figure 6.11A). Whereas in the posteriorly-derived cells, *FGFR1* expression was up-regulated by 1.75-fold after 72 hours of FGF8 stimulation only (Figure 6.11A). The FGF8-induced up-regulation of *FGFR1* expression was inhibited by U0126 only in the anteriorly-derived cells after 72 hours (Figure 6.11A). Note that the expression of *FGFR1* was up-regulated by 1.57-fold and significantly by 1.45-fold when the posteriorly-derived cells were treated with both FGF8 and U0126 for 24 and 72 hours respectively (Figure 6.11A). Thus the up-regulation of *FGFR1* expression induced by FGF8 occurred predominantly in anteriorly-derived cells but also posteriorly, and the substantial up-regulation of *FGFR1* expression anteriorly after 72 hour was potentially dependent on MAPK signalling. However, the intracellular signalling pathways involved posteriorly were potentially under the repression of MAPK signalling.

Expression of *FGFR2* in the anteriorly-derived cells was down-regulated by 1.76-fold after 24 hours of FGF8 stimulation, whereas in the posteriorly-derived cells its expression was down-regulated by 1.73-fold after 72 hours of FGF8 stimulation (Figure 6.11B). The down-regulation of *FGFR2* expression was inhibited by U0126 in the anteriorly-derived cells after 24 hours only (Figure 6.11B). Note that *FGFR2* expression was slightly but significantly down-regulated by 1.22- and 1.30-fold when the posteriorly-derived cells were treated with both FGF8 and U0126 for 24 and 72 hours respectively (Figure 6.11B). Thus the down-regulation of *FGFR2* expression was induced by FGF8 both anteriorly and posteriorly, however only the anterior down-regulation of *FGFR2* expression was potentially dependent on MAPK signalling. The intracellular signalling pathways involved posteriorly after 24 hours potentially under the repression of MAPK signalling.

Expression of *FGFR3* was up-regulated by 1.76-fold after a prolonged FGF8 stimulation (72 hours) in the anteriorly-derived cells only, and no effect was observed posteriorly (Figure 6.11C). This FGF8-induced up-regulation of *FGFR3* expression was

inhibited by U0126 (Figure 6.11C). Note that *FGFR3* expression was down-regulated by 1.52-fold when the posteriorly-derived cells were treated with both FGF8 and U0126 for 72 hours (Figure 6.11C). Thus the up-regulation of *FGFR3* expression induced by the long-term stimulation of FGF8 occurred only anteriorly, and this up-regulation of *FGFR3* expression was potentially dependent on MAPK signalling. However, prolonged stimulation of FGF8 down-regulated *FGFR3* expression and the intracellular signalling pathways involved were potentially under the repression of MAPK signalling.

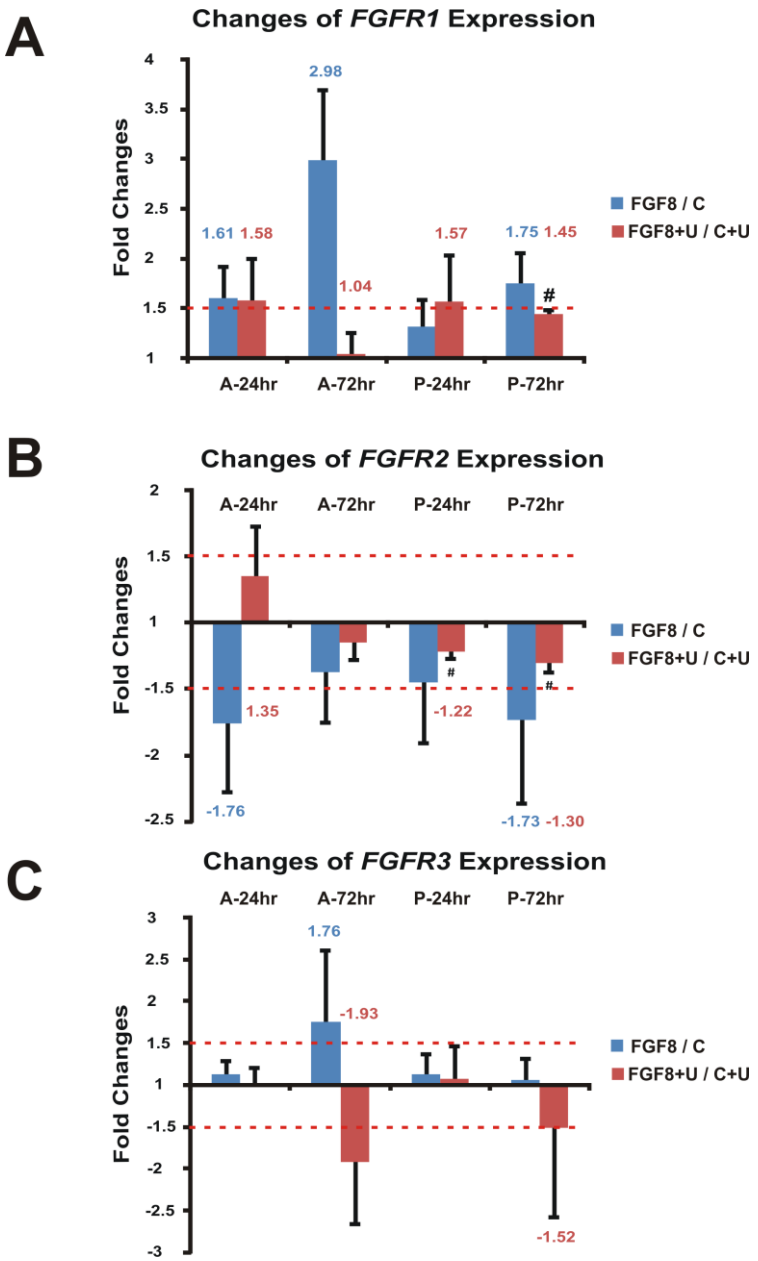

Figure 6.11. Spatiotemporal effects of FGF8 signalling on *FGFR1-3* expression.

Graphical representation of fold changes of *FGFR1* (A), *FGFR2* (B) and *FGFR3* (C) expression determined by rtPCR from RNA extracted from anteriorly- and posteriorly-derived cultures of human neocortex aged 10 (n=1), 11 (n=1) and 12 (n=1) PCW, which have been treated with FGF8 in the presence or absence of U0126 for 24 and 72 hours (24hr/72hr). Blue bars represented the fold changes in gene expression after FGF8 stimulation in comparison to non-treated control groups (FGF8/C). Pink bars represented the fold changes in gene expression after FGF8 stimulation in the presence of U0126 in comparison to U0126-treated alone groups (FGF8+U/C+U). Red dotted lines indicated 1.5-fold increase or decrease of expression level. # indicated significant differences of expression level between FGF8 and control groups or FGF8+U and C+U groups ($p \leq 0.05$). * indicated significant differences of fold changes between FGF8/C and FGF8+U/C+U ($p \leq 0.05$). A, anterior; P, posterior.

6.4 Discussion

6.4.1 Establishment of Human in-vitro Regionalisation Model

To establish whether the regulation of genes observed within the brain is dependent on their physiological environment, or whether such information is held intrinsically, we have generated dissociated cultures from neocortical tissue dissected from the anterior and posterior poles of 11 PCW neocortices. The protomap hypothesis states that progenitors possess regional intrinsic information by the time they undergo their final asymmetric division in the VZ and their progenies maintain this information, so that by the time they have migrated to the CP, they may phenotypically look like all other cortical neurones but are genetically different to their neighbours (Rakic et al., 2009; Rakic, 1991). The cell culture model employed here involves maintenance of the cells in a differentiation-inducing medium that results in the vast majority of cells reacting positively for the neuronal marker, MAP2 (Figure 6.1). The detection of GFAP- and Nestin-positive cells suggests that radial glia / astrocytes and other progenitors are also present (Figure 6.1). Cell counts from these markers showed no significant differences between anterior or posterior cultures indicating no differences in the differentiation processes occurring in the cells after 3 DIV (Figure 6.1).

6.4.2 Maintenance of the Intrinsic Regional Molecular Identity of Cells

Further characterization of these cells indicated their intrinsic molecular identity was maintained after 3 DIV. *In-situ* studies have shown that CTIP2, which is associated with corticofugal neurones, is expressed solely by post-mitotic neurones in humans (Figure 5.6) as well as in mice, involving in post-mitotic differentiation such as axonal outgrowth, fasciculation and survival (Arlotta et al., 2005). Here, neocortical cells cultured for 3DIV that were immunoreactive for CTIP2 did not co-express Nestin or GFAP (Figure 6.2), indicating CTIP2 remained to be expressed by post-mitotic neurones but not by neural progenitor or astroglial cells in the culture. Furthermore, it was demonstrated previously within the developing CP of the human neocortex, a subpopulation of post-mitotic neurones co-expressed all three corticofugal neurone-

associated markers, CTIP2, ROBO1 and SRGAP1 (Figure 5.6). These cells maintained their intrinsic molecular identity *in-vitro* as indicated by the co-localization of CTIP2/ROBO1 and CTIP2/SRGAP1 (Figure 6.2).

To confirm whether cells maintained their intrinsic regional identity, cells stained with antibodies for PAX6, EMX2 and CTIP2 were quantified. Whereas PAX6-positive cell counts from anteriorly- and posteriorly-derived cultures exhibited no significant differences, EMX2-positive cells were significantly more numerous in posteriorly-derived cell cultures and there were significantly more CTIP2-immunoreactive cells in the anteriorly-derived cell cultures (Figure 6.3). This supports our previous evidence that a PAX6 gradient is not detectable in the developing neocortex at this time point (11 PCW, (Bayatti et al., 2008b)). Furthermore, EMX2, which has been reported to be expressed in the proliferative zones during rodent development (Cecchi and Boncinelli, 2000), was observed to be expressed in the majority of cells in culture posteriorly, indicating that the protein must be expressed in post-mitotic neurones, again supporting recent evidence indicating that EMX2 is expressed within the CP during development in humans (Bayatti et al., 2008b). This observation raises the interesting question as to whether EMX2 exerts an areal influence in the CP in addition to having a regionalization function in the proliferative zones in humans. The relative levels of EMX2 in culture after 3 DIV (posterior vs. anterior) (Figure 6.3) mirror the relative *EMX2* levels measured in tissue (posterior vs. anterior) (Figure 3.3; (Ip et al., 2010a)) and this may indicate a degree of intrinsic information contained within expressing cells.

rtPCR confirmed that expression levels of *EMX2* and the other members of the subset of genes tested in cultures (Figure 6.5) showed similar posterior / anterior differences as detected by Affymetrix chip analysis (Ip et al., 2010a) and rtPCR (Figure 3.3) using tissue RNAs. Robust and consistent anterior > posterior levels of *PCDH17, CTIP2, S100A10, CNTNAP2* and *ROBO1* were detected, whereas levels of *COUPTFI, EMX2* and *FGFR3* were found to be posterior > anterior (Figure 6.5).

6.4.3 The Applications of Human in-vitro Regionalisation Model

Differences in expression between human and rodent genes are mirrored in the cell culture model presented here. Examples include detection of EMX2 expression in differentiated neuronal cells (Figure 6.3), and lack of an observable *PAX6*/PAX6 gradient (Figure 6.3, Figure 6.5). These findings highlight the usefulness of this culture system as a model of regionalisation in humans. In addition to *EMX2*, a number of known regionalisation genes were confirmed clustering posteriorly in this culture system (Figure 6.5). These include *FGFR3,* a gene postulated to be involved in regionalisation but reported to be involved in proliferation of cells and regulation of brain size (Thomson et al., 2007; Inglis-Broadgate et al., 2005). This observation is intriguing as this implies that progenitors or differentiating neurones isolated from the anterior neocortex exhibit a different balance in expression of *FGFRs* (high *FGFR1*, low *FGFR3*) than those from the posterior neocortex (high *FGFR2/ 3*), which could lead to differential signalling activity (Fortin et al., 2005). Thus FGF8, a signalling molecule released from an anterior signalling centre and a high affinity ligand for FGFR3, and FGF2, with a more widespread expression patterns throughout the CNS but a high affinity ligand for FGFR1, could potentially activate different signalling pathways in anterior compared to posterior neocortices. Therefore this *in-vitro* model initiated from anteriorly- and posteriorly-derived neocortical cells has provided two separate systems which allow identification of putative differences in cell-signalling between these populations of cells as well as downstream effects such as proliferation vs. differentiation and differential expression of genes.

The preliminary study of FGFs signalling in regulation of corticofugal neurone-associated genes and FGFRs genes yields interesting observations. For instance, differential regulation of these genes was observed in which *CTIP2* and *SRGAP1* expression was generally down-regulated anteriorly and posteriorly, whereas *ROBO1* expression was only up-regulated regionally after FGF2 and FGF8 stimulation (Figure 6.8, Figure 6.9). Similarly, expression of *FGFR1* was generally up-regulated and *FGFR2* was down-regulated both anteriorly and posteriorly, while changes of *FGFR3* expression varied after FGF2 and FGF8 stimulation (Figure 6.10, Figure 6.11). However due to time constraint, there are caveats regarding this set of experiments. Cell cultures subjected to FGFs stimulation in the presence or absence of MEK inhibitor were initiated from 3 neocortices aged 10, 11 and 12 PCW, and results obtained from each sample were averaged and graphically presented. Large error bars in graphs and

the lack of statistical significance indicate an inconsistency within a given data set, which is potentially due to the sample used. The clustering study and principal component analysis conducted previously have revealed the gestational age is a variable factor affecting total gene expression between samples, and that samples aged 8 and 12.5 PCW exhibited more variability as compared to samples aged 9-11 PCW (Figure 1.13). As this is potentially reflecting a developmental switch occurring at 8 and 12.5 PCW, different regulatory machineries may be taking place and results in different levels of gene expression as compared to samples aged 9-11 PCW. Thus the data obtained in the current studies on the basis of 3 samples of different ages could potentially be skewed by the least-related 12 PCW aged sample. Furthermore, the small sample size at each age (n=1) also limited the use of two-way ANOVA statistical test to allow for the covariate of sample ages. Ideally, at least 3 samples of each age should be used in order to acquire data with more consistent patterns, and two-way ANOVA should be performed instead of a Student's paired *t*-test. Although the data obtained by far might not be showing significant changes of gene expression after different types of stimulations, it nevertheless gives a preview of the changing trends and allows initial prediction and speculation of the regulatory mechanisms of gene expression involved.

The roles of Fgf2 in controlling proliferation and differentiation of neocortical neural progenitors(Li and DiCicco-Bloom, 2004; Raballo et al., 2000; Vaccarino et al., 1999; Qian et al., 1997; McFarlane et al., 1995; Murphy et al., 1994; Murphy et al., 1990a; Murphy et al., 1990b) and Fgf8 in patterning of the developing brain (Crossley et al., 2001; Fukuchi-Shimogori and Grove, 2001) have been widely studied. Interestingly, it is demonstrated that the Fgf2-induced proliferation of glial cells cultured from rat neocortices is activated predominantly via the MAPK signalling pathway and upon inhibition of the MAPK signalling cascade or cAMP stimulation, inhibition of the cAMP response element-binding (CREB) pathway is released, leading to the functional differentiation of cells (Figiel et al., 2003; Bayatti and Engele, 2001). As CTIP2 and potentially SRGAP1 are not expressed by GFAP- and/or Nestin-immunoreactive cells (Figure 6.2), the down-regulation of *CTIP2* and *SRGAP1* expression observed after FGF2 and FGF8 stimulation (Figure 6.8, Figure 6.9) has initially prompted us to speculate an induction of proliferation of GFAP- and/or Nestin-positive progenitor cells, which probably out-number the MAP2-positive differentiating cells and reduce the proportion of these MAP2-positive differentiating cells expressing *CTIP2* and/or

SRGAP in the neocortical cultures. However, this might be unlikely as our culture system is dominated by MAP2-positive differentiating cells (~80%), the overlapping population of GFAP- and Nestin-expressing proliferating cells are of minority (~20%) (Figure 6.1). Furthermore, an up-regulation of *ROBO1* expression is detected after stimulation of FGF2 (Figure 6.8). This observation suggests that the down-regulation of *CTIP2* or *SRGAP1* expression could not be simply due to an increase in the number of proliferating cells that do not express these genes, given that ROBO1 remained to be solely expressed by post-mitotic cells *in-vitro*. The treatment of cells with FGFs in the presence of the MEK inhibitor U0126 thus serves two purposes: to direct the downstream signalling cascade towards the CREB pathway that leads to differentiation rather than proliferation of cells and to determine whether the FGFs-induced changes in gene expression is dependent on the MAPK signalling. Yet it is necessary to determine the ratio of proliferating to differentiating cells in the cultures after various stimulations such as counting GFAP- and/or Nestin- vs. MAP2-immunostained cells at protein level, performing rtPCR to examine *GFAP*, *Nestin* and *MAP2* expression at RNA level and methylthiazol tetrazolium (MTT) cell proliferation assay. Furthermore, the co-localization of CTIP2/ROBO1/SRGAP1 with markers such as GFAP, Nestin and MAP2 via immunocytochemistry requires more thorough investigation to confirm the type of cells (e.g. proliferative vs. differentiative; neuronal vs. glial) expressing these corticofugal neurone-associated markers.

The preliminary data thus far has revealed a differential down- and up-regulation of *CTIP2*/*SRGAP1* and *ROBO1* expression (Figure 6.8, Figure 6.9). Although they are all implicated in the development of corticofugal projection neurones, by nature they are different molecules (transcription factor vs. signalling molecule vs. cell adhesion molecule) and so is not surprising that their expression might not be regulated the same way. Additionally, our data have shown that cells expressing CTIP2 do not exclusively co-express ROBO1 or SRGAP1 both *in-situ* (Figure 5.6) and *in-vitro* (Figure 6.2), and that the callosal projection neurones expressing SATB2 are found to co-express ROBO1 within Layer V (Figure 5.7). It is worth looking into the expression of SATB2 in relation to ROBO1 and CTIP2 before and after various treatments at RNA and protein level. Nevertheless the down-regulation of *CTIP2* expression after FGF8 stimulation (Figure 6.9) is somewhat unexpected. This is because *Fgf8* is known to inhibit the expression of the posterior marker *CouptfI* (Borello et al., 2008; Storm et al., 2006;

Garel et al., 2003), which represses the expression of *Ctip2* in Layer VI of the sensory areas in the mice neocortices (Tomassy et al., 2010). Thus the treatment with FGF8 should theoretically down-regulate *COUPTFI* expression as observed in the *Fgf8*$^{null/neo}$ hypomorph (Borello et al., 2008) and release the repression of *CTIP2* expression in the cultured cells. Nevertheless, the *FGF8*-mediated down-regulation of *COUPTFI* expression is probably only occurring before neocorticogenesis begins as the regionalized expression of *FGF8* in the ANR is down-regulated while its expression in the diencephalon and at the mesencephalic-rhombencephalic boundary remains strong at a relative early stage of development in humans (around CS20; 7 PCW; Subrot Sarma, unpublished data). It would be useful to probe the expression of *COUPTFI* after various treatments of cells and compared with the expression of *CTIP2*.

The additional roles of Fgf2 and Fgf8 in regulating the growth and guidance of axons in various systems have also been studied more recently. In particular, Fgf2 is able to induce functional recovery from neonatal motor cortex injury in rats, probably by re-establishing the corticospinal tract with the re-growth of neocortical cells in the lesioned region of the motor cortex and outgrowth of fibre projection towards the cervical spinal cord (Monfils et al., 2008), as Fgf2 signalling has been demonstrated to promote the growth and sprouting of axons and sustain the required cues for the guidance of axons to reach their targets (Ramirez et al., 1999; Kawamata et al., 1997; Mahler et al., 1997; McFarlane et al., 1995). Whereas Fgf8 regulates the anteriorly-directed growth of midbrain dopaminergic axons at the midbrain-hindbrain boundary by inducing expression of axon guidance molecules such as sema3F (Yamauchi et al., 2009). Likewise, a microarray analysis studying the transcriptional targets of FGF signalling has revealed *EphA2* and *A4* receptors, which play a role in axonal guidance, are positively regulated via FGF signalling during early development of *Xenopus laevis* (Branney et al., 2009). Thus it is not surprising to observe an up-regulation of *ROBO1* expression after FGF2 and FGF8 stimulations in our neocortical cultures (Figure 6.8, Figure 6.9). However what causes the differential up-regulation of *ROBO1* expression posteriorly after FGF2 stimulation (Figure 6.8) and anteriorly after FGF8 stimulation in the presence of U0126 (Figure 6.9) is not known.

The differential regulation of *FGFRs* expression by their high affinity ligands (Figure 6.10, Figure 6.11) has also been observed by other research groups within different

cellular contexts. In a rat primary cortical culture enriched with cells along the oligodendrocyte lineage, exogenous Fgf2 up-regulates the expression of *Fgfr1* in early oligodendrocyte progenitors, but down-regulates *Fgfr2* expression in mature oligodendrocytes, whereas the regulation of *Fgfr3* expression is independent of the exogenous Fgf2 (Bansal et al., 1996). A more recent study that has employed three murine cell lines with different lineages shows the expression of *Fgfrs* are differentially regulated by Fgf8 within the same and among different cell types (Mott et al., 2010). For instance *Fgfr1* expression is up-regulated in fibroblast-derived 3T3 cells and neuroendocrine GT1-7 cells, whereas expression of *Fgfr3* is down-regulated in hippocampal neuronal HT-22 cells and GT1-7 cells following Fgf8 stimulation (Mott et al., 2010). Together, the differential regulation of *FGFRs* expression detected by our groups (Figure 6.10, Figure 6.11) and others might suggest that these FGFRs are subserving different cell-specific biological functions. The up-regulation of *FGFR1* expression induced by exogenous FGF2 and FGF8 appears to be a consistent phenomenon observed by others and in our neocortical culture (Figure 6.10, Figure 6.11). A positive feedback mechanism is probably in place in which exogenous FGF2 causes newly-synthesized or internalized FGFR1 to accumulate inside the nuclei of developing neurones and glial cells and the nuclei-localized FGFR1 acts as transcriptional activator to potentially activate the transcription of other genes as well as itself, thereby increasing the synthesis of FGFR1 (Stachowiak et al., 2007; Maher, 1996). The localization and accumulation of FGFR2 and FGFR3 within the nuclei has also been found which associates with the development of other cell types such as osteoblasts and Sertoli cells within the gonad (Stachowiak et al., 2007; Marchetti et al., 2006; Sabbieti et al., 2005; Schmahl et al., 2004; Johnston et al., 1995).

The preliminary data presented here showing differential regulation of corticofugal neurone-associated genes expression by FGFs signalling (Figure 6.8, Figure 6.9) implicates that FGFs alone might not be sufficient to induce the growth or differentiation of corticofugal neurones in our neocortical cultures. Indeed, there are other potential regulators including transcription factors such as *Sp8* (Zembrzycki et al., 2007), *Pax6* (Clegg et al., 2010; Lopez-Bendito et al., 2007; Jones et al., 2002) and *CouptfI* (Tomassy et al., 2010) in which the expression of *Robo1* and *Ctip2* is reduced in their absence in rodent studies. The knock-down of *SP8, PAX6, COUPTFI* as well as other potential transcription factor genes in our *in-vitro* regionalisation model could be

carried out in order to study their role in regulating the expression of corticofugal neurone-related genes. Yet the culture system used in the current study contains a mixed population of cells and that changes in gene expression in a particular cell type after FGFs stimulation could potentially be masked. Thus combination of other *in-vitro* approaches such as purifying specific sub-populations of developing neocortical cells (e.g. radial glia) in culture (Mo and Zecevic, 2008; Mo et al., 2007) and subsequent stimulation of cells with FGFs or other factors would allow the tracking of gene expression changes in isolated populations of cells. The ultimate aim is to identify factors that are required to induce the expression of various corticofugal neurone-related genes, and induce the differentiation of pluripotent stem cells (e.g. human umbilical cord blood-derived stem cells) into corticofugal projection neurones which could potentially be used therapeutically.

Chapter 7 General Discussion and Future Work

7.1 Conclusion

In conclusion, the current project has confirmed the graded expression of a subset of putative anterior and posterior markers in the developing human neocortex aged between 8-12 PCW, including a number of transcription factors, cell adhesion and axonal guidance molecules and growth factor receptors.

Importantly, the discovery of some corticofugal projection neurone-associated genes and/or proteins (*CTIP2*, *ROBO1* and *SRGAP1*) being highly up-regulated anteriorly might mark the site of the emerging human motor cortex, which is the predominant origin of corticofugal projection neurones such as corticospinal and corticopontine projection neurones. Since the motor cortex and the corticospinal tract are common sites of developmental brain damage leading to cerebral palsy (Eyre, 2007), the identification of regulated corticofugal projection neurone-related markers and localization of the developmental origin of the above corticofugal projection neurones are crucial in order to promote mechanisms that facilitate the replacement or repair of these neurones in the affected regions.

This project has also established and characterized the dissociated human cell cultures from anteriorly- and posteriorly-derived foetal neocortex to be used as a human *in-vitro* model of regionalisation. The establishment of this model has provided a valuable tool to investigate the regulation of various genes. In particular, the identification of regulatory mechanisms of corticofugal projection neurone-associated genes would guide potential future approaches targeting to stimulate population of endogenous stem cells or those from other source to differentiate into a corticofugal neurone phenotype, which could potentially be applied therapeutically to improve functional outcomes of patients suffering from motor disorders such as cerebral palsy.

7.2 Implications of Regionalised Gene Expression during Human Neocorticogenesis

7.2.1 Age-Dependent Regulation of Regionalised Gene Expression

During early stages of neurogenesis in rodents, genes that control the establishment of the early cortical map are presumed to be expressed in gradients across the tangential dimension of the developing neocortex (Cecchi and Boncinelli, 2000). Similarly, Affymetrix chip analysis and rtPCR reveals robust consistent gradients of gene expression in 8-12.5 PCW aged human neocortical tissues in the current study. The selected ages for investigation represent early stages of corticogenesis when the intrinsic information carried by the neocortical progenitors are being passed onto their progenies (e.g. *EMX2*/EMX2 expressed by both neocortical progenitors as well as post-mitotic neurones; (Bayatti et al., 2008b)) as the CP begins to form (7.5 PCW; (Meyer et al., 2000)), but their molecular identities are not yet under the influence of extrinsic factors that are potentially brought forward via the incoming thalamocortical afferents (Kostovic and Rakic, 1990). In humans, the intrinsic information carried in a form of graded or regionalised gene expression is probably regulated by different developmental mechanisms prior to, or at around 8 PCW, as compared to later ages, evidently supported by the age-dependent clustering of samples (Chapter 3), the down-regulation of *FGF8* expression in the ANR at around CS20/7 PCW (Subrot Sarma, unpublished observation) and the deregulation of high anterolateral/low posteromedial gradient of *PAX6* expression at 9 PCW (Bayatti et al., 2008b), which is otherwise maintained in rodents throughout corticogenesis (Manuel and Price, 2005). It would also be interesting to compare the gene expression between the current samples (8-12.5 PCW) and older samples (>12.5 PCW) to identify expression of genes that are potentially under extrinsic influences via microarray analyses and rtPCR.

7.2.2 PAX6-Independent Anterior Regionalisation

Despite the persistence of *Pax6* gradient in rodents, accumulating evidence argues that this gene is not directly involved in regionalisation processes (Pinon et al., 2008; Manuel et al., 2007), as neocortical identities indicated by the distribution of area-specific thalamocortical and corticofugal projections are maintained in conditional *Pax6* knock-out mutants, and the inability of *Pax6* over-expression to alter the expression of Emx2 or other areal markers. In contrast, over-expression of *Emx2* shifts the position and increases the size of primary areas located posteriorly when compared to anterior structures (Hamasaki et al., 2004). Therefore all neocortical progenitors are proposed to carry intrinsic information that impart posterior regional identities by-default such as expressing reported regionalisation genes *EMX2, COUPTFI* and *FGFR3,* in which their expression is repressed by secreted ligands such as FGF8, -15 and -17 released from signalling centres located anteriorly (Rakic et al., 2009; O'Leary et al., 2007; O'Leary and Nakagawa, 2002), and/or by as yet undiscovered, anteriorly up-regulated regionalisation genes that are essential for specification of the anterior neocortex (Rakic et al., 2009).

The identified anteriorly up-regulated genes include *CNTNAP2,* a frontal cortex marker (Abrahams et al., 2007), *PCDH17,* an areal marker corresponding to the motor cortex in rodents (Kim et al., 2007), *CTIP2* and *S100A10,* Layer V markers for early corticospinal neurones development in rodents (Arlotta et al., 2005), *ROBO1,* gene encoding axon guidance molecule that is expressed in the corticospinal fibres before, during and after crossing the midline in the caudal medulla in rodents (Sundaresan et al., 2004), and *SRGAP1,* the downstream signalling molecule of ROBO1 (Wong et al., 2001). However, it is important to distinguish whether these genes are regionalisation genes that are expressed by progenitor cells or areal genes expressed by post-mitotic neurones in the developing CP and regulated by regionalisation genes to induce their graded expression patterns (O'Leary et al., 2007). More thorough investigation is therefore required to localize their expression on human neocortical tissues spatially and temporally via tissue *in-situ* hybridization and immunohistochemistry to classify them as regionalisation or areal genes.

7.2.3 Anterior Clustering of Corticofugal Neurone-associated Genes

Among the identified genes up-regulated anteriorly, the laminar and cellular expression of CTIP2, ROBO1 and SRGAP1, which are shown to be important in the development of corticofugal projection neurones, were examined on human neocortical tissues. Although their expression was detected in the proliferative SVZ, an elaborate transient layer constituting a heterogeneous population of cells in humans (Bayatti et al., 2008a), they were shown to be expressed by post-mitotic neurones. Thus they are not regionalisation genes that specify progenitors to become corticofugal projection neurones, rather they are areal genes that clustered at the anterior neocortex relatively early in cortical development, potentially marking the primitive site of origin of the later developing motor cortex and/or corticofugal neurones at a similar location of the motor cortex observed in rodents (O'Leary and Nakagawa, 2002). The adult human motor cortex is not found to be predominantly located towards the anterior pole of the neocortex as it is in rodents. This may be due to the prefrontal cortex, a much larger structure in humans compared to the rodent brains, starts to expand during later stages of development (Fuster, 2002) resulting in its adult position being in the centre and anterior to the central sulcus. Tissue ISH and IHC demonstrating the localization of genes and proteins that delineate the motor and prefrontal cortex at later stages would potentially reveal the developmental relationship between the two neocortical areas in humans.

The anterior up-regulation of these corticofugal neurone-associated genes has further implications on the development of various corticofugal projection neurones originating from different neocortical areas:

1) It may potentially be highlighting a much higher proportion of corticofugal neurones generated from the frontal/motor areas as compared to the occipital cortex as observed in adult macaque (Lock et al., 2003; Galea and Darian-Smith, 1994; Glickstein et al., 1985). It would be useful to retrogradely trace these different projection neurones from their terminals and identify the proportions of various neocortical origins by DiI tracing studies or diffusion tensor imaging tractography in human tissues if possible.

2) It may also be showing the importance of ROBO1, SRGAP1 and CTIP2 in the growth and maintenance of the corticospinal axons beyond the pons and across the medullary decussation (Lopez-Bendito et al., 2007; Arlotta et al., 2005), in comparison to the other major subcerebral cortical projections that terminate, in maturity, ipsilaterally in the midbrain and pons. Additionally, regionalised expression of specific cell-cell signalling molecules such as ROBO1/SRGAP1 may protect corticospinal axons from retraction from the spinal cord and promote their removal from inappropriate target areas, in a similar way as arealized expression of Plexin 3A and -4A in the rodent visual cortex that promotes pruning of their corticospinal projections and protection of appropriate projections to the superior colliculus (Low et al., 2008). If achievable, explant cultures initiated from sagittally dissected human brain tissue that retain all of the corticofugal projection tracts in combination with RNA interference (siRNA) of *CTIP2/ROBO1/SRGAP1* and DiI tracing would potentially reveal the importance of the three genes in maintaining appropriate corticofugal axonal projections during development.

7.3 Ontogenesis of Layer V Pyramidal Neurones in the Developing Human Neocortex

Studies of various gene expression patterns not only provided information regarding the development of neocortical areas, their laminar-specific expression patterns also revealed the formation of cortical layers in the developing human neocortex. In particular, the formation of Layer V is of primary interest as it harbours a heterogeneous population of pyramidal neurones projecting subcerebrally and callosally, expressing some of the markers used in the current project (Molnar and Cheung, 2006). Previous molecular neuroanatomical studies by our group have shown that by 16 PCW, Layer V is visualized by ER81 immunoreactivity in the human neocortex (Bayatti et al., 2008a). The expression of ER81 observed in this project suggested Layer V is already formed by 12 PCW and also strongly expressing SATB2, above the TBR1- and NURR1-positive Layer VI and GAP43-, Synaptophysin-immunoreactive SP in the developing human neocortex.

The spatiotemporal expression of the studied genes and proteins observed in the present project not only delineated the formation of various cortical layers, it potentially reflects the development of pyramidal projection neurones residing in these layers. Within the developing neocortex, a subpopulation of post-mitotic neurones was demonstrated to co-express ROBO1, SRGAP1 and CTIP2, which are related to the corticofugal projection neurones, when the CP is forming at around 10 PCW. At the caudal medulla level, the pyramids containing corticospinal axons were immunoreactive for both ROBO1 and SRGAP1 which was observed as early as 11 PCW, however the decussation of these fibres only took place at around 14 PCW, visualized by prominent ROBO1- and SRGAP1-positive fibres extending to the decussation and beyond. Expression of ROBO1 and SRGAP1 was not restricted to the putative Layer V during its emergence, but only at 15 PCW. Thus the present study have found at least a subset of ROBO1+/SRGAP1+/CTIP2+ corticofugal neurones to be restricted to Layer V by the time that presumptive ROBO1- and SRGAP1- positive corticospinal fibres are crossing the decussation in large numbers.

In addition to the corticofugal projection neurones, Layer V also contains callosal projection neurones expressing markers such as SATB2. As corticogenesis begins, SATB2-positive cells were sparsely distributed in the SVZ, whereas CTIP2 was already abundantly expressed by post-mitotic neurones in both the SVZ and CP. This might be suggesting that although some SATB2-expressing neurones are destined to occupy Layer V alongside CTIP2-expressing neurones, the callosal projection neurones are probably generated later than subcerebral projection neurones. Alternatively, it might be due to some differential regulatory machineries causing SATB2 expression to be switched on later than CTIP2, for instance the repression and promotion of SATB2 and CTIP2 expression respectively by their upstream gene *FEZF2*, which is under the repression of *SOX5* further upstream of *FEZF2*. Further investigation is required to study the expression of SATB2 such as rtPCR and cell counting of immunostained cells to confirm the high anterior - low posterior expression across the developing neocortex at RNA and protein levels. Co-localization studies of SATB2 with TBR2 (INPs markers) or TBR1 (early post-mitotic neuronal markers) are necessary to identify the types of cells expressing SATB2 within the heterogeneous SVZ.

7.4 Characterization and Application of the Human *in-vitro* Regionalisation Model

Important differences between human and rodent gene expression patterns and localization have been identified previously (Bayatti et al., 2008b; Bayatti et al., 2008a), thus highlighting the insufficiency of animal models for human studies. Human model systems are therefore necessary and important to allow the manipulation of human gene expression. Dissociated cultures from human neocortical tissue were dissected from the anterior and posterior poles of 11 PCW neocortices and cells were maintained in a differentiation-inducing medium. After 3DIV, the anteriorly- and posteriorly-derived cells showed no difference in differentiation processes and the vast majority of them became immunoreactive for the neuronal marker, MAP2, whereas GFAP- and Nestin-positive cells were also detected suggesting radial glia/astrocytes and other progenitors were also present. Further characterization of these cells indicated their intrinsic molecular identities were maintained after 3 DIV, as shown by the co-expression of CTIP2, ROBO1 and SRGAP1 as well as the expression of CTIP2 and EMX2 in post-mitotic neurones. In addition, rtPCR and cell counting of immunoreactive cells confirmed these cultured cells also maintained their intrinsic regional identities by displaying similar graded expression of genes and proteins after 3 DIV.

The differential expression of FGFRs is intriguing as this implicates that progenitors or differentiating neurones isolated from the anterior neocortex exhibit a different balance in expression of *FGFRs* (high *FGFR1*, low *FGFR3*) than those from the posterior neocortex (high *FGFR2/3*), which could lead to differential signalling activity (Fortin et al., 2005). Therefore, a preliminary study was carried out to investigate the gene expression regulation by FGF signalling. FGF2 and FGF8, high affinity ligands for FGFR1 and FGFR3 respectively, were applied to two separate systems initiated from the anteriorly- and posteriorly-derived neocortical cells in the presence or absence of MEK inhibitor to show a dependence or independence of MAPK signalling cascade to regulate gene expression.

Differential regulation of corticofugal neurone-associated genes and FGFRs genes was observed in which *CTIP2* and *SRGAP1* expression was generally down-regulated

anteriorly and posteriorly, whereas *ROBO1* expression was only up-regulated regionally after FGF2 and FGF8 stimulation. Although they are all implicated in the development of corticofugal projection neurones, it should not be surprising that genes encoding for transcription factor (*CTIP2*), signalling molecule (*SRGAP1*) and cell adhesion molecule (*ROBO1*) are regulated differentially. Additionally, ROBO1 has been implicated in mediating axon guidance of other neuronal subtypes in addition to corticofugal projection neurones, such as the callosal projection neurones expressing SATB2. Nevertheless the down-regulation of *CTIP2* expression after FGF8 stimulation is somewhat unexpected. This is because *Fgf8* is known to inhibit the expression of the posterior marker *CouptfI* (Borello et al., 2008; Storm et al., 2006; Garel et al., 2003), which represses the expression of *Ctip2* in Layer VI of the sensory areas in the mice (Tomassy et al., 2010). Thus the treatment with FGF8 should theoretically down-regulate *COUPTFI* expression and release the repression of *CTIP2* expression in the cultured cells. Yet, the *FGF8*-mediated down-regulation of *COUPTFI* expression is probably only occurring before neocorticogenesis begins as the regionalised expression of *FGF8* in the ANR is weakened at a relative early stage of development in humans (around CS20; 7 PCW) while its expression in the diencephalon and at the mesencephalic-rhombencephalic boundary remains strong (Subrot Sarma, unpublished observation). On the other hand, the up-regulation of *ROBO1* expression observed after FGF2 and FGF8 stimulation in our neocortical cultures might suggest roles for FGF2 and FGF8 in regulating the growth and guidance of axons as well as sustaining the expression of guidance cues as proposed by other researchers (Branney et al., 2009; Yamauchi et al., 2009; Monfils et al., 2008; Ramirez et al., 1999; Kawamata et al., 1997; Mahler et al., 1997; McFarlane et al., 1995).

Similarly, expression of *FGFR1* was generally up-regulated and *FGFR2* was down-regulated both anteriorly and posteriorly, while changes of *FGFR3* expression varied after FGF2 and FGF8 stimulation. The differential regulation of *FGFRs* expression by their high affinity ligands has also been observed by other research groups in primary cortical cultures (Bansal et al., 1996) as well as in various cell lines (Mott et al., 2010), potentially suggesting that these FGFRs are subserving different cell-specific biological functions. The up-regulation of *FGFR1* expression induced by exogenous FGF2 and FGF8 appears to be a consistent phenomenon observed by others and in our neocortical culture. A positive feedback mechanism is probably in place in which exogenous FGF2

causes newly-synthesized or internalized FGFR1 to accumulate inside the nuclei of developing neurones and glial cells that potentially activates the transcription of other genes as well as itself, thereby increasing the synthesis of FGFR1 (Stachowiak et al., 2007; Maher, 1996). The localization and accumulation of FGFR2 and FGFR3 within the nuclei has also been found associating with the development of other cell types (Stachowiak et al., 2007; Marchetti et al., 2006; Sabbieti et al., 2005; Schmahl et al., 2004; Johnston et al., 1995).

7.5 Further Investigation of Gene Expression Regulation

Despite the interesting changes in gene expression observed preliminarily after various treatments, there were caveats in the pilot study of FGF signalling in regulation of gene expression. Due to the limited time and availability of samples, cell cultures subjected to FGFs stimulation in the presence or absence of MEK inhibitor were initiated from 3 neocortices aged 10, 11 and 12 PCW. However, data obtained from the three samples of various ages have shown large deviation and lack of statistical significances. The clustering studies conducted previously have revealed that samples aged 8 and 12.5 PCW exhibited more variability as compared to samples aged 9-11 PCW (Chapter 3). Thus the data obtained in the current studies on the basis of 3 samples of different ages could potentially be skewed by the least-related 12 PCW aged sample. Further experiments should be carried out with at least 3 samples of each selected age in order to acquire data with more consistent patterns.

It is demonstrated that the Fgf2-induced proliferation of glial cells cultured from rat neocortices is activated predominantly via the MAPK signalling pathway and upon inhibition of the MAPK signalling cascade or cAMP stimulation, the inhibition of CREB pathway is released, leading to the functional differentiation of cells (Figiel et al., 2003; Bayatti and Engele, 2001). As genes such as *CTIP2*, *ROBO1* and *SRGAP1* are potentially expressed by post-mitotic neurones exclusively, it is necessary to determine the effects of proliferation and differentiation of cells after various treatments. This is because drastic changes in the proportion of proliferating and differentiating cells would potentially masked the actual effects of FGFs on expression of genes of interest. This could be achieved by counting GFAP and/or Nestin vs. MAP2-immunostained cells at protein level, performing rtPCR to examine *GFAP*, *Nestin* and *MAP2* expression at RNA level, or with a MTT cell proliferation assay. Furthermore, the co-localization of CTIP2/ROBO1/SRGAP1 with markers such as GFAP, Nestin and MAP2 via immunocytochemistry requires more thorough investigation to confirm the type of cells (e.g. proliferative vs. differentiative; neuronal vs. glial) expressing the corticofugal neurone-associated proteins.

The inhibition of MAPK signalling pathway requires further attention and confirmation which involves the use of non-phosphorylated and phospho-specific antibodies to p42/p44 (ERK1/2), downstream MAPKs of MEK, to reveal the ratio of non-activated and MAPK-activated cells after various treatments. Additionally, double-labelling of cells with markers such as GFAP, Nestin and β–Tubulin (in replacement of MAP2) with non-phospho and phospho-p42/p44 would identify the types of cells that are affected after different treatments. It is also necessary to investigate the involvement of additional downstream signalling pathways using various phospho-specific antibodies such as CREB, AKT and PKC or by FGF signal transduction pathway-focused arrays.

The preliminary data obtained currently showed differential regulation of corticofugal neurone-associated genes expression by FGFs signalling. This implicates that FGFs alone might not be sufficient to induce the growth or differentiation of corticofugal neurones in our neocortical cultures. Transcription factors such as *Sp8* (Zembrzycki et al., 2007), *Pax6* (Clegg et al., 2010; Lopez-Bendito et al., 2007; Jones et al., 2002) and *CouptfI* (Tomassy et al., 2010) have been shown to affect the expression of *Robo1* and *Ctip2* in rodent knock-out studies. Utilizing our in-vitro regionalisation model, the regulation of corticofugal neurone-related genes expression by various transcription factors would be achievable by knocking-down *SP8*, *PAX6*, *COUPTFI* as well as other potential transcription factor genes. Nonetheless the culture system used in the current study contains a heterogeneous population of cells and that changes in gene expression in a particular cell type after FGFs stimulation could potentially be masked. Thus combination of other *in-vitro* approaches such as purifying specific sub-populations of developing neocortical cells (e.g. radial glia) in culture (Mo and Zecevic, 2008; Mo et al., 2007) and subsequent stimulation of cells with FGFs or other factors would allow the tracking of gene expression changes in isolated populations of cells. The ultimate aim is to identify factors that are required to induce the expression of various corticofugal neurone-related genes, and induce the differentiation of pluripotent stem cells (e.g. human umbilical cord blood-derived stem cells) into corticofugal projection neurones which could potentially be used therapeutically.

Appendix

Accession	Description	Max Score	Total Score	Query Coverage	E-Value	Sequence Homology
NP_001139317.1	roundabout 1 isoform d [Homo sapiens]	44.8	58.5	100%	3e-05	Query 1 VLGGYERGEDNNE 13 VLGGYERGEDNNE Sbjct 1532 VLGGYERGEDNNE 1544 Query 5 YERG 8 Y+RG Sbjct 904 YQRG 907
NP_001139316.1	roundabout 1 isoform c [Homo sapiens] >gb|AAI57862.1| ROBO1 protein [Homo sapiens] >gb|AAI71855.1| ROBO1 protein [Homo sapiens]	44.8	58.5	100%	3e-05	Query 1 VLGGYERGEDNNE 13 VLGGYERGEDNNE Sbjct 1587 VLGGYERGEDNNE 1599
EAW68887.1	roundabout, axon guidance receptor, homolog 1 (Drosophila), isoform CRA_c [Homo sapiens]	44.8	58.5	100%	3e-05	Query 1 VLGGYERGEDNNE 13 VLGGYERGEDNNE Sbjct 1513 VLGGYERGEDNNE 1525
EAW68888.1	roundabout, axon guidance receptor, homolog 1 (Drosophila), isoform CRA_d [Homo sapiens]	44.8	58.5	100%	3e-05	Query 1 VLGGYERGEDNNE 13 VLGGYERGEDNNE Sbjct 1512 VLGGYERGEDNNE 1524
AAI15023.1	ROBO1 protein [Homo sapiens]	44.8	58.5	100%	3e-05	Query 1 VLGGYERGEDNNE 13 VLGGYERGEDNNE Sbjct 1532 VLGGYERGEDNNE 1544 Query 5 YERG 8 Y+RG

						Sbjct 904 YQRG 907 Query 1 VLGGYERGEDNNE 13 VLGGYERGEDNNE Sbjct 1587 VLGGYERGEDNNE 1599 Query 5 YERG 8 Y+RG Sbjct 904 YQRG 907
AAI15021.1	ROBO1 protein [Homo sapiens]	44.8	58.5	100%	3e-05	
XP_941372.3	PREDICTED: similar to roundabout 1 isoform 2 [Homo sapiens]	44.8	72.8	100%	3e-05	Query 1 VLGGYERGEDNNE 13 VLGGYERGEDNNE Sbjct 1596 VLGGYERGEDNNE 1608 Query 1 VLGG 4 VLGG Sbjct 1498 VLGG 1501
AAH01969.1	Similar to roundabout (axon guidance receptor, Drosophila) homolog 1 [Homo sapiens]	44.8	44.8	100%	3e-05	Query 1 VLGGYERGEDNNE 13 VLGGYERGEDNNE Sbjct 475 VLGGYERGEDNNE 487
AAI12337.1	ROBO1 protein [Homo sapiens]	44.8	58.5	100%	3e-05	Query 1 VLGGYERGEDNNE 13 VLGGYERGEDNNE Sbjct 1588 VLGGYERGEDNNE 1600 Query 5 YERG 8 Y+RG Sbjct 904 YQRG 907
NP_598334.1	roundabout 1 isoform b [Homo sapiens] >gb|EAW68884.1| roundabout, axon guidance receptor, homolog 1 (Drosophila), isoform CRA_a [Homo sapiens] >gb|EAW68885.1| roundabout, axon guidance receptor,	44.8	58.5	100%	3e-05	Query 1 VLGGYERGEDNNE 13 VLGGYERGEDNNE Sbjct 1593 VLGGYERGEDNNE 1605

	homolog 1 (Drosophila), isoform CRA_a [Homo sapiens]					Query 5 YERG 8 Y+RG Sbjct 910 YQRG 913
CAD98093.1	hypothetical protein [Homo sapiens] GENE ID: 6091 ROBO1 | roundabout, axon guidance receptor, homolog 1 (Drosophila) [Homo sapiens]	44.8	58.5	100%	3e-05	Query 1 VLGGYERGEDNNE 13 VLGGYERGEDNNE Sbjct 1271 VLGGYERGEDNNE 1283 Query 5 YERG 8 Y+RG Sbjct 588 YQRG 591
NP_002932.1	roundabout 1 isoform a [Homo sapiens] >sp|Q9Y6N7.1|ROBO1_HUMAN RecName: Full=Roundabout homolog 1; AltName: Full=H-Robo-1; AltName: Full=Deleted in U twenty twenty; Flags: Precursor >gb|AAC39575.1| roundabout 1 [Homo sapiens]	44.8	58.5	100%	3e-05	Query 1 VLGGYERGEDNNE 13 VLGGYERGEDNNE Sbjct 1632 VLGGYERGEDNNE 1644 Query 5 YERGEDNN 12 YER EDNN Sbjct 114 YERDEDNN 121
2V53-A	Chain A, Crystal Structure Of A Sparc-Collagen Complex	26.5	26.5	61%	8.5	Query 5 YERGEDNN 12 YER EDNN Sbjct 88 YERDEDNN 95
BAG61416.1	highly similar to secreted protein, acidic and rich in cysteine, SPARC (Osteonectin) [Homo sapiens]	26.5	26.5	61%	8.5	Query 5 YERGEDNN 12 YER EDNN Sbjct 88 YERDEDNN 95
BAG37963.1	highly similar to secreted protein, acidic and rich in cysteine, SPARC (Osteonectin) [Homo sapiens]	26.5	26.5	61%	8.5	Query 5 YERGEDNN 12 YER EDNN Sbjct 179 YERDEDNN 186
EAW61667.1	secreted protein, acidic, cysteine-rich (Osteonectin), isoform CRA_a [Homo sapiens] >gb|EAW61671.1|	26.5	26.5	61%	8.5	Query 5 YERGEDNN 12

	secreted protein, acidic, cysteine-rich (Osteonectin), isoform CRA_a [Homo sapiens]					YER EDNN Sbjct 191 YERDEDNN 198
AAS50152.1	cysteine-rich protein (SPARC) [Homo sapiens]	26.5	26.5	61%	8.5	Query 5 YERGEDNN 12 YER EDNN Sbjct 31 YERDEDNN 38
AAA60993.1	osteonectin [Homo sapiens]	26.5	26.5	61%	8.5	Query 5 YERGEDNN 12 YER EDNN Sbjct 178 YERDEDNN 185
1BMO-A	Chain A, Bm-40, FsEC DOMAIN PAIR >pdb|1BMO|B Chain B, Bm-40, FsEC DOMAIN PAIR	26.5	26.5	61%	8.5	Query 5 YERGEDNN 12 YER EDNN Sbjct 109 YERDEDNN 116
1NUB-A	Chain A, Helix C Deletion Mutant Of Bm-40 Fs-Ec Domain Pair >pdb|1NUB|B Chain B, Helix C Deletion Mutant Of Bm-40 Fs-Ec Domain Pair	26.5	26.5	61%	8.5	Query 5 YERGEDNN 12 YER EDNN Sbjct 113 YERDEDNN 120
1SRA-A	Chain A, Structure Of A Novel Extracellular Ca2+-Binding Module In Bm-40(Slash)sparc(Slash)osteonectin	26.5	26.5	61%	8.5	Query 5 YERGEDNN 12 YER EDNN Sbjct 27 YERDEDNN 34
NP_003109.1	secreted protein, acidic, cysteine-rich precursor [Homo sapiens] >sp|P09486.1|SPRC_HUMAN RecName: Full=SPARC; AltName: Full=Secreted protein acidic and rich in cysteine; AltName: Full=Osteonectin; Short=ON; AltName: Full=Basement-membrane protein 40; Short=BM-40; Flags: Precursor >emb|CAA68724.1| unnamed protein product [Homo sapiens] >gb|AAA60570.1| osteonectin [Homo sapiens] >gb|AAH04974.1| Secreted protein, acidic, cysteine-rich (osteonectin) [Homo sapiens] >gb|AAH08011.1| Secreted protein, acidic, cysteine-rich (osteonectin) [Homo sapiens] >gb|AAH72457.1| Secreted protein, acidic, cysteine-rich	26.5	26.5	61%	8.5	Query 5 YERGEDNN 12 YER EDNN Sbjct 179 YERDEDNN 186

	(osteonectin) [Homo sapiens] >emb|CAG33080.1| SPARC [Homo sapiens] >gb|EAW61668.1| secreted protein, acidic, cysteine-rich (osteonectin), isoform CRA_b [Homo sapiens] >gb|EAW61669.1| secreted protein, acidic, cysteine-rich (osteonectin), isoform CRA_b [Homo sapiens] >gb|EAW61670.1| secreted protein, acidic, cysteine-rich (osteonectin), isoform CRA_b [Homo sapiens] >gb|EAW61672.1| secreted protein, acidic, cysteine-rich (osteonectin), isoform CRA_b [Homo sapiens]					
BAG35170.1	highly similar to Chromogranin B, CHGB (Secretogranin 1) [Homo sapiens]	22.7	38.6	61%	120	Query 6 ERGEDNNE 13 ERGED++E Sbjct 177 ERGEDSSE 184 Query 8 GEDNNE 13 GE+ NE Sbjct 549 GEEENE 554
NP_001810.2	chromogranin B precursor [Homo sapiens] >emb|CAB55272.1| chromogranin B (secretogranin 1) [Homo sapiens]	22.7	38.6	61%	120	Query 6 ERGEDNNE 13 ERGED++E Sbjct 177 ERGEDSSE 184 Query 8 GEDNNE 13 GE+ NE Sbjct 549 GEEENE 554
CAC34360.1	chromogranin B (secretogranin 1) [Homo sapiens]	22.7	22.7	61%	120	Query 6 ERGEDNNE 13 ERGED++E Sbjct 157 ERGEDSSE 164
P05060.1	RecName: Full=Secretogranin-1; AltName: Full=Secretogranin I; Short=SgI; AltName: Full=Chromogranin-B; Short=CgB; Contains: RecName: Full=GAWK peptide; Contains: RecName: Full=CCB	22.7	38.6	61%	120	Query 6 ERGEDNNE 13 ERGED++E Sbjct 177 ERGEDSSE 184

	peptide; Flags: Precursor >emb|CAA68271.1| unnamed protein product [Homo sapiens] >gb|AAH00375.1| Chromogranin B (Secretogranin 1) [Homo sapiens] >emb|CAG33007.1| CHGB [Homo sapiens] >gb|EAX10410.1| Chromogranin B (Secretogranin 1) [Homo sapiens]					Query 8 GEDNNE 13 GE+ NE Sbjct 549 GEEENE 554
NP_001157281.1	WD repeat domain 81 isoform 1 [Homo sapiens]	22.3	22.3	92%	161	Query 2 LGGYER-GEDNNE 13 L YER ED NE Sbjct 303 LSAYERPEEDENE 315
BAH13164.1	Ankyrin 2, neuronal, ANK2 [Homo sapiens]	21.8	21.8	61%	216	Query 6 ERGEDNNE 13 E+ EDNNE Sbjct 816 EQSEDNNE 823
BAH11860.1	Ankyrin 2, neuronal, ANK2 [Homo sapiens]	21.8	21.8	61%	216	Query 6 ERGEDNNE 13 E+ EDNNE Sbjct 1041 EQSEDNNE 1048
Q01484.3	RecName: Full=Ankyrin-2; Short=ANK-2; AltName: Full=Brain ankyrin; AltName: Full=Ankyrin-B; AltName: Full=Non-erythroid ankyrin	21.8	21.8	61%	216	Query 6 ERGEDNNE 13 E+ EDNNE Sbjct 3917 EQSEDNNE 3924
NP_001120965.1	Ankyrin 2 isoform 3 [Homo sapiens]	21.8	21.8	61%	216	Query 6 ERGEDNNE 13 E+ EDNNE Sbjct 1856 EQSEDNNE 1863
EAX06288.1	Ankyrin 2, neuronal, isoform CRA_b [Homo sapiens] >gb|EAX06291.1| ankyrin 2, neuronal, isoform CRA_b [Homo sapiens]	21.8	21.8	61%	216	Query 6 ERGEDNNE 13 E+ EDNNE Sbjct 3929 EQSEDNNE 3936
EAX06287.1	Ankyrin 2, neuronal, isoform CRA_a [Homo sapiens] >gb|EAX06292.1| ankyrin 2, neuronal, isoform CRA_a [Homo sapiens]	21.8	21.8	61%	216	Query 6 ERGEDNNE 13 E+ EDNNE Sbjct 1844 EQSEDNNE 1851

AAI25236.1	ANK2 protein [Homo sapiens]	21.8	21.8	61%	216	Query 6 ERGEDNNE 13 E+ EDNNE Sbjct 548 EQSEDNNE 555
AAI25237.1	ANK2 protein [Homo sapiens]	21.8	21.8	61%	216	Query 6 ERGEDNNE 13 E+ EDNNE Sbjct 466 EQSEDNNE 473
NP_001139.3	Ankyrin 2 isoform 1 [Homo sapiens] >gb|EAX06290.1| Ankyrin 2, neuronal, isoform CRA_d [Homo sapiens]	21.8	21.8	61%	216	Query 6 ERGEDNNE 13 E+ EDNNE Sbjct 3950 EQSEDNNE 3957
NP_066187.2	Ankyrin 2 isoform 2 [Homo sapiens] >gb|EAX06289.1| ankyrin 2, neuronal, isoform CRA_c [Homo sapiens]	21.8	21.8	61%	216	Query 6 ERGEDNNE 13 E+ EDNNE Sbjct 1865 EQSEDNNE 1872
CAD97827.1	ANK2 [Homo sapiens]	21.8	21.8	61%	216	Query 6 ERGEDNNE 13 E+ EDNNE Sbjct 1856 EQSEDNNE 1863
CAA40279.2	Ankyrin (brank-2) [Homo sapiens]	21.8	21.8	61%	216	Query 6 ERGEDNNE 13 E+ EDNNE Sbjct 1865 EQSEDNNE 1872
2003319A	Ankyrin B:ISOTYPE=440kD	21.8	21.8	61%	216	Query 6 ERGEDNNE 13 E+ EDNNE Sbjct 3917 EQSEDNNE 3924
NP_001003700.1	Ras responsive element binding protein 1, RREB1, isoform 3 [Homo sapiens]	21.0	36.9	61%	388	Query 6 ERGEDNNE 13 ERGE+++E Sbjct 1368 ERGEEDSE 1375

						Query 7 RGED 10 RGED Sbjct 844 RGED 847
BAG54712.1	NIMA (never in mitosis gene a)- related kinase 9, NEK9 [Homo sapiens]	21.0	21.0	53%	388	Query 1 VLGGYER 7 VLG YER Sbjct 3 VLGEYER 9
Q58DX5.2	RecName: Full=Inactive N-acetylated-alpha-linked acidic dipeptidase-like protein 2; Short=NAALADase L2, NAALADL2	21.0	21.0	61%	388	Query 3 GGYERGED 10 G YE GED Sbjct 505 GSYEWGED 512
BAF84442.1	Arrestin domain-containing protein 3, ARRDC3 [Homo sapiens]	21.0	21.0	76%	388	Query 4 GYERGEDNNE 13 G+ER +DN+E Sbjct 90 GHERDDDNSE 99
NP_996898.2	N-acetylated alpha-linked acidic dipeptidase 2, NAALADL2 [Homo sapiens]	21.0	21.0	61%	388	Query 3 GGYERGED 10 G YE GED Sbjct 505 GSYEWGED 512
AAI31600.1	RREB1 protein [Homo sapiens]	21.0	21.0	61%	388	Query 6 ERGEDNNE 13 ERGE+++E Sbjct 370 ERGEEDSE 377
EAW81084.1	zinc finger, FYVE domain containing 1, ZFYVE1, isoform CRA_a [Homo sapiens]	21.0	21.0	46%	388	Query 5 YERGED 10 YERGE+ Sbjct 476 YERGEE 481
EAW81221.1	NIMA (never in mitosis gene a)- related kinase 9, NEK9, isoform CRA_b [Homo sapiens]	21.0	21.0	53%	388	Query 1 VLGGYER 7 VLG YER Sbjct 3 VLGEYER 9
CAH73521.1	Ras responsive element binding protein 1 [Homo sapiens]	21.0	36.9	61%	388	Query 6 ERGEDNNE 13

	>emb|CAI16450.1| ras responsive element binding protein 1 [Homo sapiens] >emb|CAI14574.1| ras responsive element binding protein 1, RREB1 [Homo sapiens]					ERGE+++E Sbjct 1615 ERGEEDSE 1622 Query 7 RGED 10 RGED Sbjct 825 RGED 828
CAE75743.1	TPA: putative N-acetylated alpha-linked acidic dipeptidase-like protein 2, NAALADL2 [Homo sapiens]	21.0	21.0	61%	388	Query 3 GGYERGED 10 G YE GED Sbjct 505 GSYEWGED 512
NP_001003698.1	ras responsive element binding protein 1 isoform 2 [Homo sapiens] >ref|NP_001161816.1| ras responsive element binding protein 1 isoform 2 [Homo sapiens] >sp|Q92766.3|RREB1_HUMAN RecName: Full=Ras-responsive element-binding protein 1; Short=RREB-1; AltName: Full=Raf-responsive zinc finger protein LZ321; AltName: Full=Zinc finger motif-enhancer binding-protein 1; Short=Zep-1; AltName: Full=Finger protein in nuclear bodies >gb|EAW55198.1| ras responsive element binding protein 1, isoform CRA_a [Homo sapiens] >gb|EAW55199.1| ras responsive element binding protein 1, isoform CRA_a [Homo sapiens] >gb|EAW55200.1| ras responsive element binding protein 1, isoform CRA_a [Homo sapiens]	21.0	36.9	61%	388	Query 6 ERGEDNNE 13 ERGE+++E Sbjct 1579 ERGEEDSE 1586 Query 7 RGED 10 RGED Sbjct 844 RGED 847
AAB19094.1	Ras-responsive element binding protein, RREB1 [Homo sapiens]	21.0	21.0	61%	388	Query 6 ERGEDNNE 13 ERGE+++E Sbjct 647 ERGEEDSE 654
AAC25598.1	Raf responsive zinc finger protein, RREB1 [Homo sapiens]	21.0	21.0	61%	388	Query 6 ERGEDNNE 13 ERGE+++E Sbjct 418 ERGEEDSE 425

NP_149107.4	NIMA-related kinase 9 [Homo sapiens] >sp|Q8TD19.2|NEK9_HUMAN RecName: Full=Serine/threonine-protein kinase Nek9; AltName: Full=Never in mitosis A-related kinase 9; Short=NimA-related protein kinase 9; AltName: Full=Nercc1 kinase; AltName: Full=NimA-related kinase 8; Short=Nek8 >gb|AAH93881.1| NIMA (never in mitosis gene a)-related kinase 9 [Homo sapiens] >gb|AAI12102.1| NIMA related kinase 9 [Homo sapiens]	21.0	21.0	53%	388	Query 1 VLGGYER 7 VLG YER Sbjct 3 VLGEYER 9
NP_001003699.1	Ras responsive element binding protein 1, RREB1, isoform 1 [Homo sapiens]	21.0	36.9	61%	388	Query 6 ERGEDNNE 13 ERGE+++E Sbjct 1634 ERGEEDSE 1641 Query 7 RGED 10 RGED Sbjct 844 RGED 847
NP_065852.1	Arrestin domain containing 3 [Homo sapiens] >sp|Q96B67.1|ARRD3_HUMAN RecName: Full=Arrestin domain-containing protein 3; AltName: Full=TBP-2-like inducible membrane protein; Short=TLIMP >gb|AAH15928.1| Arrestin domain containing 3 [Homo sapiens] >gb|AAH53619.1| Arrestin domain containing 3 [Homo sapiens] >gb|EAW95997.1| arrestin domain containing 3 [Homo sapiens]	21.0	21.0	76%	388	Query 4 GYERGEDNNE 13 G+ER +DN+E Sbjct 90 GHERDDDNSE 99
NP_848535.1	zinc finger, FYVE domain containing 1 isoform 2 [Homo sapiens] >gb|AAK27339.1| tandem FYVE fingers-1 protein [Homo sapiens]	21.0	21.0	46%	388	Query 5 YERGED 10 YERGE+ Sbjct 61 YERGEE 66
AAL87410.1	NIMA-family kinase NERCC1, NEK9 [Homo sapiens]	21.0	21.0	53%	388	Query 1 VLGGYER 7 VLG YER Sbjct 3 VLGEYER 9

AAD31940.1	NEK9 [Homo sapiens]	21.0	21.0	53%	388	Query 1 VLGGYER 7 VLG YER Sbjct 3 VLGEYER 9
BAD32776.1	zinc-finger motif-enhancer binding-protein-1, RREB1 [Homo sapiens]	21.0	36.9	61%	388	Query 6 ERGEDNNE 13 ERGE+++E Sbjct 1634 ERGEEDSE 1641 Query 7 RGED 10 RGED Sbjct 844 RGED 847
BAD32779.1	Zinc-finger motif-Enhancer binding-Protein-1, RREB1, gamma [Homo sapiens]	21.0	36.9	61%	388	Query 6 ERGEDNNE 13 ERGE+++E Sbjct 1368 ERGEEDSE 1375 Query 7 RGED 10 RGED Sbjct 844 RGED 847
BAD32778.1	zinc-finger motif-enhancer binding-protein-1, RREB1, beta [Homo sapiens]	21.0	36.9	61%	388	Query 6 ERGEDNNE 13 ERGE+++E Sbjct 1579 ERGEEDSE 1586 Query 7 RGED 10 RGED Sbjct 844 RGED 847
BAB13415.1	ZFYV1 [Homo sapiens]	21.0	21.0	46%	388	Query 5 YERGED 10 YERGE+ Sbjct 515 YERGEE 520
AAL05428.1	NIMA-related kinase Nek8 [Homo sapiens] >gb|EAW81220.1| NIMA (never in mitosis gene a)-	21.0	21.0	53%	388	Query 1 VLGGYER 7 VLG YER

	related kinase 9, isoform CRA_a [Homo sapiens] >gb|EAW81222.1| NIMA (never in mitosis gene a)-related kinase 9, NEK9, isoform CRA_a [Homo sapiens]					Sbjct 3 VLGEYER 9 Query 5 YERGED 10 YERGE+ Sbjct 476 YERGEE 481
BAB55085.1	ZFYV1 [Homo sapiens]	21.0	21.0	46%	388	
NP_067083.1	zinc finger, FYVE domain containing 1 isoform 1 [Homo sapiens] >sp|Q9HBF4.1|ZFYV1_HUMAN RecName: Full=Zinc finger FYVE domain-containing protein 1; AltName: Full=Double FYVE-containing protein 1; AltName: Full=Tandem FYVE fingers-1; AltName: Full=SR3 >gb|AAG23748.1|AF251025_1 double FYVE-containing protein 1 [Homo sapiens] >emb|CAC83950.1| phosphoinositide-binding protein [Homo sapiens] >gb|AAH53520.1| Zinc finger, FYVE domain containing 1 [Homo sapiens] >gb|EAW81085.1| zinc finger, FYVE domain containing 1, isoform CRA_b [Homo sapiens]	21.0	21.0	46%	388	Query 5 YERGED 10 YERGE+ Sbjct 476 YERGEE 481
BAA23165.1	DNA-binding protein, RREB1 [Homo sapiens]	21.0	36.9	61%	388	Query 6 ERGEDNNE 13 ERGE+++E Sbjct 1559 ERGEEDSE 1566 Query 7 RGED 10 RGED Sbjct 825 RGED 828
BAA92614.1	KIAA1376 protein, ARRD3[Homo sapiens]	21.0	21.0	76%	388	Query 4 GYERGEDNNE 13 G+ER +DN+E Sbjct 113 GHERDDDNSE 122
BAC02704.1	KIAA1995 protein, NEK9 [Homo sapiens]	21.0	21.0	53%	388	Query 1 VLGGYER 7 VLG YER Sbjct 35 VLGEYER 41

BAI51368.1	immunoglobulin heavy chain variable region, IGH [Homo sapiens]	20.6	20.6	53%	521	Query 5 YERGEDN 11 +ERG+DN Sbjct 65 FERGQDN 71
BAH12057.1	Exocyst complex component 4, EXOC4 [Homo sapiens]	20.6	20.6	53%	521	Query 4 GYERGED 10 GY+RGE+ Sbjct 221 GYQRGEN 227
EAW83806.1	Exocyst complex component 4, isoform CRA_c [Homo sapiens]	20.6	20.6	53%	521	Query 4 GYERGED 10 GY+RGE+ Sbjct 322 GYQRGEN 328
EAW78858.1	ring finger protein 13, isoform CRA_a [Homo sapiens] >gb|EAW78860.1| ring finger protein 13, isoform CRA_a [Homo sapiens] >gb|EAW78862.1| ring finger protein 13, isoform CRA_a [Homo sapiens] >dbj|BAG52224.1| unnamed protein product [Homo sapiens], RNF13	20.6	20.6	69%	521	Query 5 YERGEDNNE 13 YE ED+NE Sbjct 222 YE--EDDNE 228
NP_001032203.1	Exocyst complex component 4 isoform b [Homo sapiens]	20.6	20.6	53%	521	Query 4 GYERGED 10 GY+RGE+ Sbjct 322 GYQRGEN 328
AAH67263.1	Exocyst complex component 4 [Homo sapiens]	20.6	20.6	53%	521	Query 4 GYERGED 10 GY+RGE+ Sbjct 322 GYQRGEN 328
AAH26174.1	EXOC4 protein [Homo sapiens]	20.6	20.6	53%	521	Query 4 GYERGED 10 GY+RGE+ Sbjct 322 GYQRGEN 328
BAB21790.1	KIAA1699 protein, EXOC4 [Homo sapiens]	20.6	20.6	53%	521	Query 4 GYERGED 10 GY+RGE+

						Sbjct 314 GYQRGEN 320
NP_009213.1	ring finger protein 13 [Homo sapiens] >ref|NP_899237.1| ring finger protein 13 [Homo sapiens] >sp|O43567.1|RNF13_HUMAN RecName: Full=RING finger protein 13 >gb|AAC03769.1| RING zinc finger protein [Homo sapiens] >gb|AAC28641.1| RING zinc finger protein RZF [Homo sapiens] >gb|AAH09781.1| Ring finger protein 13 [Homo sapiens] >gb|AAH09803.1| Ring finger protein 13 [Homo sapiens] >emb|CAG33085.1| RNF13 [Homo sapiens] >gb|EAW78859.1| ring finger protein 13, isoform CRA_b [Homo sapiens] >gb|EAW78861.1| ring finger protein 13, isoform CRA_b [Homo sapiens] >gb|EAW78863.1| ring finger protein 13, isoform CRA_b [Homo sapiens] >dbj|BAG36109.1| unnamed protein product [Homo sapiens] >dbj|BAG52202.1| unnamed protein product [Homo sapiens]	20.6	20.6	69%	521	Query 5 YERGEDNNE 13 YE ED+NE Sbjct 341 YE--EDDNE 347
CAD39134.1	hypothetical protein, EXOC4 [Homo sapiens]	20.6	20.6	53%	521	Query 4 GYERGED 10 GY+RGE+ Sbjct 109 GYQRGEN 115
NP_068579.3	SEC8 protein isoform a [Homo sapiens] >sp|Q96A65.1|EXOC4_HUMAN RecName: Full=Exocyst complex component 4; AltName: Full=Exocyst complex component Sec8 >gb|AAK57456.1|AF380839_1 secretory protein SEC8 [Homo sapiens] >dbj|BAB55298.1| unnamed protein product [Homo sapiens] >emb|CAD89977.1| hypothetical protein [Homo sapiens] >gb|EAL24073.1| SEC8-like 1 (S. cerevisiae) [Homo sapiens] >gb|EAW83804.1| exocyst complex component 4, isoform CRA_a [Homo sapiens]	20.6	20.6	53%	521	Query 4 GYERGED 10 GY+RGE+ Sbjct 322 GYQRGEN 328
Q9Y618.2	RecName: Full=Nuclear receptor corepressor 2; Short=N-CoR2; AltName: Full=Silencing mediator of retinoic acid	20.2	38.6	100%	699	Query 8 GEDNNE 13 GEDN+E

	and thyroid hormone receptor; Short=SMRT; AltName: Full=Thyroid-, retinoic-acid-receptor-associated corepressor; AltName: Full=T3 receptor-associating factor; Short=TRAC; AltName: Full=CTG repeat protein 26; AltName: Full=SMAP270; NCOR2					Sbjct 555 GEDNDE 560 Query 1 VLGGYERGED 10 VLGG GED Sbjct 2222 VLGG---GED 2228
BAH12506.1	Highly similar to Glutamate receptor, ionotrophic, AMPA 3, GRIA3 [Homo sapiens]	20.2	20.2	38%	699	Query 9 EDNNE 13 EDNNE Sbjct 568 EDNNE 572
BAH12200.1	Highly similar to SLIT-ROBO Rho GTPase-activating protein 2, SRGAP2 [Homo sapiens]	20.2	20.2	46%	699	Query 5 YERGED 10 +ERGED Sbjct 541 FERGED 546
BAH11812.1	Highly similar to Rho GTPase-activating protein 4, ARHGAP4 [Homo sapiens]	20.2	20.2	46%	699	Query 5 YERGED 10 +ERGED Sbjct 535 FERGED 540

Table A.1. Blastp results of ROBO1 antibody immunogen sequence.

References

Abrahams, B. S., Tentler, D., Perederiy, J. V., Oldham, M. C., Coppola, G. and Geschwind, D. H. (2007) 'Genome-wide analyses of human perisylvian cerebral cortical patterning', *Proc Natl Acad Sci U S A,* 104, (45), pp. 17849-54.

Alcamo, E. A., Chirivella, L., Dautzenberg, M., Dobreva, G., Farinas, I., Grosschedl, R. and McConnell, S. K. (2008) 'Satb2 regulates callosal projection neuron identity in the developing cerebral cortex', *Neuron,* 57, (3), pp. 364-77.

Allen, B. L. and Rapraeger, A. C. (2003) 'Spatial and temporal expression of heparan sulfate in mouse development regulates FGF and FGF receptor assembly', *J Cell Biol,* 163, (3), pp. 637-48.

Andjelic, S., Gallopin, T., Cauli, B., Hill, E. L., Roux, L., Badr, S., Hu, E., Tamas, G. and Lambolez, B. (2009) 'Glutamatergic nonpyramidal neurons from neocortical layer VI and their comparison with pyramidal and spiny stellate neurons', *J Neurophysiol,* 101, (2), pp. 641-54.

Ando, K., Yagi, H., Suda, Y., Aizawa, S., Sakashita, M., Nagano, T., Terashima, T. and Sato, M. (2008) 'Establishment of framework of the cortical area is influenced by Otx1', *Neuroscience Research,* 60, pp. 457-459.

Andrews, W., Barber, M., Hernadez-Miranda, L. R., Xian, J., Rakic, S., Sundaresan, V., Rabbitts, T. H., Pannell, R., Rabbitts, P., Thompson, H., Erskine, L., Murakami, F. and Parnavelas, J. G. (2008) 'The role of Slit-Robo signaling in the generation, migration and morphological differentiation of cortical interneurons', *Dev Biol,* 313, (2), pp. 648-58.

Andrews, W., Liapi, A., Plachez, C., Camurri, L., Zhang, J., Mori, S., Murakami, F., Parnavelas, J. G., Sundaresan, V. and Richards, L. J. (2006) 'Robo1 regulates the development of major axon tracts and interneuron migration in the forebrain', *Development,* 133, (11), pp. 2243-52.

Andrews, W. D., Barber, M. and Parnavelas, J. G. (2007) 'Slit-Robo interactions during cortical development', *J Anat,* 211, (2), pp. 188-98.

Anthony, T. E., Klein, C., Fishell, G. and Heintz, N. (2004) 'Radial glia serve as neuronal progenitors in all regions of the central nervous system', *Neuron,* 41, (6), pp. 881-90.

Arimatsu, Y., Ishida, M., Kaneko, T., Ichinose, S. and Omori, A. (2003) 'Organization and development of corticocortical associative neurons expressing the orphan nuclear receptor Nurr1', *J Comp Neurol,* 466, (2), pp. 180-96.

Arlotta, P., Molyneaux, B. J., Chen, J., Inoue, J., Kominami, R. and Macklis, J. D. (2005) 'Neuronal subtype-specific genes that control corticospinal motor neuron development in vivo', *Neuron,* 45, (2), pp. 207-21.

Armentano, M., Chou, S. J., Tomassy, G. S., Leingartner, A., O'Leary, D. D. and Studer, M. (2007) 'COUP-TFI regulates the balance of cortical patterning between frontal/motor and sensory areas', *Nat Neurosci,* 10, (10), pp. 1277-86.

Atkinson-Leadbeater, K., Bertolesi, G. E., Hehr, C. L., Webber, C. A., Cechmanek, P. B. and McFarlane, S. (2010) 'Dynamic expression of axon guidance cues required for optic tract development is controlled by fibroblast growth factor signaling', *J Neurosci,* 30, (2), pp. 685-93.

Azim, E., Shnider, S. J., Cederquist, G. Y., Sohur, U. S. and Macklis, J. D. (2009) 'Lmo4 and Clim1 progressively delineate cortical projection neuron subtypes during development', *Cereb Cortex,* 19 Suppl 1, pp. i62-9.

Bachler, M. and Neubuser, A. (2001) 'Expression of members of the Fgf family and their receptors during midfacial development', *Mech Dev,* 100, (2), pp. 313-6.

Bacon, C., Endris, V. and Rappold, G. (2009) 'Dynamic expression of the Slit-Robo GTPase activating protein genes during development of the murine nervous system', *J Comp Neurol,* 513, (2), pp. 224-36.

Bagri, A., Marin, O., Plump, A. S., Mak, J., Pleasure, S. J., Rubenstein, J. L. and Tessier-Lavigne, M. (2002) 'Slit proteins prevent midline crossing and determine the dorsoventral position of major axonal pathways in the mammalian forebrain', *Neuron,* 33, (2), pp. 233-48.

Bansal, R., Kumar, M., Murray, K., Morrison, R. S. and Pfeiffer, S. E. (1996) 'Regulation of FGF receptors in the oligodendrocyte lineage', *Mol Cell Neurosci,* 7, (4), pp. 263-75.

Basu, A., Graziadio, S., Smith, M., Clowry, G. J., Cioni, G. and Eyre, J. A. (2010) 'Developmental plasticity connects visual cortex to motoneurons after stroke', *Ann Neurol,* 67, (1), pp. 132-6.

Bates, C. A. and Killackey, H. P. (1984) 'The emergence of a discretely distributed pattern of corticospinal projection neurons', *Brain Res,* 315, (2), pp. 265-73.

Bayatti, N. and Engele, J. (2001) 'Cyclic AMP modulates the response of central nervous system glia to fibroblast growth factor-2 by redirecting signalling pathways', *J Neurochem,* 78, (5), pp. 972-80.

Bayatti, N., Moss, J. A., Sun, L., Ambrose, P., Ward, J. F., Lindsay, S. and Clowry, G. J. (2008a) 'A molecular neuroanatomical study of the developing human neocortex from 8 to 17 postconceptional weeks revealing the early differentiation of the subplate and subventricular zone', *Cereb Cortex,* 18, (7), pp. 1536-48.

Bayatti, N., Sarma, S., Shaw, C., Eyre, J. A., Vouyiouklis, D. A., Lindsay, S. and Clowry, G. J. (2008b) 'Progressive loss of PAX6, TBR2, NEUROD and TBR1 mRNA gradients correlates with translocation of EMX2 to the cortical plate during human cortical development', *Eur J Neurosci,* 28, (8), pp. 1449-56.

Bedogni, F., Hodge, R. D., Elsen, G. E., Nelson, B. R., Daza, R. A., Beyer, R. P., Bammler, T. K., Rubenstein, J. L. and Hevner, R. F. (2010) 'Tbr1 regulates regional and laminar identity of postmitotic neurons in developing neocortex', *Proc Natl Acad Sci U S A,* 107, (29), pp. 13129-34.

Bernhardt, R. and Matus, A. (1984) 'Light and electron microscopic studies of the distribution of microtubule-associated protein 2 in rat brain: a difference between dendritic and axonal cytoskeletons', *J Comp Neurol,* 226, (2), pp. 203-21.

Bishop, K. M., Garel, S., Nakagawa, Y., Rubenstein, J. L. and O'Leary, D. D. (2003) 'Emx1 and Emx2 cooperate to regulate cortical size, lamination, neuronal differentiation, development of cortical efferents, and thalamocortical pathfinding', *J Comp Neurol,* 457, (4), pp. 345-60.

Bishop, K. M., Goudreau, G. and O'Leary, D. D. (2000) 'Regulation of area identity in the mammalian neocortex by Emx2 and Pax6', *Science,* 288, (5464), pp. 344-9.

Bishop, K. M., Rubenstein, J. L. and O'Leary, D. D. (2002) 'Distinct actions of Emx1, Emx2, and Pax6 in regulating the specification of areas in the developing neocortex', *J Neurosci,* 22, (17), pp. 7627-38.

Borello, U., Cobos, I., Long, J. E., McWhirter, J. R., Murre, C. and Rubenstein, J. L. (2008) 'FGF15 promotes neurogenesis and opposes FGF8 function during neocortical development', *Neural Dev,* 3, pp. 17.

Brader, S. and Eccles, S. A. (2004) 'Phosphoinositide 3-kinase signalling pathways in tumor progression, invasion and angiogenesis', *Tumori,* 90, (1), pp. 2-8.

Branney, P. A., Faas, L., Steane, S. E., Pownall, M. E. and Isaacs, H. V. (2009) 'Characterisation of the fibroblast growth factor dependent transcriptome in early development', *PLoS One,* 4, (3), pp. e4951.

Britanova, O., Akopov, S., Lukyanov, S., Gruss, P. and Tarabykin, V. (2005) 'Novel transcription factor Satb2 interacts with matrix attachment region DNA elements in a tissue-specific manner and demonstrates cell-type-dependent expression in the developing mouse CNS', *Eur J Neurosci,* 21, (3), pp. 658-68.

Britanova, O., Alifragis, P., Junek, S., Jones, K., Gruss, P. and Tarabykin, V. (2006a) 'A novel mode of tangential migration of cortical projection neurons', *Dev Biol,* 298, (1), pp. 299-311.

Britanova, O., de Juan Romero, C., Cheung, A., Kwan, K. Y., Schwark, M., Gyorgy, A., Vogel, T., Akopov, S., Mitkovski, M., Agoston, D., Sestan, N., Molnar, Z. and Tarabykin, V. (2008) 'Satb2 is a postmitotic determinant for upper-layer neuron specification in the neocortex', *Neuron*, 57, (3), pp. 378-92.

Britanova, O., Depew, M. J., Schwark, M., Thomas, B. L., Miletich, I., Sharpe, P. and Tarabykin, V. (2006b) 'Satb2 haploinsufficiency phenocopies 2q32-q33 deletions, whereas loss suggests a fundamental role in the coordination of jaw development', *American journal of human genetics*, 79, (4), pp. 668-78.

Brodal, P. (1978) 'The corticopontine projection in the rhesus monkey. Origin and principles of organization', *Brain*, 101, (2), pp. 251-83.

Buervenich, S., Carmine, A., Arvidsson, M., Xiang, F., Zhang, Z., Sydow, O., Jonsson, E. G., Sedvall, G. C., Leonard, S., Ross, R. G., Freedman, R., Chowdari, K. V., Nimgaonkar, V. L., Perlmann, T., Anvret, M. and Olson, L. (2000) 'NURR1 mutations in cases of schizophrenia and manic-depressive disorder', *Am J Med Genet*, 96, (6), pp. 808-13.

Bystron, I., Blakemore, C. and Rakic, P. (2008) 'Development of the human cerebral cortex: Boulder Committe revisited', *Nature*, 9, pp. 110-122.

Bystron, I., Molnar, Z., Otellin, V. and Blakemore, C. (2005) 'Tangential networks of precocious neurons and early axonal outgrowth in the embryonic human forebrain', *The Journal of Neuroscience*, 25, (11), pp. 2781-2792.

Bystron, I., Rakic, P., Molnar, Z. and Blakemore, C. (2006) 'The first neurons of the human cerebral cortex', *Nat Neurosci*, 9, (7), pp. 880-6.

Cang, J., Kaneko, M., Yamada, J., Woods, G., Stryker, M. P. and Feldhem, D. A. (2005) 'Ephrin-As guide the formation of function maps in the visual cortex', *Neuron,* 48, pp. 577-589.

Casarosa, S., Fode, C. and Guillemot, F. (1999) 'Mash1 regulates neurogenesis in the ventral telencephalon', *Development,* 126, (3), pp. 525-34.

Cavallaro, U. and Christofori, G. (2004) 'Cell adhesion and signalling by cadherins and Ig-CAMs in cancer', *Nat Rev Cancer,* 4, (2), pp. 118-32.

Cecchi, C. and Boncinelli, E. (2000) 'Emx homeogenes and mouse brain development', *Trends Neurosci,* 23, (8), pp. 347-52.

Chen, B., Schaevitz, L. R. and McConnell, S. K. (2005a) 'Fezl regulates the differentiation and axon targeting of layer 5 subcortical projection neurons in cerebral cortex', *Proc Natl Acad Sci U S A,* 102, (47), pp. 17184-9.

Chen, B., Wang, S. S., Hattox, A. M., Rayburn, H., Nelson, S. B. and McConnell, S. K. (2008) 'The Fezf2-Ctip2 genetic pathway regulates the fate choice of subcortical projection neurons in the developing cerebral cortex', *Proc Natl Acad Sci U S A,* 105, (32), pp. 11382-7.

Chen, J. G., Rasin, M. R., Kwan, K. Y. and Sestan, N. (2005b) 'Zfp312 is required for subcortical axonal projections and dendritic morphology of deep-layer pyramidal neurons of the cerebral cortex', *Proc Natl Acad Sci U S A,* 102, (49), pp. 17792-7.

Chen, Y. H., Tsai, M. T., Shaw, C. K. and Chen, C. H. (2001) 'Mutation analysis of the human NR4A2 gene, an essential gene for midbrain dopaminergic neurogenesis, in schizophrenic patients', *Am J Med Genet*, 105, (8), pp. 753-7.

Cholfin, J. A. and Rubenstein, J. L. R. (2007) 'Patterning of frontal cortex subdivisions by Fgf17', *Proceedings of the National Academy of Sciences of the United States of America*, 104, (18), pp. 7652-7657.

Clegg, J. M., Manuel, M. and Price, D. J. (2010) 'Pax6 and the development of the thalamocortical tract', *7th Forum of European Neuroscience Societies (FENS)*. Amsterdam, 3-7 July 2010. pp. FENS Abstract 159.8.

Crossley, P. H. and Martin, G. R. (1995) 'The mouse Fgf8 gene encodes a family of polypeptides and is expressed in regions that direct outgrowth and patterning in the developing embryo', *Development*, 121, (2), pp. 439-51.

Crossley, P. H., Martinez, S., Ohkubo, Y. and Rubenstein, J. L. R. (2001) 'Coordinate expression of *Fgf8*, *Otx2*, *Bmp4*, and *Shh* in the rostral prosencephalon during development of the telencephalic and optic vesicles', *Neuroscience*, 108, (2), pp. 183-206.

Cubelos, B., Sebastian-Serrano, A., Kim, S., Moreno-Oritz, C., Redondo, J. M., Walsh, C. A. and Nieto, M. (2007) 'Cux-2 controls the proliferation of neuronal intermediate precursors of the cortical subventricular zone', *Cerebral Cortex*.

Danesin, C., Peres, J. N., Johansson, M., Snowden, V., Cording, A., Papalopulu, N. and Houart, C. (2009) 'Integration of telencephalic Wnt and hedgehog signaling center activities by Foxg1', *Dev Cell*, 16, (4), pp. 576-87.

DeFelipe, J., Ballesteros-Yanez, I., Inda, M. C. and Munoz, A. (2006) 'Double-bouquet cells in the monkey and human cerebral cortex with special reference to areas 17 and 18', *Prog Brain Res*, 154, pp. 15-32.

Dehay, C. and Kennedy, H. (2007) 'Cell-cycle control and cortical development', *Nat Rev Neurosci*, 8, (6), pp. 438-50.

Demyanenko, G. P., Siesser, P. F., Wright, A. G., Brennaman, L. H., Bartsch, U., Schachner, M. and Maness, P. F. (2010) 'L1 and CHL1 Cooperate in Thalamocortical Axon Targeting', *Cereb Cortex*.

Dobreva, G., Chahrour, M., Dautzenberg, M., Chirivella, L., Kanzler, B., Farinas, I., Karsenty, G. and Grosschedl, R. (2006) 'SATB2 is a multifunctional determinant of craniofacial patterning and osteoblast differentiation', *Cell*, 125, (5), pp. 971-86.

Dufour, A., Seibt, J., Passante, L., Depaepe, V., Ciossek, T., Frisen, J., Kullander, K., Flanagan, J. G., Polleux, F. and Vanderhaeghen, P. (2003) 'Area specificity and topography of thalamocortical projections are controlled by ephrin/Eph genes', *Neuron*, 39, pp. 453-465.

Englund, C., Fink, A., Lau, C., Pham, D., Daza, R. A., Bulfone, A., Kowalczyk, T. and Hevner, R. F. (2005) 'Pax6, Tbr2, and Tbr1 are expressed sequentially by radial glia, intermediate progenitor cells, and postmitotic neurons in developing neocortex', *J Neurosci*, 25, (1), pp. 247-51.

Eswarakumar, V. P., Lax, I. and Schlessinger, J. (2005) 'Cellular signaling by fibroblast growth factor receptors', *Cytokine Growth Factor Rev*, 16, (2), pp. 139-49.

Eyre, J. A. (2007) 'Corticospinal tract development and its plasticity after perinatal injury', *Neurosci Biobehav Rev,* 31, (8), pp. 1136-49.

Faedo, A., Borello, U. and Rubenstein, J. L. (2010) 'Repression of Fgf signaling by sprouty1-2 regulates cortical patterning in two distinct regions and times', *J Neurosci,* 30, (11), pp. 4015-23.

Faedo, A., Tomassy, G. S., Ruan, Y., Teichmann, H., Krauss, S., Pleasure, S. J., Tsai, S. Y., Tsai, M. J., Studer, M. and Rubenstein, J. L. (2008) 'COUP-TFI coordinates cortical patterning, neurogenesis, and laminar fate and modulates MAPK/ERK, AKT, and beta-catenin signaling', *Cereb Cortex,* 18, (9), pp. 2117-31.

Faulkner, R. L., Low, L. K., Liu, X. B., Coble, J., Jones, E. G. and Cheng, H. J. (2008) 'Dorsal turning of motor corticospinal axons at the pyramidal decussation requires plexin signaling', *Neural Dev,* 3, pp. 21.

Feng, J., Chen, J., Yan, J., Jones, I. R., Craddock, N., Cook, E. H., Jr., Goldman, D., Heston, L. L. and Sommer, S. S. (2005) 'Structural variants in the retinoid receptor genes in patients with schizophrenia and other psychiatric diseases', *Am J Med Genet B Neuropsychiatr Genet,* 133B, (1), pp. 50-3.

Ferland, R. J., Cherry, T. J., Preware, P. O., Morrisey, E. E. and Walsh, C. A. (2003) 'Characterization of Foxp2 and Foxp1 mRNA and protein in the developing and mature brain', *J Comp Neurol,* 460, (2), pp. 266-79.

Fertuzinhos, S., Krsnik, Z., Kawasawa, Y. I., Rasin, M. R., Kwan, K. Y., Chen, J. G., Judas, M., Hayashi, M. and Sestan, N. (2009) 'Selective depletion of molecularly defined cortical interneurons in human holoprosencephaly with severe striatal hypoplasia', *Cereb Cortex,* 19, (9), pp. 2196-207.

Fietz, S. A., Kelava, I., Vogt, J., Wilsch-Brauninger, M., Stenzel, D., Fish, J. L., Corbeil, D., Riehn, A., Distler, W., Nitsch, R. and Huttner, W. B. (2010) 'OSVZ progenitors of human and ferret neocortex are epithelial-like and expand by integrin signaling', *Nat Neurosci,* 13, (6), pp. 690-9.

Figiel, M., Maucher, T., Rozyczka, J., Bayatti, N. and Engele, J. (2003) 'Regulation of glial glutamate transporter expression by growth factors', *Experimental neurology,* 183, (1), pp. 124-35.

Flames, N., Long, J. E., Garratt, A. N., Fischer, T. M., Gassmann, M., Birchmeier, C., Lai, C., Rubenstein, J. L. and Marin, O. (2004) 'Short- and long-range attraction of cortical GABAergic interneurons by neuregulin-1', *Neuron,* 44, (2), pp. 251-61.

Flames, N., Pla, R., Gelman, D. M., Rubenstein, J. L., Puelles, L. and Marin, O. (2007) 'Delineation of multiple subpallial progenitor domains by the combinatorial expression of transcriptional codes', *J Neurosci,* 27, (36), pp. 9682-95.

Fode, C., Ma, Q., Casarosa, S., Ang, S. L., Anderson, D. J. and Guillemot, F. (2000) 'A role for neural determination genes in specifying the dorsoventral identity of telencephalic neurons', *Genes and Development,* 14, pp. 67-80.

Ford-Perriss, M., Abud, H. and Murphy, M. (2001) 'Fibroblast growth factors in the developing central nervous system', *Clin Exp Pharmacol Physiol,* 28, (7), pp. 493-503.

Ford-Perriss, M., Guimond, S. E., Greferath, U., Kita, M., Grobe, K., Habuchi, H., Kimata, K., Esko, J. D., Murphy, M. and Turnbull, J. E. (2002) 'Variant heparan sulfates synthesized in developing mouse brain differentially regulate FGF signaling', *Glycobiology,* 12, (11), pp. 721-7.

Fortin, D., Rom, E., Sun, H., Yayon, A. and Bansal, R. (2005) 'Distinct fibroblast growth factor (FGF)/FGF receptor signaling pairs initiate diverse cellular responses in the oligodendrocyte lineage', *J Neurosci,* 25, (32), pp. 7470-9.

Franke, B., Bayatti, N. and Engele, J. (2000) 'Neurotrophins require distinct extracellular signals to promote the survival of CNS neurons in vitro', *Exp Neurol,* 165, (1), pp. 125-35.

Fukuchi-Shimogori, T. and Grove, E. A. (2001) 'Neocortex patterning by the secreted signaling molecule FGF8', *Science,* 294, (5544), pp. 1071-1074.

Fukuchi-Shimogori, T. and Grove, E. A. (2003) 'Emx2 patterns the neocortex by regulating FGF positional signaling', *Nat Neurosci,* 6, (8), pp. 825-31.

Fuster, J. M. (2002) 'Frontal lobe and cognitive development', *J Neurocytol,* 31, (3-5), pp. 373-85.

Gal, J. S., Morozov, Y. M., Ayoub, A. E., Chatterjee, M., Rakic, P. and Haydar, T. F. (2006) 'Molecular and morphological heterogeneity of neural precursors in the mouse neocortical proliferative zones', *J Neurosci,* 26, (3), pp. 1045-56.

Galea, M. P. and Darian-Smith, I. (1994) 'Multiple corticospinal neuron populations in the macaque monkey are specified by their unique cortical origins, spinal terminations, and connections', *Cereb Cortex,* 4, (2), pp. 166-94.

Galea, M. P. and Darian-Smith, I. (1995) 'Postnatal maturation of the direct corticospinal projections in the macaque monkey', *Cereb Cortex,* 5, (6), pp. 518-40.

Garel, S., Huffman, K. J. and Rubenstein, J. L. (2003) 'Molecular regionalization of the neocortex is disrupted in Fgf8 hypomorphic mutants', *Development,* 130, (9), pp. 1903-14.

Garel, S. and Rubenstein, J. L. R. (2004) 'Intermediate targets in formation of topographic projections: inputs from the thalamocortical system', *Trends in Neurosciences,* 27, (9), pp. 533-539.

Gelman, D. M. and Marin, O. (2010) 'Generation of interneuron diversity in the mouse cerebral cortex', *Eur J Neurosci,* 31, (12), pp. 2136-41.

Gelman, D. M., Martini, F. J., Nobrega-Pereira, S., Pierani, A., Kessaris, N. and Marin, O. (2009) 'The embryonic preoptic area is a novel source of cortical GABAergic interneurons', *J Neurosci,* 29, (29), pp. 9380-9.

Gimeno, L., Brulet, P. and Martinez, S. (2003) 'Study of Fgf15 gene expression in developing mouse brain', *Gene Expr Patterns,* 3, (4), pp. 473-81.

Gimeno, L. and Martinez, S. (2007) 'Expression of chick Fgf19 and mouse Fgf15 orthologs is regulated in the developing brain by Fgf8 and Shh', *Dev Dyn,* 236, (8), pp. 2285-97.

Glickstein, M., May, J. G., 3rd and Mercier, B. E. (1985) 'Corticopontine projection in the macaque: the distribution of labelled cortical cells after large injections of horseradish peroxidase in the pontine nuclei', *J Comp Neurol,* 235, (3), pp. 343-59.

Glickstein, S. B., Monaghan, J. A., Koeller, H. B., Jones, T. K. and Ross, M. E. (2009) 'Cyclin D2 is critical for intermediate progenitor cell proliferation in the embryonic cortex', *J Neurosci,* 29, (30), pp. 9614-24.

Grigoriou, M., Tucker, A. S., Sharpe, P. T. and Pachnis, V. (1998) 'Expression and regulation of Lhx6 and Lhx7, a novel subfamily of LIM homeodomain encoding genes, suggests a role in mammalian head development', *Development,* 125, (11), pp. 2063-74.

Grimes, D. A., Han, F., Panisset, M., Racacho, L., Xiao, F., Zou, R., Westaff, K. and Bulman, D. E. (2006) 'Translated mutation in the Nurr1 gene as a cause for Parkinson's disease', *Mov Disord,* 21, (7), pp. 906-9.

Gu, H., Wang, S., Messam, C. A. and Yao, Z. (2002) 'Distribution of nestin immunoreactivity in the normal adult human forebrain', *Brain Res,* 943, (2), pp. 174-80.

Guillemot, F., Molnar, Z., Tarabykin, V. and Stoykova, A. (2006) 'Molecular mechanisms of cortical differentiation', *Eur J Neurosci,* 23, (4), pp. 857-68.

Gyorgy, A. B., Szemes, M., de Juan Romero, C., Tarabykin, V. and Agoston, D. V. (2008) 'SATB2 interacts with chromatin-remodeling molecules in differentiating cortical neurons', *Eur J Neurosci,* 27, (4), pp. 865-73.

Hamasaki, T., Leingartner, A., Ringstedt, T. and O'Leary, D. D. (2004) 'EMX2 regulates sizes and positioning of the primary sensory and motor areas in neocortex by direct specification of cortical progenitors', *Neuron,* 43, (3), pp. 359-72.

Hansen, D. V., Lui, J. H., Parker, P. R. and Kriegstein, A. R. (2010) 'Neurogenic radial glia in the outer subventricular zone of human neocortex', *Nature,* 464, (7288), pp. 554-561.

Hartfuss, E., Galli, R., Heins, N. and Gotz, M. (2001) 'Characterization of CNS precursor subtypes and radial glia', *Dev Biol,* 229, (1), pp. 15-30.

Hebert, J. M., Lin, M., Partanen, J., Rossant, J. and McConnell, S. K. (2003) 'FGF signaling through FGFR1 is required for olfactory bulb morphogenesis', *Development,* 130, (6), pp. 1101-11.

Heins, N., Cremisi, F., Malatesta, P., Gangemi, R. M., Corte, G., Price, J., Goudreau, G., Gruss, P. and Gotz, M. (2001) 'Emx2 promotes symmetric cell divisions and a multipotential fate in precursors from the cerebral cortex', *Mol Cell Neurosci,* 18, (5), pp. 485-502.

Heins, N., Malatesta, P., Cecconi, F., Nakafuku, M., Tucker, K. L., Hack, M. A., Chapouton, P., Barde, Y. A. and Gotz, M. (2002) 'Glial cells generate neurons: the role of the transcription factor Pax6', *Nat Neurosci,* 5, (4), pp. 308-15.

Hellemans, J., Mortier, G., De Paepe, A., Speleman, F. and Vandesompele, J. (2007) 'qBase relative quantification framework and software for management and automated analysis of real-time quantitative PCR data', *Genome Biol,* 8, (2), pp. R19.

Hern, W. M. (1984) 'Correlation of fetal age and measurements between 10 and 26 weeks of gestation', *Obstet Gynecol,* 63, (1), pp. 26-32.

Hevner, R. F., Daza, R. A., Rubenstein, J. L., Stunnenberg, H., Olavarria, J. F. and Englund, C. (2003) 'Beyond laminar fate: toward a molecular classification of cortical projection/pyramidal neurons', *Dev Neurosci,* 25, (2-4), pp. 139-51.

Hevner, R. F., Hodge, R. D., Daza, R. A. and Englund, C. (2006) 'Transcription factors in glutamatergic neurogenesis: conserved programs in neocortex, cerebellum, and adult hippocampus', *Neurosci Res,* 55, (3), pp. 223-33.

Hevner, R. F., Shi, L., Justice, N., Hsueh, Y., Sheng, M., Smiga, S., Bulfone, A., Goffinet, A. M., Campagnoni, A. T. and Rubenstein, J. L. (2001) 'Tbr1 regulates differentiation of the preplate and layer 6', *Neuron,* 29, (2), pp. 353-66.

Hill, R. S. and Walsh, C. A. (2005) 'Molecular insights into human brain evolution', *Nature,* 437, pp. 64-67.

Hirata, T., Suda, Y., Nakao, K., Narimatsu, M., Hirano, T. and Hibi, M. (2004) 'Zinc finger gene fez-like functions in the formation of subplate neurons and thalamocortical axons', *Dev Dyn,* 230, (3), pp. 546-56.

Hirokawa, J., Watakabe, A., Ohsawa, S. and Yamamori, T. (2008) 'Analysis of area-specific expression patterns of RORbeta, ER81 and Nurr1 mRNAs in rat neocortex by double in situ hybridization and cortical box method', *PLoS One,* 3, (9), pp. e3266.

Hirschberg, A., Deng, S., Korostylev, A., Paldy, E., Costa, M. R., Worzfeld, T., Vodrazka, P., Wizenmann, A., Gotz, M., Offermanns, S. and Kuner, R. (2010) 'Gene deletion mutants reveal a role for semaphorin receptors of the plexin-B family in mechanisms underlying corticogenesis', *Mol Cell Biol,* 30, (3), pp. 764-80.

Hisaoka, T., Nakamura, Y., Senba, E. and Morikawa, Y. (2010) 'The forkhead transcription factors, Foxp1 and Foxp2, identify different subpopulations of projection neurons in the mouse cerebral cortex', *Neuroscience,* 166, (2), pp. 551-63.

Hoerder-Suabedissen, A., Wang, W. Z., Lee, S., Davies, K. E., Goffinet, A. M., Rakic, S., Parnavelas, J., Reim, K., Nicolic, M., Paulsen, O. and Molnar, Z. (2009) 'Novel markers reveal subpopulations of subplate neurons in the murine cerebral cortex', *Cereb Cortex,* 19, (8), pp. 1738-50.

Holm, P. C., Mader, M. T., Haubst, N., Wizenmann, A., Sigvardsson, M. and Gotz, M. (2007) 'Loss- and gain-of-function analyses reveal targets of Pax6 in the developing mouse telencephalon', *Mol Cell Neurosci*, 34, (1), pp. 99-119.

Hoshikawa, M., Ohbayashi, N., Yonamine, A., Konishi, M., Ozaki, K., Fukui, S. and Itoh, N. (1998) 'Structure and expression of a novel fibroblast growth factor, FGF-17, preferentially expressed in the embryonic brain', *Biochem Biophys Res Commun*, 244, (1), pp. 187-91.

Huang, Y., Cheung, L., Rowe, D. and Halliday, G. (2004) 'Genetic contributions to Parkinson's disease', *Brain Res Brain Res Rev*, 46, (1), pp. 44-70.

Inglis-Broadgate, S. L., Thomson, R. E., Pellicano, F., Tartaglia, M. A., Pontikis, C. C., Cooper, J. D. and Iwata, T. (2005) 'FGFR3 regulates brain size by controlling progenitor cell proliferation and apoptosis during embryonic development', *Dev Biol*, 279, (1), pp. 73-85.

Ip, B. K., Bayatti, N., Howard, N. J., Lindsay, S. and Clowry, G. J. (2010b) 'The corticofugal neuron-associated genes ROBO1, SRGAP1, and CTIP2 exhibit an anterior to posterior gradient of expression in early fetal human neocortex development', *Cereb Cortex*, in press.

Ip, B. K., Wappler, I., Peters, H., Lindsay, S., Clowry, G. J. and Bayatti, N. (2010a) 'Investigating gradients of gene expression involved in early human cortical development', *Journal of Anatomy*, 217 (4), pp. 300-311.

Ishiguro, H., Okubo, Y., Ohtsuki, T., Yamakawa-Kobayashi, K. and Arinami, T. (2002) 'Mutation analysis of the retinoid X receptor beta, nuclear-related receptor 1, and peroxisome proliferator-activated receptor alpha genes in schizophrenia and alcohol

dependence: possible haplotype association of nuclear-related receptor 1 gene to alcohol dependence', *Am J Med Genet,* 114, (1), pp. 15-23.

Itoh, N. (2007) 'The Fgf families in humans, mice, and zebrafish: their evolutional processes and roles in development, metabolism, and disease', *Biol Pharm Bull,* 30, (10), pp. 1819-25.

Itoh, N. and Ornitz, D. M. (2004) 'Evolution of the Fgf and Fgfr gene families', *Trends Genet,* 20, (11), pp. 563-9.

Iwata, T. and Hevner, R. F. (2009) 'Fibroblast growth factor signaling in development of the cerebral cortex', *Dev Growth Differ,* 51, (3), pp. 299-323.

Jacobsen, K. X., MacDonald, H., Lemonde, S., Daigle, M., Grimes, D. A., Bulman, D. E. and Albert, P. R. (2008) 'A Nurr1 point mutant, implicated in Parkinson's disease, uncouples ERK1/2-dependent regulation of tyrosine hydroxylase transcription', *Neurobiol Dis,* 29, (1), pp. 117-22.

Jen, J. C., Chan, W. M., Bosley, T. M., Wan, J., Carr, J. R., Rub, U., Shattuck, D., Salamon, G., Kudo, L. C., Ou, J., Lin, D. D., Salih, M. A., Kansu, T., Al Dhalaan, H., Al Zayed, Z., MacDonald, D. B., Stigsby, B., Plaitakis, A., Dretakis, E. K., Gottlob, I., Pieh, C., Traboulsi, E. I., Wang, Q., Wang, L., Andrews, C., Yamada, K., Demer, J. L., Karim, S., Alger, J. R., Geschwind, D. H., Deller, T., Sicotte, N. L., Nelson, S. F., Baloh, R. W. and Engle, E. C. (2004) 'Mutations in a human ROBO gene disrupt hindbrain axon pathway crossing and morphogenesis', *Science,* 304, (5676), pp. 1509-13.

Jimenez, D., Lopez-Mascaraque, L., de Carlos, J. A. and Valverde, F. (2002) 'Further studies on cortical tangential migration in wild type and Pax-6 mutant mice', *J Neurocytol,* 31, (8-9), pp. 719-28.

Johnson, M. B., Kawasawa, Y. I., Mason, C. E., Krsnik, Z., Coppola, G., Bogdanovic, D., Geschwind, D. H., Mane, S. M., State, M. W. and Sestan, N. (2009) 'Functional and evolutionary insights into human brain development through global transcriptome analysis', *Neuron,* 62, (4), pp. 494-509.

Johnston, C. L., Cox, H. C., Gomm, J. J. and Coombes, R. C. (1995) 'Fibroblast growth factor receptors (FGFRs) localize in different cellular compartments. A splice variant of FGFR-3 localizes to the nucleus', *J Biol Chem,* 270, (51), pp. 30643-50.

Jones, L., Lopez-Bendito, G., Gruss, P., Stoykova, A. and Molnar, Z. (2002) 'Pax6 is required for the normal development of the forebrain axonal connections', *Development,* 129, (21), pp. 5041-52.

Kadkhodaei, B., Ito, T., Joodmardi, E., Mattsson, B., Rouillard, C., Carta, M., Muramatsu, S., Sumi-Ichinose, C., Nomura, T., Metzger, D., Chambon, P., Lindqvist, E., Larsson, N. G., Olson, L., Bjorklund, A., Ichinose, H. and Perlmann, T. (2009) 'Nurr1 is required for maintenance of maturing and adult midbrain dopamine neurons', *J Neurosci,* 29, (50), pp. 15923-32.

Kahle, W. and Frotscher, M. (2002) *Nervous System and Sensory Organs.*5 ed Stuttgart: George Thieme Verlag.

Kanatani, S., Yozu, M., Tabata, H. and Nakajima, K. (2008) 'COUP-TFII is preferentially expressed in the caudal ganglionic eminence and is involved in the caudal migratory stream', *J Neurosci,* 28, (50), pp. 13582-91.

Kang, W., Wong, L. C., Shi, S. H. and Hebert, J. M. (2009) 'The transition from radial glial to intermediate progenitor cell is inhibited by FGF signaling during corticogenesis', *J Neurosci*, 29, (46), pp. 14571-80.

Kawamata, T., Dietrich, W. D., Schallert, T., Gotts, J. E., Cocke, R. R., Benowitz, L. I. and Finklestein, S. P. (1997) 'Intracisternal basic fibroblast growth factor enhances functional recovery and up-regulates the expression of a molecular marker of neuronal sprouting following focal cerebral infarction', *Proc Natl Acad Sci U S A*, 94, (15), pp. 8179-84.

Kidd, T., Brose, K., Mitchell, K. J., Fetter, R. D., Tessier-Lavigne, M., Goodman, C. S. and Tear, G. (1998) 'Roundabout controls axon crossing of the CNS midline and defines a novel subfamily of evolutionarily conserved guidance receptors', *Cell*, 92, (2), pp. 205-15.

Kim, G. J., Shatz, C. J. and McConnell, S. K. (1991) 'Morphology of pioneer and follower growth cones in the developing cerebral cortex', *J Neurobiol*, 22, (6), pp. 629-42.

Kim, S. Y., Chung, H. S., Sun, W. and Kim, H. (2007) 'Spatiotemporal expression pattern of non-clustered protocadherin family members in the developing rat brain', *Neuroscience*, 147, (4), pp. 996-1021.

Koop, K. E., MacDonald, L. M. and Lobe, C. G. (1996) 'Transcripts of Grg4, a murine groucho-related gene, are detected in adjacent tissues to other murine neurogenic gene homologues during embryonic development', *Mech Dev*, 59, (1), pp. 73-87.

Kostovic, I. and Judas, M. (2007) 'Transient patterns of cortical lamination during prenatal life: do they have implications for treatment?', *Neurosci Biobehav Rev*, 31, (8), pp. 1157-68.

Kostovic, I. and Rakic, P. (1990) 'Developmental history of the transient subplate zone in the visual and somatosensory cortex of the macaque monkey and human brain', *J Comp Neurol*, 297, (3), pp. 441-70.

Kowalczyk, T., Pontious, A., Englund, C., Daza, R. A., Bedogni, F., Hodge, R., Attardo, A., Bell, C., Huttner, W. B. and Hevner, R. F. (2009) 'Intermediate Neuronal Progenitors (Basal Progenitors) Produce Pyramidal-Projection Neurons for All Layers of Cerebral Cortex', *Cereb Cortex*.

Kuro-o, M. (2008) 'Endocrine FGFs and Klothos: emerging concepts', *Trends Endocrinol Metab*, 19, (7), pp. 239-45.

Kwan, K. Y., Lam, M. M., Krsnik, Z., Kawasawa, Y. I., Lefebvre, V. and Sestan, N. (2008) 'SOX5 postmitotically regulates migration, postmigratory differentiation, and projections of subplate and deep-layer neocortical neurons', *Proc Natl Acad Sci U S A*, 105, (41), pp. 16021-6.

Lai, T., Jabaudon, D., Molyneaux, B. J., Azim, E., Arlotta, P., Menezes, J. R. and Macklis, J. D. (2008) 'SOX5 controls the sequential generation of distinct corticofugal neuron subtypes', *Neuron*, 57, (2), pp. 232-47.

Lavdas, A. A., Grigoriou, M., Pachnis, V. and Parnavelas, J. G. (1999) 'The medial ganglionic eminence gives rise to a population of early neurons in the developing cerebral cortex', *J Neurosci*, 19, (18), pp. 7881-8.

Lemon, R. N. (2008) 'Descending pathways in motor control', *Annu Rev Neurosci*, 31, pp. 195-218.

Leone, D. P., Srinivasan, K., Chen, B., Alcamo, E. and McConnell, S. K. (2008) 'The determination of projection neuron identity in the developing cerebral cortex', *Curr Opin Neurobiol*, 18, (1), pp. 28-35.

Leoyklang, P., Suphapeetiporn, K., Siriwan, P., Desudchit, T., Chaowanapanja, P., Gahl, W. A. and Shotelersuk, V. (2007) 'Heterozygous nonsense mutation SATB2 associated with cleft palate, osteoporosis, and cognitive defects', *Hum Mutat*, 28, (7), pp. 732-8.

Letinic, K., Zoncu, R. and Rakic, P. (2002) 'Origin of GABAergic neurons in the human neocortex', *Nature*, 417, (6889), pp. 645-9.

Li, B. and DiCicco-Bloom, E. (2004) 'Basic fibroblast growth factor exhibits dual and rapid regulation of cyclin D1 and p27 to stimulate proliferation of rat cerebral cortical precursors', *Dev Neurosci*, 26, (2-4), pp. 197-207.

Li, C. P., Olavarria, J. F. and Greger, B. E. (1995) 'Occipital cortico-pyramidal projection in hypothyroid rats', *Brain Res Dev Brain Res*, 89, (2), pp. 227-34.

Li, W., Sun, G., Yang, S., Qu, Q., Nakashima, K. and Shi, Y. (2008) 'Nuclear receptor TLX regulates cell cycle progression in neural stem cells of the developing brain', *Mol Endocrinol*, 22, (1), pp. 56-64.

Lindenmeyer, M. T., Eichinger, F., Sen, K., Anders, H. J., Edenhofer, I., Mattinzoli, D., Kretzler, M., Rastaldi, M. P. and Cohen, C. D. (2010) 'Systematic analysis of a novel human renal glomerulus-enriched gene expression dataset', *PLoS One*, 5, (7), pp. e11545.

Liodis, P., Denaxa, M., Grigoriou, M., Akufo-Addo, C., Yanagawa, Y. and Pachnis, V. (2007) 'Lhx6 activity is required for the normal migration and specification of cortical interneuron subtypes', *J Neurosci,* 27, (12), pp. 3078-89.

Liu, X., Hashimoto-Torii, K., Torii, M., Ding, C. and Rakic, P. (2010) 'Gap junctions/hemichannels modulate interkinetic nuclear migration in the forebrain precursors', *J Neurosci,* 30, (12), pp. 4197-209.

Lock, T. M., Baizer, J. S. and Bender, D. B. (2003) 'Distribution of corticotectal cells in macaque', *Exp Brain Res,* 151, (4), pp. 455-70.

Long, H., Sabatier, C., Ma, L., Plump, A., Yuan, W., Ornitz, D. M., Tamada, A., Murakami, F., Goodman, C. S. and Tessier-Lavigne, M. (2004) 'Conserved roles for Slit and Robo proteins in midline commissural axon guidance', *Neuron,* 42, (2), pp. 213-23.

Lopez-Bendito, G., Cautinat, A., Sanchez, J. A., Bielle, F., Flames, N., Garratt, A. N., Talmage, D. A., Role, L. W., Charnay, P., Marin, O. and Garel, S. (2006) 'Tangential neuronal migration controls axon guidance: a role for neuregulin-1 in thalamocortical axon navigation', *Cell,* 125, (1), pp. 127-42.

Lopez-Bendito, G., Chan, C. H., Mallamaci, A., Parnavelas, J. and Molnar, Z. (2002) 'Role of Emx2 in the development of the reciprocal connectivity between cortex and thalamus', *J Comp Neurol,* 451, (2), pp. 153-69.

Lopez-Bendito, G., Flames, N., Ma, L., Fouquet, C., Di Meglio, T., Chedotal, A., Tessier-Lavigne, M. and Marin, O. (2007) 'Robo1 and Robo2 cooperate to control the guidance of major axonal tracts in the mammalian forebrain', *J Neurosci,* 27, (13), pp. 3395-407.

Low, L. K., Liu, X. B., Faulkner, R. L., Coble, J. and Cheng, H. J. (2008) 'Plexin signaling selectively regulates the stereotyped pruning of corticospinal axons from visual cortex', *Proc Natl Acad Sci U S A,* 105, (23), pp. 8136-41.

Machon, O., Backman, M., Machonova, O., Kozmik, Z., Vacik, T., Andersen, L. and Krauss, S. (2007) 'A dynamic gradient of Wnt signaling controls initiation of neurogenesis in the mammalian cortex and cellular specification in the hippocampus', *Dev Biol,* 311, (1), pp. 223-37.

Maher, P. A. (1996) 'Nuclear Translocation of fibroblast growth factor (FGF) receptors in response to FGF-2', *J Cell Biol,* 134, (2), pp. 529-36.

Mahler, M., Ben-Ari, Y. and Represa, A. (1997) 'Differential expression of fibronectin, tenascin-C and NCAMs in cultured hippocampal astrocytes activated by kainate, bacterial lipopolysaccharide or basic fibroblast growth factor', *Brain Res,* 775, (1-2), pp. 63-73.

Mallamaci, A. and Stoykova, A. (2006) 'Gene networks controlling early cerebral cortex arealization', *European Journal of Neuroscience,* 23, pp. 847-856.

Manuel, M., Georgala, P. A., Carr, C. B., Chanas, S., Kleinjan, D. A., Martynoga, B., Mason, J. O., Molinek, M., Pinson, J., Pratt, T., Quinn, J. C., Simpson, T. I., Tyas, D. A., van Heyningen, V., West, J. D. and Price, D. J. (2007) 'Controlled overexpression of Pax6 in vivo negatively autoregulates the Pax6 locus, causing cell-autonomous defects of late cortical progenitor proliferation with little effect on cortical arealization', *Development,* 134, (3), pp. 545-55.

Manuel, M. and Price, D. J. (2005) 'Role of Pax6 in forebrain regionalization', *Brain Res Bull,* 66, (4-6), pp. 387-93.

Marchetti, L., Sabbieti, M. G., Agas, D., Menghi, M., Materazzi, G., Menghi, G. and Hurley, M. M. (2006) 'PGF2alpha increases FGF-2 and FGFR2 trafficking in Py1a rat osteoblasts via clathrin independent and importin beta dependent pathway', *J Cell Biochem,* 97, (6), pp. 1379-92.

Marin, O. and Rubenstein, J. L. R. (2001) 'A long, remarkable journey: tangential migration in the telencephalon', *Nature,* 2, pp. 780-790.

Marin, O., Yaron, A., Bagri, A., Tessier-Lavigne, M. and Rubenstein, J. L. (2001) 'Sorting of striatal and cortical interneurons regulated by semaphorin-neuropilin interactions', *Science,* 293, (5531), pp. 872-5.

Markram, H., Toledo-Rodriguez, M., Wang, Y., Gupta, A., Silberberg, G. and Wu, C. (2004) 'Interneurons of the neocortical inhibitory system', *Neurosciene* 5, pp. 793-807.

Marlow, R., Binnewies, M., Sorensen, L. K., Monica, S. D., Strickland, P., Forsberg, E. C., Li, D. Y. and Hinck, L. (2010) 'Vascular Robo4 restricts proangiogenic VEGF signaling in breast', *Proc Natl Acad Sci U S A,* 107, (23), pp. 10520-5.

Martin, J. H., Friela, K. M., Salimia, I. and Chakrabarty, S. (2007) 'Activity- and use-dependent plasticity of the developing corticospinal systems', *Neuroscience & Biobehavioral Reviews,* 31, (8), pp. 1125-1135.

Martinez-Cerdeno, V., Noctor, S. C. and Kriegstein, A. R. (2006) 'The role of intermediate progenitor cells in the evolutionary expansion of the cerebral cortex', *Cereb Cortex,* 16 Suppl 1, pp. i152-61.

Maruoka, Y., Ohbayashi, N., Hoshikawa, M., Itoh, N., Hogan, B. L. and Furuta, Y. (1998) 'Comparison of the expression of three highly related genes, Fgf8, Fgf17 and Fgf18, in the mouse embryo', *Mech Dev,* 74, (1-2), pp. 175-7.

Mason, I. (2007) 'Initiation to end point: the multiple roles of fibroblast growth factors in neural development', *Nat Rev Neurosci,* 8, (8), pp. 583-96.

McConnell, S. K., Ghosh, A. and Shatz, C. J. (1989) 'Subplate neurons pioneer the first axon pathway from the cerebral cortex', *Science,* 245, (4921), pp. 978-82.

McConnell, S. K., Ghosh, A. and Shatz, C. J. (1994) 'Subplate pioneers and the formation of descending connections from cerebral cortex', *J Neurosci,* 14, (4), pp. 1892-907.

McFarlane, S., McNeill, L. and Holt, C. E. (1995) 'FGF signaling and target recognition in the developing Xenopus visual system', *Neuron,* 15, (5), pp. 1017-28.

McKenna, W. L., Betancourt, J., Larkin, K. A., Abrams, B., Guo, C., Rubenstein, J. L. and Chen, B. (2011) 'Tbr1 and Fezf2 regulate alternate corticofugal neuronal identities during neocortical development', *J Neurosci,* 31, (2), pp. 549-64.

McSherry, G. M. and Smart, I. H. (1986) 'Cell production gradients in the developing ferret isocortex', *Journal of Anatomy,* 144, pp. 1-14.

Messam, C. A., Hou, J., Berman, J. W. and Major, E. O. (2002) 'Analysis of the temporal expression of nestin in human fetal brain derived neuronal and glial progenitor cells', *Brain Res Dev Brain Res,* 134, (1-2), pp. 87-92.

Metin, C., Baudoin, J. P., Rakic, S. and Parnavelas, J. G. (2006) 'Cell and molecular mechanisms involved in the migration of cortical interneurons', *Eur J Neurosci,* 23, (4), pp. 894-900.

Meyer, G. (2001) 'Human neocortical development: the importance of embryonic and early fetal events', *Neuroscientist,* 7, (4), pp. 303-14.

Meyer, G. (2007) 'Genetic control of neuronal migrations in human cortical development', *Adv Anat Embryol Cell Biol,* 189, pp. 1 p preceding 1, 1-111.

Meyer, G., Schaaps, J. P., Moreau, L. and Goffinet, A. M. (2000) 'Embryonic and early fetal development of the human neocortex', *J Neurosci,* 20, (5), pp. 1858-68.

Miyata, T., Kawaguchi, A., Okano, H. and Ogawa, M. (2001) 'Asymmetric inheritance of radial glial fibers by cortical neurons', *Neuron,* 31, (5), pp. 727-41.

Miyoshi, G., Hjerling-Leffler, J., Karayannis, T., Sousa, V. H., Butt, S. J., Battiste, J., Johnson, J. E., Machold, R. P. and Fishell, G. (2010) 'Genetic fate mapping reveals that the caudal ganglionic eminence produces a large and diverse population of superficial cortical interneurons', *J Neurosci,* 30, (5), pp. 1582-94.

Mizutani, K., Yoon, K., Dang, L., Tokunaga, A. and Gaiano, N. (2007) 'Differential Notch signalling distinguishes neural stem cells from intermediate progenitors', *Nature,* 449, (7160), pp. 351-5.

Mo, Z., Moore, A. R., Filipovic, R., Ogawa, Y., Kazuhiro, I., Antic, S. D. and Zecevic, N. (2007) 'Human cortical neurons originate from radial glia and neuron-restricted progenitors', *J Neurosci,* 27, (15), pp. 4132-45.

Mo, Z. and Zecevic, N. (2008) 'Is Pax6 critical for neurogenesis in the human fetal brain?', *Cereb Cortex,* 18, (6), pp. 1455-65.

Molnar, Z. and Blakemore, C. (1995) 'How do thalamic axons find their way to the cortex?', *Trends Neurosci,* 18, (9), pp. 389-97.

Molnar, Z. and Cheung, A. F. (2006) 'Towards the classification of subpopulations of layer V pyramidal projection neurons', *Neurosci Res,* 55, (2), pp. 105-15.

Molnar, Z., Metin, C., Stoykova, A., Tarabykin, V., Price, D. J., Francis, F., Meyer, G., Dehay, C. and Kennedy, H. (2006) 'Comparative aspects of cerebral cortical development', *The European journal of neuroscience,* 23, (4), pp. 921-34.

Molyneaux, B. J., Arlotta, P., Fame, R. M., MacDonald, J. L., MacQuarrie, K. L. and Macklis, J. D. (2009) 'Novel subtype-specific genes identify distinct subpopulations of callosal projection neurons', *J Neurosci,* 29, (39), pp. 12343-54.

Molyneaux, B. J., Arlotta, P., Hirata, T., Hibi, M. and Macklis, J. D. (2005) 'Fezl is required for the birth and specification of corticospinal motor neurons', *Neuron,* 47, (6), pp. 817-31.

Molyneaux, B. J., Arlotta, P., Menezes, J. R. and Macklis, J. D. (2007) 'Neuronal subtype specification in the cerebral cortex', *Nat Rev Neurosci,* 8, (6), pp. 427-37.

Monfils, M. H., Driscoll, I., Vavrek, R., Kolb, B. and Fouad, K. (2008) 'FGF-2-induced functional improvement from neonatal motor cortex injury via corticospinal projections', *Exp Brain Res,* 185, (3), pp. 453-60.

Monuki, E. S. and Walsh, C. A. (2001) 'Mechanisms of cerebral cortical patterning in mice and humans', *Nature Neuroscience,* 4 (Suppl), pp. 1199-1206.

Mott, N. N., Chung, W. C., Tsai, P. S. and Pak, T. R. (2010) 'Differential fibroblast growth factor 8 (FGF8)-mediated autoregulation of its cognate receptors, Fgfr1 and Fgfr3, in neuronal cell lines', *PLoS One,* 5, (4), pp. e10143.

Muhlfriedel, S., Kirsch, F., Gruss, P., Chowdhury, K. and Stoykova, A. (2007) 'Novel genes differentially expressed in cortical regions during late neurogenesis', *Eur J Neurosci,* 26, (1), pp. 33-50.

Murphy, M., Drago, J. and Bartlett, P. F. (1990a) 'Fibroblast growth factor stimulates the proliferation and differentiation of neural precursor cells in vitro', *Journal of neuroscience research,* 25, (4), pp. 463-75.

Murphy, M., Reid, K., Ford, M., Furness, J. B. and Bartlett, P. F. (1994) 'FGF2 regulates proliferation of neural crest cells, with subsequent neuronal differentiation regulated by LIF or related factors', *Development,* 120, (12), pp. 3519-28.

Murphy, P. R., Katsumata, N., Sato, Y., Too, C. K. and Friesen, H. G. (1990b) 'In-gel ligand blotting with 125I-heparin for detection of heparin-binding growth factors', *Anal Biochem,* 187, (1), pp. 197-201.

Muzio, L., DiBenedetto, B., Stoykova, A., Boncinelli, E., Gruss, P. and Mallamaci, A. (2002) 'Emx2 and Pax6 control regionalization of the pre-neuronogenic cortical primordium', *Cereb Cortex,* 12, (2), pp. 129-39.

Nieto, M., Monuki, E. S., Tang, H., Imitola, J., Haubst, N., Khoury, S. J., Cunningham, J., Gotz, M. and Walsh, C. A. (2004) 'Expression of Cux-1 and Cux-2 in the subventricular zone and upper layers II-IV of the cerebral cortex', *J Comp Neurol,* 479, (2), pp. 168-80.

Nobrega-Pereira, S., Kessaris, N., Du, T., Kimura, S., Anderson, S. A. and Marin, O. (2008) 'Postmitotic Nkx2-1 controls the migration of telencephalic interneurons by direct repression of guidance receptors', *Neuron,* 59, (5), pp. 733-45.

Noctor, S. C., Flint, A. C., Weissman, T. A., Dammerman, R. S. and Kriegstein, A. R. (2001) 'Neurons derived from radial glial cells establish radial units in neocortex', *Nature,* 409, (6821), pp. 714-20.

Noctor, S. C., Flint, A. C., Weissman, T. A., Wong, W. S., Clinton, B. K. and Kriegstein, A. R. (2002) 'Dividing precursor cells of the embryonic cortical ventricular zone have morphological and molecular characteristics of radial glia', *J Neurosci,* 22, (8), pp. 3161-73.

Noctor, S. C., Martinez-Cerdeno, V., Ivic, L. and Kriegstein, A. R. (2004) 'Cortical neurons arise in symmetric and asymmetric division zones and migrate through specific phases', *Nat Neurosci,* 7, (2), pp. 136-44.

Noctor, S. C., Martinez-Cerdeno, V. and Kriegstein, A. R. (2008) 'Distinct behaviors of neural stem and progenitor cells underlie cortical neurogenesis', *J Comp Neurol,* 508, (1), pp. 28-44.

O'Leary, D. D. (1992) 'Development of connectional diversity and specificity in the mammalian brain by the pruning of collateral projections', *Curr Opin Neurobiol,* 2, (1), pp. 70-7.

O'Leary, D. D. and Borngasser, D. (2006) 'Cortical ventricular zone progenitors and their progeny maintain spatial relationships and radial patterning during preplate development indicating an early protomap', *Cereb Cortex*, 16 Suppl 1, pp. i46-56.

O'Leary, D. D., Chou, S. J. and Sahara, S. (2007) 'Area patterning of the mammalian cortex', *Neuron*, 56, (2), pp. 252-69.

O'Leary, D. D. and Koester, S. E. (1993) 'Development of projection neuron types, axon pathways, and patterned connections of the mammalian cortex', *Neuron*, 10, (6), pp. 991-1006.

O'Leary, D. D. and Sahara, S. (2008) 'Genetic regulation of arealization of the neocortex', *Curr Opin Neurobiol*, 18, (1), pp. 90-100.

O'Leary, D. D. M. (1989) 'Do cortical areas emerge from a protocortex?', *Trends in Neurosciences*, 12, pp. 400-206.

O'Leary, D. D. M. and Nakagawa, Y. (2002) 'Patterning centers, regulatory genes and extrinsic mechanisms controlling arealization of the neocortex', *Current Opinion in Neurobiology*, 12, pp. 14-25.

Ohkubo, Y., Chiang, C. and Rubenstein, J. L. R. (2002) 'Coordinate regulation and synergistic actions of *Bmp4*, *Shh* and *Fgf8* in the rostral prosencephalon regulate morphogenesis of the telencephalic and optic vesicles', *Neuroscience*, 111, (1), pp. 1-17.

Oudega, M., Varon, S. and Hagg, T. (1994) 'Distribution of corticospinal motor neurons in the postnatal rat: quantitative evidence for massive collateral elimination and modest cell death', *J Comp Neurol*, 347, (1), pp. 115-26.

Petanjek, Z., Berger, B. and Esclapez, M. (2009a) 'Origins of cortical GABAergic neurons in the cynomolgus monkey', *Cereb Cortex,* 19, (2), pp. 249-62.

Petanjek, Z., Dujmovic, A., Kostovic, I. and Esclapez, M. (2008) 'Distinct origin of GABA-ergic neurons in forebrain of man, nonhuman primates and lower mammals', *Coll Antropol,* 32 Suppl 1, pp. 9-17.

Petanjek, Z., Kostovic, I. and Esclapez, M. (2009b) 'Primate-specific origins and migration of cortical GABAergic neurons', *Front Neuroanat,* 3, pp. 26.

Pilaz, L. J., Patti, D., Marcy, G., Ollier, E., Pfister, S., Douglas, R. J., Betizeau, M., Gautier, E., Cortay, V., Doerflinger, N., Kennedy, H. and Dehay, C. (2009) 'Forced G1-phase reduction alters mode of division, neuron number, and laminar phenotype in the cerebral cortex', *Proc Natl Acad Sci U S A,* 106, (51), pp. 21924-9.

Pinon, M. C., Tuoc, T. C., Ashery-Padan, R., Molnar, Z. and Stoykova, A. (2008) 'Altered molecular regionalization and normal thalamocortical connections in cortex-specific Pax6 knock-out mice', *J Neurosci,* 28, (35), pp. 8724-34.

Pinto, L., Mader, M. T., Irmler, M., Gentilini, M., Santoni, F., Drechsel, D., Blum, R., Stahl, R., Bulfone, A., Malatesta, P., Beckers, J. and Gotz, M. (2008) 'Prospective isolation of functionally distinct radial glial subtypes--lineage and transcriptome analysis', *Mol Cell Neurosci,* 38, (1), pp. 15-42.

Porter, R. (1985) 'The corticomotoneuronal component of the pyramidal tract: corticomotoneuronal connections and functions in primates', *Brain Res,* 357, (1), pp. 1-26.

Qian, X., Davis, A. A., Goderie, S. K. and Temple, S. (1997) 'FGF2 concentration regulates the generation of neurons and glia from multipotent cortical stem cells', *Neuron,* 18, (1), pp. 81-93.

Qu, Q., Sun, G., Li, W., Yang, S., Ye, P., Zhao, C., Yu, R. T., Gage, F. H., Evans, R. M. and Shi, Y. (2010) 'Orphan nuclear receptor TLX activates Wnt/beta-catenin signalling to stimulate neural stem cell proliferation and self-renewal', *Nat Cell Biol,* 12, (1), pp. 31-40; sup pp 1-9.

Raballo, R., Rhee, J., Lyn-Cook, R., Leckman, J. F., Schwartz, M. L. and Vaccarino, F. M. (2000) 'Basic fibroblast growth factor (Fgf2) is necessary for cell proliferation and neurogenesis in the developing cerebral cortex', *J Neurosci,* 20, (13), pp. 5012-23.

Rakic, P. (1988) 'Specification of cerebral cortical areas', *Science,* 241, pp. 170-176.

Rakic, P. (1991) 'Experimental manipulation of cerebral cortical areas in primates', *Philos Trans R Soc Lond B Biol Sci,* 331, (1261), pp. 291-4.

Rakic, P., Ayoub, A. E., Breunig, J. J. and Dominguez, M. H. (2009) 'Decision by division: making cortical maps', *Trends Neurosci,* 32, (5), pp. 291-301.

Rakic, S. and Zecevic, N. (2003) 'Emerging complexity of layer I in human cerebral cortex', *Cereb Cortex,* 13, (10), pp. 1072-83.

Ramirez, J. J., Finklestein, S. P., Keller, J., Abrams, W., George, M. N. and Parakh, T. (1999) 'Basic fibroblast growth factor enhances axonal sprouting after cortical injury in rats', *Neuroreport,* 10, (6), pp. 1201-4.

Ramnani, N., Behrens, T. E., Johansen-Berg, H., Richter, M. C., Pinsk, M. A., Andersson, J. L., Rudebeck, P., Ciccarelli, O., Richter, W., Thompson, A. J., Gross, C. G., Robson, M. D., Kastner, S. and Matthews, P. M. (2006) 'The evolution of prefrontal inputs to the cortico-pontine system: diffusion imaging evidence from Macaque monkeys and humans', *Cereb Cortex,* 16, (6), pp. 811-8.

Rice, D. S. and Curran, T. (2001) 'Role of the reelin signaling pathway in central nervous system development', *Annu Rev Neurosci,* 24, pp. 1005-39.

Roy, K., Kuznicki, K., Wu, Q., Sun, Z., Bock, D., Schutz, G., Vranich, N. and Monaghan, A. P. (2004) 'The Tlx gene regulates the timing of neurogenesis in the cortex', *J Neurosci,* 24, (38), pp. 8333-45.

Ruano, D., Macedo, A., Dourado, A., Soares, M. J., Valente, J., Coelho, I., Santos, V., Azevedo, M. H., Goodman, A., Hutz, M. H., Gama, C., Lobato, M. I., Belmonte-de-Abreu, P. and Palha, J. A. (2004) 'NR4A2 and schizophrenia: lack of association in a Portuguese/Brazilian study', *Am J Med Genet B Neuropsychiatr Genet,* 128B, (1), pp. 41-5.

Runker, A. E., Little, G. E., Suto, F., Fujisawa, H. and Mitchell, K. J. (2008) 'Semaphorin-6A controls guidance of corticospinal tract axons at multiple choice points', *Neural Dev,* 3, pp. 34.

Sabbieti, M. G., Marchetti, L., Gabrielli, M. G., Menghi, M., Materazzi, S., Menghi, G., Raisz, L. G. and Hurley, M. M. (2005) 'Prostaglandins differently regulate FGF-2 and FGF receptor expression and induce nuclear translocation in osteoblasts via MAPK kinase', *Cell Tissue Res,* 319, (2), pp. 267-78.

Sahara, S., Kawakami, Y., Izpisua Belmonte, J. C. and O'Leary, D. D. (2007) 'Sp8 exhibits reciprocal induction with Fgf8 but has an opposing effect on anterior-posterior cortical area patterning', *Neural Dev,* 2, pp. 10.

Saito, T., Hanai, S., Takashima, S., Nakagawa, E., Okazaki, S., Inoue, T., Miyata, R., Hoshino, K., Akashi, T., Sasaki, M., Goto, Y. I., Hayashi, M. and Itoh, M. (2010) 'Neocortical Layer Formation of Human Developing Brains and Lissencephalies: Consideration of Layer-Specific Marker Expression', *Cereb Cortex*.

Sanchez-Heras, E., Howell, F. V., Williams, G. and Doherty, P. (2006) 'The fibroblast growth factor receptor acid box is essential for interactions with N-cadherin and all of the major isoforms of neural cell adhesion molecule', *J Biol Chem,* 281, (46), pp. 35208-16.

Schmahl, J., Kim, Y., Colvin, J. S., Ornitz, D. M. and Capel, B. (2004) 'Fgf9 induces proliferation and nuclear localization of FGFR2 in Sertoli precursors during male sex determination', *Development,* 131, (15), pp. 3627-36.

Schuurmans, C., Armant, O., Nieto, M., Stenman, J. M., Britz, O., Klenin, N., Brown, C., Langevin, L. M., Seibt, J., Tang, H., Cunningham, J. M., Dyck, R., Walsh, C., Campbell, K., Polleux, F. and Guillemot, F. (2004) 'Sequential phases of cortical specification involve Neurogenin-dependent and -independent pathways', *Embo J,* 23, (14), pp. 2892-902.

Sharkey, M. A., Lund, R. D. and Dom, R. M. (1986) 'Maintenance of transient occipitospinal axons in the rat', *Brain Res,* 395, (2), pp. 257-61.

Sheldon, H., Andre, M., Legg, J. A., Heal, P., Herbert, J. M., Sainson, R., Sharma, A. S., Kitajewski, J. K., Heath, V. L. and Bicknell, R. (2009) 'Active involvement of Robo1 and Robo4 in filopodia formation and endothelial cell motility mediated via WASP and other actin nucleation-promoting factors', *FASEB J,* 23, (2), pp. 513-22.

Shimogori, T., Banuchi, V., Ng, H. Y., Strauss, J. B. and Grove, E. A. (2004) 'Embryonic signalling centres expressing BMP, WNT and FGF proteins interact to pattern the cerebral cortex', *Development,* 131, pp. 5639-5647.

Shimogori, T. and Grove, E. A. (2005) 'Fibroblast growth factor 8 regulates neocortical guidance of area-specific thalamic innervation', *The Journal of Neuroscience,* 25, (28), pp. 6550-6560.

Siegel, A. L., Atchison, K., Fisher, K. E., Davis, G. E. and Cornelison, D. D. (2009) '3D timelapse analysis of muscle satellite cell motility', *Stem Cells,* 27, (10), pp. 2527-38.

Simeone, A., Gulisano, M., Acampora, D., Stornaiuolo, A., Rambaldi, M. and Boncinelli, E. (1992) 'Two vertebrate homeobox genes related to the Drosophila empty spiracles gene are expressed in the embryonic cerebral cortex', *EMBO J,* 11, (7), pp. 2541-50.

Simon, H. H., Bhatt, L., Gherbassi, D., Sgado, P. and Alberi, L. (2003) 'Midbrain dopaminergic neurons: determination of their developmental fate by transcription factors', *Ann N Y Acad Sci,* 991, pp. 36-47.

Sleiman, P. M., Healy, D. G., Muqit, M. M., Yang, Y. X., Van Der Brug, M., Holton, J. L., Revesz, T., Quinn, N. P., Bhatia, K., Diss, J. K., Lees, A. J., Cookson, M. R., Latchman, D. S. and Wood, N. W. (2009) 'Characterisation of a novel NR4A2 mutation in Parkinson's disease brain', *Neurosci Lett,* 457, (2), pp. 75-9.

Smart, I. H., Dehay, C., Giroud, P., Berland, M. and Kennedy, H. (2002) 'Unique morphological features of the proliferative zones and postmitotic compartments of the neural epithelium giving rise to striate and extrastriate cortex in the monkey', *Cereb Cortex,* 12, (1), pp. 37-53.

Stachowiak, M. K., Maher, P. A. and Stachowiak, E. K. (2007) 'Integrative nuclear signaling in cell development--a role for FGF receptor-1', *DNA Cell Biol,* 26, (12), pp. 811-26.

Stancik, E. K., Navarro-Quiroga, I., Sellke, R. and Haydar, T. F. (2010) 'Heterogeneity in ventricular zone neural precursors contributes to neuronal fate diversity in the postnatal neocortex', *J Neurosci,* 30, (20), pp. 7028-36.

Stanfield, B. B. and O'Leary, D. D. (1985) 'Fetal occipital cortical neurones transplanted to the rostral cortex can extend and maintain a pyramidal tract axon', *Nature,* 313, (5998), pp. 135-7.

Storm, E. E., Garel, S., Borello, U., Hebert, J. M., Martinez, S., McConnell, S. K., Martin, G. R. and Rubenstein, J. L. (2006) 'Dose-dependent functions of Fgf8 in regulating telencephalic patterning centers', *Development,* 133, (9), pp. 1831-44.

Stoykova, A., Treichel, D., Hallonet, M. and Gruss, P. (2000) 'Pax6 modulates the dorsoventral patterning of the mammalian telencephalon', *J Neurosci,* 20, (21), pp. 8042-50.

Stuhmer, T., Anderson, S. A., Ekker, M. and Rubenstein, J. L. (2002) 'Ectopic expression of the Dlx genes induces glutamic acid decarboxylase and Dlx expression', *Development,* 129, (1), pp. 245-52.

Subramanian, L., Remedios, R., Shetty, A. and Tole, S. (2009) 'Signals from the edges: the cortical hem and antihem in telencephalic development', *Semin Cell Dev Biol,* 20, (6), pp. 712-8.

Sundaresan, V., Mambetisaeva, E., Andrews, W., Annan, A., Knoll, B., Tear, G. and Bannister, L. (2004) 'Dynamic expression patterns of Robo (Robo1 and Robo2) in the developing murine central nervous system', *J Comp Neurol*, 468, (4), pp. 467-81.

Super, H., Soriano, E. and Uylings, H. B. (1998) 'The functions of the preplate in development and evolution of the neocortex and hippocampus', *Brain Res Brain Res Rev*, 27, (1), pp. 40-64.

Sussel, L., Marin, O., Kimura, S. and Rubenstein, J. L. R. (1999) 'Loss of Nkx2.1 homeobox gene function results in a ventral to dorsal molecular respecification within the basal telencephalon: evidence for a transformation of the pallidum into the striatum', *Development*, 126, pp. 3359-3370.

Szemes, M., Gyorgy, A., Paweletz, C., Dobi, A. and Agoston, D. V. (2006) 'Isolation and characterization of SATB2, a novel AT-rich DNA binding protein expressed in development- and cell-specific manner in the rat brain', *Neurochem Res*, 31, (2), pp. 237-46.

Takahashi, K., Liu, F. C., Oishi, T., Mori, T., Higo, N., Hayashi, M., Hirokawa, K. and Takahashi, H. (2008) 'Expression of FOXP2 in the developing monkey forebrain: comparison with the expression of the genes FOXP1, PBX3, and MEIS2', *J Comp Neurol*, 509, (2), pp. 180-9.

Tarabykin, V., Stoykova, A., Usman, N. and Gruss, P. (2001) 'Cortical upper layer neurons derive from the subventricular zone as indicated by Svet1 gene expression', *Development*, 128, (11), pp. 1983-93.

ten Donkelaar, H. J. (2000) 'Major events in the development of the forebrain', *Eur J Morphol*, 38, (5), pp. 301-8.

Thomson, R. E., Pellicano, F. and Iwata, T. (2007) 'Fibroblast growth factor receptor 3 kinase domain mutation increases cortical progenitor proliferation via mitogen-activated protein kinase activation', *J Neurochem,* 100, (6), pp. 1565-78.

Tomasch, J. (1969) 'The numerical capacity of the human cortico-pontocerebellar system', *Brain Res Dev Brain Res,* 13, (3), pp. 476-84.

Tomassy, G. S., De Leonibus, E., Jabaudon, D., Lodato, S., Alfano, C., Mele, A., Macklis, J. D. and Studer, M. (2010) 'Area-specific temporal control of corticospinal motor neuron differentiation by COUP-TFI', *Proc Natl Acad Sci U S A,* 107, (8), pp. 3576-81.

Toresson, H., Potter, S. S. and Campbell, K. (2000) 'Genetic control of dorsal-ventral identity in the telencephalon: opposing roles for Pax6 and Gsh2', *Development,* 127, pp. 4361-4371.

Vaccarino, F. M., Schwartz, M. L., Raballo, R., Nilsen, J., Rhee, J., Zhou, M., Doetschman, T., Coffin, J. D., Wyland, J. J. and Hung, Y. T. (1999) 'Changes in cerebral cortex size are governed by fibroblast growth factor during embryogenesis', *Nat Neurosci,* 2, (3), pp. 246-53.

Van der Loos, H. and Woolsey, T. A. (1973) 'Somatosensory cortex: structural alterations following early injury to sense organs', *Science,* 179, pp. 395-298.

Vargha-Khadem, F., Gadian, D. G., Copp, A. and Mishkin, M. (2005) 'FOXP2 and the neuroanatomy of speech and language', *Nat Rev Neurosci,* 6, (2), pp. 131-8.

Wang, W. Z., Hoerder-Suabedissen, A., Oeschger, F. M., Bayatti, N., Ip, B. K., Lindsay, S., Supramaniam, V., Srinivasan, L., Rutherford, M., Mollgard, K., Clowry, G. J. and Molnar,

Z. (2010) 'Subplate in the developing cortex of mouse and human', *J Anat*, 217, (4), pp. 368-80.

Warren, N., Caric, D., Pratt, T., Clausen, J. A., Asavaritikrai, P., Mason, J. O., Hill, R. E. and Price, D. J. (1999) 'The transcription factor, Pax6, is required for cell proliferation and differentiation in the developing cerebral cortex', *Cereb Cortex*, 9, (6), pp. 627-35.

Watakabe, A., Ichinohe, N., Ohsawa, S., Hashikawa, T., Komatsu, Y., Rockland, K. S. and Yamamori, T. (2007) 'Comparative analysis of layer-specific genes in Mammalian neocortex', *Cereb Cortex*, 17, (8), pp. 1918-33.

Weimann, J. M., Zhang, Y. A., VLevin, M. E., Devine, W. P., Brulet, P. and McConnell, S. K. (1999) 'Cortical neurons require Otx1 for the refinement of exuberant axonal projections to subcortical targets', *Neuron*, 24, pp. 819-831.

Whitford, K. L., Marillat, V., Stein, E., Goodman, C. S., Tessier-Lavigne, M., Chedotal, A. and Ghosh, A. (2002) 'Regulation of cortical dendrite development by Slit-Robo interactions', *Neuron*, 33, (1), pp. 47-61.

Wichterle, H., Alvarez-Dolado, M., Erskine, L. and Alvarez-Buylla, A. (2003) 'Permissive corridor and diffusible gradients direct medial ganglionic eminence cell migration to the neocortex', *Proc Natl Acad Sci U S A*, 100, (2), pp. 727-32.

Willi-Monnerat, S., Migliavacca, E., Surdez, D., Delorenzi, M., Luthi-Carter, R. and Terskikh, A. V. (2008) 'Comprehensive spatiotemporal transcriptomic analyses of the ganglionic eminences demonstrate the uniqueness of its caudal subdivision', *Mol Cell Neurosci*, 37, (4), pp. 845-56.

Wonders, C. P. and Anderson, S. A. (2006) 'The origin and specification of cortical interneurons', *Nat Rev Neurosci,* 7, (9), pp. 687-96.

Wong, K., Ren, X. R., Huang, Y. Z., Xie, Y., Liu, G., Saito, H., Tang, H., Wen, L., Brady-Kalnay, S. M., Mei, L., Wu, J. Y., Xiong, W. C. and Rao, Y. (2001) 'Signal transduction in neuronal migration: roles of GTPase activating proteins and the small GTPase Cdc42 in the Slit-Robo pathway', *Cell,* 107, (2), pp. 209-21.

Xu, J., Lawshe, A., MacArthur, C. A. and Ornitz, D. M. (1999) 'Genomic structure, mapping, activity and expression of fibroblast growth factor 17', *Mech Dev,* 83, (1-2), pp. 165-78.

Yamauchi, K., Mizushima, S., Tamada, A., Yamamoto, N., Takashima, S. and Murakami, F. (2009) 'FGF8 signaling regulates growth of midbrain dopaminergic axons by inducing semaphorin 3F', *J Neurosci,* 29, (13), pp. 4044-55.

Yanez, I. B., Munoz, A., Contreras, J., Gonzalez, J., Rodriguez-Veiga, E. and DeFelipe, J. (2005) 'Double bouquet cell in the human cerebral cortex and a comparison with other mammals', *J Comp Neurol,* 486, (4), pp. 344-60.

Yao, J., Liu, Y., Husain, J., Lo, R., Palaparti, A., Henderson, J. and Stifani, S. (1998) 'Combinatorial expression patterns of individual TLE proteins during cell determination and differentiation suggest non-redundant functions for mammalian homologs of Drosophila Groucho', *Dev Growth Differ,* 40, (2), pp. 133-46.

Yao, Q., Jin, W. L., Wang, Y. and Ju, G. (2008) 'Regulated shuttling of Slit-Robo-GTPase activating proteins between nucleus and cytoplasm during brain development', *Cell Mol Neurobiol,* 28, (2), pp. 205-21.

Yoneshima, H., Yamasaki, S., Voelker, C. C., Molnar, Z., Christophe, E., Audinat, E., Takemoto, M., Nishiwaki, M., Tsuji, S., Fujita, I. and Yamamoto, N. (2006) 'Er81 is expressed in a subpopulation of layer 5 neurons in rodent and primate neocortices', *Neuroscience,* 137, (2), pp. 401-12.

Yue, Y., Grossmann, B., Galetzka, D., Zechner, U. and Haaf, T. (2006) 'Isolation and differential expression of two isoforms of the ROBO2/Robo2 axon guidance receptor gene in humans and mice', *Genomics,* 88, pp. 772-778.

Yun, K., Potter, S. and Rubenstein, J. L. (2001) 'Gsh2 and Pax6 play complementary roles in dorsoventral patterning of the mammalian telencephalon', *Development,* 128, pp. 193-205.

Zembrzycki, A., Griesel, G., Stoykova, A. and Mansouri, A. (2007) 'Genetic interplay between the transcription factors Sp8 and Emx2 in the patterning of the forebrain', *Neural Dev,* 2, pp. 8.

Zhao, Y., Flandin, P., Long, J. E., Cuesta, M. D., Westphal, H. and Rubenstein, J. L. (2008) 'Distinct molecular pathways for development of telencephalic interneuron subtypes revealed through analysis of Lhx6 mutants', *J Comp Neurol,* 510, (1), pp. 79-99.

Zhou, C., Qiu, Y., Pereira, F. A., Crair, M. C., Tsai, S. Y. and Tsai, M. J. (1999) 'The nuclear orphan receptor COUP-TFI is required for differentiation of subplate neurons and guidance of thalamocortical axons', *Neuron,* 24, (4), pp. 847-59.

Zschocke, J., Bayatti, N., Clement, A. M., Witan, H., Figiel, M., Engele, J. and Behl, C. (2005) 'Differential promotion of glutamate transporter expression and function by glucocorticoids in astrocytes from various brain regions', *J Biol Chem,* 280, (41), pp. 34924-32.

List of Publications

Journal Articles

Ip BK, Bayatti N, Howard NJ, Lindsay S, Clowry GJ (2010b). The corticofugal neuron-associated genes ROBO1, SRGAP1, and CTIP2 exhibit an anterior to posterior gradient of expression in early fetal human neocortex development. *Cerebral Cortex*. doi: 10.1093/cercor/bhq219.

Ip BK, Wappler I, Peters H, Lindsay S, Clowry GJ, Bayatti N (2010a). Investigating gradients of gene expression involved in early human cortical development. *Journal of Anatomy*. 217 (4): 300-311.

Wang WZ, Hoerder-Suabedissen A, Oeschger FM, Bayatti N, **Ip BK**, Lindsay S, Supramaniam V, Srinivasan L, Rutherford M, Mollgard K, Clowry GJ, Molnar Z (2010). Subplate in the developing cortex of mouse and human. *Journal of Anatomy*. 217 (4): 368-380.

Abstracts

Ip BK, Bayatti N, Howard NJ, Lindsay S, Clowry GJ. (2010) Graded expression patterns of proteins ROBO1, SRGAP1 and CTIP2 show the corticospinal tract arises from the anterior pole of the neocortex during early fetal human development. *FENS Abstr.* 127.14

Ip BK, Bayatti N, Howard NJ, Clowry GJ, Lindsay S. (2009) Localization of Expression of Motor Cortex Markers ROBO1/SRGAP1 and CTIP2 in the Early Foetal Human Neocortex. *British Neurosci. Assoc. Abstr.*, Vol 20, P52, Abstract 3.02.

Ip BK, Bayatti N, Howard N, Lindsay S, Clowry GJ. (2009) Expression of ROBO1/SRGAP1 and CTIP2 suggests that the motor cortex initially forms at the anterior pole during development of the human foetal neocortex, *Mechanisms of Development* 126:S82-S83.

Ip BK, Bayatti N, Lindsay S, Clowry GJ. (2009) Development of functional regionalization in the human neocortex: preliminary findings of SLIT/ROBO/srGAP differential expression. *Journal of Anatomy* 214:794-795.

Clowry GJ, Bayatti N, **Ip BK**, Lindsay S. (2008) Gene expression studies of the development of functional regionalization in the human neocortex. Program No. 718.14 Abstract Viewer and Itinerary Planner. *Washington, DC: Society for Neuroscience*. Online